



PHD

Approximation of the attractor and the inertial manifold of the Kuramoto-Sivashinsky equation

Falcon, Michael Andrew

Award date:
1998

Awarding institution:
University of Bath

[Link to publication](#)

Alternative formats

If you require this document in an alternative format, please contact:
openaccess@bath.ac.uk

Copyright of this thesis rests with the author. Access is subject to the above licence, if given. If no licence is specified above, original content in this thesis is licensed under the terms of the Creative Commons Attribution-NonCommercial 4.0 International (CC BY-NC-ND 4.0) Licence (<https://creativecommons.org/licenses/by-nc-nd/4.0/>). Any third-party copyright material present remains the property of its respective owner(s) and is licensed under its existing terms.

Take down policy

If you consider content within Bath's Research Portal to be in breach of UK law, please contact: openaccess@bath.ac.uk with the details. Your claim will be investigated and, where appropriate, the item will be removed from public view as soon as possible.

Approximation of the Attractor and the Inertial Manifold of the Kuramoto-Sivashinsky Equation

submitted by

Michael Andrew Falcon

for the degree of Ph.D.

of the

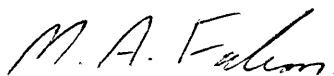
University of Bath

1998

COPYRIGHT

Attention is drawn to the fact that copyright of this thesis rests with its author. This copy of the thesis has been supplied on the condition that anyone who consults it is understood to recognise that its copyright rests with its author and that no quotation from the thesis and no information derived from it may be published without the prior written consent of the author.

This thesis may be made available for consultation within the University Library and may be photocopied or lent to other libraries for the purposes of consultation.

Signature of Author 

Michael Andrew Falcon

UMI Number: U532318

All rights reserved

INFORMATION TO ALL USERS

The quality of this reproduction is dependent upon the quality of the copy submitted.

In the unlikely event that the author did not send a complete manuscript and there are missing pages, these will be noted. Also, if material had to be removed, a note will indicate the deletion.



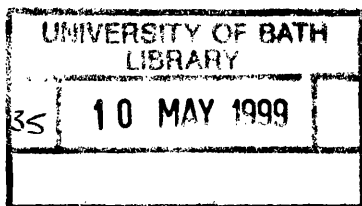
UMI U532318

Published by ProQuest LLC 2013. Copyright in the Dissertation held by the Author.
Microform Edition © ProQuest LLC.

All rights reserved. This work is protected against
unauthorized copying under Title 17, United States Code.



ProQuest LLC
789 East Eisenhower Parkway
P.O. Box 1346
Ann Arbor, MI 48106-1346



Summary

This thesis considers the numerical approximation, using the Fourier pseudospectral method, of the asymptotic dynamical behaviour of the one-dimensional Kuramoto-Sivashinsky (K-S) equation

$$\frac{\partial u}{\partial t} + 4 \frac{\partial^4 u}{\partial x^4} + \alpha \left(\frac{\partial^2 u}{\partial x^2} + u \frac{\partial u}{\partial x} \right) = 0,$$

with odd initial data and periodic boundary conditions, where α is some non-negative parameter. This equation is known to possess a global attractor, with a finite-dimensional Hausdorff dimension, and an inertial manifold. Also the solutions of this equation are contained in a Gevrey class.

The pseudospectral method is analysed by formulating a semi-discrete spatial approximation and a fully-discrete approximation which uses the Trapezoidal rule for the temporal discretization. Convergence results are obtained for both of these approximation schemes in the H^1 norm. The result for the semi-discrete approximation is an improvement on an existing one proved by López-Marcos (1994). The solutions of the semi-discrete approximation are also shown to be contained in a Gevrey class, which is the first time such a result has been shown for approximations involving the pseudospectral method. This result along with the convergence result for the semi-discrete approximation is used to show upper semi-continuity of the semi-discrete attractor to the true attractor in H^1 .

A result concerning the persistence of the bounded invariant sets of the K-S equation under semi-discrete approximation is also proved. These sets are shown to converge to the true invariant sets with a high order of accuracy. This is achieved by applying the approximation theory of Jones, Stuart and Titi (1998) and exploiting the regularity of the solutions of the K-S equation and the semi-discrete approximation.

Finally a detailed computational study of the dynamics of the K-S equation for $0 \leq \alpha \leq 40$ is carried out using the pseudospectral approximation. A variety of bifurcation phenomena is shown to exist which includes a period doubling cascade, homoclinic orbits of the Sil'nikov type and a previously undiscovered heteroclinic orbit. The existence of the Sil'nikov homoclinic orbits shows a route to chaos of the K-S equation.

Acknowledgements

I would like to thank all the members of the Department of Mathematical Sciences at the University of Bath for all their help and EPSRC for funding this project. I would especially like to thank Dr Adrian Hill for his supervision and help during this thesis. I would also like to offer my deepest thanks to my parents and Susanna Page for all their support and encouragement which has made each step of this thesis possible.

I've had some great officemates and made some good friends in the past three years, who include Dan Brown, Jenny Jones, Chris Poulton, Steve and Emma Benbow, Bill Browne, Rob Laister, Chris Brooking, Mark Penny, Paul Spencer, Graeme Boswell, Jon Wilson, Richard Cleyton, Garry Pollock and Rob Scheichl. Finally I would like to thank Stuart Hawkins and Steve Langdon who been the best of friends throughout my degree.

Contents

1	Introduction	1
1.1	General introduction	1
1.2	Aims of the thesis	8
1.3	Thesis outline	9
2	The Continuous Problem	14
2.1	Domains and function spaces	14
2.2	Sectorial operators and analytic semigroups	18
2.3	The Kuramoto-Sivashinsky equation	27
2.4	An abstract framework for the Kuramoto-Sivashinsky equation . .	30
3	The Discrete Problem	39
3.1	A semi-discrete approximation	39
3.1.1	The pseudospectral method	39
3.1.2	Discretization of the Kuramoto-Sivashinsky equation . . .	40
3.1.3	A mathematical setting for the semi-discrete approximation	45
3.2	Nonlinear stability and convergence	54
3.2.1	Stability for the semi-discrete approximation	54
3.2.2	Consistency for the semi-discrete approximation	57
3.2.3	Convergence for the semi-discrete approximation	61
3.3	Gevrey regularity of the solutions of the semi-discrete approximation	66
3.4	A fully-discrete approximation	77
3.4.1	A Crank-Nicolson scheme	77
3.4.2	A further fully-discrete scheme	77

3.4.3	Consistency for the fully-discrete scheme	79
3.4.4	Convergence for the fully-discrete scheme	80
3.4.5	Convergence for the Crank-Nicolson scheme	84
4	Attractors and upper semi-continuity of attractors	86
4.1	Attractor theory	86
4.2	Attractors of the Kuramoto-Sivashinsky equation	92
4.3	Upper semi-continuity of attractors	93
4.3.1	Introduction	93
4.3.2	General theory	97
4.4	Upper semi-continuity of attractors for the Kuramoto-Sivashinsky equation	100
4.5	Orbits homoclinic to saddle-focus points	104
5	Inertial Manifolds	108
5.1	Introduction	108
5.2	Existence and approximation theory of inertial manifolds	112
5.3	Inertial manifolds for the Kuramoto-Sivashinsky equation	121
5.4	Convergence of the Fréchet derivative of the semi-discrete approx- imation	128
5.4.1	The Fréchet derivative	128
5.4.2	Consistency	132
5.4.3	Convergence	134
5.5	Persistence of bounded invariant sets for the semi-discrete approx- imation	138
6	Numerical Analysis	144
6.1	Numerical study of the dynamics of the Kuramoto-Sivashinsky equation	144
6.1.1	Low dimensional attractor	144
6.1.2	Steady states	148
6.1.3	Periodic states	150

6.1.4	Homoclinic orbits	156
6.1.5	A heteroclinic orbit	161
6.1.6	Other periodic behaviour	163
6.2	Approximate inertial manifolds and nonlinear Galerkin methods .	166
6.2.1	Approximate inertial manifold theory	167
6.2.2	Computational aspects of NLG methods	171
6.2.3	The postprocessed Galerkin method	173
6.3	A nonlinear Galerkin method based on the pseudospectral method for the Kuramoto-Sivashinsky equation	176
6.3.1	Approximate inertial manifold approach of Wallace and Sloan	177
6.3.2	Algorithm with coarse and fine grid interactions	178
6.3.3	Numerical results	182
7	Final Conclusions and Future Work	187
	Bibliography	189

List of Figures

2-1	Graphical representation of the sector of the complex plane where $\sigma(A)$ must lie for an operator A to be sectorial for a given ϕ and a .	20
2-2	Illustration of the closure of the numerical range in the complex plane.	32
4-1	Graphical illustration of the type of convergence associated with upper semi-continuity.	95
4-2	a) Plot of the flow of the dynamical system $u_t = f(u)$; b) Plot of the flow of the perturbed dynamical system $u_t = f_\epsilon(u)$	96
4-3	Graphical illustration of the properties of the global attractor of the K-S equation.	101
4-4	Behaviour of the unstable manifold for differing values of μ	106
4-5	Stability diagram of the periodic solutions.	107
6-1	Bi-modal steady state attractor of the K-S equation with $\alpha = 40$ on the interval $[-\pi, \pi]$	146
6-2	Periodic solutions of the PS approximation for increasing sizes of N .	147
6-3	Solutions of the K-S equation with $\alpha = 32.96$ over two periods. . .	147
6-4	Bifurcation diagram of the K-S equation for $0 \leq \alpha \leq 40$, showing the L^2 norm plotted against α	149
6-5	Bifurcation diagram of the K-S equation of the fourth solution component plotted against α	150
6-6	Close-up of stable periodic solutions emanating from the Hopf bifurcation at $\alpha = 30.345$	152

6-7	Periodic solutions loosing stability at bifurcation and period doubling points.	152
6-8	Close-up of the initial period doubling points.	153
6-9	Minima of the L^2 norm of the periodic solutions plotted against α showing the period doubling cascade and beyond.	155
6-10	Interior crisis bifurcation at $\alpha \simeq 33.004$	156
6-11	Behaviour of the periodic solutions produced at the supercritical Hopf bifurcation at $\alpha = 30.345$. Solution norm plotted against α	157
6-12	Behaviour of the periodic solutions produced at the supercritical Hopf bifurcation at $\alpha = 30.345$. Period plotted against α	158
6-13	Eigenvalues of the linearization at the saddle-focus point at $\alpha = 34.366$. a) Complete spectrum; b) Close up of first three eigenvalues.	159
6-14	Phase plots of the periodic solutions. a) $\alpha = 32.971$; b) $\alpha = 32.990$; c) $\alpha = 32.994$; d) $\alpha = 32.996$; e) $\alpha = 34.336$; f) $\alpha = 34.3661$	160
6-15	Double-pulse homoclinic orbit at $\alpha = 34.3606$	161
6-16	Unstable branch of periodic solutions emanating from the bifurcation point at $\alpha = 32.853$	162
6-17	Heteroclinic orbit at $\alpha = 36.127$	162
6-18	Periodic solutions as they approach the heteroclinic orbit.	163
6-19	Periodic behaviour of the solutions at the Hopf bifurcation point at $\alpha = 34.345$	164
6-20	Behaviour of the upper branch of periodic solutions produced at Hopf bifurcation at $\alpha = 34.345$. Period plotted against α	164
6-21	Behaviour of the upper branch of periodic solutions produced at Hopf bifurcation at $\alpha = 34.345$. Homoclinic orbit at $\alpha = 35.1745$	165
6-22	Eigenvalues of the linearization at the saddle-focus point at $\alpha = 35.1745$. a) Complete spectrum; b) Close-up of first three eigenvalues.	165
6-23	Approximation of the steady state attractor of Burgers' equation with $\nu = 1$. The L^2 error plotted against the number of high modes used by the NLG method.	172

6-24	The L^2 error of the approximation to the periodic behaviour of the reaction-diffusion equation with $\nu = 0.002$ at $T = 15$ for different mode sizes n . — Spectral Galerkin Method, NLG method, — — — Postprocessed Galerkin Method.	175
6-25	Efficiency diagram for the approximation of the periodic behaviour of the reaction-diffusion equation with $\nu = 0.002$ at $T = 15$. — Spectral Galerkin Method, NLG method, — — — Postprocessed Galerkin Method.	176
6-26	Coarse grid points (\times) and fine grid points (\times, \circ) on the interval $(0, \pi)$ for $N = 5$	178
6-27	Bifurcation diagram for the K-S equation for $0 \leq \alpha \leq 80$ using the PS method with $N = 12$	183
6-28	Bifurcation diagram for the K-S equation for $0 \leq \alpha \leq 80$ using Algorithm 2 with $N = 6$	183
6-29	Bifurcation diagram for the K-S equation for $0 \leq \alpha \leq 80$ using Algorithm 2 with $N = 9$	184
6-30	Periodic solutions produced by the Hopf bifurcation at $\alpha = 30.345$, computed using Algorithm 2 with $N = 9$	185
6-31	Heteroclinic orbit at $\alpha = 36.127$, computed using Algorithm 2 with $N = 9$	185

List of Tables

6.1	PS approximation to a steady state solution of the K-S equation with $\alpha = 40$ at $x = \pi/3$ and $x = 2\pi/3$, for varying sizes of the discretization parameter N	145
6.2	The period of the PS approximations to a periodic solution of the K-S equation which exists at $\alpha = 32.96$	146
6.3	Attracting states of the K-S equation and their bifurcations. . . .	151
6.4	First seven period doubling bifurcation points and the ratio of the successive subwindow lengths.	154

Chapter 1

Introduction

1.1 General introduction

Problems in dynamics have greatly interested mathematicians and scientists for many years. In the context of celestial mechanics, nonlinear dynamics has some claim to be one of the oldest scientific problems studied by man. In many cases systems involving dynamical problems can be modelled by differential equations. These equations are often simple in form, however they can be extremely difficult to study and indeed solve. For this reason progress in the area of nonlinear dynamics was slow to begin with, as work was restricted to obtaining analytical solutions of dynamical systems. Many great mathematicians were involved in this work, such as Newton, Leibniz, Euler, Gauss, Lagrange and Laplace.

However despite these great names, Henri Poincaré (1854-1912) is largely seen as the father of nonlinear dynamics. His approach to dynamical problems, introduced in the 1880's, was much more geometrical and he emphasised the importance of studying such problems qualitatively by looking at the global properties of the phase space of dynamical orbits. Poincaré's approach was a major breakthrough in the study of nonlinear dynamics and led to many new methods for exploring dynamical systems.

In the 1920's the foundations laid down by Poincaré's original work were strengthened analytically by Birkhoff, who also characterised the possibility of

complicated dynamics occurring for nonlinear equations. Also Van der Pol discovered the possibility of multiple terminal behaviour in a second-order ordinary differential equation which he was using to model an electric circuit. Other contributions came from Andronov and Liapunov who studied the structural stability of dynamical systems.

In the 1940's Cartwright and Littlewood gave a precise mathematical proof that Van der Pol's equation has a family of solutions which are *chaotic*. Roughly speaking, for a system to be chaotic it means that the distance between two nearby orbits may become arbitrarily large as time evolves. This is sometimes termed *sensitive dependence on initial conditions*. The discovery of chaotic behaviour in turn stimulated many talented mathematicians to study nonlinear dynamical systems.

The invention of digital computers in the 1940's also brought with it many advances in dynamical systems. Initially these computers were used only to obtain numerical solutions of differential equations which could not be solved analytically. However, they were later used to great effect by mathematicians such as von Neumann and Ulam as an interactive tool for discovering new dynamical properties by studying the interplay between computations and analysis.

Before the 1950's work in nonlinear dynamics was restricted to systems which modelled celestial and classical mechanics where energy is conserved, as these were the problems originally considered by Poincaré and Birkhoff. However as computers became more and more accessible to physical scientists and engineers, the period following the 1950's was particularly rich in new ideas and in the growing applications of these ideas to a wide range of disciplines, such as physics, chemistry, biology and economics.

One of the major area of interest was in the study of systems which are said to be *dissipative*. These systems have an evolving ensemble of states which occupy a region of the phase space whose volume decreases with time. Over the long term the volume concentration has a strong tendency to simplify the structure of orbits. A set in the phase space which the orbits of these equations enter after a finite time and remain thereafter is called an *absorbing set*. The existence of

absorbing sets is a step towards proving the existence of the *global attractor*, a set which all the orbits of the equation converge to and therefore contains all possible asymptotic dynamics. The attractor is also invariant for the flow of the equation, which means that any point in the system belongs to a complete orbit lying in the attractor.

Dissipative problems are frequently governed by partial differential equations (PDE's) and these equations can arise in the modelling of fluid dynamics and pattern formation problems. Examples are the Navier-Stokes equations which is used to model fluid flow, the Ginzburg-Landau equation which is used to model Taylor-Couette flow and super-conductivity and the Kuramoto-Sivashinsky equation which is used to model the Belousov-Zhabotinskii reaction which exhibits coherent, periodic oscillations in chemical reactions. Usually the systems which are modelled by dissipative PDE's exhibit turbulence, which has become a growing area of interest to many scientists and engineers in recent years. It was initially suggested by Ruelle and Takens that chaotic attractors of these equations are important objects in gaining some insight into turbulence.

In most cases it is not possible to obtain analytic solutions of dissipative PDE's. This has led to the numerical approximation of these equations where one finds an approximate solution of the PDE at a time t_1 or the approximate long-time (or asymptotic) solution. In order to capture essential global dynamical behaviour of dissipative PDE's by a numerical approximation, the dimension of the approximation has to be very large. The development of more powerful computers in terms of speed and memory capacity has lead to a deeper investigation of nonlinear dynamics of these equations by mathematicians and numerical analysts. Also much analysis has gone on to produce new numerical methods which model the dynamics of the underlying equations with a greater deal of accuracy. This is the case for numerical methods that have analogous properties as the original systems which they are approximating, such as dissipativity.

As well as the study of dissipative equation, the 1960's and 1970's saw many other important developments in the study of nonlinear dynamics. Lorenz, who studied a system of ordinary differential equations which models two-dimensional

convection in a horizontal layer of fluid heated from below, found that the solutions bifurcate to chaos and that homoclinic orbits exist. Illustrations of this behaviour can be seen, for example, in Drazin [15, Chapter 8]. The logistic map was developed by Sarkovskii as a one-dimensional model for population growth and has a great abundance of interesting dynamical behaviour. As well as numerical investigations of various dynamical systems, there were also many mathematical advances during this time. For example the analysis of the horseshoe map by Smale, which has an attractor made up of a complicated invariant set containing an infinite family of periodic and nonperiodic orbits. The existence of horseshoe maps can be used to prove the existence of chaotic dynamics for nonlinear differential equations. Mandelbrot studied fractal sets which are characterised by having different Hausdorff and topological dimensions. Also Sil'nikov proved some abstract results on orbits which are homoclinic to saddle-focus steady states.

In this thesis we are only concerned with the approximation of dissipative PDE's using numerical methods. In the 1980's there have been a number of theoretical results in this area which we will look at in detail next. There have also been advances on the computation side due to the introduction of more sophisticated computers.

Obviously predicting and understanding the dynamical behaviour of the global attractors of dissipative PDE's by numerical methods is a very important subject and due to the possibility of complicated behaviour it can become a very challenging problem. We note that the numerical approximation of a PDE will yield a finite-dimensional system. It is reasonable to question whether this finite-dimensional system will give a good representation of the true asymptotic dynamics of the PDE, given that the attractor may contain chaotic behaviour, as occurs for many dissipative PDE's. There have been two important theoretical advances in the study of dissipative PDE's which have helped answer this question.

The first advance is that many dissipative PDE's have been shown to have global attractors which have finite Hausdorff dimension, see Hale [37], Mallet-Paret [62] and Temam [87]. This implies that there are a finite number of parameters describing the configuration of the asymptotic dynamics. Hence although

the transient behaviour of the PDE may be infinite-dimensional, it is possible to justify the modelling of the asymptotic behaviour by a finite system.

The second advance in this area is that many dissipative PDE's have been shown to possess *inertial manifolds*. An inertial manifold is a finite-dimensional Lipschitz manifold which attracts all the orbits of the equation at an exponential rate and therefore contains the global attractor. Many equations have been shown to possess inertial manifolds, these include the Kuramoto-Sivashinsky equation see [8], [9], [22] and [24], the Cahn-Hilliard equation, see [8] and [69], the Ginzburg-Landau equation, see [14], several reaction-diffusion equations, see [8], [46],[65] and [63] and the Swift-Hohenberg equation, see [86]. The one notable exception is the Navier-Stokes equations. A necessary condition for inertial manifolds to exist is the existence of large gaps in the spectrum of the linear operator of the dissipative PDE. This is referred to as the *spectral gap condition*. Inertial manifolds are given by the graphs of Lipschitz functions which relate finite-dimensional sets of low frequency modes of the solutions of PDE's to a set of high frequency modes.

The existence of an inertial manifold implies that the PDE reduces to a finite-dimensional system called the *inertial form* in its asymptotic limit. Since the manifold is exponentially attracting, one can expect this reduction to occur in a relatively short time. We note that the inertial form of the PDE will have identical asymptotic dynamical behaviour to the original equation as the inertial manifold contains the global attractor. The existence of inertial manifolds has been a major breakthrough in the study of dissipative PDE's, which possess inertial manifolds, as it rigorously justifies that the asymptotic dynamics of these equations can be modelled by systems of ODE's.

The existence of inertial manifolds has lead to the introduction of a number of new numerical methods called *nonlinear Galerkin methods* which approximate the inertial form. This is so that one can obtain an approximation which is much closer to the system which describes the asymptotic dynamics. Unfortunately inertial manifolds have no explicit representation, so in order to construct nonlinear Galerkin methods, these manifolds have to be approximated. Many

nonlinear Galerkin methods have been introduced based on approximate inertial manifolds. These methods were first of all used with the spectral Galerkin method, see Debussche and Marion [10], Foias, Jolly, Kevrekidis, Sell and Titi [19], Foias, Manley and Temam [21], Jolly, Kevrekidis and Titi [47] and Temam [88]. However they have also been extended to other numerical approximation methods, see Frutos, García-Archilla and Novo [29], Gottlieb and Temam [35], Margolin and Jones [64], Marion and Xu [66], Temam [89] and Wallace and Sloan [94]. It has been shown, as one would expect, that these methods are much more accurate than existing approximation methods. However, from a practical point of view, it is not clear at present whether nonlinear Galerkin methods offer a viable alternative to the existing methods. For many model problems it has been shown that the additional accuracy of these methods is far outweighed by the extra computational cost of solving the nonlinear Galerkin method on an approximate inertial manifold, see García-Archilla and Frutos [31].

Having discussed objects which contain the global asymptotic dynamical behaviour of dissipative PDE's, we now turn our attention to their approximation by numerical methods. First of all, we note that there are two types of convergence associated with attractors for the approximation and the attractor for the true equation. These are *upper semi-continuity* and *lower semi-continuity*. Roughly speaking upper semi-continuity means that in the limit (as the discretization parameter tends to zero) the approximate attractor is contained in the true attractor, whereas lower semi-continuity means that in the limit the true attractor is contained in the approximate attractor. These two results together give set convergence in the Hausdorff metric. Upper semi-continuity results have been shown for many different numerical approximation schemes, see Elliott and Larson [18], Hale, Lin and Raugel, [38], Hill and Süli [40], Lord and Stuart [61] and the references therein. However, on its own, upper semi-continuity does not tell us, in a strong sense, whether the approximate attractor captures the essential dynamical behaviour contained in the true global attractor. Although proving upper semi-continuity results is nontrivial, in general it is much easier than proving lower semi-continuity results. Nevertheless, lower semi-continuity results have

only been shown for attractors which have certain types of structure, such as being made up of a union of unstable manifolds, see Stuart and Humphries [85] for details.

In Jones and Stuart [51] it is shown that under certain conditions a numerical approximation of a PDE can be shown to possess an inertial manifold, which is both upper and lower semi-continuous under numerical approximation. This result is shown for the spectral Galerkin and a finite-element method and implies that the inertial forms of the PDE and its numerical approximation are close. This is an important step towards establishing a good relationship between the dynamics of a PDE and its approximation. In Jones, Stuart and Titi [52] the theory in [51] is extended to numerical schemes which approximate dissipative equations, with inertial manifolds, on bounded sets in the C^1 norm. The essential improvement here is that the distance between the inertial forms for the approximation and the true inertial form can be made arbitrarily small in the C^1 norm. Since the inertial forms are finite-dimensional it is possible to apply results from standard finite-dimensional dynamical systems theory concerning the C^1 perturbations. The sort of results that can be applied are those which involve the persistence of bounded invariant sets of the perturbation or approximation. In particular these bounded invariant sets include hyperbolic steady states (and their stable and unstable manifolds) and periodic orbits. Results of this type can be found in texts such as Hirsch and Smale [41], Hirsch, Pugh and Shub [42] and Pliss and Sell [76].

The results of [52] show that if a numerical method approximates the solution of a dissipative equation which possesses an inertial manifold in a C^1 sense, then realistic deductions can be made about the relationships between the true and approximate flows on the attractor. This is because understanding the invariant manifolds of equations is an important step towards understanding how the asymptotic dynamics behave. Hence any insight into how the invariant manifolds of the approximation and its underlying equation are related is useful.

1.2 Aims of the thesis

The aim of this thesis is to carry out a detailed theoretical and computational study of the long-time dynamical behaviour of the one-dimensional Kuramoto-Sivashinsky (K-S) equation using the pseudospectral method. The K-S equation is a fourth order dissipative PDE which arises in pattern formation and interfacial turbulence in various physical contexts, see Hyman and Nicolaenko [43] and Kuramoto [56] for details. The K-S equation has also been shown to possess a finite-dimensional global attractor and an inertial manifold. These results are shown in Nicolaenko, Scheurer and Temam [68] and Foias, Nicolaenko, Sell and Temam [22] respectively. It is for these two reasons that, in recent years, the K-S equation has been extensively used as a model for studying long-time dynamical behaviour of dissipative equations under numerical approximation, both theoretically and computationally. In this thesis we only consider the K-S equation with odd initial data and periodic boundary conditions. The reason for this is that the K-S equation was originally shown to possess an inertial manifold under these conditions and most of the important theoretical results have only been shown to hold for this case. However the K-S equation has also been shown to possess an inertial manifold for general unsymmetric initial data and periodic boundary conditions in Wang and Temam [90], but we will not consider this case.

We have used the Fourier pseudospectral approximation for the K-S equation introduced in the paper Wallace and Sloan [94]. This method has been chosen due to its high accuracy, which is essential when computing complicated long-time dynamics. The method is generally easier to implement than the standard spectral Galerkin method when considering equations which possess complicated nonlinearities. We are also motivated by the fact that the pseudospectral method has been used extensively in many recent computational studies of the K-S equation and other dissipative equations. Since we are primarily interested in the spatial discretization of the K-S equation using the pseudospectral method, we concentrate theoretically on a semi-discrete approximation. However for practical purposes we also briefly consider a fully-discrete approximation using the

Crank-Nicolson method for the time integration.

For the pseudospectral discretization our aim is to prove high order convergence results for attractors and inertial manifolds of the approximation by exploiting the regularity of the solutions of the K-S equation and its pseudospectral approximation. One of the main results which we use is that the solutions of the K-S equation are in a Gevrey class, which implies that they are real and analytic. It is possible to show that other dissipative equations have solutions in a Gevrey class. These include the Ginzburg-Landau equation, see Duan, Titi and Holmes [16], the Cahn-Hilliard equation, see Promislow [77], reaction-diffusion equations with polynomial nonlinearity, see also [77] and the Navier-Stokes equation in space dimensions 2 and 3, see Foias and Temam [26], see also Liu [59]. We note that all the above results only hold for periodic boundary conditions. The idea of using Gevrey regularity of the solution and the approximation to prove convergence of attractors was first used in Lord and Stuart [61] for a finite difference approximation to the Ginzburg-Landau equation.

1.3 Thesis outline

Below we outline the contents of this thesis. We begin Chapter 2 by introducing some important mathematical function spaces and in particular Sobolev spaces. We then state some results, mainly from Adams [1], involving these spaces, such as the Gagliardo-Nirenberg Theorem. In Section 2.2 we state the definitions for sectorial operators, their fractional powers and analytic semigroups. We then state some results involving the existence, uniqueness and regularity of the solutions of evolution equations from Henry [39]. We also introduce the concept of Gevrey regularity and state some properties of Gevrey spaces. In Section 2.3 the K-S equation and its derivative form are introduced with periodic boundary conditions and odd initial data on the interval $(-L/2, L/2)$, where L is an arbitrary parameter. We consider the derivative form of the K-S equation in this thesis and for convenience this equation is rescaled onto the interval $(-\pi, \pi)$. This procedure gives rise to an equation involving a real parameter $\alpha = (L/\pi)^2$. In Section 2.4

we formulate this equation into the form of an evolution equation. We apply the results from Section 2.2 to this equation to prove existence and regularity of its solutions. Finally we show that the solutions of the K-S equation are contained in a Gevrey class, a result which follows from Liu [58].

We begin Chapter 3 by introducing the semi-discrete pseudospectral approximation which we consider in this thesis. Prior to the discretization we write the nonlinearity of the K-S equation in an equivalent form. This gives rise to a slightly different approximation from previous ones considered. However in the paper by Wallace and Sloan [94] it is pointed out that the dissipative properties of the K-S equation are likely to carry over to this approximation. A mathematical setting is given for the semi-discrete approximation and we also define relevant discrete Sobolev spaces. We then state a stability result for the approximation in the discrete L^2 space which was given in Wallace and Sloan [94]. This result depends upon an assumption which has so far only been verified numerically. We conclude this section with some useful discrete Sobolev inequalities.

In Section 3.2 we prove some convergence results for the solutions of the approximations in the discrete L^2 and H^1 norms. These results essentially follow a proof by López-Marcos [60], who also considered a pseudospectral discretization for the K-S equation with periodic boundary conditions. However, we have managed to eliminate the unnecessary assumptions for convergence result given in this paper, due to the way we have split the nonlinearity. In the paper [60] it is assumed that the approximation is bounded in the L^∞ norm.

We begin Section 3.3 by proving some bounds on the nonlinear terms of the semi-discrete approximation. This enables us to prove that the solutions of the semi-discrete approximation are contained in a Gevrey class for a small interval of time. The method of proof follows that of Liu [58].

In Section 3.4 we prove a convergence result for a fully-discrete approximation scheme for the K-S equation which uses the Crank-Nicolson method for the temporal discretization. This fully-discrete approximation was used in [94]; however no convergence result was proved in this paper. In order to obtain this result we first of all prove convergence for a similar fully-discrete approximation which is

related to the Crank-Nicolson approximation. We then use this result to prove a corresponding result for the approximation involving the Crank-Nicolson method.

In Chapter 4 we consider how well our semi-discrete method approximates the asymptotic dynamical behaviour of the K-S equation. We begin Section 4.1 by stating some standard definitions from dynamical systems theory, given in Temam [87]. We then give formal definitions of global attracting sets for dissipative equations and state some results concerning these sets. In Section 4.2 we state some known results involving the absorbing sets and the global attractor for the K-S equation. We also give an upper bound on the Hausdorff dimension of the global attractor in the H^1 space, which was obtained in Nicolaenko, Scheurer and Temam [68].

In Section 4.3 we briefly discuss the concept of upper semi-continuity and lower semi-continuity and illustrate, using a simple example, why lower semi-continuity does not always follow. We then outline the general theory from Hale, Lin and Rangel [38] for proving upper semi-continuity of approximation methods. In Section 4.4 we prove an upper semi-continuity result for our semi-discrete pseudospectral approximation. Usually these sort of results involve rough initial data error estimates and can be difficult to prove. We have simplified this approach by using the property that the equation and its approximation have solutions in a Gevrey class even for rough initial data. This approach was first introduced in Lord and Stuart [61]. We have improved the generality of this approach by removing the requirement of high order stability bounds for the approximation, which are required in [61].

In Section 4.5 we change tack slightly by outlining some general theory involving homoclinic orbits about steady state points of saddle-focus type from Glendinning and Sparrow [33]. In this paper it is shown that a system which has these type homoclinic orbits will produce chaotic behaviour under certain conditions. This theory is essential when we carry out a dynamical study of the K-S equation using the pseudospectral approximation later in the thesis.

In Chapter 5 we consider inertial manifolds for dissipative PDE's. We begin by giving a formal definition of an inertial manifold and briefly discuss a number of

methods used to prove the existence of these manifolds. In Section 5.2 we outline the existence and approximation theory from the paper by Jones, Stuart and Titi [52]. The work in this paper is a step towards building a general framework for proving the existence of inertial manifolds for numerical approximation and their convergence to the true inertial manifold of the underlying equation. In this theory, the variation of constants approach is used to replace differential equations by discrete time maps. The results are then proved for these maps and are shown to carry over to the continuous equation. The approximation theory in this paper requires that the numerical approximation is C^1 close to the solution of the original equation.

In Section 5.3 we prove the existence of a C^1 inertial manifold for the K-S equation with periodic boundary conditions, using the theory in [52]. In order to apply the approximation theory we prove a convergence result, similar to the one in Section 3.2, for the Fréchet derivative of the solutions of the K-S equation and its pseudospectral approximation. In Section 5.4 we use our error estimates for the solution and the Fréchet derivative to verify the conditions of the approximation theory in [52] and prove the persistence of bounded invariant sets of the K-S equation under our semi-discrete approximation. If we assume sufficient regularity of the initial data of the K-S equation, this gives a high order of convergence of these sets. This is a new result and was not considered in [52].

In Section 6.1, we carry out a detailed examination of the asymptotic dynamics of the K-S equation using the pseudospectral method. This first of all involves determining a maximum value for the discretization parameter h , in order to capture the essential dynamics in a fixed parameter range. The range which we consider is $0 \leq \alpha \leq 40$ due to the abundance of bifurcation phenomena in this interval. Having done this we use AUTO 97, which is a FORTRAN continuation and bifurcation software package for ODE's, to compute steady and periodic states for the K-S equation. We then carry out an extensive study of periodic orbits which are produced at a supercritical Hopf bifurcation in the parameter range under consideration. This reveals the existence of a Feigenbaum period doubling cascade and homoclinic orbits of the Sil'nikov type which we

described in Section 4.5. The formation of these orbits is likely to give rise to the chaotic behaviour in the original K-S equation. In our computational study we also reveal the existence of a heteroclinic orbit connecting two saddle-focus steady states. As far as we are aware this orbit has not previously been observed.

In Section 6.2 we briefly introduce approximate inertial manifolds and illustrate how they can be used to compute asymptotic behaviour of dissipative PDE's by nonlinear Galerkin methods. We illustrate the main disadvantage of nonlinear Galerkin methods, which is that they are not as computationally efficient as existing approximation methods. We also discuss a new type of method in this field which uses approximate inertial manifolds called *postprocessed* nonlinear Galerkin methods. These methods achieve much of the extra accuracy of nonlinear Galerkin methods at a single point on the orbit, but have the computational cost of standard methods.

Finally in Section 6.3 we consider a nonlinear Galerkin method for fully-discrete approximation which involves the Crank-Nicolson method. This method was introduced by Wallace and Sloan in [94]. Here one replaces the Lipschitz mapping relating high and low Fourier modes with a multi-grid method relating coarse and fine grid interactions. We illustrate some of numerical results from their work using FORTRAN and AUTO 97.

Chapter 2

The Continuous Problem

2.1 Domains and function spaces

We begin by introducing some basic notation. Let $\mathbf{x} = (x_1, x_2, \dots, x_n)$ be a point in the space \mathbb{R}^n , $n \in \mathbb{N}$, and define

$$D_i^\alpha = \frac{\partial^\alpha}{\partial x_i}, \quad 1 \leq i \leq n \text{ and } \alpha \in \mathbb{N} \cup \{0\},$$

and for the multi-index $\alpha = \{\alpha_1, \dots, \alpha_n\} \in [\mathbb{N} \cup \{0\}]^n$, D^α will be the differentiation operator

$$D^\alpha = D_1^{\alpha_1} \cdots D_n^{\alpha_n} = \frac{\partial^{|\alpha|}}{\partial x_1^{\alpha_1} \cdots \partial x_n^{\alpha_n}},$$

where

$$|\alpha| = \alpha_1 + \cdots + \alpha_n.$$

If $\alpha_i = 0$ for some i , then $D_i^{\alpha_i}$ is the identity operator and in particular if $|\alpha| = 0$, then the entire operator D^α is the identity.

We let Ω be an open set of \mathbb{R}^n , with boundary $\partial\Omega$, and denote by $C(\Omega)$ and $C^k(\Omega)$, $k \in \mathbb{N}$, the space of real valued continuous functions on Ω and the space of k times continuously differentiable functions on Ω respectively. The space

$C^\infty(\Omega)$ is the space of real valued infinitely differentiable functions on Ω . The spaces $C_0(\Omega)$ and $C_0^k(\Omega)$, $k \in \mathbb{N}$ or $k = \infty$, denote the subspaces of $C(\Omega)$ and $C^k(\Omega)$ respectively, that consist of those functions which have compact support in Ω .

For $1 \leq p < \infty$, $L^p(\Omega)$ is the space of all measurable real valued functions on Ω , which are p^{th} order integrable. These spaces are Banach spaces with norm defined by

$$\|u\|_{L^p} = \left\{ \int_{\Omega} |u(\mathbf{x})|^p d\mathbf{x} \right\}^{1/p}.$$

For $p = \infty$, $L^\infty(\Omega)$ is the space of all measurable real valued functions on Ω , such that

$$\|u\|_{L^\infty} := \text{ess sup}_{\mathbf{x} \in \Omega} |u(\mathbf{x})| < \infty.$$

If \mathcal{X} is a Banach space, $k \in \mathbb{N}$ and $-\infty \leq a < b \leq \infty$, then we denote by $C([a, b]; \mathcal{X})$ the space of continuous functions from $[a, b]$ into \mathcal{X} and by $C^k([a, b]; \mathcal{X})$ the space of k times continuously differentiable functions from $[a, b]$ into \mathcal{X} . These are Banach spaces with norms

$$\begin{aligned} \|u\|_{C([a, b]; \mathcal{X})} &= \sup_{t \in [a, b]} \|u(t)\|_{\mathcal{X}}, \\ \|u\|_{C^k([a, b]; \mathcal{X})} &= \sum_{j=0}^k \left\| \frac{d^j u}{dt^j} \right\|_{C([a, b]; \mathcal{X})}, \end{aligned}$$

respectively.

Next we introduce Sobolev spaces.

Definition 2.1.1 We define $\mathcal{D}(\Omega)$ to be the space $C_0^\infty(\Omega)$ with the topology given by the following definition of convergence. The sequence $\{\phi_j\}_{j=1}^\infty$, $\phi_j \in C_0^\infty(\Omega)$, converges to $\phi \in C_0^\infty(\Omega)$ if

- (i) there exists a compact subset $K \subset \Omega$ such that, for each j , $\phi_j = 0$ in $\Omega \setminus K$;
- (ii) for every multi-index α , the sequence $\{D^\alpha \phi_j\}$ converges to $D^\alpha \phi$ uniformly

on K , as $j \rightarrow \infty$.

Definition 2.1.2 *The space of distributions $\mathcal{D}'(\Omega)$, is the space of continuous linear functionals on $\mathcal{D}(\Omega)$.*

Definition 2.1.3 *For $p \in [1, \infty)$ and $m \in \mathbb{N} \cup \{0\}$, the Sobolev space $W^{m,p}(\Omega)$ is the space of functions $u \in \mathcal{D}'(\Omega)$ with finite norms given by*

$$\|u\|_{W^{m,p}} = \left\{ \int_{\Omega} \sum_{|\alpha| \leq m} |D^{\alpha} u|^p d\mathbf{x} \right\}^{1/p},$$

where $\mathbf{x} \in \mathbb{R}^n$.

For $m = 0$ the spaces $W^{0,p}(\Omega)$ are the $L^p(\Omega)$ spaces we introduced earlier.

Definition 2.1.4 *We denote by $H^m(\Omega)$ the Hilbert space whose inner product is determined by the norm of $W^{m,2}(\Omega)$ for $m \in \mathbb{N} \cup \{0\}$. We write $H(\Omega)$ for $H^0(\Omega)$.*

The space $H_0^m(\Omega)$, $m \in \mathbb{N} \cup \{0\}$, is defined to be the completion in the norm $\|\cdot\|_{H^m}$ of $C_0^\infty(\Omega)$. Poincaré's inequality, see Adams [1], states that

$$\|u\|_{L^2} \leq c(\Omega) \|Du\|_{L^2}, \quad u \in H_0^1(\Omega),$$

and by induction, for any $m \in \mathbb{N} \cup \{0\}$,

$$\|u\|_{L^2} \leq [c(\Omega)]^m \|D^m u\|_{L^2}, \quad u \in H_0^m(\Omega).$$

This implies that the space $H_0^m(\Omega)$ is a Hilbert space with norm

$$\|u\|_{H_0^m} = \|D^m u\|_{L^2},$$

which is equivalent to the norm induced by the space $H^m(\Omega)$.

The space $H_{per}^m(\Omega)$, $m \in \mathbb{N} \cup \{0\}$, denotes the subspace of the Hilbert space $H^m(\Omega)$ consisting of functions which, along with their derivatives up to order

$m - 1$, are periodic. The norm induced on the space $H_{per}^m(\Omega)$ is equivalent to the norm on the space $H^m(\Omega)$.

We denote by $\dot{H}^m(\Omega)$, $m \in \mathbb{N} \cup \{0\}$, the subspace of $H^m(\Omega)$ consisting of functions which have the following property

$$\int_{\Omega} u(x) dx = 0. \quad (2.1.1)$$

This corresponds to the solutions having zero average. As with the $H_0^m(\Omega)$ spaces we can apply Poincaré's inequality, so that $\dot{H}_{per}^m(\Omega)$ is a Hilbert space with norm

$$\|u\|_{\dot{H}_{per}^m} = \|D^m u\|_{L^2},$$

which is equivalent to the norm induced by the space $H^m(\Omega)$.

We now state some useful imbeddings and results involving the spaces we have defined above.

Theorem 2.1.5 (Rellich-Kondrachov)

Let Ω be a bounded domain in \mathbb{R}^n with boundary $\partial\Omega$ of class C^1 ; then the following imbeddings are compact

$$W^{m,p}(\Omega) \subset W^{k,p}(\Omega), \quad \text{for } m > k \geq 0 \text{ and } p \in [1, \infty), \quad (2.1.2)$$

$$W^{m,p}(\Omega) \subset C^\nu(\bar{\Omega}), \quad \text{if } mp > n \geq (m-1)p, \quad (2.1.3)$$

and $0 \leq \nu < m - n/p$, for $m \in \mathbb{N}$.

Proof: See Adams [1, Theorem 6.2, p.144].

□

Theorem 2.1.6 (Nirenberg-Gagliardo)

If Ω is a bounded domain in \mathbb{R}^n with boundary $\partial\Omega$ of class C^1 and let $u \in W^{m,q}(\Omega) \cap L^r(\Omega)$ where $1 \leq q, r < \infty$ and $m \in \mathbb{N} \cup \{0\}$. Then for any $k \in \mathbb{N} \cup \{0\}$ the following inequality holds

$$\|u\|_{W^{k,p}} \leq c(\Omega) \|u\|_{W^{m,q}}^\theta \|u\|_{L^r}^{1-\theta},$$

if $k - n/p \leq \theta(m - n/q) - n(1 - \theta)/r$, (with strict inequality if q or r is 1,) $1 \leq p < \infty$ and $k/m \leq \theta \leq 1$.

Proof: See Nirenberg [70].

□

Theorem 2.1.7 *Let Ω be a bounded domain in \mathbb{R}^n with smooth boundary $\partial\Omega$ of class C^m , and $mp > n$; then there exists a constant c depending on m, p, n and the domain Ω such that for all $u, v \in W^{m,p}(\Omega)$ the product uv , defined pointwise a.e. in Ω , belongs to $W^{m,p}(\Omega)$ and satisfies*

$$\|uv\|_{W^{m,p}} \leq c(\Omega)\|u\|_{W^{m,p}}\|v\|_{W^{m,p}}.$$

Proof: See [1, Theorem 5.23, p.115].

□

We conclude this section with the definition of differentiability of functions defined on Banach spaces.

Definition 2.1.8 *Let \mathcal{X} and \mathcal{Y} be Banach spaces. The map $f : \mathcal{X} \rightarrow \mathcal{Y}$ is **Fréchet differentiable** at a point $u_0 \in \mathcal{X}$ if there exists a continuous linear map $Df(u_0) : \mathcal{X} \rightarrow \mathcal{Y}$ such that*

$$\|f(u) - f(u_0) - Df(u_0)(u - u_0)\|_{\mathcal{Y}} = o(\|u - u_0\|_{\mathcal{X}}), \quad \text{as } u \rightarrow u_0.$$

The map f is continuously differentiable on an open set $U \subset \mathcal{X}$ if it is differentiable at each point of U and if $u \rightarrow Df(u) : U \rightarrow \mathcal{L}(\mathcal{X}, \mathcal{Y})$ is continuous.

2.2 Sectorial operators and analytic semigroups

When we consider existence and regularity of solutions of equations in Banach spaces, knowledge of sectorial operators and consequently analytic semigroups is required. We also need to consider fractional powers of sectorial operators and their domains. We begin, therefore, by stating some standard definitions and

theorems on semigroup theory from Henry [39] and Pazy [75]. We will assume that we are working in a Banach space \mathcal{X} with inner product $\langle \cdot, \cdot \rangle_{\mathcal{X}}$ and norm $\|\cdot\|_{\mathcal{X}}^2 = \langle \cdot, \cdot \rangle_{\mathcal{X}}$.

Definition 2.2.1 *If A is a linear operator on the Banach space \mathcal{X} , then $\lambda \in \mathbb{C}$ is said to be an **eigenvalue** of A if and only if there exists $\omega \in \mathcal{X} \setminus \{0\}$ such that*

$$A\omega = \lambda\omega,$$

*where ω is termed the **eigenfunction** of A corresponding to λ .*

Definition 2.2.2 *If A is a linear operator on the space \mathcal{X} , then the **resolvent set** of A , $\rho(A)$, is defined to be the set of all complex numbers $\lambda \in \mathbb{C}$ such that $(\lambda I - A)^{-1}$ exists, and we refer to the operator $R(\lambda : A) := (\lambda I - A)^{-1}$, for $\lambda \in \rho(A)$, as the **resolvent** of A . The **spectrum** of A , $\sigma(A)$, is defined by $\sigma(A) := \mathbb{C} \setminus \rho(A)$.*

Definition 2.2.3 *The linear operator A on the space \mathcal{X} , is said to be **sectorial** if*

- (i) *A is closed; i.e., if $\{x_n\} \in D(A)$, $x_n \rightarrow x$ and $Ax_n \rightarrow y$, then $x \in D(A)$ and $Ax=y$;*
- (ii) *A is densely defined; i.e., the closure in \mathcal{X} of $D(A)$ is the entire space \mathcal{X} ;*
- (iii) *there exists $\phi \in (0, \pi/2)$, $M \geq 1$ and $a \in \mathbb{C}$ such that*

$$\rho(A) \subseteq \Sigma_{a,\phi} = \{\lambda \in \mathbb{C} : \phi < |\arg(\lambda - a)| \leq \pi, \lambda \neq a\},$$

and

$$\|R(\lambda : A)\|_{\mathcal{X}} \leq \frac{M}{|a - \lambda|}, \quad \lambda \in \Sigma_{a,\phi}. \quad (2.2.1)$$

An operator is therefore sectorial if it has no residual spectrum and its point spectrum lies in a sector of the complex plane which contains a subset of the positive real axis. An illustration of this can be seen in Figure 2-1.

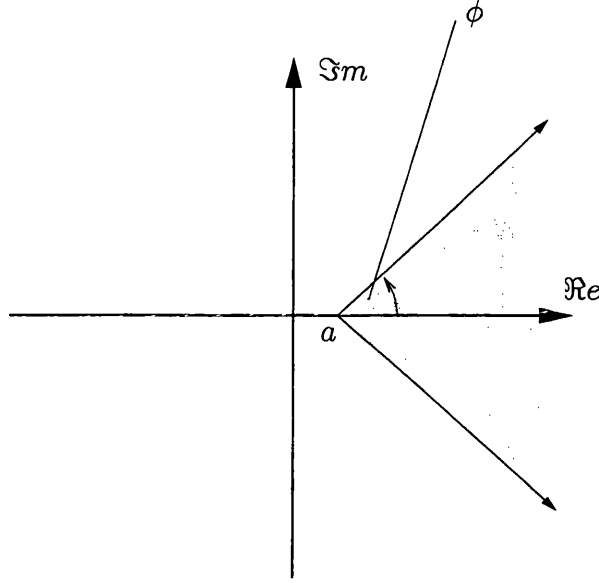


Figure 2-1: Graphical representation of the sector of the complex plane where $\sigma(A)$ must lie for an operator A to be sectorial for a given ϕ and a .

Definition 2.2.4 *An analytic semigroup on the space \mathcal{X} is the family of continuous linear operators on \mathcal{X} , $\{T(t)\}_{t \geq 0}$, satisfying*

- (i) $T(0) = I$ and $T(t)T(s) = T(t+s)$, for $t, s \geq 0$;
- (ii) $T(t)x \rightarrow x$ as $t \rightarrow 0^+$ for each $x \in \mathcal{X}$;
- (iii) $t \rightarrow T(t)x$ is real analytic on $0 < t < \infty$ for each $x \in \mathcal{X}$.

The linear operator $-A$ defined by

$$-Ax = \lim_{z \rightarrow 0^+} \frac{T(z)x - x}{z}, \quad x \in D(A),$$

where

$$D(A) = \{x \in \mathcal{X} : \lim_{z \rightarrow 0^+} \frac{T(z)x - x}{z} \text{ exists}\},$$

and is said to be the *infinitesimal generator* of the semigroup $T(z)$. Sectorial operators and analytic semigroups are linked by the following theorem.

Theorem 2.2.5 *The operator A is sectorial if and only if $-A$ is the infinitesimal*

generator of an analytic semigroup, e^{-At} , defined by the integral

$$e^{-At} = \frac{1}{2\pi i} \int_{\Gamma} (\lambda I + A)^{-1} e^{\lambda t} d\lambda,$$

where Γ is the contour in $\rho(-A)$ with $\arg \lambda \rightarrow \pm\theta$ as $|\lambda| \rightarrow \infty$ for some $\theta \in (\pi/2, \pi)$.

Proof: See [39, Theorem 1.3.4, p.20].

□

We now define fractional powers of sectorial operators.

Definition 2.2.6 Let A be a sectorial operator on the space \mathcal{X} and $\Re\{\sigma(A)\} > 0$. Then for any $\alpha > 0$ we define $A^{-\alpha}$ by

$$A^{-\alpha} := \frac{1}{\Gamma(\alpha)} \int_0^{\infty} t^{\alpha-1} e^{-At} dt,$$

and we define A^{α} , for all $\alpha > 0$, by

$$A^{\alpha} = (A^{-\alpha})^{-1}.$$

For $\alpha = 0$, A^{α} is the identity on \mathcal{X} .

Definition 2.2.7 If A is a sectorial operator on the space \mathcal{X} , then for each $\alpha \geq 0$ we define

$$\mathcal{X}^{\alpha} = D(A^{\alpha}) = \{u \in \mathcal{X} : \|A^{\alpha}u\|_{\mathcal{X}} < \infty\},$$

with associated norm $\|\cdot\|_{\mathcal{X}^{\alpha}}$ given by

$$\|\cdot\|_{\mathcal{X}^{\alpha}} := \|A^{\alpha} \cdot\|_{\mathcal{X}}.$$

Theorem 2.2.8 Let A be a sectorial operator on the space \mathcal{X} . Then \mathcal{X}^{α} is a Banach space with norm $\|\cdot\|_{\mathcal{X}^{\alpha}}$ and for $\alpha \geq \beta \geq 0$, \mathcal{X}^{α} is a dense subspace of \mathcal{X}^{β} with continuous inclusion. Furthermore if A has compact resolvent, then the inclusion $\mathcal{X}^{\alpha} \subset \mathcal{X}^{\beta}$ is compact.

Proof: See [39, Theorem 1.4.8, p.29].

□

Sectorial operators can be shown to have smoothing properties.

Theorem 2.2.9 *Let $-A$ be the infinitesimal generator of an analytic semigroup e^{-At} . If $0 \in \rho(A)$ then*

(i) $e^{-At} : \mathcal{X} \rightarrow D(A^\alpha)$ for every $t > 0$ and $\alpha \geq 0$;

(ii) for every $x \in D(A^\alpha)$ and $t > 0$ and $\alpha \geq 0$,

$$e^{-At} A^\alpha x = A^\alpha e^{-At} x;$$

(iii) if $\Re\{\sigma(A)\} > \delta > 0$ then, for any $\alpha > 0$ there exists $M = M(\alpha) < \infty$ such that

$$\|A^\alpha e^{-At}\|_{\mathcal{X}} \leq M t^{-\alpha} e^{-\delta t} \quad \forall t > 0;$$

(iv) for $0 < \alpha \leq 1$ and $x \in D(A^\alpha)$,

$$\|(e^{-At} - I)x\|_{\mathcal{X}} \leq C t^\alpha \|A^\alpha x\|_{\mathcal{X}}.$$

Proof: See [75, Theorem 2.6.13, p.74].

□

Let us now consider the evolution equation which has the following abstract form

$$\begin{aligned} \frac{du}{dt} + Au + R(u) &= 0, \\ u_0 &= u(0), \end{aligned} \tag{2.2.2}$$

in the space \mathcal{X} , say, where A is sectorial and R is some nonlinear function of u . We will now state some important results from Henry [39] which involve equations of this form and we begin by giving the definition of a solution of this equation.

Definition 2.2.10 (Hale [37])

A **solution** of (2.2.2) on $[0, \tau)$ is a continuous function $u : [0, \tau) \rightarrow \mathcal{X}^\alpha$, $\alpha \geq 0$, with the following properties

- (i) $u(0) = u_0$;
- (ii) $R(u(\cdot)) : [0, \tau) \rightarrow \mathcal{X}$ is continuous;
- (iii) $u(t) \in D(A)$ for $t \in (0, \tau)$;
- (iv) u satisfies (2.2.2) on $(0, \tau)$.

Lemma 2.2.11 *If $u(t)$ is a solution of (2.2.2) on $[0, \tau)$, then*

$$u(t) = e^{-At}u_0 - \int_0^t e^{-A(t-s)}R(u(s))ds, \quad 0 < t < \tau. \quad (2.2.3)$$

Proof: See [39, Lemma 3.3.2, p.53].

□

Theorem 2.2.12 *Assume A is a sectorial operator, $0 \leq \alpha < 1$, and $R : U \rightarrow \mathcal{X}$, U is an open set of \mathcal{X}^α , $R(u)$ is locally Lipschitzian in u ; then for any $u_0 \in U$ there exists $\tau = \tau(u_0) > 0$ such that (2.2.2) has a unique solution $u(t)$ on $(0, \tau)$ with initial condition $u(0) = u_0$.*

Proof: See [39, Theorem 3.3.3, p.54].

□

It is possible to generalise this theorem for fractional power spaces with $\alpha \geq 1$ by the following theorem.

Theorem 2.2.13 *Suppose A is sectorial on $\mathcal{X}^{s+\alpha}$ and $R : \mathcal{X}^{s+\alpha} \rightarrow \mathcal{X}^s$ is Lipschitz in a neighbourhood of u_0 for some $s \geq 0$ and $0 \leq \alpha < 1$. If $u_0 \in \mathcal{X}^{s+\alpha}$ then there exists a unique solution $u(t) = u(t; u_0)$ of (2.2.2), on some interval $(0, \tau)$ and $t \rightarrow u(t) \in \mathcal{X}^{s+\alpha}$ is continuous.*

Proof: See [39, Exercise 1, p.73].

□

The last theorem shows the existence of a semigroup $T(t) : \mathcal{X}^{s+\alpha} \rightarrow \mathcal{X}^{s+\alpha}$ for equation (2.2.2), such that $u(t) = T(t)u_0$ for $t \in [0, \tau]$. The next result from [39] concerns the regularity of this semigroup.

Theorem 2.2.14 *Suppose that A is a sectorial operator in the Hilbert space $\mathcal{X}^{s+\alpha}$, $0 \leq \alpha < 1$, U an open set in $\mathcal{X}^{s+\alpha}$ and $R : U \rightarrow \mathcal{X}^s$ is C^1 with derivative continuous on U . Also for $u_0 \in U$, let $u(t)$ be the maximally defined solution of (2.2.2). Then the semigroup $T(t)$ is $C^1(\mathcal{X}^{s+\alpha}, \mathcal{X}^{s+\alpha})$ for each $t > 0$ on its interval of existence. Furthermore, the derivative with respect to initial data is $v(t) = DT(t, u_0)$, see Definition 2.1.8, which is the solution of*

$$\begin{aligned} \frac{dv}{dt} + Av + DR(u)v &= 0, \\ v(0) &= I. \end{aligned}$$

Proof: See [39, Theorem 3.4.4, p.64]. Let us consider the proof for a short time interval, say $[0, \tau]$. The solution $u(t)$ is obtained as the fixed point of the map $S \in C([0, \tau]; \mathcal{X}^{s+\alpha})$ defined by

$$S(u(t)) = e^{-At}u_0 - \int_0^t e^{-A(t-s)}R(u(s))ds, \quad 0 \leq t \leq \tau.$$

This map is a contraction mapping in a small neighbourhood of u_0 and since S is the composition map of R with the analytic map $e^{-At}u_0$ it is continuously differentiable. Given these two properties, it can be shown that the fixed point of S is continuously differentiable for all $t \in [0, \tau]$, see [39, Section 1.2.6, p.12].

□

This theorem implies that for $\mu_0 \in \mathcal{X}^{s+\alpha}$, $\mu(t) := DT(t, u_0)\mu_0$ is the solution of

$$\begin{aligned} \frac{d\mu}{dt} + A\mu + DR(u)\mu &= 0, \quad 0 < t \leq \tau, \\ \mu(0) &= \mu_0, \end{aligned}$$

for some $\tau > 0$.

Fractional powers of sectorial operators are also useful when we need to define certain function spaces such as Sobolev spaces. Let us suppose that $u \in L^2(\Omega)$, where Ω is a bounded domain in \mathbb{R}^n . Suppose also that we have a linear self-adjoint operator A defined on $L^2(\Omega)$ with eigenvalues $\{\lambda_k\}_{k=1}^\infty$ and corresponding eigenvectors $\{\omega_k\}_{k=1}^\infty$, which form a complete orthonormal basis for $L^2(\Omega)$. This implies that u can be expressed by the following Fourier expansion

$$u = \sum_{k=1}^{\infty} a_k \omega_k, \quad a_k = \langle u, \omega_k \rangle_{L^2}.$$

The space \mathcal{X}^α , $\alpha \geq 0$, is then a Sobolev space with norm

$$\|u\|_{\mathcal{X}^\alpha}^2 := \|A^\alpha u\|_{L^2}^2 = \sum_{k=1}^{\infty} \lambda_k^{2\alpha} |a_k|^2.$$

The powers of linear operators can also be used to define an important class of spaces.

Definition 2.2.15 *Let $u \in L^2(\Omega)$ have the Fourier expansion*

$$u = \sum_{k=1}^{\infty} a_k \omega_k.$$

Then we define the Gevrey Space $G_{\tau,\alpha}$ by

$$G_{\tau,\alpha} := D(A^\alpha e^{\tau A^\alpha}) = \{u \in L^2(\Omega) : \|A^\alpha e^{\tau A^\alpha} u\|_{L^2}^2 < \infty\},$$

with norm

$$\|u\|_{G_{\tau,\alpha}}^2 := \|A^\alpha e^{\tau A^\alpha} u\|_{L^2}^2 = \sum_{k=1}^{\infty} \lambda_k^{2\alpha} e^{2\tau \lambda_k^\alpha} |a_k|^2, \quad (2.2.4)$$

where $\tau > 0$ and $\alpha \geq 0$.

The τ given in Definition 2.2.15 is referred to as the order of Gevrey regularity of $G_{\tau,\alpha}$ and we say that $u \in G_{\tau,\alpha}$ is of Gevrey class regularity τ . The following theorem relates Gevrey classes of different regularity.

Theorem 2.2.16 *If $\tau > \sigma > 0$, then the following inclusion holds $G_{\tau,\alpha} \subset G_{\sigma,\alpha}$.*

Proof: For $u \in G_{\tau,\alpha}$ we have that

$$\begin{aligned} \|u\|_{G_{\sigma,\alpha}}^2 &= \sum_{k=1}^{\infty} \lambda_k^{2\alpha} e^{2\sigma\lambda_k^\alpha} |a_k|^2, \\ &\leq \sum_{k=1}^{\infty} \lambda_k^{2\alpha} e^{2\tau\lambda_k^\alpha} |a_k|^2, \\ &= \|u\|_{G_{\tau,\alpha}}^2, \end{aligned}$$

therefore $u \in G_{\sigma,\alpha}$ which implies that $G_{\tau,\alpha} \subset G_{\sigma,\alpha}$. □

From the definition of a Gevrey class, in particular (2.2.4), we can see that if $u \in G_{\tau,\alpha}$ then the Fourier coefficients of u must decay exponentially as k increases and hence u must be a smooth function. The following theorem states exactly how smooth u is in this case.

Theorem 2.2.17 *If $u \in G_{\tau,\alpha}$ for some $\tau > 0$ then u is real analytic and hence in $C^\infty(\Omega)$.*

Proof: See John [45, p.64-65]. □

Theorem 2.2.18 *For all $\tau > 0$ and $\alpha \geq 0$ we have the following inclusion*

$$G_{\tau,\alpha} \subset \mathcal{X}^\alpha.$$

Proof: By definition

$$\begin{aligned} \|u\|_{\mathcal{X}^\alpha}^2 &= \|A^\alpha u\|_{L^2}^2 = \sum_{k=1}^{\infty} \lambda_k^{2\alpha} |a_k|^2, \\ &= \sum_{k=1}^{\infty} \lambda_k^{1/2} e^{2\tau\lambda_k^{1/4}} |a_k|^2 \left(\lambda_k^{2\alpha-1/2} e^{-2\tau\lambda_k^{1/4}} \right), \end{aligned}$$

and the function $x^{2\alpha-1/2} e^{-2\tau x}$, $x = \lambda_k^{1/4}$, is uniformly bounded for $x \geq \lambda_1$ for all $\alpha \in \mathbb{R}$. Hence the result follows since there exists a constant $C > 0$ such that

$$\|u\|_{\mathcal{X}^\alpha} \leq C < \infty.$$

□

In this thesis we will be only interested in the case when $\alpha = 1/4$ and $\tau > 0$ and will therefore write G_τ instead of $G_{\tau,\alpha}$.

2.3 The Kuramoto-Sivashinsky equation

The Kuramoto-Sivashinsky (K-S) equation is the following fourth order dissipative partial differential equation

$$\frac{\partial w}{\partial t} + \frac{\partial^4 w}{\partial x^4} + \frac{\partial^2 w}{\partial x^2} + \frac{1}{2} \left(\frac{\partial w}{\partial x} \right)^2 = 0. \quad (2.3.1)$$

Primarily this equation is used to model pattern formation and inter-facial turbulence in various physical contexts. It was initially derived by Kuramoto in the study of phase turbulence in the Belousov-Zhabotinskii reaction, see Kuramoto [56]. This reaction, both theoretically and experimentally, is one of the most widely studied oscillatory reactions in Chemistry and exhibits remarkable spatial patterns and colour oscillations. The K-S equation was also derived in the two-dimensional form by Sivashinsky [81], in the study of thermal diffusive instabilities for laminar flame fronts. Other applications of the equation are in the modelling of directional solidification in dilute binary alloys, see Kassner, Hobbs and Metzener [54] and Novick-Cohen and Sivashinsky [71], soliton like pulses in nonlinear optical fibres, see Kutz and Kath [57] and free surface flows, see Benney [3], see also Hyman and Nicolaenko [43] and Nicolaenko, Scheurer and Temam [68] for further applications. A generalised form, of which (2.3.1) is a special case, has been derived by an asymptotic analysis of the Navier-Stokes equations in the context of two phase flows in cylindrical geometries, see Papageorgiou, Maldarelli and Rumschitzki [72]. This has applications in lubricated pipe lining and oil recovery through porous media.

Alternatively we can consider the space derivative of the solution of equation

(2.3.1), $v = \partial w / \partial x$, which satisfies

$$\frac{\partial v}{\partial t} + \frac{\partial^4 v}{\partial x^4} + \frac{\partial^2 v}{\partial x^2} + v \frac{\partial v}{\partial x} = 0. \quad (2.3.2)$$

This equation is called the derivative form of (2.3.1) and has an identical linear part to equation (2.3.1), however the nonlinear term is now of Burgers' type. We consider this equation on the interval $\Omega_L = (-L/2, L/2)$ with the periodic boundary conditions

$$\frac{\partial^j v}{\partial x} \left(-\frac{L}{2}, t \right) = \frac{\partial^j v}{\partial x} \left(\frac{L}{2}, t \right), \quad t \in (0, \infty); j = 0, 1, 2, 3, \quad (2.3.3)$$

and initial condition

$$v(x, 0) = v_0(x), \quad x \in \Omega_L, \quad (2.3.4)$$

where $v_0 = dw_0/dx$. Since v should be thought of as the derivative of a periodic function, we always require that

$$\int_{\Omega_L} v(x, t) dx = 0, \quad t \in [0, \infty). \quad (2.3.5)$$

Equation (2.3.2) was derived independently as a general mechanism for studying the stability of liquid films flowing under heavier fluids with respect to small disturbances in Babchin, Frenkel, Levich and Sivashinsky [2].

As well as all the applications mentioned above, the K-S equation is known to exhibit low dimensional asymptotic dynamical behaviour and possess an inertial manifold. It is for these reasons that the K-S equation has been extensively studied in recent years, both numerically and theoretically, as a model example for understanding and predicting complex dynamical behaviour. This is illustrated by the abundance of literature which investigates the numerical approximation of various bifurcation phenomena for this equation, see [20], [43], [44], [55], [60], [67], [91] and [94]. The existence of an inertial manifold was first shown for solutions in the invariant subspace of odd functions by Foias, Nicolaenko, Sell and Temam

[22] and later for general solutions which satisfy the condition (2.3.5) in Temam and Wang [90].

In this thesis we will impose the following condition on equation (2.3.2),

$$v(x, t) = -v(-x, t), \quad x \in \Omega_L \times [0, \infty). \quad (2.3.6)$$

This will ensure that we can use all the theoretical results which have been proved for the equation with solutions in the odd subspace.

It is convenient to map equation (2.3.2) from the interval Ω_L , where L is arbitrary, onto the fixed interval $\Omega_\pi = (-\pi, \pi)$ which will be useful when we need to use Fourier analysis. This mapping procedure of the K-S equation has been widely used when considering numerical approximation, see for example [19], [30], [31], [48], [55], [60] and [78]. We start by setting $\hat{x} = 2\pi x/L$, $\hat{t} = 2\pi t/4L$ and $u = (L/2\pi)v(\hat{x}, \hat{t})$ so equation (2.3.2) becomes

$$\frac{\partial u}{\partial \hat{t}} + 4 \frac{\partial^4 u}{\partial \hat{x}^4} + \alpha \left(\frac{\partial^2 u}{\partial \hat{x}^2} + u \frac{\partial u}{\partial \hat{x}} \right) = 0, \quad (\hat{x}, \hat{t}) \in \Omega_\pi \times (0, \infty),$$

where $\alpha = (L/\pi)^2$. Therefore the form of the K-S equation which will be considered in this thesis is

$$\frac{\partial u}{\partial t} + 4 \frac{\partial^4 u}{\partial x^4} + \alpha \left(\frac{\partial^2 u}{\partial x^2} + u \frac{\partial u}{\partial x} \right) = 0, \quad (x, t) \in \Omega_\pi \times (0, \infty), \quad (2.3.7)$$

where

$$\begin{aligned} u(x, 0) &= u_0(x), & x &\in \Omega_\pi, \\ \frac{\partial^j u}{\partial x}(-\pi, t) &= \frac{\partial^j u}{\partial x}(\pi, t), & t &\in (0, \infty); j = 0, 1, 2, 3, \\ u(x, t) &= -u(-x, t), & (x, t) &\in \Omega_\pi \times (0, \infty). \end{aligned} \quad (2.3.8)$$

Note that for simplicity the variables \hat{x} and \hat{t} have been renamed as x and t respectively. We will discuss existence and uniqueness of the solutions of this equation in the next section.

2.4 An abstract framework for the Kuramoto-Sivashinsky equation

In order to apply some of the theory which we introduced in Section 2.2, it is convenient to write equation (2.3.7) in the form of an abstract evolution equation. Hence we denote by A the operator $4\partial^4/\partial x^4$ with domain

$$\begin{aligned} D(A) &= \{u \in H_{per}^4(\Omega_\pi) : u(x) = -u(-x), \quad \forall x \in \Omega_\pi\}, \\ &= \dot{H}_{per}^4(\Omega_\pi), \end{aligned} \quad (2.4.1)$$

and define the nonlinear function F by

$$F(u) = \alpha(u_{xx} + uu_x), \quad u \in D(A). \quad (2.4.2)$$

We can therefore rewrite equation (2.3.7) along with conditions (2.3.8) as

$$u_t + Au + F(u) = 0, \quad (2.4.3)$$

$$u(0) = u_0, \quad (2.4.4)$$

in the Hilbert space $X = \dot{L}_{per}^2(\Omega_\pi)$.

Theorem 2.4.1 *The linear operator A which has domain (2.4.1) has eigenvalues $\{\lambda_k\}_{k=1}^\infty$, given by*

$$\lambda_k = 4k^4,$$

which have corresponding eigenfunctions $\{\omega_k\}_{k=1}^\infty$, such that

$$\omega_k = \sin(kx).$$

The solution $u(x, t)$ of (2.3.7) can be expressed in terms of the Fourier series

$$u(x, t) = \sum_{k=1}^{\infty} a_k(t) \sin kx,$$

and from the previous section we can define the Sobolev spaces X^s , $s \geq 0$, as the normed linear spaces with norm

$$\|u\|_{X^s}^2 := \|A^s u\|_{L^2}^2 = \pi \sum_{k=1}^{\infty} (4k^4)^{2s} |a_k|^2 < \infty,$$

for $u \in X^s$. Alternatively we could write

$$X^s := \{u : u = \sum_{k=1}^{\infty} a_k \omega_k \text{ \& } \sum_{k=1}^{\infty} (4k^4)^{2s} |a_k|^2 < \infty\}.$$

In the thesis we will assume that $4s \in \mathbb{N} \cup \{0\}$.

Theorem 2.4.2 *The linear operator A is sectorial on the space X .*

Proof: First we prove that A is a closed densely defined operator in X . By definition

$$\|Au\|_{L^2}^2 = 16 \int_{-\pi}^{\pi} \frac{\partial^4 u}{\partial x^4} \frac{\partial^4 u}{\partial x^4} dx, \quad u \in D(A),$$

so that $D(A)$ is norm-equivalent to the Sobolev space $\dot{H}_{per}^4(\Omega_\pi)$. Now Theorem 2.1.5 implies that $\dot{H}_{per}^4(\Omega_\pi)$ is compactly imbedded in X . Therefore A is a closed densely defined operator in X .

To satisfy part iii) of Definition 2.2.3 we note that

$$\begin{aligned} \langle Au, u \rangle_{L^2} &= 4 \int_{-\pi}^{\pi} \frac{\partial^4 u}{\partial x^4} u dx, \\ &= 4 \int_{-\pi}^{\pi} \frac{\partial^2 u}{\partial x^2} \frac{\partial^2 u}{\partial x^2} dx, \\ &= \|2 \frac{\partial^2 u}{\partial x^2}\|_{L^2}^2, \\ &\geq \lambda_1 \|u\|_{L^2}^2, \quad \text{by Poincaré's inequality,} \end{aligned}$$

which implies that the numerical range of A defined by

$$\Theta(A) := \{\langle Au, u \rangle_{L^2} : u \in D(A) : \|u\|_{L^2} = 1\},$$

has closure, $\Gamma(A)$, such that

$$\Gamma(A) \subseteq [\lambda_1, \infty) = \mathcal{I}.$$

Therefore by Edmunds and Evans [17, Theorem 2.3, p.100] we have that

$$\begin{aligned} \|(A - \lambda I)^{-1}\|_{L^2} &\leq \frac{1}{d(\lambda, \Gamma(A))}, & \lambda \in \mathbb{C} \setminus \Gamma(A), \\ &\leq \frac{1}{d(\lambda, \mathcal{I})}, & \lambda \in \mathbb{C} \setminus \mathcal{I}, \end{aligned} \quad (2.4.5)$$

since $d(\lambda, \mathcal{I}) \leq d(\lambda, \Gamma(A))$, where $d(\cdot, \cdot)$ is the distance function on X .

We now use inequality (2.4.5) to prove that (2.2.1) in Definition 2.2.3 holds for this specific case. In order to aid us, a picture has been plotted in Figure 2-2, which shows two general points P_1 and P_2 and the interval \mathcal{I} in the complex plane.

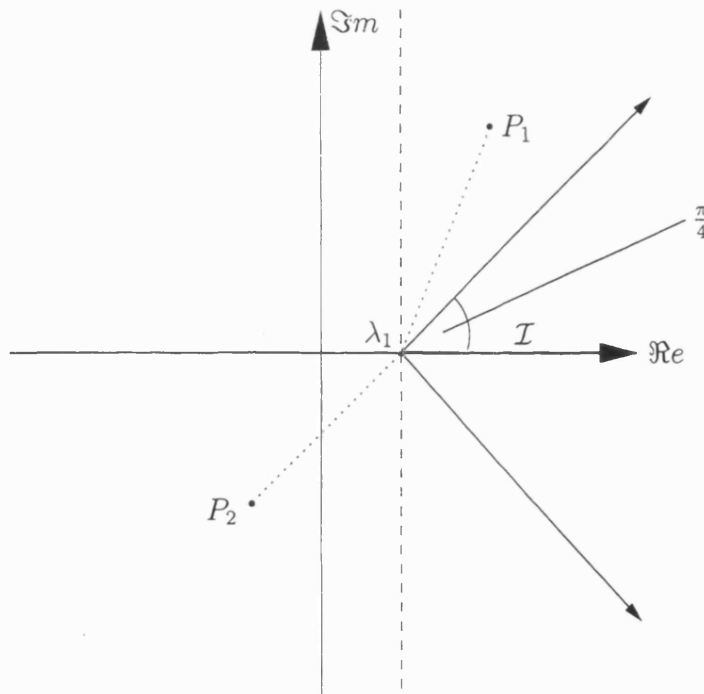


Figure 2-2: Illustration of the closure of the numerical range in the complex plane.

Now for any $\lambda \in \mathbb{C}$, with $\Re\{\lambda\} \geq \lambda_1$ and $|\arg(\lambda - \lambda_1)| = |\theta| \in (\pi/4, \pi/2)$, say the point P_1 in Figure 2-2, we have that

$$\begin{aligned} d(\lambda, \mathcal{I}) &= |\lambda_1 - \lambda| \sin \theta, \\ &\geq \frac{|\lambda_1 - \lambda|}{\sqrt{2}}, \end{aligned}$$

which implies that

$$\frac{1}{d(\lambda, \mathcal{I})} \leq \frac{\sqrt{2}}{|\lambda_1 - \lambda|}. \quad (2.4.6)$$

Also for a point with $\Re\{\lambda\} \leq \lambda_1$ and $|\arg(\lambda - \lambda_1)| \in (\pi/2, \pi)$, say the point P_2 , we have that

$$|\lambda_1 - \lambda| = d(\lambda, \mathcal{I}),$$

which implies that

$$\frac{1}{d(\lambda, \mathcal{I})} \leq \frac{1}{|\lambda_1 - \lambda|}. \quad (2.4.7)$$

Hence from (2.4.6) and (2.4.7), we have that

$$\|(A - \lambda I)^{-1}\|_{L^2} \leq \frac{\sqrt{2}}{|\lambda_1 - \lambda|},$$

for all λ such that $|\theta| = |\arg(\lambda_1 - \lambda)| \geq \pi/4$. So we have satisfied part iii) of Definition 2.2.3 with $a = \lambda_1$ and $M = \sqrt{2}$.

□

Remark 2.4.3 We note that if we were to take $A = 4\partial^4/\partial x^4 + \alpha\partial^2/\partial x^2$ in equation (2.4.3) we would obtain eigenvalues

$$\lambda_k = 4k^4 - \alpha k^2,$$

which are negative for $k < (\alpha/4)^{1/2} = L/2\pi$. This means that the eigenvalues will no longer be positive and thus A will no longer be sectorial. This could be rectified by subtracting off the first few Fourier modes which correspond to the negative eigenvalues. This approach has been taken in Constantin, Foias, Nicolaenko and Temam [9].

We can generalise Theorem 2.4.2 in the following way.

Lemma 2.4.4 *If A , defined in (2.4.1) is a sectorial operator, then A^s is a closed operator with domain X^s , for $s \geq 0$.*

Proof: See Pazy [75, Theorem 6.8a), p.72].

□

Lemma 2.4.5 *The operator $A : X^{s+1} \rightarrow X^s$ is sectorial.*

Proof: From the last lemma, the operator A^{s+1} is closed. Hence for $u_n \in X^{s+1}$, we have that

$$\left. \begin{array}{l} u_n \rightarrow u, \quad \text{in } X^{s+1}, \\ A^{s+1}u_n \rightarrow v, \quad \text{in } L^2, \end{array} \right\} \Rightarrow \begin{cases} u \in X^{s+1}, \\ A^{s+1}u = v. \end{cases}$$

Therefore,

$$\|Au_n - w\|_{X^s} = \|A^{s+1}u_n - A^{s+1}u\|_{L^2},$$

where $w = Au$ and

$$Au_n \rightarrow w, \quad \text{in } X^s.$$

Hence A is closed on X^s . Also, A is densely defined since the space $C_0^\infty \subset X^{s+1}$, and C_0^∞ is dense in X^s . Finally we need to show that $\sigma(A)$ consists of a set of strictly positive real points. Since $A : X^1 \rightarrow X$ is sectorial, by Theorem 2.4.2, we have that

$$\|(A - \lambda)^{-1}\|_{L^2} \leq \frac{M}{|\lambda - a|}, \quad \forall \lambda \in S \subset \rho(A),$$

where $M \geq 0$ and a is a real constant. We can generalise this result so that $A : X^{s+1} \rightarrow X^s$ is sectorial by considering the equation

$$(A - \lambda)u = g,$$

where $u \in X^{s+1}$ and $g \in X^s$. Premultiplying by A^s and taking the L^2 norm gives

$$\|A^s u\|_{L^2} \leq \|(A - \lambda)^{-1}\|_{L^2} \|A^s g\|_{L^2},$$

so that

$$\|u\|_{X^s} \leq \frac{M}{|\lambda - a|} \|g\|_{X^s}.$$

Hence A is a sectorial operator on X^s .

□

Before stating the existence and uniqueness theorem of the K-S equation we prove the following lemma.

Lemma 2.4.6 *The function F defined by (2.4.2) is Lipschitz continuous from an open set U in X^s into $X^{s-1/2}$, for $s > 5/8$ with $4s \in \mathbb{N} \cup \{0\}$.*

Proof: Let $u, v \in U$, then

$$\begin{aligned} \|F(u) - F(v)\|_{X^{s-1/2}} &= \alpha \|u_{xx} - v_{xx} + uu_x - vv_x\|_{X^{s-1/2}}, \\ &\leq \alpha (\|u_{xx} - v_{xx}\|_{X^{s-1/2}} + \|uu_x - vv_x\|_{X^{s-1/2}}), \\ &\leq C_1 \|u - v\|_{X^s} + \alpha (\|u_x(u - v)\|_{X^{s-1/2}} \\ &\quad + \|v(u - v)_x\|_{X^{s-1/2}}). \end{aligned}$$

We recall from Section 2.1 that the norms $\|\cdot\|_{W^{4s-2,2}}$ and $\|\cdot\|_{X^{s-1/2}}$ are equivalent for $4s \in \mathbb{N} \cup \{0\}$. Hence if $s - 1/2 > 1/8$ then we can apply Theorem 2.1.7 to

the last two norms in the above inequality, to obtain

$$\begin{aligned} \|F(u) - F(v)\|_{X^{s-1/2}} &= C_1 \|u - v\|_{X^s} + C_2 \|u_x\|_{W^{4s-2,2}} \|(u - v)\|_{W^{4s-2,2}} \\ &\quad + C_3 \|v\|_{W^{4s-2,2}} \|(u - v)_x\|_{W^{4s-2,2}}. \end{aligned}$$

Finally applying Theorem 2.1.5 to the norms on the right hand side gives

$$\|F(u) - F(v)\|_{X^{s-1/2}} = C (\|u\|_{X^s}, \|v\|_{X^s}) \|u - v\|_{X^s}.$$

□

Theorem 2.4.7 *If A is a sectorial operator and F is locally Lipschitz from an open set U in X^s into $X^{s-1/2}$, for $s > 5/8$ and $4s \in \mathbb{N}$, then for any $u_0 \in X^s$, there exists $\tau = \tau(u_0) > 0$ such that (2.4.3) has a unique solution $u(t) \in C([0, \tau); X^s)$ which is uniformly bounded.*

Proof: Follows from Theorem 2.4.7 given the results of Lemma 2.4.5 and Lemma 2.4.6.

□

Theorem 2.4.7 gives us the existence of a semigroup $S(t) : X^s \rightarrow X^s$, for $s > 5/8$ and $t \in [0, \tau)$ for the K-S equation. The interval of existence of this semigroup can be extended to $[0, \infty)$. This follows from the results concerning the existence of absorbing balls in X^s for the solutions of the K-S equation in Section 4.2. The next theorem is concerned with the regularity of this semigroup.

Theorem 2.4.8 *Let U be an open set in X^s . Then if $u_0 \in U$, the semigroup $S(t)$ defined by (2.4.3) is continuously differentiable with respect to u_0 from X^s into X^s , for $s > 5/8$, $4s \in \mathbb{N}$, and for each $t > 0$ on its domain of existence $[0, \tau)$.*

Proof: We need to verify the assumptions of Theorem 2.2.14. We have that the operator A is sectorial by Lemma 2.4.5 and that the operator F is continuous. Now for $u \in X^s$ the Fréchet derivative of F is given by

$$DF(u)w = \alpha \left(\frac{\partial u}{\partial x} w + u \frac{\partial w}{\partial x} + \frac{\partial^2 w}{\partial x^2} \right), \quad \forall w \in X^s. \quad (2.4.8)$$

Hence for $u, v, w \in X^s$ we have that

$$\| [DF(u) - DF(v)]w \|_{X^{s-1/2}} \leq \alpha (\| (u-v)w_x \|_{X^{s-1/2}} + \| (u-v)_x w \|_{X^{s-1/2}}).$$

Following the proof of Lemma 2.4.6 and applying Theorem 2.1.7, we obtain

$$\begin{aligned} \| (DF(u) - DF(v))w \|_{X^{s-1/2}} &\leq C_1 \| w_x \|_{W^{4s-2,2}} \| (u-v) \|_{W^{4s-2,2}} \\ &\quad + C_2 \| w \|_{W^{4s-2,2}} \| (u-v)_x \|_{W^{4s-2,2}}, \\ &\leq C_3 \| w \|_{X^s} \| u-v \|_{X^s}, \end{aligned} \quad (2.4.9)$$

where we have used the equivalence of the norms of $W^{4s,2}$ and X^s for $4s \in \mathbb{N} \cup \{0\}$.

Hence the operator DF is also continuous from X^s into X^s .

□

Theorem 2.4.8 implies that the Fréchet derivative $DS(t, u_0)$, of the semi-group $S(t)$ with respect to initial data, exists. Furthermore for $v_0 \in X^s$, $v(t) := DS(t, u_0)v_0 \in X^s$ and satisfies the following equation

$$\begin{aligned} \frac{dv}{dt} + Av + DF(u)v &= 0, \\ v(0) &= v_0. \end{aligned} \quad (2.4.10)$$

It is also possible to show that the solutions of (2.4.3) are contained in a Gevrey space, given uniform bounds in the $X^{1/4}$ space.

Theorem 2.4.9 *Let $u_0 \in X^{1/4}$; then there exists $t_1 = t_1(\|u_0\|_{X^{1/4}})$ such that*

$$u(t) \in G_t = D(A^{1/4} e^{tA^{1/4}}), \quad t \in [0, t_1),$$

with norm defined by

$$\|u(t)\|_{G_t} = \|A^{1/4} e^{tA^{1/4}} u(t)\|_{L^2} = \pi \sum_{k=1}^{\infty} \lambda_k^{1/2} e^{2t\lambda_k^{1/4}} a_k^2 < \infty.$$

Furthermore if $\|u(t)\|_{X^{1/4}} \leq M$ for $t \geq t^ > 0$ then there exists some $\tau > 0$*

independent of u_0 such that

$$u(t) \in G_\tau, \quad \forall t \geq \tau + t^*.$$

Proof: The first part of this proof is given in Liu [58]. In this paper it is shown that

$$\|A^{1/4}e^{tA^{1/4}}u(t)\|_{L^2} \leq \sqrt{2}\|u_0\|_{X^{1/4}}, \quad (2.4.11)$$

for

$$0 \leq t < t_1(\|u_0\|_{X^{1/4}}) := \frac{1}{16K\|u_0\|_{X^{1/4}}^2 + 12\sqrt{2}},$$

where K is some positive constant. In order to prove the remaining part of this theorem we let $v(s) = u(s + t)$ for $s \geq 0$ and $t \geq t^*$. Hence

$$\|v(0)\|_{X^{1/4}} = \|u(t)\|_{X^{1/4}} \leq M,$$

which implies that

$$v(s) \in G_s, \quad 0 \leq s \leq \tau := t_1(M),$$

from the first part of the proof. In particular this gives

$$v(\tau) = u(t + \tau) \in G_\tau,$$

so that

$$u(t) \in G_\tau, \quad t \geq \tau + t^*.$$

□

Chapter 3

The Discrete Problem

3.1 A semi-discrete approximation

3.1.1 The pseudospectral method

In this thesis we will consider the pseudospectral method for the spatial discretization of equation (2.3.7) with conditions (2.3.8) and we will begin this chapter by briefly outlining this type of approximation method. Text books which offer a good description of applications of the pseudospectral method to differential equations are Canuto, Hussaini, Quarteroni and Zang [5], Fornberg and Sloan [28], Gottlieb and Orszag [34] and Voigt, Gottlieb and Hussaini [92].

The pseudospectral (PS) method belongs to a class of approximation methods called spectral methods, which includes the spectral Galerkin method. The methods in this class approximate functions by means of expressing them as a truncated finite series of globally defined orthogonal polynomials and calculating the expansion coefficients of the series. For the PS method these expansion coefficients can be expressed in terms of the functions at a finite set of nodal values, which differs slightly from the Galerkin method. The PS method was first applied to ordinary differential equations in the 1930's and to PDE's in the early 1970's. When using spectral methods for solving PDE's, the PS method is usually preferred unless the problem is quite simple. This is because the spectral Galerkin method can be difficult to implement when dealing with complicated

nonlinearities.

The main disadvantages of the PS method is that difficulties may arise when applying it to problems with complicated boundary conditions. There is also an incomplete understanding of the theory for the PS method, particularly for nonlinear equations.

However the PS method is highly desirable when a high degree of computational accuracy is required, as is the case when considering turbulence in fluids, nonlinear waves, seismic modelling and weather prediction, which can all produce complicated dynamical behaviour. It is for this reason that we have chosen to study the PS method in this thesis. We have considered the Fourier PS method as this type of method is suited to dealing with problems with periodic boundary conditions. The PS method has also been used to analyse and compute solutions to the K-S equation in the following papers [11], [30], [31], [43], [44], [55], [91], and [94].

3.1.2 Discretization of the Kuramoto-Sivashinsky equation

Prior to the discretization of equation (2.3.7) we will write the nonlinear term uu_x in the equivalent form

$$[(1 - \theta)u \frac{\partial u}{\partial x} + \frac{\theta}{2} \frac{\partial}{\partial x}(u^2)], \quad 0 \leq \theta \leq 1. \quad (3.1.1)$$

The basic idea of representing the nonlinear term in this way was introduced by Foias, Jolly, Kevrekidis and Titi [20]. In this paper a semi-discrete spatial approximation to the K-S equation was analysed using the finite difference method. It was shown that when the nonlinear term was written in the form of the linear combination (3.1.1) with $\theta = 2/3$, the resulting approximation scheme had the same dissipative properties as the equation it was approximating. However when the two factors were considered separately the semi-discrete approximations were no longer dissipative and tended to blow up in a finite time.

As a result of the oddness of the solutions of the K-S equation we are considering, it will suffice to approximate it on the half interval $[0, \pi]$ and we introduce the uniform grid $\{x_j\}_{j=0}^N$ given by

$$x_j = jh = j(\pi/N), \quad j = 0, 1, \dots, N. \quad (3.1.2)$$

We require the finite-dimensional subspace of $\mathcal{H} = \dot{H}_{per}^4(\Omega_\pi)$ given by

$$X_h^o = \text{span}\{\omega_k\}_{k=1}^{N-1} = \{\sin(kx)\}_{k=1}^{N-1},$$

and also the (even) finite-dimensional subspace of \mathcal{H} ,

$$X_h^e = \text{span}\{\cos(kx)\}_{k=0}^N,$$

as writing the nonlinearity in the form (3.1.1) gives rise to an even term u^2 .

Now for $u \in \mathcal{H}$ we choose the coefficients $\{a_k\}_{k=1}^{N-1}$ such that

$$\sum_{k=1}^{N-1} a_k \sin(kx_j) = u(x_j), \quad j = 1, \dots, N-1, \quad (3.1.3)$$

where $u \in \mathcal{H}$. These coefficients can be found by solving the following system

$$\mathbf{a} = S\mathbf{u}, \quad (3.1.4)$$

where

$$\mathbf{a} = [a_1, a_2, \dots, a_{N-1}]^T, \quad \mathbf{u} = [u(x_1), u(x_2), \dots, u(x_{N-1})]^T,$$

and

$$S_{ij} = (2/N) \sin(ix_j), \quad 1 \leq i, j \leq N-1, \quad (3.1.5)$$

using the discrete orthogonality condition

$$\frac{2}{N} \sum_{j=1}^{N-1} \sin\left(\frac{jk\pi}{N}\right) \sin\left(\frac{jl\pi}{N}\right) = \begin{cases} 1, & k = l, \\ 0, & k \neq l, \end{cases} \quad (3.1.6)$$

where $0 \leq k, l \leq N$. Given these coefficients we can define the operator $I_h^o : \mathcal{H} \rightarrow X_h^o$, by

$$I_h^o u(x) := \sum_{k=1}^{N-1} a_k \sin(kx), \quad u \in \mathcal{H}, \quad (3.1.7)$$

which is an interpolation operator since

$$I_h^o u(x_j) = u(x_j), \quad j = 0, 1, \dots, N,$$

by (3.1.3). The interpolation operator I_h^o can be regarded as an orthogonal projection onto the space X_h^o with respect to the discrete inner product

$$(u, v)_{L_h^2} = 2h \sum_{j=0}^N c_j u(x_j) v(x_j), \quad (3.1.8)$$

where

$$c_j = \begin{cases} 1/2, & \text{if } j = 0, N, \\ 0, & \text{otherwise.} \end{cases} \quad (3.1.9)$$

We have introduced a factor of 2 in the inner product (3.1.8) since the K-S equation is defined on the interval $[-\pi, \pi]$ and we are only approximating it over the half interval $[0, \pi]$. This will be convenient later when we prove some results which relate the discrete and continuous inner products. If u and v are in the space X_h^o , then

$$(u, v)_{L_h^2} = \langle u, v \rangle_{L^2},$$

by the orthogonality conditions (3.1.6), hence (3.1.8) is also an inner product on

X_h^o .

Differentiation in the space X_h^o is based upon the values of the function u at the grid points. Hence in our case, the PS approximation to the first order derivative in (2.3.7) at the grid points is given by

$$(\mathcal{D}_h^o u)(x_j) = \sum_{k=1}^{N-1} k a_k \cos(kx_j), \quad j = 0, 1, \dots, N. \quad (3.1.10)$$

This procedure amounts to computing the grid values of the derivative of the interpolation (3.1.7), i.e.,

$$\mathcal{D}_h^o \cdot = (I_h^o \cdot)'$$

Hence if $u \in X_h^o$ then $\mathcal{D}_h^o u = \partial u / \partial x$. PS differentiation can also be represented in the form of a matrix and by considering the coefficients (3.1.3) and the orthogonality conditions (3.1.6) it is possible to write (3.1.10) in the following form

$$(\mathcal{D}_h^o u)(x_j) = \sum_{k=1}^{N-1} [\hat{D}_h^o]_{jk} u(x_k), \quad j = 0, 1, \dots, N,$$

where $\hat{D}_h^o \in \mathbb{R}^{(N+1) \times (N-1)}$, which we refer to as the first order PS differentiation matrix. Similarly we can represent differentiation in the even space X_h^e by the matrix $\hat{D}_h^e \in \mathbb{R}^{(N-1) \times (N+1)}$. In order to write down our semi-discrete approximation we need to express these matrices as $(N-1) \times (N-1)$ square matrices. This can be achieved by removing the first and last rows of \hat{D}_h^o and the first and last columns of \hat{D}_h^e . We will denote these two new matrices as D_h^o and D_h^e respectively.

It is possible to obtain matrices which approximate the second and fourth order spatial derivatives in equation (2.3.7) in a similar way in which we outlined above. We will denote these two $(N-1) \times (N-1)$ square matrices as D_h^2 and D_h^4 respectively. A rigorous construction of all the above mentioned matrices is

given in Wallace [93], and have the following explicit representation

$$[\widehat{D}_h^o]_{jk} = \begin{cases} (-1)^{j+k} \left[\frac{\sin(x_k)}{\cos(x_k) - \cos(x_j)} \right], & k \neq j; \\ -\frac{1}{2} \cot(x_k), & k = j; \end{cases} \quad (3.1.11)$$

$$[\widehat{D}_h^e]_{jk} = \begin{cases} c_k (-1)^{j+k} \left[\frac{\sin(x_j)}{\cos(x_k) - \cos(x_j)} \right], & j \neq k; \\ \frac{1}{2} \cot(x_k), & j = k; \end{cases} \quad (3.1.12)$$

where c_k is defined in (3.1.9) and second order differentiation matrix is given by

$$[D_h^2]_{jk} = \begin{cases} 2(-1)^{j+k+1} \left[\frac{\sin(x_j) \sin(x_k)}{(\cos(x_k) - \cos(x_j))^2} \right], & k \neq j; \\ \frac{1}{3}(1 - (N+1)^2) + \frac{1}{2} \cot^2(x_k), & k = j; \end{cases} \quad (3.1.13)$$

These matrices have the following properties

$$D_h^e = -[D_h^o]^T, \quad (3.1.16a)$$

$$[\widehat{D}_h^e]_{jk} = -\frac{1}{2}[\widehat{D}_h^o]_{kj}, \quad \text{for } k = 0, N \text{ and } j = 1, 2, \dots, N-1, \quad (3.1.16b)$$

$$D_h^2 = \widehat{D}_h^e \times \widehat{D}_h^o, \quad (3.1.16c)$$

$$D_h^2 = [D_h^2]^T, \quad (3.1.16d)$$

$$D_h^4 = D_h^2 \times D_h^2. \quad (3.1.16e)$$

Finally we denote by $U_j(t) = u_h(x_j, t)$, the PS approximation to $u(x_j, t)$ for $j = 0, 1, \dots, N$ and introduce the following notation

$$\mathbf{U} = [U_1, U_2, \dots, U_{N-1}]^T,$$

$$\mathbf{U} \otimes \mathbf{V} = [U_1 V_1, U_2 V_2, \dots, U_{N-1} V_{N-1}]^T,$$

where $\mathbf{V} \in \mathbb{R}^{N-1}$, with components V_1, V_2, \dots, V_{N-1} . Having discussed the form

of the PS approximation and differentiation matrices we can now introduce the PS semi-discretization of the K-S equation. The PS spatially discrete system which approximates (2.3.7) at the grid points $\{x_j\}_{j=1}^{N-1}$ is

$$\frac{d}{dt}\mathbf{U} + 4D_h^4\mathbf{U} + \alpha D_h^2\mathbf{U} + \frac{\alpha}{3}(\mathbf{U} \otimes D_h^o\mathbf{U} + D_h^e(\mathbf{U} \otimes \mathbf{U})) = \mathbf{0}, \quad (3.1.17)$$

3.1.3 A mathematical setting for the semi-discrete approximation

We now introduce a mathematical setting for equation (3.1.17) and begin by defining the matrix operator $A_h : \mathbb{R}^{N-1} \rightarrow \mathbb{R}^{N-1}$ by

$$A_h = 4D_h^4. \quad (3.1.18)$$

The following theorem gives the eigenvalues and eigenfunctions of this finite-dimensional operator.

Theorem 3.1.1 *The linear operator A_h has eigenvalues*

$$\lambda_{h,k} = 4k^4, \quad 1 \leq k \leq N-1,$$

with corresponding eigenfunctions

$$\omega_{h,k} = (\sin(kx_1), \sin(kx_2), \dots, \sin(kx_{N-1}))^T, \quad 1 \leq k \leq N-1.$$

The eigenvalues of A_h are identical to the first $N-1$ eigenvalues of A defined in the previous chapter.

For $\mathbf{U} \in \mathbb{R}^{N-1}$, we denote by L_h^p the discrete L^p spaces on $(0, \pi)$, with corresponding norms

$$\|\mathbf{U}\|_{L_h^p} = \begin{cases} (2h \sum_{j=1}^{N-1} |U_j|^p)^{1/p}, & \text{for } 1 \leq p < \infty, \\ \sup_{1 \leq j \leq N-1} |U_j|, & \text{for } p = \infty, \end{cases} \quad (3.1.19)$$

so that the L_h^2 inner product is given by

$$\langle \mathbf{U}, \mathbf{V} \rangle_{L_h^2} = 2h \sum_{k=1}^{N-1} U_k V_k, \quad (3.1.20)$$

where $\mathbf{V} \in \mathbb{R}^{N-1}$. This gives a slightly different definition to the inner product given in (3.1.8). However these two norms are identical on the odd space, since for $\mathbf{U} \in \mathbb{R}^{N+1} \cap X_h^o$, we have that

$$\begin{aligned} (\mathbf{U}, \mathbf{V})_{L_h^2} &= 2h \sum_{j=0}^N U_j V_j, \\ &= 2h(U_0 V_0 + \sum_{j=1}^{N-1} U_j V_j + U_N V_N), \end{aligned}$$

and $U_0 = U_N = 0$, so that

$$\begin{aligned} (\mathbf{U}, \mathbf{V})_{L_h^2} &= 2h \sum_{j=1}^N U_j V_j, \\ &= \langle \mathbf{U}, \mathbf{V} \rangle_{L_h^2}, \end{aligned}$$

We will use (3.1.8) as the L_h^2 inner product for any element $\mathbf{U} \in \mathbb{R}^{N+1} \cap X_h^e$.

We can also define discrete Sobolev spaces in an analogous manner to the one in which we used for the continuous problem in Section 2.2. We consider the expansion of the vector $\mathbf{U} = (U_1, U_2, \dots, U_{N-1})^T \in L_h^2$ as a Fourier series based on the eigenfunctions $\omega_{h,k}$ of A_h , so that

$$\mathbf{U} = \sum_{k=1}^{N-1} \eta_k \omega_{h,k}. \quad (3.1.21)$$

Then, for $s \geq 0$, we define the discrete Sobolev space X_h^s as the normed linear space with norm

$$\|\mathbf{U}\|_{X_h^s}^2 = \|A_h^s \mathbf{U}\|_{L_h^2}^2 = \pi \sum_{k=1}^{N-1} \lambda_{h,k}^{2s} |\eta_k|^2.$$

Remark 3.1.2

- i) For $s = 0$ we simply recover the L_h^2 norm and the discrete space X_h will be identical to our definition of the L_h^2 space, given that the elements are the grid restricted functions of the space X_h^o .
- ii) For $\alpha = 1/4$ we obtain the space $X_h^{1/4}$ which approximates the space $X^{1/4}$, with norm

$$\|\mathbf{U}\|_{X_h^{1/4}}^2 = \|A_h^{1/4}\mathbf{U}\|_{L_h^2}^2 = \pi \sum_{k=1}^{N-1} \lambda_{h,k}^{1/2} \eta_k^2.$$

Lemma 3.1.3 *The linear operator A_h is sectorial in the space X_h .*

Proof: A_h is closed and densely defined by its finite dimensionality. Also by considering the proof of Theorem 2.4.2 we note that a similar analysis will show that $\Gamma(A_h) \subseteq \mathcal{I}$ so that

$$\frac{1}{d(\lambda, \Gamma(A_h))} \leq \frac{1}{d(\lambda, \mathcal{I})},$$

which implies that A_h satisfies part iii) of Definition 2.2.3.

□

We now state and prove some important properties of these discrete Sobolev spaces.

Lemma 3.1.4 *Let $\mathbf{U} \in X_h^{1/4}$ with $\mathbf{U} = \sum_{k=1}^{N-1} \eta_k \boldsymbol{\omega}_{h,k}$. Then*

$$\|D_h^o \mathbf{U}\|_{L_h^2} = \frac{1}{\sqrt{2}} \|A_h^{1/4} \mathbf{U}\|_{L_h^2}.$$

Proof: We recall that $D_h^\circ \mathbf{U}$ is just a grid restricted element of X_h^e , hence

$$\begin{aligned} \|D_h^\circ \mathbf{U}\|_{L_h^2}^2 &= \frac{2\pi}{N} \sum_{j=0}^N c_j \sum_{k=1}^{N-1} k \eta_k \cos kx_j \sum_{l=1}^{N-1} l \eta_l \cos lx_j, \\ &= \pi \sum_{k=1}^{N-1} k^2 \eta_k^2, \\ &= \frac{1}{2} \left(\pi \sum_{k=1}^{N-1} \lambda_{h,k}^{1/2} \eta_k^2 \right), \end{aligned}$$

where $\lambda_{h,k}$ is given in Theorem 3.1.1, so that

$$\|D_h^\circ \mathbf{U}\|_{L_h^2}^2 = \frac{1}{2} \|A_h^{1/4} \mathbf{U}\|_{L_h^2}^2.$$

□

Lemma 3.1.5 *Let $\mathbf{U} \in X_h^{1/2}$ with $\mathbf{U} = \sum_{k=1}^{N-1} \eta_k \omega_{h,k}$. Then*

$$\|D_h^2 \mathbf{U}\|_{L_h^2} = \frac{1}{2} \|A_h^{1/2} \mathbf{U}\|_{L_h^2}.$$

Proof:

$$\begin{aligned} \|D_h^2 \mathbf{U}\|_{L_h^2}^2 &= \frac{2\pi}{N} \sum_{j=1}^{N-1} \sum_{k=1}^{N-1} k^2 \eta_k \sin kx_j \sum_{l=1}^{N-1} l^2 \eta_l \sin lx_j, \\ &= \pi \sum_{k=1}^{N-1} k^4 \eta_k^2 \quad \text{by (3.1.6),} \\ &= \frac{1}{4} \left(\pi \sum_{k=1}^{N-1} \lambda_{h,k} \eta_k^2 \right), \\ &= \frac{1}{4} \|A_h^{1/2} \mathbf{U}\|_{L_h^2}^2. \end{aligned}$$

□

Lemma 3.1.6 *Let $\mathbf{U} \in L_h^2$ with $\mathbf{U} = \sum_{k=1}^{N-1} \eta_k \omega_{h,k}$. Then*

$$\langle D_h^2 \mathbf{U}, \mathbf{U} \rangle_{L_h^2} = -\|\hat{D}_h^\circ \mathbf{U}\|_{L_h^2}^2,$$

where \widehat{D}_h^o is given in (3.1.11).

Proof:

$$\begin{aligned}
\langle D_h^2 \mathbf{U}, \mathbf{U} \rangle_{L_h^2} &= \frac{2\pi}{N} \sum_{j=1}^{N-1} (D_h^2 \mathbf{U})_j U_j, \\
&= \frac{2\pi}{N} \sum_{j=1}^{N-1} \sum_{k=1}^{N-1} [D_h^2]_{jk} U_k U_j, \\
&= \frac{2\pi}{N} \sum_{j=1}^{N-1} \sum_{k=1}^{N-1} \sum_{l=0}^N [\widehat{D}_h^e]_{jl} [\widehat{D}_h^o]_{lk} U_k U_j, \quad \text{by (3.1.16c),} \\
&= -\frac{2\pi}{N} \sum_{l=0}^N c_l \sum_{j=1}^{N-1} [\widehat{D}_h^o]_{lj} U_j \sum_{k=1}^{N-1} [\widehat{D}_h^o]_{lk} U_k, \quad \text{by (3.1.16a) and (3.1.16b),} \\
&= -\|\widehat{D}_h^o\|_{L_h^2}^2.
\end{aligned}$$

□

Lemma 3.1.7 Let $\mathbf{U} \in L_h^2$ with $\mathbf{U} = \sum_{k=1}^{N-1} \eta_k \boldsymbol{\omega}_{h,k}$. Then

$$\|D_h^o \mathbf{U}\|_{L_h^2}^2 \leq \|\widehat{D}_h^o \mathbf{U}\|_{L_h^2}^2.$$

Proof:

$$\begin{aligned}
\|\widehat{D}_h^o\|_{L_h^2}^2 &= \frac{2\pi}{N} \sum_{j=0}^N \left[\sum_{k=1}^{N-1} [\widehat{D}_h^o]_{jk} U_k \right]^2, \\
&= \frac{2\pi}{N} \left[\sum_{k=1}^{N-1} [\widehat{D}_h^o]_{0k} U_k \right]^2 + \|D_h^o\|_{L_h^2}^2 + \frac{2\pi}{N} \left[\sum_{k=1}^{N-1} [\widehat{D}_h^o]_{Nk} U_k \right]^2.
\end{aligned}$$

□

Lemma 3.1.8 Let $\mathbf{U} \in X_h^\sigma$ then for $\sigma \geq s \geq 0$,

$$\|A_h^s \mathbf{U}\|_{L_h^2} \leq \frac{1}{4^{\sigma-s}} \|A_h^\sigma \mathbf{U}\|_{L_h^2}.$$

Proof: By definition

$$\|A_h^s \mathbf{U}\|_{L_h^2}^2 = \pi \sum_{k=1}^{N-1} \lambda_{h,k}^{2s} \eta_k^2,$$

so that

$$\begin{aligned}
\|A_h^s \mathbf{U}\|_{L_h^2}^2 &= \pi \sum_{k=1}^{N-1} \lambda_{h,k}^{2\sigma} \eta_k^2 \lambda_{h,k}^{2s-2\sigma}, \\
&\leq 4^{2s-2\sigma} \left(\pi \sum_{k=1}^{N-1} \lambda_{h,k}^{2\sigma} \eta_k^2 \right), \quad \sigma \geq s, \\
&= \frac{1}{4^{2(\sigma-s)}} \|A_h^\sigma \mathbf{U}\|_{L_h^2}^2.
\end{aligned}$$

□

Lemma 3.1.9 *Let $\beta, \delta \geq 0$ and $\mathbf{U} \in X_h^s$ for $s = \max\{\beta, \delta\}$. Then for $\alpha = \beta\theta + (1-\theta)\delta$ with $0 < \theta < 1$, $\beta \geq 0$ the following is true*

$$\|A_h^\alpha \mathbf{U}\|_{L_h^2} \leq \|A_h^\beta \mathbf{U}\|_{L_h^2}^\theta \|A_h^\delta \mathbf{U}\|_{L_h^2}^{1-\theta}.$$

Proof: By definition

$$\begin{aligned}
\|A_h^\alpha \mathbf{U}\|_{L_h^2}^2 &= \pi \sum_{k=1}^{N-1} \lambda_{h,k}^{2\alpha} \eta_k^2, \\
&= \pi \sum_{k=1}^{N-1} \lambda_{h,k}^{2\beta\theta+2(1-\theta)\delta} \eta_k^{2\theta} \eta_k^{2(1-\theta)}, \\
&= \pi \sum_{k=1}^{N-1} \left(\lambda_{h,k}^{2\beta} \eta_k^2 \right)^\theta \left(\lambda_{h,k}^{2\delta} \eta_k^2 \right)^{1-\theta},
\end{aligned}$$

and applying Hölder's inequality gives

$$\|A_h^\alpha \mathbf{U}\|_{L_h^2}^2 \leq \left\{ \pi \sum_{k=1}^{N-1} \lambda_{h,k}^{2\beta} \eta_k^2 \right\}^\theta \left\{ \pi \sum_{l=1}^{N-1} \lambda_{h,l}^{2\delta} \eta_l^2 \right\}^{1-\theta},$$

so that

$$\|A_h^\alpha \mathbf{U}\|_{L_h^2}^2 = \|A_h^\beta \mathbf{U}\|_{L_h^2}^{2\theta} \|A_h^\delta \mathbf{U}\|_{L_h^2}^{2(1-\theta)}.$$

□

Lemma 3.1.10 *Let $\mathbf{U} \in X_h^{1/4}$ with $\mathbf{U} = \sum_{k=1}^{N-1} \eta_k \boldsymbol{\omega}_{h,k}$. Then*

$$\|\mathbf{U}\|_{L_h^\infty} \leq \sqrt{2} \|\mathbf{U}\|_{L_h^2}^{1/2} \|A_h^{1/4} \mathbf{U}\|_{L_h^2}^{1/2}.$$

Proof: Let $u_h(x)$ be the interpolant of the vector \mathbf{U} then

$$\begin{aligned} \|\mathbf{U}\|_{L_h^\infty} &= \max_{1 \leq j \leq N-1} |U_j|, \\ &\leq \max_{0 \leq x \leq \pi} |u_h(x)|, \\ &\leq \sqrt{2} \|u_h(x)\|_{L^2}^{1/2} \left\| \frac{\partial u_h(x)}{\partial x} \right\|_{L^2}^{1/2}, \end{aligned} \quad (3.1.22)$$

by Agmon's inequality, which is

$$\|u\|_{L^\infty} \leq \sqrt{2} \|u\|_{L^2}^{1/2} \|u_x\|_{L^2}^{1/2}, \quad (3.1.23)$$

so that (3.1.22) becomes

$$\begin{aligned} \|\mathbf{U}\|_{L_h^\infty} &= \sqrt{2} \|\mathbf{U}\|_{L_h^2}^{1/2} \|A_h^{1/4} \mathbf{U}\|_{L_h^2}^{1/2}, \\ &= \sqrt{2} \|\mathbf{U}\|_{L_h^2}^{1/2} \|A_h^{1/4} \mathbf{U}\|_{L_h^2}^{1/2}, \end{aligned}$$

by definition of the discrete norm, since $u_h \in X_h^o$.

□

Discrete Gevrey spaces can also be defined for the semi-discrete equation (3.1.17). Given $\mathbf{U} \in L_h^2$ with Fourier expansion $\mathbf{U} = \sum_{k=1}^{N-1} \eta_k \boldsymbol{\omega}_{h,k}$ we define the discrete Gevrey class of regularity τ , $G_{\tau,h}$, to be the space of L_h^2 functions with norm defined by

$$\|\mathbf{U}\|_{G_{\tau,h}}^2 = \|A_h^s e^{\tau A_h^s} \mathbf{U}\|_{L_h^2}^2 = \pi \sum_{k=1}^{N-1} \lambda_{h,k}^{2s} e^{2\tau \lambda_{h,k}^s} \eta_k^2.$$

As with the continuous case we will only consider the Gevrey spaces with $s = 1/4$. Given these spaces it is possible to formulate analogous results to the ones in

Theorems 2.2.16 and 2.2.18.

Theorem 3.1.11 *Let $\mathbf{U} \in L_h^2$ and suppose there exists positive constants $C, \tau > 0$ such that*

$$\|A_h^{1/4} e^{\tau A_h^{1/4}} \mathbf{U}\|_{L_h^2}^2 \leq C < \infty.$$

Then for all $0 < \sigma < \tau$ we have that

$$\|A_h^{1/4} e^{\sigma A_h^{1/4}} \mathbf{U}\|_{L_h^2}^2 \leq \|A_h^{1/4} e^{\tau A_h^{1/4}} \mathbf{U}\|_{L_h^2}^2 \leq C.$$

Proof: The proof is similar to the proof of Theorem 2.2.16. □

Theorem 3.1.12 *For all $\tau > 0$ and $s \geq 0$ we have the following inclusion*

$$G_{\tau,h} \subset X_h^s.$$

Proof: The proof is similar to the proof of Theorem 2.2.18. □

We now state an important result which relates continuous Gevrey spaces and the discrete Gevrey spaces we have just defined.

Theorem 3.1.13 *Let $\mathbf{U} \in L_h^2$ and suppose that there exists constants $C, \tau > 0$, so that \mathbf{U} satisfies*

$$\|A_h^{1/4} e^{\tau A_h^{1/4}} \mathbf{U}\|_{L_h^2} \leq C,$$

then there exists $u \in G_\tau$, such that

$$\|A^{1/4} e^{\tau A^{1/4}} u\|_{L^2} \leq C,$$

where $u(x_j) = U_j$ for $j = 1, 2, \dots, N-1$.

Proof: For $\mathbf{U} \in L_h^2$ we have the following Fourier expansion

$$\mathbf{U} = \sum_{k=1}^{N-1} \eta_k \boldsymbol{\omega}_{h,k}.$$

We define

$$u(x) = \sum_{k=1}^{N-1} \eta_k \omega_k,$$

where $\omega_k = \sin(kx)$ so that $u \in L^2$. This implies that

$$\begin{aligned} \|A^{1/4} e^{\tau A^{1/4}} u\|_{L^2}^2 &= \pi \sum_{k=1}^{N-1} \lambda_k^{1/2} e^{2\tau \lambda_k^{1/4}} \eta_k^2, \\ &= \|A_h^{1/4} e^{\tau A_h^{1/4}} \mathbf{U}\|_{L_h^2}^2, \\ &\leq C. \end{aligned}$$

Hence $u \in G_\tau$.

□

3.2 Nonlinear stability and convergence

3.2.1 Stability for the semi-discrete approximation

We now consider the dissipative properties of the semi-discrete system (3.1.17) in the L_h^2 space. Premultiplying (3.1.17) by $2h\mathbf{U}^T$ gives

$$\begin{aligned} \frac{1}{2} \frac{d}{dt} \|\mathbf{U}\|_{L_h^2}^2 + 4\langle D_h^4 \mathbf{U}, \mathbf{U} \rangle_{L_h^2} + \alpha \langle D_h^2 \mathbf{U}, \mathbf{U} \rangle_{L_h^2} \\ + 2h \frac{\alpha}{3} \sum_{i,j=1}^{N-1} [U_i^2 d_{ij}^o U_j + U_i d_{ij}^e U_j^2] = 0, \end{aligned} \quad (3.2.1)$$

where d_{ij}^o and d_{ij}^e denote elements in the matrices D_h^o and D_h^e respectively. Matrix property (3.1.16a) implies that

$$\sum_{i,j=1}^{N-1} [d_{ij}^o U_i^2 U_j + d_{ij}^e U_i U_j^2] = \sum_{i,j=1}^{N-1} U_i^2 U_j (d_{ij}^o + d_{ji}^e) = 0,$$

hence equation (3.2.1) becomes

$$\frac{1}{2} \frac{d}{dt} \|\mathbf{U}\|_{L_h^2}^2 + 4\langle D_h^4 \mathbf{U}, \mathbf{U} \rangle_{L_h^2} + \alpha \langle D_h^2 \mathbf{U}, \mathbf{U} \rangle_{L_h^2} = 0.$$

Finally, by considering the eigenvalues of D_h^2 and D_h^4 which are k^4 and k^2 respectively, for $0 \leq k \leq N-1$, we obtain

$$\frac{1}{2} \frac{d}{dt} \|\mathbf{U}\|_{L_h^2}^2 \leq [-4 + \alpha(N-1)^2] \|\mathbf{U}\|_{L_h^2}^2.$$

This inequality however gives no information on the growth of \mathbf{U} in the L_h^2 norm if $\alpha(N-1)^2 > 4$. A much more involved stability analysis has been carried by Wallace and Sloan in [94]. For completeness we state and prove their main stability result below.

Theorem 3.2.1 *Let $\mathbf{U} \in L_h^2$ and assume that the matrix*

$$\mathcal{D} - \gamma D_h^4,$$

is positive semi-definite, where \mathcal{D} is given below by (3.2.6) and $0 \leq \gamma \leq 4$. Then for $\mathbf{U}(0)$ in the set $\{\mathbf{V} \in L_h^2 : \|\mathbf{V}\|_{L_h^2} \leq \rho, \}$ we have that

$$\|\mathbf{U}(t)\|_{L_h^2} \leq \rho \quad \forall t \geq 0. \quad (3.2.2)$$

Proof: We set $\mathbf{U}(t) := \mathbf{Z} + \mathbf{W}(t)$ in equation (3.1.17) where \mathbf{Z} is independent of t , which gives the following equation

$$\frac{d\mathbf{W}}{dt} + 4D_h^4\mathbf{W} + \alpha D_h^2\mathbf{W} + B_h(\mathbf{W}, \mathbf{Z}) + B_h(\mathbf{Z}, \mathbf{W}) + B_h(\mathbf{W}, \mathbf{W}) = \mathbf{f}, \quad (3.2.3)$$

where

$$B_h(\mathbf{U}, \mathbf{V}) = \frac{\alpha}{3} [\mathbf{U} \otimes D_h^o \mathbf{V} + D_h^e(\mathbf{U} \otimes \mathbf{V})],$$

and

$$\mathbf{f} = -B_h(\mathbf{Z}, \mathbf{Z}) - 4D_h^4\mathbf{Z} - \alpha D_h^2\mathbf{Z}.$$

Premultiplying (3.2.3) by $2h\mathbf{W}^T$ gives

$$\begin{aligned} \frac{1}{2} \frac{d}{dt} \|\mathbf{W}\|_{L_h^2}^2 + 4\langle D_h^4\mathbf{W}, \mathbf{W} \rangle_{L_h^2} + \alpha \langle D_h^2\mathbf{W}, \mathbf{W} \rangle_{L_h^2} \\ + \frac{2h\alpha}{3} \sum_{i,j=1}^{N-1} W_i [d_{ij}^o(W_i Z_j + W_j Z_i) + 2d_{ij}^e W_j Z_j] = \langle \mathbf{W}, \mathbf{f} \rangle_{L_h^2}. \end{aligned} \quad (3.2.4)$$

Now

$$\begin{aligned} \sum_{i,j=1}^{N-1} W_i [d_{ij}^o(W_i Z_j + W_j Z_i) + 2W_j Z_j d_{ij}^e] &= \sum_{i,j=1}^{N-1} W_i d_{ij}^o(W_i Z_j - W_j Z_i), \\ &= \mathbf{W}^T (R - S) \mathbf{W}, \end{aligned}$$

where

$$R = \text{diag}(R_1, R_2, \dots, R_{N-1}) \quad \text{with} \quad R_i = \sum_{j=1}^{N-1} d_{ij}^o Z_j,$$

and S is the $(N - 1) \times (N - 1)$ square matrix defined by

$$S_{ij} = \frac{1}{2}(Z_i d_{ij}^o + Z_j d_{ji}^o).$$

Hence equation (3.2.4) becomes

$$\begin{aligned} \frac{1}{2} \frac{d}{dt} \|\mathbf{W}\|_{L_h^2}^2 + 4 \langle D_h^4 \mathbf{W}, \mathbf{W} \rangle_{L_h^2} + \alpha \langle D_h^2 \mathbf{W}, \mathbf{W} \rangle_{L_h^2} \\ + \frac{2h\alpha}{3} \mathbf{W}^T (R - S) \mathbf{W} = \langle \mathbf{W}, \mathbf{f} \rangle_{L_h^2}. \end{aligned}$$

Applying Young's inequality to the right hand side of this equation gives

$$\frac{1}{2} \frac{d}{dt} \|\mathbf{W}\|_{L_h^2}^2 + 2h \mathbf{W}^T \mathcal{D} \mathbf{W} \leq \frac{\epsilon}{2} \|\mathbf{W}\|_{L_h^2}^2 + \frac{1}{2\epsilon} \|\mathbf{f}\|_{L_h^2}^2, \quad (3.2.5)$$

where $\epsilon > 0$ and

$$\mathcal{D} = 4D_h^4 + \alpha D_h^2 + \frac{\alpha}{3}(R - S). \quad (3.2.6)$$

If the matrix $\mathcal{D} - \gamma D_h^4$ is assumed to be positive semi-definite for some real number $0 \leq \gamma \leq 4$ and some choice of \mathbf{Z} then (3.2.5) becomes

$$\frac{1}{2} \frac{d}{dt} \|\mathbf{W}\|_{L_h^2}^2 + 2h\gamma \mathbf{W}^T D_h^4 \mathbf{W} - \frac{\epsilon}{2} \|\mathbf{W}\|_{L_h^2}^2 \leq \frac{1}{2\epsilon} \|\mathbf{f}\|_{L_h^2}^2,$$

which implies that

$$\frac{1}{2} \frac{d}{dt} \|\mathbf{W}\|_{L_h^2}^2 + \gamma \|D_h^2 \mathbf{W}\|_{L_h^2}^2 - \frac{\epsilon}{2} \|\mathbf{W}\|_{L_h^2}^2 \leq \frac{1}{2\epsilon} \|\mathbf{f}\|_{L_h^2}^2.$$

Applying Poincaré's inequality to the second norm on the left hand side of this equation and setting $\epsilon = \gamma$ gives

$$\frac{d}{dt} \|\mathbf{W}\|_{L_h^2}^2 + \gamma \|\mathbf{W}\|_{L_h^2}^2 \leq \frac{1}{\gamma} \|\mathbf{f}\|_{L_h^2}^2.$$

If we now integrate this equation we obtain

$$\|\mathbf{W}(t)\|_{L_h^2}^2 \leq e^{-\gamma t} \|\mathbf{W}(0)\|_{L_h^2}^2 + \frac{1}{\gamma^2} (1 - e^{-\gamma t}) \|\mathbf{f}\|_{L_h^2}^2,$$

and (3.2.2) follows with

$$\rho = \frac{\|\mathbf{f}\|_{L_h^2}^2}{\gamma} + \epsilon,$$

for any $\epsilon > 0$.

□

Remark 3.2.2 The condition that the matrix $\mathcal{D} - \gamma D_h^4$ is positive semi-definite has been verified numerically in [94] with the vector \mathbf{Z} defined by

$$\mathbf{Z} = \eta[h, 2h, \dots, (N-1)h]^T,$$

for some positive parameter η .

3.2.2 Consistency for the semi-discrete approximation

We now consider the consistency of the PS approximation method (3.1.17). In order to prove that this approximation method is consistent we will need the following results which give estimates on the interpolation error produced by the PS method.

Lemma 3.2.3 *Assume that $u(x) \in X^s$, $s > 1/8$, then for any real σ , with $0 \leq \sigma \leq s$, we have*

$$\|I_h^\sigma(u(x)) - u(x)\|_{X^\sigma} \leq Ch^{4(s-\sigma)} \|u(x)\|_{X^s},$$

where C is some positive constant independent of u .

Proof: See Voigt, Gottlieb and Hussaini [92, Theorem 2.1, p.6].

□

This means that if $u(x)$ has more than a ‘one-half’ bounded derivative then we can control the aliasing error that arises in PS collocation. We now state a more applicable result for our discrete Sobolev spaces.

Lemma 3.2.4 *Assume that $u(x) \in X^s$, $s > 1/8$, then for any real σ , with $0 \leq \sigma \leq s$, we have*

$$\|I_h^o(\mathbf{u}) - \mathbf{u}\|_{X_h^\sigma} \leq Ch^{4(s-\sigma)} \|u(x)\|_{X^s},$$

where C is some positive constant independent of u .

Proof: See [92, Theorem 2.4, p.7]. □

Below we will denote by $\mathbf{u}(t) \in \mathbb{R}^{N-1}$, for $t \in [0, T]$, the restriction of the continuous solution of the K-S equation (2.3.7) to the internal grid points of (3.1.2), i.e.,

$$\mathbf{u}(t) = [u(x_1, t), u(x_2, t), \dots, u(x_{N-1}, t)]^T.$$

Hence the truncation error, $\tau(t)$, for our PS discretization is given by

$$\tau(t) = \frac{d\mathbf{u}}{dt} + 4D_h^4\mathbf{u} + \alpha D_h^2\mathbf{u} + \frac{\alpha}{3}(\mathbf{u} \otimes D_h^o\mathbf{u} + D_h^e(\mathbf{u} \otimes \mathbf{u})). \quad (3.2.7)$$

Before we state and prove our consistency result we will need the following lemma.

Lemma 3.2.5 *Let $u(x) \in X^{1/2}$, then*

$$\|D_h^o\mathbf{u}(t)\|_{L_h^\infty} \leq C\|u(x)\|_{X^{1/2}},$$

where C is some constant independent of u .

Proof: By definition

$$\|D_h^o\mathbf{u}\|_{L_h^\infty} \leq \max_{0 \leq j \leq N} \left| \sum_{i=1}^{N-1} [\hat{D}_h^o]_{ji} u(x_i) \right|,$$

which implies that

$$\begin{aligned} \|D_h^o \mathbf{u}\|_{L_h^\infty} &\leq \max_{0 \leq j \leq N} |\mathcal{D}_h^o u(x_j)|, \\ &\leq \max_{0 \leq x \leq \pi} \left| \frac{\partial}{\partial x} I_h^o u \right|, \\ &\leq \sqrt{2} \left\| \frac{\partial}{\partial x} I_h^o u \right\|_{L^2}^{1/2} \left\| \frac{\partial^2}{\partial x^2} I_h^o u \right\|_{L^2}^{1/2}, \end{aligned}$$

by Agmon's inequality (3.1.23). Hence applying Lemma 3.2.3 and Theorem 2.1.5 gives

$$\|D_h^o \mathbf{u}\|_{L_h^\infty} \leq C \|u(x, t)\|_{X^{1/2}}.$$

□

Theorem 3.2.6 *Let $h > 0$ be sufficiently small and the initial condition u_0 of the K-S equation (2.3.7) be in the space X^s , for $s > 9/8$ with $4s \in \mathbb{N}$. Then given any $T > 0$ there exists a positive constant C such that*

$$\|\tau(t)\|_{L_h^2} \leq C(\alpha, T, \|u_0\|_{X^s}) h^{4(s-1)}, \quad \forall t \in [0, T]. \quad (3.2.8)$$

Proof: We let $\mathbf{u}_{xxxx}, \mathbf{u}_{xx}, \mathbf{u}_x$ and $(\mathbf{u}^2)_x$ denote the grid restrictions of the functions u_{xxxx}, u_{xx}, u_x and $(u^2)_x$ in equation (2.3.7), so that the truncation error can be written as

$$\begin{aligned} \tau(t) &= 4 [D_h^4 \mathbf{u} - \mathbf{u}_{xxxx}] + \alpha [D_h^2 \mathbf{u} - \mathbf{u}_{xx}] \\ &\quad + \frac{\alpha}{3} [\mathbf{u} \otimes D_h^o \mathbf{u} - \mathbf{u} \otimes \mathbf{u}_x + D_h^e (\mathbf{u} \otimes \mathbf{u}) - (\mathbf{u}^2)_x]. \end{aligned} \quad (3.2.9)$$

Taking the L_h^2 norm of this equation gives

$$\begin{aligned} \|\tau(t)\|_{L_h^2} &\leq 4 \|D_h^4 \mathbf{u} - \mathbf{u}_{xxxx}\|_{L_h^2} + \alpha \|D_h^2 \mathbf{u} - \mathbf{u}_{xx}\|_{L_h^2} \\ &\quad + \frac{\alpha}{3} \left(\|\mathbf{u}\|_{L_h^\infty} \|D_h^o \mathbf{u} - \mathbf{u}_x\|_{L_h^2} + \|D_h^e (\mathbf{u} \otimes \mathbf{u}) - (\mathbf{u}^2)_x\|_{L_h^2} \right), \end{aligned}$$

which is equivalent to

$$\begin{aligned} \|\tau(t)\|_{L_h^2} &\leq 4\|(I_h^\circ \mathbf{u})_{xxxx} - \mathbf{u}_{xxxx}\|_{L_h^2} + \alpha\|(I_h^\circ \mathbf{u})_{xx} - \mathbf{u}_{xx}\|_{L_h^2} \\ &\quad + \frac{\alpha}{3} \left(\|\mathbf{u}\|_{L_h^\infty} \|(I_h^\circ \mathbf{u})_x - \mathbf{u}_x\|_{L_h^2} + \|I_h^\circ((\mathbf{u}^2)_x) - (\mathbf{u}^2)_x\|_{L_h^2} \right). \end{aligned} \quad (3.2.10)$$

If we apply Lemma 3.2.4 to the first term on the right hand side of the above equation, then we obtain

$$\|(I_h^\circ \mathbf{u})_{xxxx} - \mathbf{u}_{xxxx}\|_{L_h^2} \leq C_1 h^{4\sigma} \|u_{xxxx}\|_{X^\sigma},$$

for some $\sigma \geq 0$, which implies that

$$\|(I_h^\circ \mathbf{u})_{xxxx} - \mathbf{u}_{xxxx}\|_{L_h^2} \leq C_2 h^{4\sigma} \|u\|_{X^{\sigma+1}},$$

by Theorem 2.1.5. Now letting $\sigma = s - 1$, $s \geq 0$, gives

$$\|(I_h^\circ \mathbf{u})_{xxxx} - \mathbf{u}_{xxxx}\|_{L_h^2} \leq C_2 h^{4(s-1)} \|u\|_{X^s}.$$

In order to satisfy the assumptions in Lemma 3.2.4 we must choose $\sigma = s - 1 > 1/8$ which implies that $s > 9/8$. Hence applying Lemma 3.2.4 to all the L_h^2 norms on the right hand side of equation (3.2.10) gives

$$\begin{aligned} \|\tau(t)\|_{L_h^2} &\leq C_2 \|u(t)\|_{X^s} h^{4(s-1)} + C_3 \|u(t)\|_{X^s} h^{4(s-1/2)} \\ &\quad + C_4 \|\mathbf{u}\|_{L_h^\infty} \|u(t)\|_{X^s} h^{4(s-1/4)} + C_5 \|(u(t))^2\|_{X^s} h^{4(s-1/4)}. \end{aligned} \quad (3.2.11)$$

Now since $s > 9/8$ we have that

$$\|\mathbf{u}(t)\|_{L_h^\infty} \leq \sqrt{2} \|u(t)\|_{L^2}^{1/2} \|u(t)\|_{X^{1/4}}^{1/2} \leq C_6 \|u(t)\|_{X^s},$$

by Agmon's inequality (3.1.23) and Theorem 2.1.5 respectively. Also Theorem 2.1.7 implies that

$$\|(u(t))^2\|_{X^s} \leq C_7 \|u(t)\|_{X^s}^2.$$

Hence the truncation error in equation (3.2.11) can be bounded as follows

$$\|\tau(t)\|_{L_h^2} \leq C_8(\alpha, \|u(x, t)\|_{X^s})h^{4(s-1)}, \quad (3.2.12)$$

for $t > 0$. Finally extending the result of Theorem 2.2.12 to the interval $[0, T]$ implies that it is possible to obtain this bound in terms of the initial condition u_0 .

□

3.2.3 Convergence for the semi-discrete approximation

Given the consistency result of our approximation above, we are now in a position to prove a convergence result.

Theorem 3.2.7 *Let $h > 0$ be sufficiently small, $u_0 \in X^s$ for $s > 9/8$ with $4s \in \mathbb{N}$. Then given $T > 0$ there exists a positive constant C such that*

$$\|\mathbf{u}(t) - \mathbf{U}(t)\|_{L_h^2} \leq C(\alpha, T, \|u_0\|_{X^s})h^{4(s-1)}, \quad \forall t \in [0, T]. \quad (3.2.13)$$

Proof: Subtracting (3.1.17) from (3.2.7) gives

$$\begin{aligned} \frac{d}{dt}\mathbf{E} + 4D_h^4\mathbf{E} + \alpha D_h^2\mathbf{E} + \frac{\alpha}{3}(\mathbf{u} \otimes D_h^\circ \mathbf{u} - \mathbf{U} \otimes D_h^\circ \mathbf{U}) \\ + \frac{\alpha}{3}(D_h^e(\mathbf{u} \otimes \mathbf{u}) - D_h^e(\mathbf{U} \otimes \mathbf{U})) = \tau, \end{aligned}$$

where $\mathbf{E} = \mathbf{u} - \mathbf{U}$ and $\tau = \tau(t)$. Premultiplying by $2h\mathbf{E}^T$ gives

$$\begin{aligned} \frac{1}{2} \frac{d}{dt} \|\mathbf{E}\|_{L_h^2}^2 &= -4\|D_h^2\mathbf{E}\|_{L_h^2}^2 - \alpha \langle D_h^2\mathbf{E}, \mathbf{E} \rangle_{L_h^2} \\ &\quad - \frac{\alpha}{3} \left(\langle \mathbf{u} \otimes D_h^\circ \mathbf{u} - \mathbf{U} \otimes D_h^\circ \mathbf{U}, \mathbf{E} \rangle_{L_h^2} \right. \\ &\quad \left. + \langle \mathbf{U} \otimes \mathbf{U} - \mathbf{u} \otimes \mathbf{u}, D_h^\circ \mathbf{E} \rangle_{L_h^2} \right) + \langle \tau, \mathbf{E} \rangle_{L_h^2}, \\ &= -4\|D_h^2\mathbf{E}\|_{L_h^2}^2 - \alpha \langle D_h^2\mathbf{E}, \mathbf{E} \rangle_{L_h^2} \\ &\quad - \frac{\alpha}{3} \left(\langle (\mathbf{u} - \mathbf{U}) \otimes D_h^\circ \mathbf{u} + \mathbf{U} \otimes D_h^\circ (\mathbf{u} - \mathbf{U}), \mathbf{E} \rangle_{L_h^2}^2 \right. \\ &\quad \left. + \langle (\mathbf{U} - \mathbf{u}) \otimes (\mathbf{U} - \mathbf{u}) + 2\mathbf{u} \otimes \mathbf{U} - 2\mathbf{u} \otimes \mathbf{u}, D_h^\circ \mathbf{E} \rangle_{L_h^2} \right) \\ &\quad + \langle \tau, \mathbf{E} \rangle_{L_h^2}, \end{aligned}$$

so that

$$\begin{aligned} \frac{1}{2} \frac{d}{dt} \|\mathbf{E}\|_{L_h^2}^2 &= -4 \|D_h^2 \mathbf{E}\|_{L_h^2}^2 - \alpha \langle D_h^2 \mathbf{E}, \mathbf{E} \rangle_{L_h^2} \\ &\quad - \frac{\alpha}{3} \left(\langle \mathbf{E} \otimes D_h^\circ \mathbf{u} - (\mathbf{u} - \mathbf{U}) \otimes D_h^\circ \mathbf{E} + \mathbf{u} \otimes D_h^\circ (\mathbf{u} - \mathbf{U}), \mathbf{E} \rangle_{L_h^2}^2 \right. \\ &\quad \left. + \langle \mathbf{E} \otimes \mathbf{E} - 2\mathbf{u} \otimes \mathbf{E}, D_h^\circ \mathbf{E} \rangle_{L_h^2} \right) + \langle \boldsymbol{\tau}, \mathbf{E} \rangle_{L_h^2}, \end{aligned}$$

which can be written as

$$\begin{aligned} \frac{1}{2} \frac{d}{dt} \|\mathbf{E}\|_{L_h^2}^2 &= -4 \|D_h^2 \mathbf{E}\|_{L_h^2}^2 - \alpha \langle D_h^2 \mathbf{E}, \mathbf{E} \rangle_{L_h^2}, \\ &\quad - \frac{\alpha}{3} \left(\langle \mathbf{E} \otimes D_h^\circ \mathbf{u}, \mathbf{E} \rangle_{L_h^2} - \langle \mathbf{E} \otimes D_h^\circ \mathbf{E}, \mathbf{E} \rangle_{L_h^2} + \langle \mathbf{u} \otimes D_h^\circ \mathbf{E}, \mathbf{E} \rangle_{L_h^2}^2 \right. \\ &\quad \left. + \langle \mathbf{E} \otimes \mathbf{E}, D_h^\circ \mathbf{E} \rangle_{L_h^2} - 2 \langle \mathbf{u} \otimes \mathbf{E}, D_h^\circ \mathbf{E} \rangle_{L_h^2} \right) + \langle \boldsymbol{\tau}, \mathbf{E} \rangle_{L_h^2}. \quad (3.2.14) \end{aligned}$$

Equating the terms together in this equation gives

$$\begin{aligned} \frac{1}{2} \frac{d}{dt} \|\mathbf{E}\|_{L_h^2}^2 &= -4 \|D_h^2 \mathbf{E}\|_{L_h^2}^2 - \alpha \langle D_h^2 \mathbf{E}, \mathbf{E} \rangle_{L_h^2} \\ &\quad - \frac{\alpha}{3} \left(\langle \mathbf{E} \otimes D_h^\circ \mathbf{u}, \mathbf{E} \rangle_{L_h^2} - \langle \mathbf{u} \otimes \mathbf{E}, D_h^\circ \mathbf{E} \rangle_{L_h^2} \right) \\ &\quad + \langle \boldsymbol{\tau}, \mathbf{E} \rangle_{L_h^2}, \quad (3.2.15) \end{aligned}$$

so that

$$\begin{aligned} \frac{1}{2} \frac{d}{dt} \|\mathbf{E}\|_{L_h^2}^2 &\leq -4 \|D_h^2 \mathbf{E}\|_{L_h^2}^2 - \alpha \langle D_h^2 \mathbf{E}, \mathbf{E} \rangle_{L_h^2} + \frac{\alpha}{3} C_1 \|\mathbf{E}\|_{L_h^2}^2 \\ &\quad + \frac{\alpha}{3} C_2 \|\mathbf{E}\|_{L_h^2} \|D_h^\circ \mathbf{E}\|_{L_h^2} + \|\boldsymbol{\tau}\|_{L_h^2} \|\mathbf{E}\|_{L_h^2}. \quad (3.2.16) \end{aligned}$$

In this equation we have bounded $\|D_h^\circ \mathbf{u}\|_{L_h^\infty}$ by C_1 using Lemma 3.2.5 and $\|\mathbf{u}\|_{L_h^\infty}$ by C_2 using the argument in the proof of Theorem 3.2.6. Now applying Young's inequality to the last two products in (3.2.16) and using the fact that $\|D_h^\circ \mathbf{E}\|_{L_h^2} \leq \|\widehat{D}_h^\circ \mathbf{E}\|_{L_h^2}$, gives

$$\begin{aligned} \frac{1}{2} \frac{d}{dt} \|\mathbf{E}\|_{L_h^2}^2 &\leq -4 \|D_h^2 \mathbf{E}\|_{L_h^2}^2 + \left(\alpha + \frac{\alpha}{6} C_2 \right) \|\widehat{D}_h^\circ \mathbf{E}\|_{L_h^2}^2 \\ &\quad + \left(\frac{\alpha}{3} C_1 + \frac{\alpha}{6} C_2 + \frac{1}{2} \right) \|\mathbf{E}\|_{L_h^2}^2 + \frac{1}{2} \|\boldsymbol{\tau}\|_{L_h^2}^2, \end{aligned}$$

which implies that

$$\frac{d}{dt} \|\mathbf{E}\|_{L_h^2}^2 \leq \left[\frac{2\alpha}{3} C_1 + \frac{\alpha}{3} C_2 + \left(\frac{2\alpha + \alpha C_2/3}{2\sqrt{8}} \right)^2 + 1 \right] \|\mathbf{E}\|_{L_h^2}^2 + \|\boldsymbol{\tau}\|_{L_h^2}^2, \quad (3.2.17)$$

since

$$-8\|D_h^2 \mathbf{E}\|_{L_h^2}^2 + \left(2\alpha + \frac{\alpha C_2}{3} \right) \|D_h^2 \mathbf{E}\|_{L_h^2}^2 \leq \left(\frac{2\alpha + \alpha C_2/3}{2\sqrt{8}} \right)^2 \|\mathbf{E}\|_{L_h^2}^2.$$

Integrating (3.2.17) with respect to time gives

$$\|\mathbf{E}(t)\|_{L_h^2}^2 \leq e^{Kt} \left[\|\mathbf{E}(0)\|_{L_h^2}^2 + \int_0^t e^{-Ks} \|\boldsymbol{\tau}(s)\|_{L_h^2}^2 ds \right], \quad (3.2.18)$$

where

$$K = \left[\frac{2\alpha}{3} C_1 + \frac{\alpha}{3} C_2 + \left(\frac{2\alpha + \alpha C_2/3}{2\sqrt{8}} \right)^2 + 1 \right].$$

Given that $\mathbf{E}(0) = \mathbf{u}(0) - \mathbf{U}(0) = 0$ and using the bound for the truncation error in Theorem 3.2.6, we can obtain the following error bound

$$\|\mathbf{U}(t) - \mathbf{u}(t)\|_{L_h^2} = C(\alpha, T, \|u_0\|_{X^s}) h^{4(s-1)},$$

for $t \in [0, T]$.

□

We can extend the last theorem to obtain error estimates in the L^2 and $X^{1/4}$ norms.

Corollary 3.2.8 *Let $h > 0$ be sufficiently small, $u_0 \in X^s$ for $s > 9/8$ with $4s \in \mathbb{N}$ and let $u_h(x, t)$ be the interpolant, on the interval $[0, \pi]$, of the vector $\mathbf{U}(t)$ given in Theorem 3.2.7. Then given $T > 0$ there exists a positive constant C such that*

$$\|u(x, t) - u_h(x, t)\|_{L^2} \leq C(\alpha, T, \|u_0\|_{X^s}) h^{4(s-1)}, \quad \forall t \in [0, T], \quad (3.2.19)$$

Proof: We have that

$$\begin{aligned} \|u(x, t) - u_h(x, t)\|_{L^2} &\leq \|u(x, t) - I_h^o(u(x, t))\|_{L^2} + \|I_h^o(u(x, t)) - u_h(x, t)\|_{L^2}, \\ &= \|u(x, t) - I_h^o(u(x, t))\|_{L^2} + \|\mathbf{u}(t) - \mathbf{U}(t)\|_{L_h^2}, \end{aligned}$$

by definition of the operator I_h^o . Hence the above equation becomes

$$\begin{aligned} \|u(x, t) - u_h(x, t)\|_{L^2} &\leq C'(\alpha, T, \|u_0\|_{X^s})h^{4s} + \|\mathbf{u}(t) - \mathbf{U}\|_{L_h^2}, \\ &\leq C(\alpha, T, \|u_0\|_{X^s})h^{4(s-1)}, \end{aligned}$$

by Lemma 3.2.3 and Theorem 3.2.7 .

□

Corollary 3.2.9 *Let $h > 0$ be sufficiently small, $u_0 \in X^s$ for $s \geq 5/4$ with $4s \in \mathbb{N}$ and $u_h(x, t)$ be the interpolant, on the interval $[0, \pi]$, of the vector $\mathbf{U}(t)$ given in Theorem 3.2.7. Then given $T > 0$ there exists a positive constant C such that*

$$\|u(x, t) - u_h(x, t)\|_{X^{1/4}} \leq C(\alpha, T, \|u_0\|_{X^s})h^{4(s-5/4)}, \quad \forall t \in [0, T], \quad (3.2.20)$$

Proof: We note that

$$\|u - u_h\|_{X^{1/4}} \leq \|u - I_h^o(u)\|_{X^{1/4}} + \|A^{1/4}(I_h^o(u) - u_h)\|_{L^2},$$

so that

$$\|u - u_h\|_{X^{1/4}} \leq C'\|u\|_{X^s}h^{4(s-1/4)} + \sqrt{2}N\|I_h^o(u) - u_h\|_{L^2},$$

by the eigenvalues of the operator A and Lemma 3.2.3. Therefore we obtain

$$\|u - u_h\|_{X^{1/4}} \leq C(\alpha, T, \|u_0\|_{X^s})h^{4(s-5/4)},$$

by Corollary 3.2.8.

□

A similar error estimate, to the one obtained in Theorem 3.2.7, for the PS approximation of the K-S equation with periodic boundary conditions is given in López-Marcos [60]. However in order to obtain the estimate in this paper artificial assumptions have to be made on the approximation, notably that $\|\mathbf{U}\|_{L_h^\infty}$ is bounded. These terms will arise in bounding the inner product $\langle \mathbf{E} \otimes D_h^\circ \mathbf{E}, \mathbf{E} \rangle_{L_h^2}$ in (3.2.14). We have managed to overcome this assumption due to the way in which we split the nonlinear term uu_x , see (3.1.1), prior to the discretization. This has enabled us to use the fact that

$$\langle \mathbf{E} \otimes D_h^\circ \mathbf{E}, \mathbf{E} \rangle_{L_h^2} + \langle D_h^\circ (\mathbf{E} \otimes \mathbf{E}), \mathbf{E} \rangle_{L_h^2} = 0,$$

in order to go from step (3.2.14) to step (3.2.15), in the proof of Theorem 3.2.7. In [60], the nonlinear term uu_x is approximated only by $D_h^\circ (\mathbf{U} \otimes \mathbf{U})$. Hence in the error analysis in this paper, one obtains

$$\langle \mathbf{u}^2 - \mathbf{U}^2, D_h^\circ \mathbf{E} \rangle_{L_h^2},$$

and this is bounded by

$$(\|\mathbf{u}\|_{L_h^\infty} + \|\mathbf{U}\|_{L_h^\infty}) \|\mathbf{E}\|_{L_h^2} \|D_h^\circ \mathbf{E}\|_{L_h^2},$$

which involve the $\|\mathbf{U}\|_{L_h^\infty}$ term.

The L_h^∞ bounds in [60] are justified by using the concept of stability thresholds. A good discussion of this idea can be found in Sanz-Serna [79]. The basic idea here is that a nonlinear discretization is referred to as being stable if, for a local perturbation of the problem, the solution remains bounded in terms of the perturbation. However it is possible that the discretization will not remain well behaved for large perturbations. This led to the concept of a stability threshold which is an upper bound such that the discretization is well behaved for perturbations whose size is below the threshold. This idea of stability thresholds was

first introduced in Stetter [83].

3.3 Gevrey regularity of the solutions of the semi-discrete approximation

In the previous chapter we introduced the concept of Gevrey regularity and proved that the solutions of the K-S equation, with initial data in $X^{1/4}$ are in a Gevrey class for $t > 0$. In this section we will prove an analogous result for the solutions of the semi-discrete approximation (3.1.17). In this proof we require bounds on the nonlinear terms

$$N_1(U) := U \otimes D_h^o U, \quad N_2(U) := D_h^e(U \otimes U),$$

and in order to obtain these bounds we will need the following eigenvalue results.

Lemma 3.3.1 *Let $1 \leq k, l \leq N-1$, $N \in \mathbb{N}$, such that $1 \leq k-l < k+l \leq N-1$. Then*

$$|\lambda_{h,k \pm l}^{1/4}| \leq \lambda_{h,k}^{1/4} + \lambda_{h,l}^{1/4},$$

where $\lambda_{h,k \pm l}$ are eigenvalues of the operator A_h .

Proof: By definition

$$\begin{aligned} |\lambda_{h,k \pm l}^{1/4}| &\leq |(4(k \pm l)^4)^{1/4}|, \\ &= \sqrt{2} |k \pm l|, \\ &\leq \sqrt{2} k + \sqrt{2} l, \\ &= \lambda_{h,k}^{1/4} + \lambda_{h,l}^{1/4}. \end{aligned}$$

□

Lemma 3.3.2 *Let $k, l, N \in \mathbb{N}$ be such that $1 \leq k \leq N-1$ and $1 \leq l \leq k$. Then*

$$|\lambda_{h,N-k+l}^{1/4}| \leq \lambda_{h,k}^{1/4} + \lambda_{h,N-l}^{1/4}.$$

Proof: By definition

$$\begin{aligned} |\lambda_{h,N-k+l}^{1/4}| &\leq \sqrt{2}|N-k+l|, \\ &\leq \sqrt{2}(|2l-k|+|N-l|), \\ &\leq \sqrt{2}(|k|+|N-l|), \end{aligned}$$

since $1 \leq l \leq k$, so that

$$\begin{aligned} |\lambda_{h,N-k+l}^{1/4}| &\leq \sqrt{2}k + \sqrt{2}(N-l), \\ &= \lambda_{h,k}^{1/4} + \lambda_{h,N-l}^{1/4}. \end{aligned}$$

□

Lemma 3.3.3 *Let $\mathbf{U} \in D(A_h^{3/4}e^{tA_h^{1/4}})$ for fixed $t \geq 0$. Then*

$$\|A_h^{1/4}e^{tA_h^{1/4}}\mathbf{N}_1(\mathbf{U})\|_{L_h^2} \leq 4\|A_h^{1/4}\mathbf{U}\|_{t,L_h^2}\|A_h^{3/4}\mathbf{U}\|_{t,L_h^2},$$

where $\|\cdot\|_{t,L_h^2} = \|e^{tA_h^{1/4}}\cdot\|_{L_h^2}$.

Proof: We recall that our approximation is in the form

$$u_h(x) = \sum_{k=1}^{N-1} \beta_k \sin kx,$$

so that

$$\begin{aligned} u_h(x) \frac{\partial}{\partial x} u_h(x) &= \sum_{k=1}^{N-1} \beta_k \sin kx \sum_{l=1}^{N-1} \beta_l l \cos lx, \\ &= \sum_{k=1}^{N-1} \sum_{l=1}^{N-1} \beta_k \beta_l l \sin kx \cos lx, \\ &= \sum_{k=1}^{N-1} \sum_{l=1}^{N-1} \beta_k \beta_l \frac{l}{2} [\sin(k+l)x + \sin(k-l)x], \end{aligned}$$

which gives

$$\begin{aligned}
 u_h(x) \frac{\partial}{\partial x} u_h(x) = & \frac{1}{2} \left(\sum_{k=1}^{N-2} \sum_{l=1}^{N-k-1} \beta_k \beta_l l \sin(k+l)x \right. \\
 & + \sum_{k=1}^{N-1} \sum_{l=N-k}^{N-1} \beta_k \beta_l l \sin(k+l)x \\
 & + \sum_{k=2}^{N-1} \sum_{l=1}^{k-1} \beta_k \beta_l l \sin(k-l)x \\
 & \left. + \sum_{k=1}^{N-1} \sum_{l=k}^{N-1} \beta_k \beta_l l \sin(k-l)x \right),
 \end{aligned}$$

which is the interpolant for $N_1(\mathbf{U}) = \mathbf{U} \otimes D_h^\circ \mathbf{U}$. Hence if we consider this expression on the uniform grid (3.1.2) it is possible to obtain $N_1(\mathbf{U})$ in terms of the eigenfunctions of A_h , $\omega_{h,\cdot}$,

$$\begin{aligned}
 N_1(\mathbf{U}) = & \frac{1}{2} \left(\sum_{k=1}^{N-2} \sum_{l=1}^{N-k-1} \beta_k \beta_l l \omega_{h,k+l} \right. \\
 & - \sum_{k=2}^{N-1} \sum_{l=1}^{k-1} \beta_k \beta_{N-l} (N-l) \omega_{h,N-k+l} \\
 & + \sum_{k=2}^{N-1} \sum_{l=1}^{k-1} \beta_k \beta_l l \omega_{h,k-l} \\
 & \left. - \sum_{k=1}^{N-2} \sum_{l=k+1}^{N-1} \beta_k \beta_l l \omega_{h,l-k} \right).
 \end{aligned}$$

Therefore we have that

$$\begin{aligned}
 A_h^{1/4} e^{tA_h^{1/4}} N_1(\mathbf{U}) = & \frac{1}{2} \left(\sum_{k=1}^{N-2} \sum_{l=1}^{N-k-1} \beta_k \beta_l l \lambda_{h,k+l}^{1/4} e^{t\lambda_{h,k+l}^{1/4}} \omega_{h,k+l} \right. \\
 & - \sum_{k=2}^{N-1} \sum_{l=1}^{k-1} \beta_k \beta_{N-l} (N-l) \lambda_{h,N-k+l}^{1/4} e^{t\lambda_{h,N-k+l}^{1/4}} \omega_{h,N-k+l} \\
 & + \sum_{k=2}^{N-1} \sum_{l=1}^{k-1} \beta_k \beta_l l \lambda_{h,k-l}^{1/4} e^{t\lambda_{h,k-l}^{1/4}} \omega_{h,k-l}, \\
 & \left. - \sum_{k=1}^{N-2} \sum_{l=k+1}^{N-1} \beta_k \beta_l l \lambda_{h,l-k}^{1/4} e^{t\lambda_{h,l-k}^{1/4}} \omega_{h,l-k} \right).
 \end{aligned}$$

Now we let \mathbf{W} be such that $\mathbf{W} = \sum_{k=1}^{N-1} \eta_k \omega_{h,k} \in D(e^{tA_h^{1/4}})$, then premultiplying the last equation by $2h(e^{tA_h^{1/4}} \mathbf{W})^T$ and taking the modulus gives

$$\begin{aligned} \mathcal{I}_1 \leq & \frac{\pi}{2} \left(\sum_{k=1}^{N-2} \sum_{l=1}^{N-k-1} |\beta_k| |\beta_l| |\eta_{k+l}| l |\lambda_{h,k+l}^{1/4}| e^{2t\lambda_{h,k+l}^{1/4}} \right. \\ & + \sum_{k=2}^{N-1} \sum_{l=1}^{k-1} |\beta_k| |\beta_{N-l}| |\eta_{N-k+l}| (N-l) |\lambda_{h,N-k+l}^{1/4}| e^{2t\lambda_{h,N-k+l}^{1/4}} \\ & + \sum_{k=2}^{N-1} \sum_{l=1}^{k-1} |\beta_k| |\beta_l| |\eta_{k-l}| l |\lambda_{h,k-l}^{1/4}| e^{2t\lambda_{h,k-l}^{1/4}} \\ & \left. + \sum_{k=1}^{N-2} \sum_{l=k+1}^{N-1} |\beta_k| |\beta_l| |\eta_{l-k}| l |\lambda_{h,l-k}^{1/4}| e^{2t\lambda_{h,l-k}^{1/4}} \right), \end{aligned}$$

where $\mathcal{I}_1 = |\langle A_h^{1/4} e^{tA_h^{1/4}} \mathbf{N}_1(\mathbf{U}), e^{tA_h^{1/4}} \mathbf{W} \rangle_{L_h^2}|$, and this equation can be written as

$$\begin{aligned} \mathcal{I}_1 \leq & \frac{\pi}{2\sqrt{2}} \left(\sum_{k=1}^{N-2} \sum_{l=1}^{N-k-1} |\beta_k| |\beta_l| |\eta_{k+l}| \lambda_{h,l}^{1/4} (\lambda_{h,k}^{1/4} + \lambda_{h,l}^{1/4}) e^{t(\lambda_{h,k}^{1/4} + \lambda_{h,l}^{1/4} + \lambda_{h,k+l}^{1/4})} \right. \\ & + \sum_{k=2}^{N-1} \sum_{l=1}^{k-1} |\beta_k| |\beta_{N-l}| |\eta_{N-k+l}| \lambda_{h,N-l}^{1/4} (\lambda_{h,k}^{1/4} + \lambda_{h,N-l}^{1/4}) e^{t(\lambda_{h,k}^{1/4} + \lambda_{h,N-l}^{1/4} + \lambda_{h,N-k+l}^{1/4})} \\ & + \sum_{k=2}^{N-1} \sum_{l=1}^{k-1} |\beta_k| |\beta_l| |\eta_{k-l}| \lambda_{h,l}^{1/4} (\lambda_{h,k}^{1/4} + \lambda_{h,l}^{1/4}) e^{t(\lambda_{h,k}^{1/4} + \lambda_{h,l}^{1/4} + \lambda_{h,k-l}^{1/4})} \\ & \left. + \sum_{k=1}^{N-2} \sum_{l=k+1}^{N-1} |\beta_k| |\beta_l| |\eta_{l-k}| \lambda_{h,l}^{1/4} (\lambda_{h,k}^{1/4} + \lambda_{h,l}^{1/4}) e^{t(\lambda_{h,k}^{1/4} + \lambda_{h,l}^{1/4} + \lambda_{h,l-k}^{1/4})} \right). \quad (3.3.1) \end{aligned}$$

Here we have used the fact that

$$l = \lambda_{h,l}^{1/4} / \sqrt{2} \quad \text{and} \quad N-l = \lambda_{h,N-l}^{1/4} / \sqrt{2},$$

by the properties of the eigenvalues of the matrix operator A_h and we have also used Lemma 3.3.2 which gives the following bound

$$\lambda_{h,N-k+l}^{1/4} \leq \lambda_{h,k}^{1/4} + \lambda_{h,N-l}^{1/4}.$$

Applying the Cauchy-Schwartz inequality to (3.3.1) gives

$$\begin{aligned}
\mathcal{I}_1 \leq & \frac{\pi}{2\sqrt{2}} \left(\sum_{k=1}^{N-2} |\beta_k| \lambda_{h,k}^{1/4} e^{t\lambda_{h,k}^{1/4}} \left[\sum_{l=1}^{N-k-1} |\beta_l|^2 \lambda_{h,l}^{1/2} e^{2t\lambda_{h,l}^{1/4}} \right]^{1/2} \left[\sum_{l=1}^{N-k-1} |\eta_{k+l}|^2 e^{2t\lambda_{h,k+l}^{1/4}} \right]^{1/2} \right. \\
& + \sum_{k=1}^{N-2} |\beta_k| e^{t\lambda_{h,k}^{1/4}} \left[\sum_{l=1}^{N-k-1} |\beta_l|^2 \lambda_{h,l} e^{2t\lambda_{h,l}^{1/4}} \right]^{1/2} \left[\sum_{l=1}^{N-k-1} |\eta_{k+l}|^2 e^{2t\lambda_{h,k+l}^{1/4}} \right]^{1/2} \\
& + \sum_{k=2}^{N-1} |\beta_k| \lambda_{h,k}^{1/4} e^{t\lambda_{h,k}^{1/4}} \left[\sum_{l=1}^{k-1} |\beta_{N-l}|^2 \lambda_{h,N-l}^{1/2} e^{2t\lambda_{h,N-l}^{1/4}} \right]^{1/2} \left[\sum_{l=1}^{k-1} |\eta_{N-k+l}|^2 e^{2t\lambda_{h,N-k+l}^{1/4}} \right]^{1/2} \\
& + \sum_{k=2}^{N-1} |\beta_k| e^{t\lambda_{h,k}^{1/4}} \left[\sum_{l=1}^{k-1} |\beta_{N-l}|^2 \lambda_{h,N-l} e^{2t\lambda_{h,N-l}^{1/4}} \right]^{1/2} \left[\sum_{l=1}^{k-1} |\eta_{N-k+l}|^2 e^{2t\lambda_{h,N-k+l}^{1/4}} \right]^{1/2} \\
& + \sum_{k=2}^{N-1} |\beta_k| \lambda_{h,k}^{1/4} e^{t\lambda_{h,k}^{1/4}} \left[\sum_{l=1}^{k-1} |\beta_l|^2 \lambda_{h,l}^{1/2} e^{2t\lambda_{h,l}^{1/4}} \right]^{1/2} \left[\sum_{l=1}^{k-1} |\eta_{k-l}|^2 e^{2t\lambda_{h,k-l}^{1/4}} \right]^{1/2} \\
& + \sum_{k=2}^{N-1} |\beta_k| e^{t\lambda_{h,k}^{1/4}} \left[\sum_{l=1}^{k-1} |\beta_l|^2 \lambda_{h,l} e^{2t\lambda_{h,l}^{1/4}} \right]^{1/2} \left[\sum_{l=1}^{k-1} |\eta_{k-l}|^2 e^{2t\lambda_{h,k-l}^{1/4}} \right]^{1/2} \\
& + \sum_{k=1}^{N-2} |\beta_k| \lambda_{h,k}^{1/4} e^{t\lambda_{h,k}^{1/4}} \left[\sum_{l=k+1}^{N-1} |\beta_l|^2 \lambda_{h,l}^{1/2} e^{2t\lambda_{h,l}^{1/4}} \right]^{1/2} \left[\sum_{l=k+1}^{N-1} |\eta_{l-k}|^2 e^{2t\lambda_{h,l-k}^{1/4}} \right]^{1/2} \\
& \left. + \sum_{k=1}^{N-2} |\beta_k| e^{t\lambda_{h,k}^{1/4}} \left[\sum_{l=k+1}^{N-1} |\beta_l|^2 \lambda_{h,l} e^{2t\lambda_{h,l}^{1/4}} \right]^{1/2} \left[\sum_{l=k+1}^{N-1} |\eta_{l-k}|^2 e^{2t\lambda_{h,l-k}^{1/4}} \right]^{1/2} \right)
\end{aligned}$$

which can be bounded as follows

$$\begin{aligned}
\mathcal{I}_1 \leq & \sqrt{2} \left(\sum_{k=1}^{N-1} |\beta_k| \lambda_{h,k}^{1/4} e^{t\lambda_{h,k}^{1/4}} \|A_h^{1/4} \mathbf{U}\|_{t, L_h^2} \|\mathbf{W}\|_{t, L_h^2} \right. \\
& \left. + \sum_{k=1}^{N-1} |\beta_k| e^{t\lambda_{h,k}^{1/4}} \|A_h^{1/2} \mathbf{U}\|_{t, L_h^2} \|\mathbf{W}\|_{t, L_h^2} \right),
\end{aligned}$$

which gives

$$\begin{aligned}
\mathcal{I}_1 \leq & \sqrt{2} \left(\max_{0 \leq x \leq \pi} \left| \sum_{k=1}^{N-1} |\beta_k| \lambda_{h,k}^{1/4} e^{t\lambda_{h,k}^{1/4}} \sin kx \right| \|A_h^{1/4} \mathbf{U}\|_{t, L_h^2} \|\mathbf{W}\|_{t, L_h^2} \right. \\
& \left. + \max_{0 \leq x \leq \pi} \left| \sum_{k=1}^{N-1} |\beta_k| e^{t\lambda_{h,k}^{1/4}} \sin kx \right| \|A_h^{1/4} \mathbf{U}\|_{t, L_h^2} \|\mathbf{W}\|_{t, L_h^2} \right).
\end{aligned}$$

This is equivalent to

$$\begin{aligned} \mathcal{I}_1 \leq & \sqrt{2} \left(\|A_h^{1/4} e^{tA_h^{1/4}} \hat{u}_h\|_{L^\infty} \|A_h^{1/4} \mathbf{U}\|_{t, L_h^2} \|\mathbf{W}\|_{t, L_h^2} \right. \\ & \left. + \|e^{tA_h^{1/4}} \hat{u}_h\|_{L^\infty} \|A_h^{1/2} \mathbf{U}\|_{t, L_h^2} \|\mathbf{W}\|_{t, L_h^2} \right), \end{aligned}$$

where $\hat{u}_h(x) = \sum_{k=1}^{N-1} |\beta_k| \sin kx$. We can now apply Agmon's inequality and replace the L^∞ norms with L^2 norms, so that we obtain

$$\begin{aligned} \mathcal{I}_1 \leq & 2 \left(\|A_h^{1/4} \mathbf{U}\|_{t, L_h^2}^{3/2} \|A_h^{1/2} \mathbf{U}\|_{t, L_h^2}^{1/2} \|\mathbf{W}\|_{t, L_h^2} \right. \\ & \left. + \|\mathbf{U}\|_{t, L_h^2}^{1/2} \|A_h^{1/4} \mathbf{U}\|_{t, L_h^2}^{1/2} \|A_h^{1/2} \mathbf{U}\|_{t, L_h^2} \|\mathbf{W}\|_{t, L_h^2} \right). \end{aligned}$$

Finally if we repeatedly apply Lemma 3.1.8 to the various norms in the above equation it is possible to bound \mathcal{I}_1 as follows

$$|\langle A_h^{1/4} e^{tA_h^{1/4}} \mathbf{N}_1(\mathbf{U}), e^{tA_h^{1/4}} \mathbf{W} \rangle_{L_h^2}| \leq 4 \|A_h^{1/4} \mathbf{U}\|_{t, L_h^2} \|A_h^{3/4} \mathbf{U}\|_{t, L_h^2} \|\mathbf{W}\|_{t, L_h^2}.$$

□

Lemma 3.3.4 *Let $\mathbf{U} \in D(A_h^{3/4} e^{tA_h^{1/4}})$ for fixed $t > 0$. Then*

$$\|A_h^{1/4} e^{tA_h^{1/4}} \mathbf{N}_2(\mathbf{U})\|_{L_h^2} \leq 8 \|A_h^{1/4} \mathbf{U}\|_{t, L_h^2} \|A_h^{3/4} \mathbf{U}\|_{t, L_h^2},$$

where $\|\cdot\|_{t, L_h^2} = \|e^{tA_h^{1/4}} \cdot\|_{L_h^2}$.

Proof: We have that

$$\begin{aligned} (u_h(x))^2 &= \sum_{k=1}^{N-1} \beta_k \sin kx \sum_{l=1}^{N-1} \beta_l \sin lx, \\ &= \sum_{k=1}^{N-1} \sum_{l=1}^{N-1} \beta_k \beta_l \sin kx \sin lx, \\ &= \frac{1}{2} \sum_{k=1}^{N-1} \sum_{l=1}^{N-1} \beta_k \beta_l [\cos(k-l)x - \cos(k+l)x], \end{aligned}$$

which gives

$$(u_h(x))^2 = \frac{1}{2} \left(\sum_{k=2}^{N-1} \sum_{l=1}^{k-1} \beta_k \beta_l \cos(k-l)x + \sum_{k=1}^{N-1} \sum_{l=k}^{N-1} \beta_k \beta_l \cos(k-l)x \right. \\ \left. - \sum_{l=1}^{N-2} \sum_{k=1}^{N-k-1} \beta_k \beta_l \cos(k+l)x - \sum_{k=1}^{N-1} \sum_{l=N-k}^{N-1} \beta_k \beta_l \cos(k+l)x \right),$$

and differentiating with respect to x gives

$$\frac{\partial}{\partial x} (u_h(x))^2 = -\frac{1}{2} \left(\sum_{k=2}^{N-1} \sum_{l=1}^{k-1} \beta_k \beta_l (k-l) \sin(k-l)x + \sum_{k=1}^{N-1} \sum_{l=k}^{N-1} \beta_k \beta_l (k-l) \sin(k-l)x \right. \\ \left. - \sum_{k=1}^{N-2} \sum_{l=1}^{N-k-1} \beta_k \beta_l (k+l) \sin(k+l)x - \sum_{k=1}^{N-1} \sum_{l=N-k}^{N-1} \beta_k \beta_l (k+l) \sin(k+l)x \right).$$

Hence $A_h^{1/4} e^{tA_h^{1/4}} \mathbf{N}_2(\mathbf{U})$ is of the form

$$A_h^{1/4} e^{tA_h^{1/4}} \mathbf{N}_2(\mathbf{U}) = -\frac{1}{2} A_h^{1/4} e^{tA_h^{1/4}} \left(\sum_{k=2}^{N-1} \sum_{l=1}^{k-1} \beta_k \beta_l (k-l) \omega_{h,k-l} \right. \\ \left. + \sum_{k=1}^{N-2} \sum_{l=k+1}^{N-1} \beta_k \beta_l (l-k) \omega_{h,l-k} - \sum_{k=1}^{N-2} \sum_{l=1}^{N-k-1} \beta_k \beta_l (k+l) \omega_{h,k+l} \right. \\ \left. + \sum_{k=2}^{N-1} \sum_{l=1}^{k-1} \beta_k \beta_{N-l} (N+k-l) \omega_{h,N-k+l} \right).$$

Following the same type of analysis as we did in the proof of Lemma 3.3.3, for any $\mathbf{W} \in D(e^{tA_h^{1/4}})$ we have that

$$\mathcal{I}_2 \leq \frac{\pi}{2} \left(\sum_{k=1}^{N-1} \sum_{l=1}^{k-1} |\beta_k| |\beta_l| |\eta_{k-l}| (k-l) |\lambda_{h,k-l}^{1/4}| e^{2t\lambda_{h,k-l}^{1/4}} \right. \\ \left. + \sum_{k=1}^{N-2} \sum_{l=k+1}^{N-1} |\beta_k| |\beta_l| |\eta_{l-k}| (l-k) |\lambda_{h,l-k}^{1/4}| e^{2t\lambda_{h,l-k}^{1/4}} \right. \\ \left. + \sum_{k=1}^{N-2} \sum_{l=1}^{N-k-1} |\beta_k| |\beta_l| |\eta_{k+l}| (k+l) |\lambda_{h,k+l}^{1/4}| e^{2t\lambda_{h,k+l}^{1/4}} \right. \\ \left. + \sum_{k=2}^{N-1} \sum_{l=1}^{k-1} |\beta_k| |\beta_{N-l}| |\eta_{N-k+l}| (N+k-l) |\lambda_{h,N-k+l}^{1/4}| e^{2t\lambda_{h,N-k+l}^{1/4}} \right),$$

where $\mathcal{I}_2 = |\langle A_h^{1/4} e^{tA_h^{1/4}} \mathbf{N}_2(\mathbf{U}), e^{tA_h^{1/4}} \mathbf{W} \rangle_{L_h^2}|$. Also equating the $(k \pm l)$ terms as eigenvalues of A_h and applying Lemmas 3.3.1 and 3.3.2 gives

$$\begin{aligned} \mathcal{I}_2 \leq & \frac{\pi}{2\sqrt{2}} \left(\sum_{k=2}^{N-1} \sum_{l=1}^{k-1} |\beta_k| |\beta_l| |\eta_{k-l}| (\lambda_{h,k}^{1/4} + \lambda_{h,l}^{1/4})^2 e^{t(\lambda_{h,k}^{1/4} + \lambda_{h,l}^{1/4} + \lambda_{h,k-l}^{1/4})} \right. \\ & + \sum_{k=1}^{N-2} \sum_{l=k+1}^{N-1} |\beta_k| |\beta_l| |\eta_{l-k}| (\lambda_{h,k}^{1/4} + \lambda_{h,l}^{1/4})^2 e^{t(\lambda_{h,k}^{1/4} + \lambda_{h,l}^{1/4} + \lambda_{h,l-k}^{1/4})} \\ & + \sum_{k=1}^{N-2} \sum_{l=k}^{N-k-1} |\beta_k| |\beta_l| |\eta_{k+l}| (\lambda_{h,k}^{1/4} + \lambda_{h,l}^{1/4})^2 e^{t(\lambda_{h,k}^{1/4} + \lambda_{h,l}^{1/4} + \lambda_{h,k+l}^{1/4})} \\ & \left. + \sum_{k=2}^{N-1} \sum_{l=1}^{k-1} |\beta_k| |\beta_{N-l}| |\eta_{N-k+l}| (\lambda_{h,k}^{1/4} + \lambda_{h,N-l}^{1/4})^2 e^{t(\lambda_{h,k}^{1/4} + \lambda_{h,N-l}^{1/4} + \lambda_{h,N-k+l}^{1/4})} \right). \end{aligned}$$

Now if we apply the Cauchy-Schwartz inequality to the above equation and follow the relevant part of the proof for Lemma 3.3.3 it is possible to show that

$$\begin{aligned} \mathcal{I}_2 \leq & \sqrt{2} \left(\|A_h^{1/2} \hat{u}_h\|_{t,L^\infty} \|\mathbf{U}\|_{t,L_h^2} + 2 \|A_h^{1/4} \hat{u}_h\|_{t,L^\infty} \|A_h^{1/4} \mathbf{U}\|_{t,L_h^2} \right. \\ & \left. + \|\hat{u}_h\|_{t,L^\infty} \|A_h^{1/2} \mathbf{U}\|_{t,L_h^2} \right) \|\mathbf{W}\|_{t,L_h^2}, \end{aligned}$$

where $\hat{u}_h(x) = \sum_{k=1}^{N-1} |\beta_k| \sin kx$, which gives

$$\begin{aligned} \mathcal{I}_2 \leq & 2 \left(\|\mathbf{U}\|_{t,L_h^2} \|A_h^{1/2} \mathbf{U}\|_{t,L_h^2}^{1/2} \|A_h^{3/4} \mathbf{U}\|_{t,L_h^2}^{1/2} + 2 \|A_h^{1/4} \mathbf{U}\|_{t,L_h^2}^{3/2} \|A_h^{1/2} \mathbf{U}\|_{t,L_h^2}^{1/2} \right. \\ & \left. + \|\mathbf{U}\|_{t,L_h^2}^{1/2} \|A_h^{1/4} \mathbf{U}\|_{t,L_h^2}^{1/2} \|A_h^{1/2} \mathbf{U}\|_{t,L_h^2} \right) \|\mathbf{W}\|_{t,L_h^2}, \end{aligned}$$

by Agmon's inequality. Finally applying Lemma 3.1.8 to the norms in the above equation it is possible to show that

$$|\langle A_h^{1/4} e^{tA_h^{1/4}} \mathbf{N}_2(\mathbf{U}), e^{tA_h^{1/4}} \mathbf{W} \rangle_{L_h^2}| \leq 8 \|A_h^{1/4} \mathbf{U}\|_{t,L_h^2} \|A_h^{3/4} \mathbf{U}\|_{t,L_h^2} \|\mathbf{W}\|_{t,L_h^2}.$$

□

We now state the following discrete Gevrey result for our semi-discrete PS approximation.

Theorem 3.3.5 *Let the initial condition $\mathbf{U}(0)$ for the semi-discrete equation*

(3.1.17) be contained in the space $X_h^{1/4}$ such that $\|\mathbf{U}_0\|_{X_h^{1/4}} \leq \rho$. Then there exists $t_{1,h} = t_{1,h}(\|\mathbf{U}(0)\|_{X_h^{1/4}})$ such that

$$\mathbf{U}(t) \in G_{t,h} = D(A_h^{1/4} e^{tA_h^{1/4}}),$$

with

$$\|A_h^{1/4} e^{tA_h^{1/4}} \mathbf{U}(t)\|_{L_h^2} \leq \sqrt{2}\rho, \quad \forall t \in (0, t_{1,h}].$$

Proof: Let $\mathbf{V}(t) = e^{tA_h^{1/4}} \mathbf{U}(t)$, so that

$$\begin{aligned} \frac{d\mathbf{V}}{dt} &= A_h^{1/4} e^{tA_h^{1/4}} \mathbf{U} + e^{tA_h^{1/4}} \frac{d\mathbf{U}}{dt}, \\ &= A_h^{1/4} e^{tA_h^{1/4}} \mathbf{U} + e^{tA_h^{1/4}} [-A_h \mathbf{U} - \alpha D_h^2 \mathbf{U} - \frac{\alpha}{3} (\mathbf{N}_1(\mathbf{U}) + \mathbf{N}_2(\mathbf{U}))], \\ &= A_h^{1/4} \mathbf{V} - A_h \mathbf{V} - \alpha D_h^2 \mathbf{V} - \frac{\alpha}{3} e^{tA_h^{1/4}} [\mathbf{N}_1(\mathbf{U}) + \mathbf{N}_2(\mathbf{U})]. \end{aligned}$$

Premultiplying by $2h(A_h^{1/2} \mathbf{V})^T$ gives

$$\begin{aligned} \frac{1}{2} \frac{d}{dt} \|A_h^{1/4} \mathbf{V}\|_{L_h^2}^2 &\leq \|A_h^{3/8} \mathbf{V}\|_{L_h^2}^2 - \|A_h^{3/4} \mathbf{V}\|_{L_h^2}^2 + \alpha \|D_h^2 \mathbf{V}\|_{L_h^2} \|A_h^{1/2} \mathbf{V}\|_{L_h^2} \\ &\quad + \frac{\alpha}{3} \left(|\langle e^{tA_h^{1/4}} \mathbf{N}_1(\mathbf{U}), A_h^{1/2} \mathbf{V} \rangle_{L_h^2}| + |\langle e^{tA_h^{1/4}} \mathbf{N}_2(\mathbf{U}), A_h^{1/2} \mathbf{V} \rangle_{L_h^2}| \right), \end{aligned}$$

which becomes

$$\begin{aligned} \frac{1}{2} \frac{d}{dt} \|A_h^{1/4} \mathbf{V}\|_{L_h^2}^2 &\leq \frac{1-2\sqrt{2}}{2\sqrt{2}} \|A_h^{3/4} \mathbf{V}\|_{L_h^2}^2 + \frac{\alpha}{2} \|A_h^{1/2} \mathbf{V}\|_{L_h^2}^2 \\ &\quad + \frac{\alpha}{3} \left(|\langle e^{tA_h^{1/4}} \mathbf{N}_1(\mathbf{U}), A_h^{1/2} \mathbf{V} \rangle_{L_h^2}| + |\langle e^{tA_h^{1/4}} \mathbf{N}_2(\mathbf{U}), A_h^{1/2} \mathbf{V} \rangle_{L_h^2}| \right), \end{aligned}$$

since

$$\|D_h^2 \mathbf{V}\|_{L_h^2} = \frac{1}{2} \|A_h^{1/2} \mathbf{V}\|_{L_h^2}, \quad \|A_h^{3/8} \mathbf{V}\|_{L_h^2} = \frac{1}{2\sqrt{2}} \|A_h^{3/4} \mathbf{V}\|_{L_h^2},$$

by Lemmas 3.1.5 and 3.1.8 respectively. Now applying the bounds in Lemmas 3.3.3 and 3.3.4 to the nonlinear terms, gives

$$\begin{aligned} \frac{d}{dt} \|A_h^{1/4} \mathbf{V}\|_{L_h^2}^2 &\leq \frac{1-2\sqrt{2}}{\sqrt{2}} \|A_h^{3/4} \mathbf{V}\|_{L_h^2}^2 + \alpha \|A_h^{1/2} \mathbf{V}\|_{L_h^2}^2 \\ &\quad + 8\alpha \|A_h^{1/4} \mathbf{V}\|_{L_h^2}^2 \|A_h^{3/4} \mathbf{V}\|_{L_h^2}, \end{aligned}$$

which implies that

$$\begin{aligned} \frac{d}{dt} \|A_h^{1/4} \mathbf{V}\|_{L_h^2}^2 &\leq \frac{1-2\sqrt{2}}{\sqrt{2}} \|A_h^{3/4} \mathbf{V}\|_{L_h^2}^2 + \alpha \|A_h^{1/4} \mathbf{V}\|_{L_h^2} \|A_h^{3/4} \mathbf{V}\|_{L_h^2} \\ &\quad + 8\alpha \|A_h^{1/4} \mathbf{V}\|_{L_h^2}^2 \|A_h^{3/4} \mathbf{V}\|_{L_h^2}, \end{aligned} \quad (3.3.2)$$

since

$$\|A_h^{1/2} \mathbf{V}\|_{L_h^2} \leq \|A_h^{1/4} \mathbf{V}\|_{L_h^2}^{1/2} \|A_h^{3/4} \mathbf{V}\|_{L_h^2}^{1/2},$$

by Lemma 3.1.9. Applying Young's inequality to the two products of norms on the right hand side of (3.3.2) then gives

$$\begin{aligned} \frac{d}{dt} \|A_h^{1/4} \mathbf{V}\|_{L_h^2}^2 &\leq \frac{1-2\sqrt{2}}{\sqrt{2}} \|A_h^{3/4} \mathbf{V}\|_{L_h^2}^2 + \alpha \left[\frac{1}{2\epsilon_1} \|A_h^{1/4} \mathbf{V}\|_{L_h^2}^2 + \frac{\epsilon_1}{2} \|A_h^{3/4} \mathbf{V}\|_{L_h^2}^2 \right] \\ &\quad + 8\alpha \left[\frac{1}{2\epsilon_2} \|A_h^{1/4} \mathbf{V}\|_{L_h^2}^4 + \frac{\epsilon_2}{2} \|A_h^{3/4} \mathbf{V}\|_{L_h^2}^2 \right] \end{aligned}$$

and if we set $\epsilon_1 = (2 - \sqrt{2})/\alpha$ and $\epsilon_2 = 1/(4\alpha)$ this becomes

$$\frac{d}{dt} \|A_h^{1/4} \mathbf{V}\|_{L_h^2}^2 \leq \frac{\alpha^2}{2(2 - \sqrt{2})} \|A_h^{1/4} \mathbf{V}\|_{L_h^2}^2 + 16\alpha^2 \|A_h^{1/4} \mathbf{V}\|_{L_h^2}^4. \quad (3.3.3)$$

Letting $y(t) = \|A_h^{1/4} \mathbf{V}(t)\|_{L_h^2}^2$ and integrating (3.3.3) with respect to time gives

$$\frac{y(t)}{y(t) + B} \leq e^{ABt} \frac{y(0)}{y(0) + B}, \quad (3.3.4)$$

where $A = 16\alpha^2$ and $B = 1/(32(2 - \sqrt{2}))$. Hence if we choose

$$0 < t \leq \frac{1}{AB} \ln \left[\frac{2(y(0) + B)}{2y(0) + B} \right],$$

which is equivalent to

$$e^{ABt} \frac{y(0)}{y(0) + B} \leq \frac{2y(0)}{2y(0) + B}.$$

then (3.3.4) becomes

$$\frac{y(t)}{y(t) + B} \leq \frac{2y(0)}{2y(0) + B},$$

which implies that

$$\|A_h^{1/4} \mathbf{V}(t)\|_{L_h^2}^2 \leq 2\|A_h^{1/4} \mathbf{U}(0)\|_{L_h^2}^2, \quad (3.3.5)$$

for $0 \leq t \leq t_{1,h}$ where

$$t_{1,h} = \frac{2(2 - \sqrt{2})}{\alpha^2} \ln \left[\frac{2 \left(\|A_h^{1/4} \mathbf{U}(0)\|_{L_h^2}^2 + 1/(32(2 - \sqrt{2})) \right)}{2\|A_h^{1/4} \mathbf{U}(0)\|_{L_h^2}^2 + 1/(32(2 - \sqrt{2}))} \right].$$

Hence we have obtained the result. □

Remark 3.3.6 If we could assume uniform bounds on the approximate solution in the space $X_h^{1/4}$ then we could extend the result in Theorem 3.3.5 to show that the approximate solution is in a Gevrey class for all $t > 0$, using a similar argument as we did in Theorem 2.4.9.

3.4 A fully-discrete approximation

3.4.1 A Crank-Nicolson scheme

Although our theoretical results are mainly concerned with the semi-discrete equation (3.1.17), we need to discretize in time in order to construct a practical numerical scheme. Therefore in this section we prove an analogous convergence result, to the one in Theorem 3.2.7, for a fully-discrete approximation involving the Crank-Nicolson method for the temporal discretization. This is a fully-implicit second order accurate method. This method was used along with the pseudospectral method in Wallace and Sloan [94], however no convergence result was proved in this paper.

We let $[0, T]$ be some interval of time and let k denote the time step, where $0 < k < T$. Also we denote the time levels by $t_n = nk$ for $n = 0, 1, \dots, M$, where $M = [T/k]$ and $[T/k]$ is highest integer less than or equal to T/k . The vector \mathbf{u}^n refers to $u(\cdot, t_n)$ restricted to the internal grid points of (3.1.2).

Therefore using the Crank-Nicolson method, the approximations \mathbf{U}^n of \mathbf{u}^n are computed by the following fully-discrete scheme

$$\frac{\mathbf{U}^n - \mathbf{U}^{n-1}}{k} = \frac{\mathbf{G}(\mathbf{U}^n) + \mathbf{G}(\mathbf{U}^{n-1})}{2}, \quad 1 \leq n \leq M, \quad (3.4.1)$$

where

$$\mathbf{G}(\mathbf{U}) = - \left(4 D_h^4 \mathbf{U} + \alpha D_h^2 \mathbf{U} + \frac{\alpha}{3} [\mathbf{U} \otimes D_h^o \mathbf{U} + D_h^e (\mathbf{U} \otimes \mathbf{U})] \right), \quad (3.4.2)$$

and $\mathbf{U}^0 = \mathbf{u}_0$. Equation (3.4.1) can be solved by Newton iteration and we will consider this in much more detail in Section 6.3.

3.4.2 A further fully-discrete scheme

In order to prove a convergence result for (3.4.1) similar to the one we proved in the previous section, it is convenient to consider another fully-discrete implicit

scheme. We begin by defining

$$\mathbf{U}^{n+1/2} = \mathbf{U}^n + \frac{k}{2} \mathbf{G}(\mathbf{U}^n), \quad 0 \leq n \leq M, \quad (3.4.3)$$

with $\mathbf{U}^{-1/2} = \mathbf{U}^0 - k/2 \mathbf{G}(\mathbf{U}^0)$, where \mathbf{U}^n are given by (3.4.1) for $1 \leq n \leq M$. Hence

$$\begin{aligned} \mathbf{U}^{n+1/2} - \mathbf{U}^{n-1/2} &= \mathbf{U}^n - \mathbf{U}^{n-1} + \frac{k}{2} [\mathbf{G}(\mathbf{U}^n) - \mathbf{G}(\mathbf{U}^{n-1})], \\ &= \frac{k}{2} [\mathbf{G}(\mathbf{U}^n) + \mathbf{G}(\mathbf{U}^{n-1}) + \mathbf{G}(\mathbf{U}^n) - \mathbf{G}(\mathbf{U}^{n-1})], \end{aligned}$$

by (3.4.1), which gives

$$\mathbf{U}^{n+1/2} - \mathbf{U}^{n-1/2} = k \mathbf{G}(\mathbf{U}^n), \quad 1 \leq n \leq M,$$

and we have by definition that $\mathbf{U}^{1/2} - \mathbf{U}^{-1/2} = k \mathbf{G}(\mathbf{U}^0)$, so that

$$\mathbf{U}^{n+1/2} - \mathbf{U}^{n-1/2} = k \mathbf{G}(\mathbf{U}^n), \quad 0 \leq n \leq M. \quad (3.4.4)$$

Combining (3.4.3) and (3.4.4) then gives

$$\mathbf{U}^n = \frac{\mathbf{U}^{n+1/2} + \mathbf{U}^{n-1/2}}{2}, \quad 0 \leq n \leq M,$$

and substituting this expression back into (3.4.3) gives the following fully-discrete implicit scheme

$$\mathbf{U}^{n+1/2} - \mathbf{U}^{n-1/2} - k \mathbf{G} \left(\frac{\mathbf{U}^{n+1/2} + \mathbf{U}^{n-1/2}}{2} \right) = 0, \quad 1 \leq n \leq M, \quad (3.4.5)$$

where

$$\mathbf{U}^{1/2} = \mathbf{U}^0 + k/2 \mathbf{G}(\mathbf{U}^0). \quad (3.4.6)$$

We will now prove a convergence result for this scheme and use it to prove a similar result for the Crank-Nicolson scheme (3.4.1).

3.4.3 Consistency for the fully-discrete scheme

Let $\tau^{n+1/2}$, for $0 \leq n \leq M$, be the grid restriction of the truncation error of the fully-discrete scheme (3.4.5) at $t = t_{n+1/2}$, which is given by the following

$$\tau^{n+1/2} = [\mathbf{u}(t_{n+1/2}) - \mathbf{u}(t_{n-1/2})] - k\mathbf{G}\left(\frac{1}{2}[\mathbf{u}(t_{n+1/2}) + \mathbf{u}(t_{n-1/2})]\right), \quad (3.4.7)$$

for $1 \leq n \leq M$, and

$$\tau^{1/2} = \mathbf{u}(t_{1/2}) - \mathbf{u}(0) - k/2 \mathbf{G}(\mathbf{u}(0)), \quad (3.4.8)$$

for $n = 0$, by (3.4.6).

Theorem 3.4.1 *Let $h, k > 0$ be sufficiently small and the initial condition of the K-S equation (2.3.7) be in the space X^s , for $s \geq 2$ with $4s \in \mathbb{N}$. Then given any $T > 0$ there exists a positive constant C such that*

$$\|\tau^{n+1/2}\|_{L_h^2} = C(\alpha, T, \|u_0\|_{X^s})(h^{4(s-1)} + k^2). \quad (3.4.9)$$

for $0 \leq n \leq M$.

Proof: Applying a Taylor Series expansion about the point t_n in (3.4.7) gives

$$\tau^{n+1/2} = k[\mathbf{u}'(t_n) - \mathbf{G}(\mathbf{u}(t_n))] + \mathcal{O}(k^2), \quad (3.4.10)$$

for $1 \leq n \leq M$. Similarly if we apply an expansion about $t = 0$ for equation (3.4.8) we obtain

$$\tau^{1/2} = \frac{k}{2}[\mathbf{u}'(0) - \mathbf{G}(\mathbf{u}(0))] + \mathcal{O}(k^2). \quad (3.4.11)$$

In order for the above equation to make sense we have to assume that the initial data is in at least the space X^2 , since the $\mathcal{O}(k^2)$ terms contain $u''(0)$. Hence taking the L_h^2 norm of (3.4.10) and (3.4.11) gives

$$\|\tau^{n+1/2}\|_{L_h^2} \leq k\|\mathbf{u}'(t_n) - \mathbf{G}(\mathbf{u}(t_n))\|_{L_h^2} + ck^2\|u''(\theta)\|_{L^2}, \quad (3.4.12)$$

for $0 \leq n \leq M$, where $\theta \in (0, t_{n+1/2})$ and c is some arbitrary constant. If we apply a similar analysis to $\|\mathbf{u}'(t_n) - \mathbf{G}(\mathbf{u}(t_n))\|_{L_h^2}$ as we did for the semi-discrete equation in Subsection 3.2.2, it is possible to obtain

$$\|\tau^{n+1/2}\|_{L_h^2} = C'(\alpha, \|u(t_n)\|_{X^s})h^{4(s-1)} + ck^2\|u(\theta)\|_{X^s},$$

for $0 \leq n \leq M$ and $s \geq 2$. Therefore given that $u_0 \in X^s$ we can again use Theorem 2.2.12 extended to the interval $[0, T]$ to obtain the following bound of the truncation error in terms of the initial data

$$\|\tau^{n+1/2}\|_{L_h^2} = C(\alpha, T, \|u_0\|_{X^s})(h^{4(s-1)} + k^2),$$

for $0 \leq n \leq M$.

□

3.4.4 Convergence for the fully-discrete scheme

We begin by stating the following lemma which is necessary in the proof for our convergence result.

Lemma 3.4.2 *If $x \in [0, 1/3]$ then the following inequality holds*

$$e^{3x} \geq \frac{1+x}{1-x}.$$

Proof: Consider the following real valued function

$$f(x) = e^{3x}(1-x) - (1+x), \quad x \geq 0,$$

where $f(0) = 0$ and $f'(x) = e^{3x}(2-3x) - 1$. If $x \in [0, 1/3]$, then $f'(x) > 0$ which implies that $f(x) \geq 0$, and so the result holds.

□

Theorem 3.4.3 *Let $h, k > 0$ be sufficiently small and $u_0 \in X^s$ for $s \geq 2$ with*

$4s \in \mathbb{N}$. Then given any $T > 0$ there exists a positive constant C such that

$$\|\mathbf{u}^{n+1/2} - \mathbf{U}^{n+1/2}\|_{L_h^2} \leq C(\alpha, T, \|u_0\|_{X^s})(h^{4(s-1)} + k^2),$$

for $0 \leq n \leq M$, where $\mathbf{U}^{n+1/2}$ is given by (3.4.5).

Proof: Subtracting (3.4.5) from (3.4.7) gives

$$\begin{aligned} \frac{\mathbf{E}^{n+1/2} - \mathbf{E}^{n-1/2}}{k} &= \boldsymbol{\tau}^{n+1/2} - 2D_h^4(\mathbf{E}^{n+1/2} + \mathbf{E}^{n-1/2}) \\ &\quad - \frac{\alpha}{2}D_h^2(\mathbf{E}^{n+1/2} + \mathbf{E}^{n-1/2}) - \frac{\alpha}{12}[(\mathbf{u}^{n+1/2} + \mathbf{u}^{n-1/2}) \otimes D_h^o(\mathbf{u}^{n+1/2} + \mathbf{u}^{n-1/2}) \\ &\quad - (\mathbf{U}^{n+1/2} + \mathbf{U}^{n-1/2}) \otimes D_h^o(\mathbf{U}^{n+1/2} + \mathbf{U}^{n-1/2}) \\ &\quad + D_h^e((\mathbf{u}^{n+1/2} + \mathbf{u}^{n-1/2})^2 - (\mathbf{U}^{n+1/2} + \mathbf{U}^{n-1/2})^2)], \end{aligned}$$

for $1 \leq n \leq M$, where $\mathbf{E}^{n-1/2} = \mathbf{u}^{n-1/2} - \mathbf{U}^{n-1/2}$, for $1 \leq n \leq M+1$. Premultiplying by $2h(\mathbf{E}^{n+1/2} + \mathbf{E}^{n-1/2})^T$ gives

$$\begin{aligned} \frac{1}{k} \left(\|\mathbf{E}^{n+1/2}\|_{L_h^2}^2 - \|\mathbf{E}^{n-1/2}\|_{L_h^2}^2 \right) &= \langle \boldsymbol{\tau}^{n+1/2}, \mathbf{E}^{n+1/2} + \mathbf{E}^{n-1/2} \rangle_{L_h^2} \\ &\quad - 2\|D_h^2(\mathbf{E}^{n+1/2} + \mathbf{E}^{n-1/2})\|_{L_h^2}^2 - \frac{\alpha}{2} \langle D_h^2(\mathbf{E}^{n+1/2} + \mathbf{E}^{n-1/2}), \mathbf{E}^{n+1/2} + \mathbf{E}^{n-1/2} \rangle_{L_h^2} \\ &\quad - \frac{\alpha}{12} \left[\langle (\mathbf{u}^{n+1/2} + \mathbf{u}^{n-1/2}) \otimes D_h^o(\mathbf{u}^{n+1/2} + \mathbf{u}^{n-1/2}), \mathbf{E}^{n+1/2} + \mathbf{E}^{n-1/2} \rangle_{L_h^2} \right. \\ &\quad - \langle (\mathbf{U}^{n+1/2} + \mathbf{U}^{n-1/2}) \otimes D_h^o(\mathbf{U}^{n+1/2} + \mathbf{U}^{n-1/2}), \mathbf{E}^{n+1/2} + \mathbf{E}^{n-1/2} \rangle_{L_h^2} \\ &\quad \left. - \langle (\mathbf{u}^{n+1/2} + \mathbf{u}^{n-1/2})^2 - (\mathbf{U}^{n+1/2} + \mathbf{U}^{n-1/2})^2, D_h^o(\mathbf{E}^{n+1/2} + \mathbf{E}^{n-1/2}) \rangle_{L_h^2} \right], \end{aligned}$$

for $1 \leq n \leq M$, which is equivalent to

$$\begin{aligned} \frac{1}{k} \left(\|\mathbf{E}^{n+1/2}\|_{L_h^2}^2 - \|\mathbf{E}^{n-1/2}\|_{L_h^2}^2 \right) &\leq \|\boldsymbol{\tau}^{n+1/2}\|_{L_h^2} \|\mathbf{E}^{n+1/2} + \mathbf{E}^{n-1/2}\|_{L_h^2} \\ &\quad - 2\|D_h^2(\mathbf{E}^{n+1/2} + \mathbf{E}^{n-1/2})\|_{L_h^2}^2 - \frac{\alpha}{2} \langle D_h^2(\mathbf{E}^{n+1/2} + \mathbf{E}^{n-1/2}), \mathbf{E}^{n+1/2} + \mathbf{E}^{n-1/2} \rangle_{L_h^2} \\ &\quad - \frac{\alpha}{12} \left[\langle (\mathbf{E}^{n+1/2} + \mathbf{E}^{n-1/2}) \otimes D_h^o(\mathbf{u}^{n+1/2} + \mathbf{u}^{n-1/2}), \mathbf{E}^{n+1/2} + \mathbf{E}^{n-1/2} \rangle_{L_h^2} \right. \\ &\quad - \langle (\mathbf{E}^{n+1/2} + \mathbf{E}^{n-1/2}) \otimes D_h^o(\mathbf{E}^{n+1/2} + \mathbf{E}^{n-1/2}), \mathbf{E}^{n+1/2} + \mathbf{E}^{n-1/2} \rangle_{L_h^2} \\ &\quad + \langle (\mathbf{u}^{n+1/2} + \mathbf{u}^{n-1/2}) \otimes D_h^o(\mathbf{E}^{n+1/2} + \mathbf{E}^{n-1/2}), \mathbf{E}^{n+1/2} + \mathbf{E}^{n-1/2} \rangle_{L_h^2} \\ &\quad + \langle (\mathbf{E}^{n+1/2} + \mathbf{E}^{n-1/2}) \otimes \mathbf{E}^{n+1/2} + \mathbf{E}^{n-1/2}, D_h^o(\mathbf{E}^{n+1/2} + \mathbf{E}^{n-1/2}) \rangle_{L_h^2} \\ &\quad \left. - 2\langle (\mathbf{u}^{n+1/2} + \mathbf{u}^{n-1/2}) \otimes (\mathbf{E}^{n+1/2} + \mathbf{E}^{n-1/2}), D_h^o(\mathbf{E}^{n+1/2} + \mathbf{E}^{n-1/2}) \rangle_{L_h^2} \right]. \end{aligned}$$

Equating the terms together in the last equation gives

$$\begin{aligned} \frac{1}{k} \left(\|\mathbf{E}^{n+1/2}\|_{L_h^2}^2 - \|\mathbf{E}^{n-1/2}\|_{L_h^2}^2 \right) &\leq \|\boldsymbol{\tau}^{n+1/2}\|_{L_h^2} \|\mathbf{E}^{n+1/2} + \mathbf{E}^{n-1/2}\|_{L_h^2} \\ &- 2\|D_h^2(\mathbf{E}^{n+1/2} + \mathbf{E}^{n-1/2})\|_{L_h^2}^2 - \frac{\alpha}{2} \langle D_h^2(\mathbf{E}^{n+1/2} + \mathbf{E}^{n-1/2}), \mathbf{E}^{n+1/2} + \mathbf{E}^{n-1/2} \rangle_{L_h^2} \\ &+ \frac{\alpha}{12} \left(C_1^{(n)} \|\mathbf{E}^{n+1/2} + \mathbf{E}^{n-1/2}\|_{L_h^2}^2 + C_2^{(n)} \|\mathbf{E}^{n+1/2} + \mathbf{E}^{n-1/2}\|_{L_h^2} \|D_h^o(\mathbf{E}^{n+1/2} + \mathbf{E}^{n-1/2})\|_{L_h^2} \right), \end{aligned}$$

where we have bounded $\|D_h^o(\mathbf{u}^{n+1/2} + \mathbf{u}^{n-1/2})\|_{L_h^\infty}$ and $\|\mathbf{u}^{n+1/2} + \mathbf{u}^{n-1/2}\|_{L_h^\infty}$ by $C_1^{(n)}$ and $C_2^{(n)}$ respectively, for $1 \leq n \leq M$, using the same argument as in the proof of Theorem 3.2.7. Applying Young's inequality to the two products of L_h^2 norms in the last equation gives

$$\begin{aligned} \frac{1}{k} \left(\|\mathbf{E}^{n+1/2}\|_{L_h^2}^2 - \|\mathbf{E}^{n-1/2}\|_{L_h^2}^2 \right) &\leq \frac{1}{2} \|\boldsymbol{\tau}^{n+1/2}\|_{L_h^2}^2 + \frac{1}{2} \|\mathbf{E}^{n+1/2} + \mathbf{E}^{n-1/2}\|_{L_h^2}^2 \\ &- 2\|D_h^2(\mathbf{E}^{n+1/2} + \mathbf{E}^{n-1/2})\|_{L_h^2}^2 - \frac{\alpha}{2} \langle D_h^2(\mathbf{E}^{n+1/2} + \mathbf{E}^{n-1/2}), \mathbf{E}^{n+1/2} + \mathbf{E}^{n-1/2} \rangle_{L_h^2} \\ &+ \frac{\alpha C_1^{(n)}}{12} \|\mathbf{E}^{n+1/2} + \mathbf{E}^{n-1/2}\|_{L_h^2}^2 + \frac{\alpha C_2^{(n)}}{24} \|\mathbf{E}^{n+1/2} + \mathbf{E}^{n-1/2}\|_{L_h^2}^2 \\ &+ \frac{\alpha C_2^{(n)}}{24} \|D_h^o(\mathbf{E}^{n+1/2} + \mathbf{E}^{n-1/2})\|_{L_h^2}^2, \end{aligned} \quad (3.4.13)$$

which becomes

$$\begin{aligned} \frac{1}{k} \left(\|\mathbf{E}^{n+1/2}\|_{L_h^2}^2 - \|\mathbf{E}^{n-1/2}\|_{L_h^2}^2 \right) &\leq \frac{1}{2} \|\boldsymbol{\tau}^{n+1/2}\|_{L_h^2}^2 + C_3^{(n)} \|\mathbf{E}^{n+1/2} + \mathbf{E}^{n-1/2}\|_{L_h^2}^2 \\ &- 2\|D_h^2(\mathbf{E}^{n+1/2} + \mathbf{E}^{n-1/2})\|_{L_h^2}^2 + C_4^{(n)} \|\widehat{D}_h^o(\mathbf{E}^{n+1/2} + \mathbf{E}^{n-1/2})\|_{L_h^2}^2, \end{aligned} \quad (3.4.14)$$

by Lemmas 3.1.6 and 3.1.7, where

$$C_3^{(n)} = \left(\frac{1}{2} + \frac{\alpha}{12} C_1^{(n)} + \frac{\alpha}{24} C_2^{(n)} \right), \quad C_4^{(n)} = \left(\frac{\alpha}{2} + \frac{\alpha}{24} C_2^{(n)} \right).$$

Also it is possible to bound the last two terms in (3.4.14) in the following way

$$\begin{aligned} -2\|D_h^2(\mathbf{E}^{n+1/2} + \mathbf{E}^{n-1/2})\|_{L_h^2}^2 + C_4^{(n)} \|\widehat{D}_h^o(\mathbf{E}^{n+1/2} + \mathbf{E}^{n-1/2})\|_{L_h^2}^2 \\ \leq \frac{(C_4^{(n)})^2}{8} \|\mathbf{E}^{n+1/2} + \mathbf{E}^{n-1/2}\|_{L_h^2}^2, \end{aligned}$$

so that (3.4.14) becomes

$$\frac{1}{k} \left(\|\mathbf{E}^{n+1/2}\|_{L_h^2}^2 - \|\mathbf{E}^{n-1/2}\|_{L_h^2}^2 \right) \leq \frac{1}{2} \|\boldsymbol{\tau}^{n+1/2}\|_{L_h^2}^2 + C_5^{(n)} \|\mathbf{E}^{n+1/2} + \mathbf{E}^{n-1/2}\|_{L_h^2}^2,$$

where $C_5^{(n)} = C_3^{(n)} + (C_4^{(n)})^2/8$. Equating the terms together and assuming that $C_5^{(n)}k \leq 1/3$ gives

$$\|\mathbf{E}^{n+1/2}\|_{L_h^2}^2 \leq \frac{k}{2(1 - C_5^{(n)}k)} \|\boldsymbol{\tau}^{n+1/2}\|_{L_h^2}^2 + \frac{1 + C_5^{(n)}k}{1 - C_5^{(n)}k} \|\mathbf{E}^{n-1/2}\|_{L_h^2}^2,$$

which can be written as

$$\begin{aligned} \|\mathbf{E}^{n+1/2}\|_{L_h^2}^2 &\leq \frac{k}{2(1 - C_5^{(n)}k)} \sum_{i=1}^n \left[\frac{1 + C_5^{(n)}k}{1 - C_5^{(n)}k} \right]^{n-i} \|\boldsymbol{\tau}^{i+1/2}\|_{L_h^2}^2 \\ &\quad + \left[\frac{1 + C_5^{(n)}k}{1 - C_5^{(n)}k} \right]^n \|\mathbf{E}^{1/2}\|_{L_h^2}^2. \end{aligned} \quad (3.4.15)$$

Now Lemma 3.4.2 implies that

$$\frac{1 + C_5^{(n)}k}{1 - C_5^{(n)}k} \leq e^{3C_5^{(n)}k},$$

so that

$$\left[\frac{1 + C_5^{(n)}k}{1 - C_5^{(n)}k} \right]^n \leq e^{3C_5^{(n)}nk}.$$

Hence substituting this into inequality (3.4.15) gives

$$\begin{aligned} \|\mathbf{E}^{n+1/2}\|_{L_h^2}^2 &\leq e^{3C_5^{(n)}nk} \|\mathbf{E}^{1/2}\|_{L_h^2}^2 + \frac{3k}{4} \sum_{i=1}^n e^{3C_5^{(n)}(n-i)k} \|\boldsymbol{\tau}^{i+1/2}\|_{L_h^2}^2, \\ &\leq K^{(n)} \left[\|\mathbf{E}^{1/2}\|_{L_h^2}^2 + \frac{3k}{4} \sum_{i=1}^M \|\boldsymbol{\tau}^{i+1/2}\|_{L_h^2}^2 \right], \end{aligned} \quad (3.4.16)$$

where $K^{(n)} = e^{3C_5^{(n)}T}$. We also have that

$$\|\mathbf{E}^{1/2}\|_{L_h^2} = \|\mathbf{u}^{1/2} - \mathbf{U}^{1/2}\|_{L_h^2} = \|\mathbf{u}(1/2) - \mathbf{U}^0 - \frac{k}{2}\mathbf{G}(\mathbf{U}^0)\|_{L_h^2},$$

by (3.4.6) which implies that

$$\|\mathbf{E}^{1/2}\|_{L_h^2} \leq \frac{k}{2} \|\mathbf{u}'(0) - \mathbf{G}(\mathbf{U}_0)\|_{L_h^2} + ck^2 \|u''(\theta)\|_{L^2}, \quad \theta \in (0, t_{1/2}),$$

which is identical to the right hand side of (3.4.12), hence we have that

$$\|\mathbf{E}^{1/2}\|_{L_h^2} \leq C(\alpha, \|u_0\|_{X^s}) (h^{4(s-1)} + k^2),$$

for $s \geq 2$. Therefore (3.4.16) becomes

$$\|\mathbf{E}^{n+1/2}\|_{L_h^2} \leq C(\alpha, T, \|u_0\|_{X^s}) (h^{4(s-1)} + k^2).$$

□

3.4.5 Convergence for the Crank-Nicolson scheme

We now use Theorem 3.4.3 to prove a similar result for the Crank-Nicolson Scheme (3.4.1).

Theorem 3.4.4 *Let $h, k > 0$ be sufficiently small and $u_0 \in X^s$ for $s \geq 2$ with $4s \in \mathbb{N}$. Then given any $T > 0$, there exists a positive constant C such that*

$$\|\mathbf{u}^n - \mathbf{U}^n\|_{L_h^2} \leq C(\alpha, T, \|u_0\|_{X^s}) (h^{4(s-1)} + k^2),$$

for $1 \leq n \leq M$, where \mathbf{U}^n is given by (3.4.1).

Proof: We note that

$$\|\mathbf{u}^n - \mathbf{U}^n\|_{L_h^2} = \|\mathbf{u}^n - \frac{1}{2}(\mathbf{U}^{n+1/2} - \mathbf{U}^{n-1/2})\|_{L_h^2}, \quad 1 \leq n \leq M,$$

so that taking a Taylor series expansion about \mathbf{u}^n gives

$$\|\mathbf{u}^n - \mathbf{U}^n\|_{L_h^2} \leq \left\| \frac{1}{2}(\mathbf{u}^{n+1/2} - \mathbf{U}^{n+1/2}) + \frac{1}{2}(\mathbf{u}^{n-1/2} - \mathbf{U}^{n-1/2}) \right\|_{L_h^2} + \mathcal{O}(k^2), \quad (3.4.17)$$

for all $1 \leq n \leq M$, which implies that

$$\|\mathbf{u}^n - \mathbf{U}^n\|_{L_h^2} \leq C(\alpha, T, \|u_0\|_{X^s})(h^{4(s-1)} + k^2), \quad (3.4.18)$$

by Theorem 3.4.3.

□

Chapter 4

Attractors and upper semi-continuity of attractors

4.1 Attractor theory

The long-time behaviour of dissipative PDE's is characterised by the presence of a global attractor towards which all orbits converge. To introduce the basic theory of the attractors for these equations, we state some standard definitions and results, which can be found in most dynamical systems text books, such as Guckenheimer and Holmes [36], Temam [87] and Wiggins [95]. We begin by introducing the notion of distance in a Banach space.

Definition 4.1.1 *Let A and B be two nonempty subsets of a Banach space \mathcal{X} , with norm $\|\cdot\|_{\mathcal{X}}$, then*

*(i) the **distance** between a point $u \in \mathcal{X}$ and the set B is defined by*

$$d(u, B) := \inf_{v \in B} \|u - v\|_{\mathcal{X}};$$

*(ii) the **semi-distance** from the set A to B is defined by*

$$\delta_{\mathcal{X}}(A, B) := \sup_{u \in A} d(u, B);$$

(iii) the **Hausdorff distance** between A and B is defined by

$$d_H(A, B) := \max\{\delta_{\mathcal{X}}(A, B), \delta_{\mathcal{X}}(B, A)\}.$$

Definition 4.1.2 Let A be a nonempty subset of \mathcal{X} and $\epsilon > 0$, then we define an **ϵ -neighbourhood** of A by

$$\mathcal{N}_{\mathcal{X}}(A, \epsilon) := \{u \in \mathcal{X} : d(u, A) < \epsilon\}.$$

Definition 4.1.3 A C^0 semigroup, defined on a Banach space \mathcal{X} , is a family of operators, $\{T(t)\}_{t \geq 0}$, that map \mathcal{X} into itself and have the following properties

- (i) $T(0) = I$, where I is the identity of \mathcal{X} ;
- (ii) $T(t + s) = T(t)T(s)$, for all $t, s \geq 0$;
- (iii) $T(t)u$ is continuous as a function of $(t, u) \in [0, \infty) \times \mathcal{X}$.

C^0 semigroups define dynamical systems for nonlinear autonomous partial or ordinary differential equations. For example, let us recall the result of Theorem 2.2.12 for equation (2.2.2) given in Section 2.2. This implies that if $u_0 \in \mathcal{X}^\alpha$, $0 \leq \alpha < 1$, then there exists a unique solution $u(t) \in \mathcal{X}^\alpha$ for all $t \in [0, \tau)$, for $\tau > 0$. If denote by $u(t; u_0)$ the solution at time t with initial condition $u(0; u_0) = u_0$ then

$$T(t)u_0 = u(t; u_0), \quad u_0 \in \mathcal{X}^\alpha,$$

defines a dynamical system on \mathcal{X}^α .

Definition 4.1.4 The **orbit** (or **trajectory**) of the point $u_0 \in \mathcal{X}$, is defined by the set

$$\gamma(u_0) := \bigcup_{t \geq 0} T(t)u_0.$$

Definition 4.1.5 The ω -limit set of the point u_0 , is defined by

$$\omega(u_0) = \bigcap_{s \geq 0} \overline{\bigcup_{t \geq s} T(t)u_0},$$

The ω -limit set of a nonempty subset $A \subset \mathcal{X}$, is defined by

$$\omega(A) = \bigcap_{s \geq 0} \overline{\bigcup_{t \geq s} T(t)A}.$$

Definition 4.1.6 The α -limit set of the point u_0 , is defined by

$$\alpha(u_0) = \bigcap_{s \leq 0} \overline{\bigcup_{t \leq s} T(-t)^{-1}u_0},$$

The α -limit set of a nonempty subset $A \subset \mathcal{X}$, is defined by

$$\alpha(A) = \bigcap_{s \leq 0} \overline{\bigcup_{t \leq s} T(-t)^{-1}A}.$$

Definition 4.1.7 Let u_0 and v_0 be two equilibrium solutions for a dynamical system. Then u_0 is said to be **connected** to v_0 if there exists an orbit γ such that

$$\alpha(\gamma) = u_0 \quad \text{and} \quad \omega(\gamma) = v_0.$$

If $u_0 = v_0$ then this orbit is referred to as a **homoclinic connection** (or **homoclinic orbit**), and when $u_0 \neq v_0$ it is referred as a **heteroclinic connection** (or **heteroclinic orbit**).

Definition 4.1.8 A nonempty set $A \subset \mathcal{X}$ is said to be **positively invariant** for the semigroup $\{T(t)\}_{t \geq 0}$, defined on \mathcal{X} , if

$$T(t)A \subset A, \quad \forall t \geq 0.$$

The set A is **invariant** for $\{T(t)\}_{t \geq 0}$ if

$$T(t)A = A, \quad \forall t \in \mathbb{R}.$$

We now quote the following lemma which gives an important property of the ω -limit set.

Lemma 4.1.9 *Assume that for some nonempty subset $A \subset \mathcal{X}$, and for some $t_0 > 0$ the set $\bigcup_{t \geq t_0} T(t)A$ is relatively compact in \mathcal{X} . Then $\omega(A)$ is nonempty, compact and invariant.*

Proof: See [87, Lemma 1.1.1, p.19].

□

We now state mathematically what we mean by attracting and attractor.

Definition 4.1.10 *A set $\mathcal{A} \subset \mathcal{X}$ is said to **attract** a set $B \subset \mathcal{X}$, under $T(t)$ if for any $\epsilon > 0$ there exists $\tau = \tau(\epsilon, \mathcal{A}, B)$ such that*

$$T(t)B \subset \mathcal{N}_{\mathcal{X}}(\mathcal{A}, \epsilon), \quad \forall t \geq \tau.$$

Definition 4.1.11 *A set $\mathcal{A} \subset \mathcal{X}$ is said to be an **attractor** if \mathcal{A} is a compact, invariant set which attracts an open neighbourhood of itself.*

Definition 4.1.12 *We say that $\mathcal{A} \subset \mathcal{X}$ is a **global or universal attractor** for the semigroup $\{T(t)\}_{t \geq 0}$ if \mathcal{A} is a compact attractor that attracts all the bounded sets of \mathcal{X} .*

The convergence to this global attractor can be arbitrarily slow, thus we may be interested in finding sets into which bounded sets enter after a finite time.

Definition 4.1.13 *A closed bounded subset \mathcal{B} of an open set U in \mathcal{X} is said to be an **absorbing set** in U if for each bounded set $B \subset U$ there exists a time $\tau(B) \geq 0$ such that*

$$T(t)B \subset \mathcal{B}, \quad \forall t \geq \tau.$$

A dynamical system is usually referred to as being *dissipative* if it is known to contain an absorbing set in its phase space.

Definition 4.1.14 A semigroup $T(t)$, $t \geq 0$ on a Banach space \mathcal{X} is said to be **asymptotically smooth**, if for any bounded set $B \subset \mathcal{X}$, there is a compact set $J = J(B) \subset \mathcal{X}$ such that J attracts the set $\{u \in B : T(t)u \in B \text{ for } t \geq 0\}$.

Theorem 4.1.15 (Billoti-LaSalle [4])

Assume that $T(t)$ is a C^0 semigroup defined on a subset U of a Banach space \mathcal{X} , and that it is asymptotically smooth on $V \subset U$, and furthermore that there exists an absorbing set \mathcal{B} , in V . Then the set \mathcal{A} defined by

$$\mathcal{A} := \omega(\mathcal{B}),$$

is a compact attractor. If V is convex, then \mathcal{A} is connected, and if V is the entire space \mathcal{X} then \mathcal{A} is a global attractor.

Proof: See [87, Theorem 1.1, p.23].

□

Before we can discuss the implications of this theorem we need to state the following definition.

Definition 4.1.16 Suppose that U is a compact set in the space \mathcal{X} , $d \in [0, \infty)$, $\epsilon > 0$ and

$$\mu(U, d, \epsilon) = \inf \sum r_i^d,$$

where the infimum is taken over all coverings $\{B_i\}$ of the set U , and B_i are the balls in \mathcal{X} of radii $r_i < \epsilon$, then the **d-dimensional Hausdorff measure** is defined by

$$\mu_H := \mu(U, d) = \lim_{\epsilon \rightarrow 0} \mu(U, d, \epsilon).$$

From the above definition it can be seen that if $\mu_H(U, d') < \infty$ for some d' , then $\mu_H(U, d) = 0$ for every $d > d'$; thus there exists $d_0 \in [0, \infty)$ such that $\mu_H(U, d) = 0$ for $d > d_0$ and $\mu_H(U, d) = +\infty$ for $d < d_0$. Here $\mu_H(U, d) \in [0, \infty]$ and is called the *Hausdorff dimension* of U and is denoted by $d_H(U)$.

A dynamical system which defines a semigroup that satisfies Theorem 4.1.15 and Lemma 4.1.9 will possess a nonempty global attractor which describes all the possible long-time dynamics that the system produces. For low values of the certain physical parameters that may govern a dynamical system, e.g. Reynolds or Grashof number, the dynamics may involve stable fixed points or stable time periodic orbits. Unfortunately, little is known about the structure of the attractor when these parameters enter regions which permit non-trivial behaviour, such as chaos where the behaviour may look completely random for all time. However it is known that for certain evolution PDE's, the long-time behaviour of solutions is relatively low dimensional, see Hale [37] and Temam [87]. In this case characterisation of the attractor is limited to bounds on its Hausdorff dimension. This result was first shown for a delay evolution equation by Mallet-Paret [62] and has been shown to be true for the two-dimensional Navier-Stokes equations by Foias and Temam [25]. The dimensions of the attractors for a wide range of other nonlinear equations can be found in [87, Section IV]. Physically we can regard these bounds on the Hausdorff dimension as bounds on the number of degrees of freedom in the global asymptotic dynamical behaviour of the system.

As stated above the attractors of these nonlinear equation may exhibit chaotic behaviour for certain parameter values. For completeness we will define what we actually mean by chaos, after giving some preliminary definitions.

Definition 4.1.17 *The semigroup $T(t)$ on \mathcal{X} is said to be **topologically transitive** on \mathcal{X} if given any pair of disjoint open sets $A, B \subset \mathcal{X}$ there exists a time $\tau_1 > 0$ such that $\{T(\tau_1)A\} \cap B \neq \emptyset$.*

Definition 4.1.18 *The semigroup $T(t)$ on \mathcal{X} is to have **sensitive dependence on initial conditions** if there exists a $\delta > 0$ such that given any $u \in \mathcal{X}$ and $\epsilon > 0$, there exists $v \in \mathcal{X}$ and $\tau_2 > 0$ with $\|u - v\|_{\mathcal{X}} < \epsilon$ and $\|T(\tau_2)u - T(\tau_2)v\|_{\mathcal{X}} > \delta$.*

Definition 4.1.19 An attractor \mathcal{A} is said to be **chaotic** (or **strange**) if the semigroup $T(t)\mathcal{X} \rightarrow \mathcal{X}$,

- (i) has sensitive dependence on initial conditions;
- (ii) and is topologically transitive on \mathcal{A} .

Remark 4.1.20 We can see that if $T(t)$ is topologically transitive then we cannot split the attractor \mathcal{A} into two disjoint sets which are invariant under $T(t)$, so we have a degree of indecomposability. The sensitive dependence on initial conditions gives rise to unpredictability, as small round-off errors become magnified during numerical computation. A third criteria for chaos, given in Devaney [12], is that the periodic orbits are dense in \mathcal{A} , i.e. any point in \mathcal{A} is arbitrarily close to a periodic orbit. This gives rise to a degree of regularity amongst the chaos.

4.2 Attractors of the Kuramoto-Sivashinsky equation

Having stated the results and definitions in the previous section, we now give corresponding known results for the K-S equation (2.3.7).

Lemma 4.2.1 *Let the initial data of the K-S equation (2.3.7) be in the space X . Then there exists a constant $\rho_0 > 0$ such that the ball*

$$\mathcal{B}_X(\rho_0) := \{u \in X : \|u\|_{L^2} \leq \rho_0\},$$

is absorbing and positively invariant for the semigroup, $S(t)$, defined by (2.3.7).

Proof: See Foias, Nicolaenko, Sell and Temam [22, Lemma 2.1, p.202] or Collet, Eckmann, Epstein and Stuble [7, Theorem 2.2, p.206].

□

In the paper [7], it has been shown that $\rho_0 = \mathcal{O}(\alpha^{4/5})$, where α is the bifurcation parameter of equation (2.3.7). This bound holds for all initial data in the space X which satisfies condition (2.3.5). Lemma 4.2.1 has been generalised to higher order spaces by the following result.

Lemma 4.2.2 *Let $u_0 \in X^s$ then there exists a constant $\rho_{4s} > 0$ for $4s \in \mathbb{N}$ which only depends on s and α such that the ball*

$$\mathcal{B}_{X^s}(\rho_{4s}) := \{u \in X^s : \|u\|_{X^s} \leq \rho_{4s}\},$$

is absorbing and positively invariant for the semigroup defined by the K-S equation and $\rho_{4s} = \mathcal{O}(\alpha^{(8s+5)/4})$.

Proof: See [90, Lemma 1, p.1099].

□

It is worth noting that the results of Lemmas 4.2.1 and 4.2.2 cover the global existence of solutions of the K-S equation as well as the existence of absorbing sets. We can now state the following theorem.

Theorem 4.2.3 *The K-S equation (2.3.7) possesses a global attractor in the space $X^{1/4}$ which is given by*

$$\mathcal{A} = \omega(\mathcal{B}_{X^{1/4}}(\rho_1)).$$

Proof: See [22, Lemma 2.3, p.204].

□

In Nicolaenko, Scheurer and Temam [68] it was shown that, for all odd initial data, the Hausdorff dimension of \mathcal{A} is such that

$$\mu_H(\mathcal{A}) = \mathcal{O}(\alpha^{3/4}).$$

4.3 Upper semi-continuity of attractors

4.3.1 Introduction

We now consider the convergence of the asymptotic behaviour of the PS approximation to that of the K-S equation (2.3.7). In general, it is extremely difficult to approximate the structure of any long-time dynamical behaviour. Also for

complicated attracting sets which have sensitive dependence on initial conditions there is little prospect of closely following a given orbit using a numerical method, as convergence results which we can obtain are of the form

$$\|u_{\text{true}}(t) - u_{\text{numerical}}(t)\| \leq C(T)h^p, \quad \forall t \in (0, T], \quad (4.3.1)$$

where the constant C is exponentially dependent on T and p is some positive constant, which is dependent on the order of the method and the regularity of the solutions.

The type of result that one can prove is the convergence of the attractors of the approximation to the global attractor of the system which is being approximated. In order to discuss this idea we recall the notion of semi-distance in the space \mathcal{X} , given in Definition 4.1.1, and we introduce the following notions of convergence.

Definition 4.3.1 *A family of sets A_ϵ , where $\epsilon \geq 0$, is **upper semi-continuous** at $\epsilon = 0$ if*

$$\delta_{\mathcal{X}}(A_\epsilon, A) \rightarrow 0 \text{ as } \epsilon \rightarrow 0, \quad (4.3.2)$$

*and **lower semi-continuous** at $\epsilon = 0$ if*

$$\delta_{\mathcal{X}}(A, A_\epsilon) \rightarrow 0 \text{ as } \epsilon \rightarrow 0. \quad (4.3.3)$$

*The family is **continuous** at $\epsilon = 0$ so that*

$$d_H(A, A_\epsilon) \rightarrow 0 \text{ as } \epsilon \rightarrow 0. \quad (4.3.4)$$

The basic method of proof for upper semi-continuity was introduced in Hale, Lin and Raugel [38] and it considers systems that have families of semigroups $\{T(t)\}_{t \geq 0}$, which possess a local attractor \mathcal{A} . Under certain conditions, it is possible use this theory to show that for a family of semigroups $\{T_h(t)\}_{t \geq 0}$, which depend on some discretization parameter $h > 0$ and approximate $\{T(t)\}_{t \geq 0}$, there exists local attractors \mathcal{A}_h for $\{T_h(t)\}_{t \geq 0}$ which have the property (4.3.2).

We illustrate upper semi-continuity graphically in Figure 4-1.

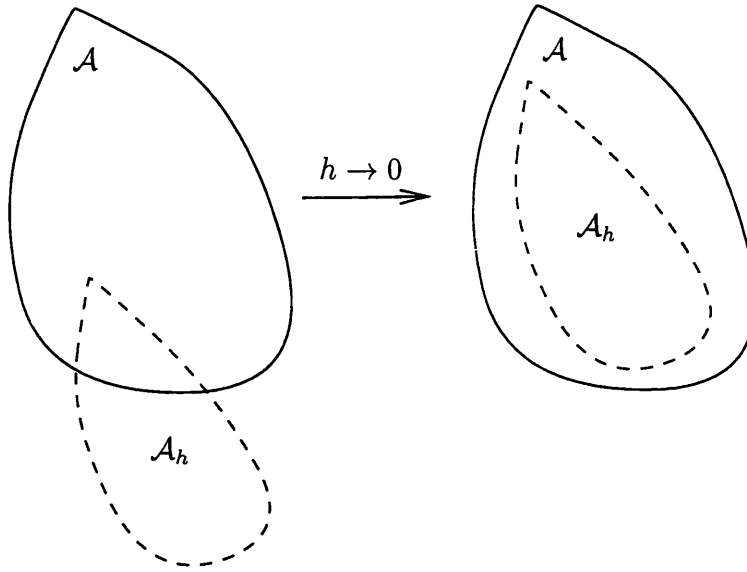


Figure 4-1: Graphical illustration of the type of convergence associated with upper semi-continuity.

Obviously upper semi-continuity alone does not provide us with a good relationship between the approximate attractor and the true attractor and in order to achieve this we must also show lower semi-continuity. However it is not always possible to prove lower semi-continuity results and we will illustrate this with the following example.

Example 4.3.2 Consider the one-dimensional autonomous ordinary differential equation

$$u_t = f(u) = -(u + 1)(u - 1)^2. \quad (4.3.5)$$

We have plotted the phase portrait for this equation in Figure 4-2a). From this figure we can see that there is a stable fixed point at $u = -1$, a fixed point at $u = 1$ of marginal stability and a heteroclinic orbit connecting these two fixed points. Therefore the global attractor for the system is given by the closed interval

$$\mathcal{A} = \{[-1, 1]\},$$

since the attractor consists of the fixed points and the orbit which connects them.

Let us now consider the perturbed system

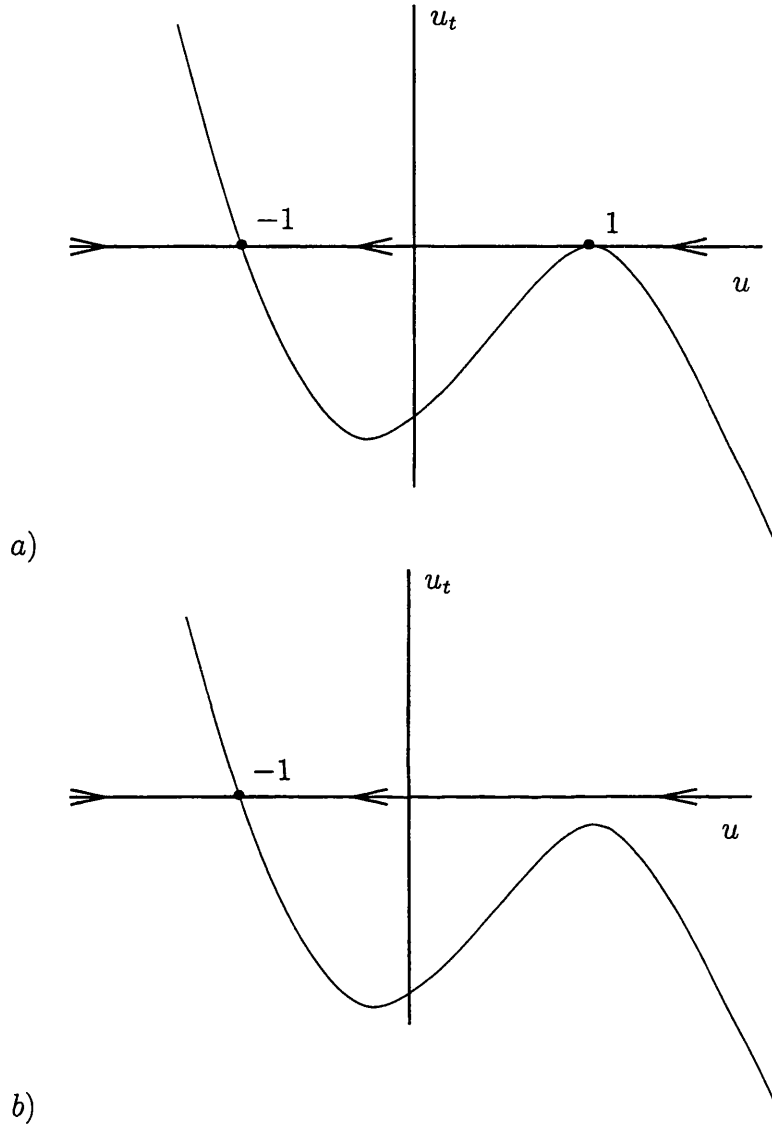


Figure 4-2: a) Plot of the flow of the dynamical system $u_t = f(u)$; b) Plot of the flow of the perturbed dynamical system $u_t = f_\epsilon(u)$.

$$u_t = f_\epsilon(u) = -(u+1)((u-1)^2 + \epsilon), \quad (4.3.6)$$

where $\epsilon > 0$. We have also plotted the phase portrait in Figure 4-2b). The perturbed system has only one stable fixed point at $u = -1$, so the attractor of

this system is simply given by

$$\mathcal{A}_\epsilon = \{-1\}.$$

Therefore as $\epsilon \rightarrow 0$ we would only be able to detect the fixed point at $u = -1$ of the original system which means that

$$\delta_{\mathcal{X}}(\mathcal{A}_\epsilon, \mathcal{A}) \rightarrow 0 \quad \text{as} \quad \epsilon \rightarrow 0,$$

however

$$\delta_{\mathcal{X}}(\mathcal{A}, \mathcal{A}_\epsilon) \not\rightarrow 0 \quad \text{as} \quad \epsilon \rightarrow 0.$$

The above example illustrates that lower semi-continuity does not always follow when a system is perturbed. We note that our example did not consider how such a perturbation might arise from a numerical approximation, however the general idea, in this example, to some extent reflects the difficulties that may be encountered. Lower semi-continuity results can be proved when systems are in gradient form or when their attractors are made up of unions of unstable manifolds, see Stuart and Humphries [85] for details. However for the rest of this section we will concentrate on proving an upper semi-continuity result for our PS approximation. This can be achieved by using the theory of Hale, Lin and Raugel [38], which we will introduce next.

4.3.2 General theory

Definition 4.3.3 *The semigroup $T(t)$, defined on the Banach space \mathcal{X} is said to be conditionally approximated on a bounded set $E \subset \mathcal{X}$, **uniformly** on compact subintervals $I \subset (0, \infty)$, by the discrete semigroup $T_h(t)$, dependent on $h \geq 0$, if for all I there exists a constant $h_0(I, E) > 0$ and a function $\eta(h, I, E)$ defined for*

all $h \in (0, h_0]$ such that

$$\lim_{h \rightarrow 0} \eta(h, I, E) = 0,$$

and

$$\|T(t)u - T_h(t)u\|_{\mathcal{X}} \leq \eta(h, I, E), \quad \forall t \in I,$$

where $u \in E \cap \mathcal{X}_h$ has the property that $T(t)u, T_h(t)u$ are defined and belong to E for all $t \in I$ and \mathcal{X}_h is the approximation space, which has the following property

$$\lim_{h \rightarrow 0} d_{\mathcal{X}}(x, \mathcal{X}_h) = 0, \quad \forall x \in \mathcal{X}. \quad (4.3.7)$$

Lemma 4.3.4 Assume that there exists a bounded set $\mathcal{B}_0 \subset \mathcal{X}$ and an open set $E_0 \supset \mathcal{N}(\mathcal{B}_0, d_0)$ for some $d_0 > 0$ such that \mathcal{B}_0 attracts E_0 under $T(t)$. Moreover, assume that there exists an open set $E_1 \supset \mathcal{N}(\mathcal{B}_0, d_1)$ for some $d_1 > 0$ and a constant $t_0 \geq 0$ such that $T_h(t)$ approximates $T(t)$ on E_1 uniformly on compact sets of $[t_0, \infty)$. Then, for any $\epsilon_0 > 0$ there are $h_0 > 0$ and $\tau_0 > t_0$ such that, for $0 < h \leq h_0$ and $t \geq \tau_0$,

$$T_h(t)(E_0 \cap E_1 \cap \mathcal{X}_h) \subset \mathcal{N}(\mathcal{B}_0, \epsilon_0).$$

Proof: See [38, Lemma 2.1].

□

Theorem 4.3.5 Assume that there exist a compact set $\mathcal{A} \subset \mathcal{X}$ and an open neighbourhood N_1 of \mathcal{A} such that \mathcal{A} attracts N_1 . Suppose that there are constants $h_0 > 0$, $\delta_0 > 0$, $t_0 \geq 0$ and two open neighbourhoods N_2, N_3 of \mathcal{A} , with $N_1 \subset N_2 \subset \mathcal{N}(N_2, \delta_0) \subset N_3$, such that, for $0 < h \leq h_0$,

- (i) $T(t)N_1 \subseteq N_2$ for all $t \geq 0$;
- (ii) $T_h(t)(N_1 \cap \mathcal{X}_h) \subseteq N_2$ for all $t \in [0, t_0]$;
- (iii) for any $u_h \in \mathcal{N}(N_2, \delta_0) \cap \mathcal{X}_h$, there exists $t(u_h) > 0$ such that $T_h(t)u_h \in N_3$ for $0 \leq t \leq t(u_h)$.

Also assume that $T_h(t)$ conditionally approximates $T(t)$ on N_3 uniformly on compact sets of $[t_0, \infty)$. Then, for any $\epsilon_0 > 0$ there are $\bar{h} > 0$ and $\tau_0 > t_0$ such that for $0 < h \leq \bar{h}$ and $t \geq \tau_0$,

$$T_h(t)(N_1 \cap \mathcal{X}_h) \subset \mathcal{N}(\mathcal{A}, \epsilon_0).$$

Proof: See [38, Proposition 2.2].

□

The next result gives conditions for the existence of compact attractors \mathcal{A}_h for $T_h(t)$ and the upper semi-continuity of these sets at $h = 0$.

Theorem 4.3.6 *Assume that $T(t)$ has a local, compact attractor \mathcal{A} and that the hypotheses of Theorem 4.3.5 are satisfied. If each $T_h(t)$ is asymptotically smooth, then there is $h_0 > 0$ such that, for $0 < h \leq h_0$, $T_h(t)$ admits a local, compact attractor \mathcal{A}_h , which attracts $N_1 \cap \mathcal{X}_h$. Moreover*

$$d_{\mathcal{X}}(\mathcal{A}_h, \mathcal{A}) \rightarrow 0 \quad \text{as } h \rightarrow 0.$$

Proof: By Theorem 4.3.5 the set $N_1 \cap \mathcal{X}_h$ is attracted by $\mathcal{N}(\mathcal{A}, \epsilon) \cap \mathcal{X}_h$. Therefore the set $\mathcal{B}_h := \mathcal{N}(\mathcal{A}, \epsilon) \cap \mathcal{X}_h$ is absorbing and the semigroup $T_h(t)$ is asymptotically smooth so we can apply Theorem 4.1.15 to obtain

$$\mathcal{A}_h := \omega_h(\mathcal{B}_h),$$

where

$$\omega_h(\cdot) = \bigcap_{s \geq 0} \overline{\bigcup_{t \geq s} T_h(t)(\cdot)}, \quad (4.3.8)$$

which implies that $\mathcal{A}_h \subset \mathcal{N}(\mathcal{A}, \epsilon) \cap \mathcal{X}_h$.

□

Remark 4.3.7 The condition on $T_h(t)$ being asymptotically smooth on the space N_2 holds if the approximation space \mathcal{X}_h is finite-dimensional. This follows from

the Heine-Borel Theorem.

4.4 Upper semi-continuity of attractors for the Kuramoto-Sivashinsky equation

In order to apply the theory of Hale, Lin and Raugel it is necessary to obtain an error estimate similar to (4.3.1), which will depend on the regularity of the solutions. It is not known a priori if the solution will be sufficiently regular, in which case nonsmooth error estimates are required. This leads to an estimate of the form

$$\|u_{\text{true}}(t) - u_{\text{numerical}}(t)\|_{H^s} \leq C(T, \|u_0\|_{H^\sigma}) h^{r-s} t^{-\alpha}, \quad \forall t \in (0, T],$$

where $\sigma \leq s$, r depends on the order of the spatial discretization and α depends on r and s . Such an estimate for the Cahn-Hilliard equation with a finite-element approximation is given in Elliott and Larsson [18].

We have avoided proving an error estimate of this form by adapting an alternative approach of proving upper semi-continuity, given in Lord and Stuart [61], for our PS semi-discrete approximation. This approach uses the Gevrey regularity of the solution and the approximate solution.

By Theorem 4.2.3 we know that the global attractor of the K-S equation, \mathcal{A} , is a compact set contained in some subdomain D of the space $X^{1/4}$ and given any $\epsilon > 0$ there exists $T = T(\epsilon)$ such that

$$u(t) \in \mathcal{N}_{X^{1/4}}(\mathcal{A}, \epsilon/2), \quad \forall t \geq T, \quad (4.4.1)$$

where $u_0 \in D$. This is graphically illustrated in Figure 4-3.

In order to prove the existence of local attractors that converge to the attractor of the K-S equation, it is sufficient to show that for a sequence of values of $h \rightarrow 0^+$,

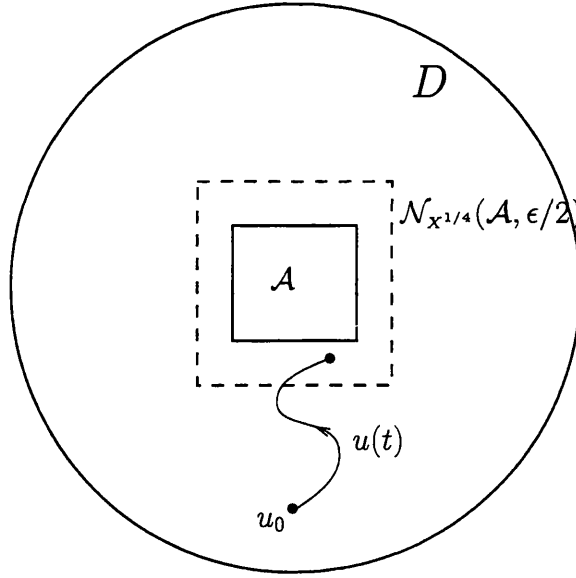


Figure 4-3: Graphical illustration of the properties of the global attractor of the K-S equation.

there exists a time $T_h = T_h(\epsilon)$ such that

$$u_h(t) \in \mathcal{N}_{X^{1/4}}(\mathcal{A}, \epsilon) \cap X_h^\circ, \quad \forall t \geq T_h,$$

where $u_h(0) \in I_h^\circ D$ and X_h° is the approximation space we defined in Section 3.1. This result follows from the next theorem.

Theorem 4.4.1 *Let \mathcal{A} denote the global attractor for the continuous equation (2.3.7) and assume that $u_h(0)$ is in a ball, $\mathcal{B}_{X^{1/4}}(\rho) \cap X_h^\circ$, with ρ large enough so that*

$$\mathcal{N}_{X^{1/4}}(\mathcal{A}, \epsilon) \subset \mathcal{B}_{X^{1/4}}(\rho).$$

Then there exists a local attractor, \mathcal{A}_h for the semigroup $S_h(t)$ of the approximation in the ball $\mathcal{B}_{X^{1/4}}(\rho) \cap X_h^\circ$ such that

$$\delta_{X^{1/4}}(\mathcal{A}_h, \mathcal{A}) \rightarrow 0 \quad \text{as } h \rightarrow 0. \quad (4.4.2)$$

Proof: Since $u_h(0) \in \mathcal{B}_{X^{1/4}}(\rho) \cap X_h^\circ$ we have that the approximate solution $u_h(t)$ is contained in a Gevrey ball $G_t(\sqrt{2}\rho) \cap X_h^\circ$ with radius $\sqrt{2}\rho$ by Theorem 3.3.5,

for $t \in (0, t_{1,h}]$ where $t_{1,h} > 0$. Now if we choose some $t_0 \in (0, t_{1,h})$ and take $u(t_0)$ for the initial data for the continuous equation such that $\mathbf{u}(t_0) = \mathbf{u}_h(t_0)$ then $u(t_0) \in G_{t_0}(\sqrt{2}\rho)$ by Theorem 3.1.13. Hence by Theorem 2.4.9 $u(t)$ will be in a Gevrey class for all $t > t_0$ which implies that $u(t) \in X^s$ for all $s \geq 0$ and $t > t_0$. Therefore if we choose $s = \alpha + 5/4$, with $\alpha \geq 0$ then by Corollary 3.2.9 we have that

$$\|u(t) - u_h(t)\|_{X^{1/4}} \leq C(T^*, \|u(t_0)\|_{X^{\alpha+5/4}})h^{4\alpha}, \quad 0 < t_0 \leq t \leq T^*, \quad (4.4.3)$$

where T^* will be chosen later. Now we have that

$$\begin{aligned} \delta_{X^{1/4}}(u_h, \mathcal{A}) &= \inf_{w \in \mathcal{A}} \|u_h - w\|_{X^{1/4}}, \\ &\leq \delta_{X^{1/4}}(u, w) + \|u_h - u\|_{X^{1/4}}, \end{aligned}$$

where u is a solution of the continuous equation, which implies that

$$\delta_{X^{1/4}}(u_h, \mathcal{A}) \leq \frac{\epsilon}{2} + \|u_h - u\|_{X^{1/4}},$$

by (4.4.1) for all $t \geq t_0 + T$. Thus taking (4.4.3) with $h \leq 1/(\sqrt[4]{\epsilon/(2C)})$ gives

$$\delta_{X^{1/4}}(u_h, \mathcal{A}) \leq \epsilon, \quad \forall t \in [t_0 + T, 2(t_0 + T)], \quad (4.4.4)$$

where we have chosen T^* such that $2(t_0 + T) \leq T^*$. Hence from (4.4.4) we have that

$$u_h(t) \in \mathcal{N}_{X^{1/4}}(\mathcal{A}, \epsilon) \cap X_h^o, \quad \forall t \in [t_0 + T, 2(t_0 + T)], \quad (4.4.5)$$

We now prove that this result holds for all $t \geq t_0 + T$. Let P_n be the statement

$$S_h(t) (\mathcal{B}_{X^{1/4}}(\rho) \cap X_h^o) \subset \mathcal{N}_{X^{1/4}}(\mathcal{A}, \epsilon) \cap X_h^o, \quad \forall t \in [n(t_0 + T), (n+1)(t_0 + T)],$$

and assume that it is true for $n = m$, so that

$$S_h(m(t_0 + T))(\mathcal{B}_{X^{1/4}}(\rho) \cap X_h^o) \subset \mathcal{N}_{X^{1/4}}(\mathcal{A}, \epsilon) \cap X_h^o. \quad (4.4.6)$$

Hence

$$\begin{aligned} S_h(t)(\mathcal{B}_{X^{1/4}}(\rho) \cap X_h^o) &= S_h(t - m(t_0 + T))S_h(m(t_0 + T))(\mathcal{B}_{X^{1/4}}(\rho) \cap X_h^o), \\ &\subset S_h(t - m(t_0 + T))(\mathcal{N}_{X^{1/4}}(\mathcal{A}, \epsilon) \cap X_h^o) \quad \text{by (4.4.6),} \\ &\subset S_h(t - m(t_0 + T))(\mathcal{B}_{X^{1/4}}(\rho) \cap X_h^o) \quad \text{by (4.4.2),} \end{aligned}$$

and by (4.4.5),

$$S_h(t)(\mathcal{B}_{X^{1/4}}(\rho) \cap X_h^o) \subset \mathcal{N}_{X^{1/4}}(\mathcal{A}, \epsilon) \cap X_h^o, \quad (4.4.7)$$

for all $t \in [(m+1)(t_0 + T), (m+2)(t_0 + T)]$. Therefore P_n is true for $n = m+1$, so by induction P_n is true for all $n \in \mathbb{N}$. Therefore $\mathcal{N}_{X^{1/4}}(\mathcal{A}, \epsilon) \cap X_h^o$ is an absorbing ball in $\mathcal{B}_{X^{1/4}}(\rho) \cap X_h^o$ and since $S_h(t)$ is asymptotically smooth, there exists a local attractor in $\mathcal{B}_{X^{1/4}}(\rho) \cap X_h^o$ for $S_h(t)$ defined by

$$\mathcal{A}_h = \omega_h(\mathcal{N}_{X^{1/4}}(\mathcal{A}, \epsilon) \cap X_h^o),$$

by Theorem 4.1.15, where ω_h is defined in (4.3.8). So by definition

$$S_h(t)\mathcal{A}_h \subset \mathcal{N}_{1/4}(\mathcal{A}, \epsilon) \cap X_h^o, \quad \forall t \geq t_0 + T,$$

which implies that

$$\mathcal{A}_h \subset \mathcal{N}_{1/4}(\mathcal{A}, \epsilon) \cap X_h^o, \quad \forall t \geq t_0 + T,$$

since \mathcal{A}_h is invariant, and we have that

$$\lim_{h \rightarrow 0} \delta_{X^{1/4}}(\mathcal{A}_h, \mathcal{A}) = 0.$$

□

As mentioned before the approach that we have adopted here for proving upper semi-continuity is similar to the type of argument used in Lord and Stuart [61]. However in this paper it is necessary to prove the existence of an absorbing Gevrey Ball for the approximation, which contains the approximate attractor. In order to show the existence of this absorbing ball it is necessary to prove time independent bounds on the solution of the approximation in the $X^{1/4}$ norm. We have managed to avoid this and therefore increase the generality of this approach.

Theorem 4.4.1 implies that there exists a time $t_h^* > 0$ such that

$$\|\mathbf{U}(t)\|_{X_h^{1/4}} \leq \mathcal{R}_A, \quad \forall t \geq t_h^*, \quad (4.4.8)$$

where $\mathcal{R}_A = \sup_{u \in \mathcal{A}} \|u\|_{X_h^{1/4}}$. Hence we can extend the discrete Gevrey result for the PS discretization in Theorem 3.3.5.

Theorem 4.4.2 *Let $u_h(0) \in \mathcal{B}_{X^{1/4}}(\rho) \cap X_h^\rho$, where ρ is given in Theorem 4.4.1. Then there exists τ_h independent of u_0 such that*

$$\mathbf{U}(t) \in G_{\tau_h, h}, \quad \forall t \geq \tau_h + t_h^*.$$

Proof: Similar to the proof of the analogous result for the solutions of the K-S equation given in Theorem 2.4.9.

□

4.5 Orbits homoclinic to saddle-focus points

We now digress briefly from considering the approximation of attractors by numerical methods and introduce some background theory from Glendinning and Sparrow [33] and Wiggins [95], concerning a certain type of homoclinic orbit. This will be important when we look at the asymptotic global dynamics of the K-S equation in more detail, later in this thesis. Let us consider the one parameter family of autonomous third order ODE's, which can be written in the

form

$$\begin{aligned}\dot{x} &= -\eta_2 x - \nu y + P(x, y, z; \mu), \\ \dot{y} &= \nu x - \eta_2 y + Q(x, y, z; \mu), \\ \dot{z} &= \eta_1 z + R(x, y, z; \mu),\end{aligned}\tag{4.5.9}$$

where $\eta_1, \eta_2 > 0$ and P, Q, R are analytic functions which vanish along with their derivatives when $x = y = z = 0$. Hence the origin is a steady state which is of saddle-focus type as the linearization of (4.5.9) about this point has eigenvalues $\eta_1, -\eta_2 \pm i\nu$. We also suppose that (4.5.9) possesses a homoclinic orbit connecting the origin to itself at $\mu = 0$. We illustrate the behaviour of this orbit for the differing values of μ in Figure 4-4. This type of system was first studied by Sil'nikov in [80].

It is possible to construct a Poincaré map for (4.5.9) in order to analyse the periodic behaviour for different values of μ . In the papers [33] and [95] this behaviour is considered when $\delta := (\eta_2/\eta_1) > 1$ and $\delta < 1$, we will only consider the latter of these two cases. It has been shown that when $\mu < 0$ and $\mu > 0$ there is a finite number of periodic orbits and when $\mu = 0$ there is a countable infinity of periodic orbits, we summarise this behaviour and the stability properties in a bifurcation diagram in Figure 4-5. This figure shows that the periodic orbits tends to having infinite orbits as they wind around the unstable manifold of the origin as μ tends to zero.

Now if we consider stability, we note that when $\delta > 1/2$ the solutions undergo a period doubling bifurcation followed by a reverse period doubling. The stable solutions produced here then loose stability at a saddle node bifurcation, which is regained at a further saddle node. This pattern repeats itself for a countable infinity of times as the orbits wind around the unstable manifold. In fact on each branch we have not only a period doubling bifurcation but a complete period doubling cascade following or preceding the saddle node bifurcations, which leads to the formation of a horseshoe map. Therefore the Poincaré map associated with the homoclinic orbit at $\mu = 0$ contains an infinite number of horseshoe maps.

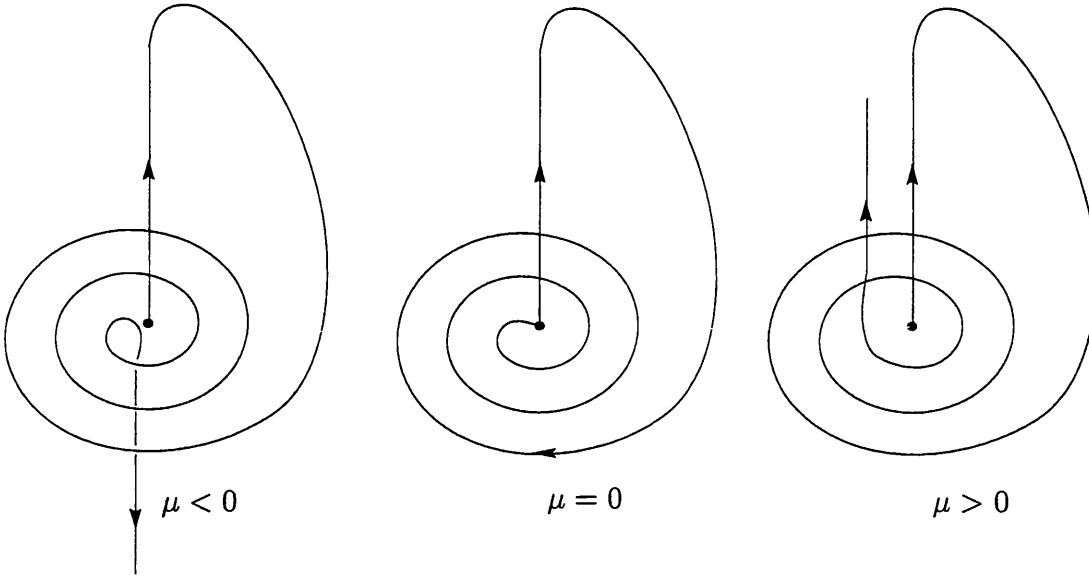


Figure 4-4: Behaviour of the unstable manifold for differing values of μ .

These maps give rise to chaotic behaviour in the system as they are topologically conjugate to the shift map. Hence there exists a strange invariant set made up of a countable infinity of periodic orbits of arbitrarily high period, an uncountable infinity of non-periodic orbits (or aperiodic behaviour) and a dense orbit. These results are also valid in an open interval of the parameter set containing the parameter value at homoclinicity.

The chaotic behaviour observed for the third order system (4.5.9) can be generalised to higher dimensional systems. Suppose that we have the system

$$\dot{\mathbf{x}} = f(\mathbf{x}, \alpha), \quad \mathbf{x} \in \mathbb{R}^n, \quad (4.5.10)$$

with fixed point \mathbf{x}_0 and linearization $Df(\mathbf{x}_0)$ which has one positive real eigenvalue, σ_1 , a complex eigenvalue pair with negative real part, $\lambda_2 = \overline{\lambda_3} = \sigma_2 + iw$ and all remaining eigenvalues, $\lambda_4, \lambda_5, \dots, \lambda_n$, with negative real parts, such that

$$\sigma_1 > 0 > \sigma_2 > \Re\{\lambda_4\} \geq \Re\{\lambda_5\} \geq \dots,$$

Now if we suppose also that there exists a homoclinic orbit at \mathbf{x}_0 for some α ,

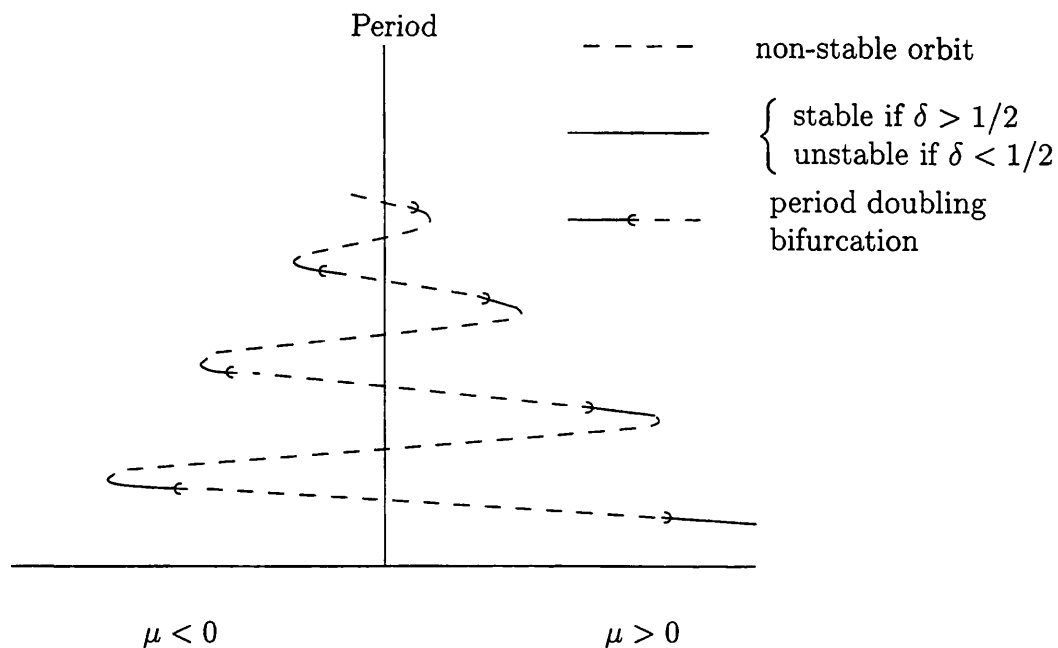


Figure 4-5: Stability diagram of the periodic solutions.

then the system (4.5.10) will be chaotic, as outlined above, if

$$\delta := |\sigma_2|/\sigma_1 < 1. \quad (4.5.11)$$

This condition is often referred to as *Sil'nikov's inequality* and the homoclinic orbits associated with this are usually referred to as Sil'nikov homoclinic orbits. The complicated behaviour implied by this condition has been observed for the Rössler system and the Lorenz equations, see [33] for details.

Chapter 5

Inertial Manifolds

5.1 Introduction

In the previous chapter we showed that the solutions of dissipative PDE's converge as $t \rightarrow \infty$ to a global attracting set \mathcal{A} which is finite-dimensional in a Hausdorff sense. Since \mathcal{A} 's dimension is finite, one may suspect that it is possible to model the dynamics on \mathcal{A} by a large system of ordinary differential equations (ODE's). The theory of inertial manifolds provides us with a rigorous method to do this. The concept of inertial manifolds was introduced by Foias, Sell and Temam in [23] and [24] and we now give a formal definition.

Definition 5.1.1 *A subset \mathcal{M} in the Hilbert space \mathcal{X} is said to be an **inertial manifold** of a dissipative equation if the following conditions hold*

- (i) \mathcal{M} is a finite-dimensional Lipschitz manifold in \mathcal{X} ;*
- (ii) \mathcal{M} is positively invariant under the action of the semigroup $T(t)$, defined by the equation;*
- (iii) \mathcal{M} is exponentially attracting, i.e. there is a $\mu > 0$ such that for every $u_0 \in \mathcal{X}$ there is a constant $C = C(u_0)$ such that*

$$\text{dist}(T(t)u_0, \mathcal{M}) \leq Ce^{-\mu t}, \quad t \geq 0.$$

Remark 5.1.2 Property (iii) in Definition 5.1.1 implies that the inertial manifold contains the global attractor of the underlying system. Also the μ given here is usually referred to as the decay rate and in many cases it has been shown to be very large. This being the case, it is reasonable to expect the inertial manifold to provide useful information about medium-time behaviour of solutions as well as long-time behaviour.

In order to bring out the main ideas of inertial manifolds we consider the following abstract evolution equation

$$\begin{aligned} \frac{du}{dt} + Au + R(u) &= 0, \\ u(0) &= u_0, \end{aligned} \tag{5.1.1}$$

on a separable Hilbert space \mathcal{X} , and we assume that this equation arises from a dissipative PDE. We denote the inner product in \mathcal{X} by $\langle \cdot, \cdot \rangle_{\mathcal{X}}$ and norm by $\| \cdot \|_{\mathcal{X}}^2 = \langle \cdot, \cdot \rangle_{\mathcal{X}}$. We assume that A is a closed, densely defined, self-adjoint, positive operator with compact inverse. The associated eigenfunctions of A are given by $\{\psi_i\}_{i=1}^{\infty}$ with corresponding real eigenvalues $\{\eta_i\}_{i=1}^{\infty}$, such that

$$0 < \eta_1 \leq \eta_2 \leq \dots$$

The assumptions on A imply that the space \mathcal{X} is spanned by the eigenfunctions given above and since \mathcal{X} is considered to be infinite-dimensional we have that $\eta_n \rightarrow \infty$ as $n \rightarrow \infty$. The properties of A also ensure that it is a sectorial operator which implies that it generates an analytic semigroup $L(t)$ and its fractional powers are well defined. The fractional powers can then be used to define the Hilbert spaces $\mathcal{X}^{\alpha} = D(A^{\alpha})$ for $\alpha \geq 0$, which have the inner product $\langle A^{\alpha}u, A^{\alpha}v \rangle_{\mathcal{X}}$ and norm $\|u\|_{\mathcal{X}^{\alpha}} = \|A^{\alpha}u\|_{\mathcal{X}}$ for all $u, v \in \mathcal{X}^{\alpha}$.

We assume that $R(u)$ satisfies sufficient conditions for the initial value problem (5.1.1) to generate a locally Lipschitz continuous semigroup $T(t) : \mathcal{X}^{\alpha} \rightarrow \mathcal{X}^{\alpha}$, for

some $\alpha \geq 0$, i.e.,

$$\|T(t)u - T(t)v\|_{\mathcal{X}^\alpha} \leq C\|u - v\|_{\mathcal{X}^\alpha},$$

where C depends on $\|u\|_{\mathcal{X}^\alpha}$, $\|v\|_{\mathcal{X}^\alpha}$ and t . We suppose further that the system (5.1.1) is dissipative in \mathcal{X}^α , i.e there exists an absorbing ball $\mathcal{B}_{\mathcal{X}^\alpha}(\rho)$ with radius $\rho > 0$ in \mathcal{X}^α .

To date inertial manifolds of dissipative equations, of the form of (5.1.1), have been constructed as graphs of Lipschitz functions. These functions relate the high frequency eigenfunctions of the linear operator A to a finite set of low frequency eigenfunctions. On the inertial manifold the equation can be reduced to a system of ODE's characterised by these low eigenfunctions. This system will have the same asymptotic dynamics as the original equation and is referred to as the *inertial form*.

There are several methods to prove the existence of inertial manifolds for dissipative equations and we will briefly outline some of these before discussing a particular one in detail. In order to apply the various existence methods we must assume that equation (5.1.1) is in a *prepared* (or *modified*) form. This form of the equation is identical to the original equation in a ball containing the asymptotic behaviour, i.e. $\mathcal{B}_{\mathcal{X}^\alpha}(\sigma)$, for $\sigma > \rho$. However outside the ball, the nonlinear operator R is taken to be zero. The reason for this is so that it is possible to obtain uniform estimates for this operator in the $\mathcal{X}^{\alpha-\beta}$ norm, $\beta \in [0, 1)$, in terms of $\|u\|_{\mathcal{X}^\alpha}$. If an inertial manifold exists for the prepared equation then it is possible to show that some open neighbourhood of the global attractor in this inertial manifold is an inertial manifold for the original equation.

The first method used to prove the existence of inertial manifolds is the Liapunov-Perron method, see Chow, Lu and Sell [6] and Foias *et al.* [22], [24] for details. This method involves reducing the search for an invariant manifold, to finding a fixed point for an integral equation which is based on the variation of constants formula of (5.1.1). Extra work is required to show that the manifold obtained by this method attracts all the orbits exponentially.

Other methods of constructions of inertial manifolds rely on a much more geometrical approach. First of all there is the Hadamard or graph transform method, which has been previously used to construct invariant manifolds for finite-dimensional systems. This method has recently been applied to reaction-diffusion equations by Mallet-Paret and Sell [63]. The method involves constructing a finite-dimensional invariant manifold, \mathcal{M}_0 , and then considering the evolution of this manifold under the action of the semigroup $T(t)$, thereby obtaining a set \mathcal{M}_t at each time $t > 0$. It is then possible to prove that, under certain conditions, the limit

$$\lim_{t \rightarrow \infty} \mathcal{M}_t = \mathcal{M},$$

exists and that \mathcal{M} is an invariant manifold which is exponentially attracting. Another geometrical approach used to construct inertial manifolds is the Cauchy method, see Constantin, Foias, Nicolaenko and Temam [8]. In this method the inertial manifold is constructed by considering an integral manifold (or surface) Σ given by

$$\Sigma = \bigcup_{t \geq 0} T(t)\Gamma,$$

where Γ is a smooth boundary chosen so that it is contained in \mathcal{M} . In this method it is shown that under appropriate conditions $\bar{\Sigma}$ is an inertial manifold for (5.1.1).

In order to prove the existence of an inertial manifold using the above methods, the spectrum of the linear operator A must satisfy a *spectral gap* condition. This condition requires that there exists sufficiently large gaps between consecutive eigenvalues of A . This condition is essential in proving the exponential attraction of inertial manifolds.

5.2 Existence and approximation theory of inertial manifolds

In this section we outline the existence and approximation theory of inertial manifolds for dissipative PDE's given in Jones and Stuart [51], Jones, Stuart and Titi [52] and Stuart [84]. The motivation behind these papers is to use the idea of inertial manifolds to prove that the long-time dynamics of approximation schemes accurately reflect the long-time dynamics of the original equation. Other works in this area are Jones [49] and Jones and Titi [53].

We recall from the previous chapter that, in general, it is not possible to approximate individual orbits of dissipative equations over long time intervals, using numerical approximation methods. However, one possible way to interpret data from numerical computations over long time intervals is to study the effect of approximation on sets which are invariant under the action of the semigroup of the original equation. As well as the global attractor, other invariant sets are equilibria, periodic orbits, stable and unstable manifolds and inertial manifolds. Knowledge of these sets is crucial in understanding the asymptotic global dynamics.

In [51] a general framework is set up for proving the existence of inertial manifolds for approximation schemes and the convergence of these inertial manifolds to the true inertial manifold of the underlying equation, as the approximation is refined. In this paper, it is shown that inertial manifolds are both upper and lower semi-continuous under numerical approximation. Since the inertial manifold contains the global attractor this is a step towards establishing a good relationship between the asymptotic global dynamics of the true equation and its approximation.

In [84] the theory in [51] is extended to numerical schemes which approximate dissipative equations, with inertial manifolds, on bounded sets in the C^1 norm. The essential improvement here is that inertial manifolds are shown to persist under numerical approximation and the distance between the inertial forms for

the approximation and the true inertial form can be made arbitrarily small in the C^1 norm. This persistence is considered in much more detail in [52].

Since the inertial forms are finite-dimensional it is possible to apply results from Hirsch and Smale [41], Hirsch, Pugh and Shub [42] and Pliss and Sell [76] concerning the C^1 perturbations of finite-dimensional dynamical systems to the study of infinite-dimensional problems. In particular it is known that certain bounded invariant sets, which include hyperbolic equilibria (and their stable and unstable manifolds) and periodic orbits, persist under such perturbations.

The results in [52] show that if a numerical method approximates the solutions of dissipative equations which possess inertial manifolds in a C^1 sense, then the asymptotic dynamics of the numerical method will give a good representation of the underlying dynamics.

We now look at the theory in the paper [52] in much more detail. In this theory, the variation of constants approach to evolution equations is used to replace the differential equation by a discrete time map. All the main results are proved for this map and are shown to carry over to the continuous equation. Also the contraction mapping principle is extensively used to prove existence and uniqueness of invariant manifolds.

Therefore using the variation of constants approach on (5.1.1), the solution at time τ can be written as

$$u(\tau) = T(\tau)u_0 = L(\tau)u_0 + N(\tau, u_0),$$

where

$$L(\tau)u_0 := e^{-A\tau}u_0, \quad N(\tau, u_0) := - \int_0^\tau L(\tau-s)R(S(s)u_0)ds. \quad (5.2.1)$$

Let $G : \mathcal{X}^\alpha \rightarrow \mathcal{X}^\alpha$ be the mapping

$$G(u) = Lu + N(u), \quad (5.2.2)$$

where L, N are given above and we have dropped the explicit dependence on τ .

If we define $u^{(n)} := u(n\tau)$, then this mapping gives

$$u^{(n+1)} = G(u^{(n)}). \quad (5.2.3)$$

If M is a bounded invariant subset of the semigroup $T(t)$, then M will also be invariant under time τ map G . Also if M is a bounded invariant subset of G then the set $\widehat{M} = \bigcup_{0 \leq t \leq \tau} T(t)M$ is a bounded invariant set of $T(t)$. It therefore suffices to study the behaviour of the invariant sets of G .

To construct an inertial manifold for the map G we must decompose the space \mathcal{X} into a finite-dimensional space and its orthogonal complement. We let $\Lambda > 0$ and let P_Λ denote the orthogonal projection onto the space spanned by the eigenfunctions of A which correspond to the eigenvalues with real part less than or equal to Λ and we let $Q_\Lambda = I - P_\Lambda$. We can now define the spaces

$$\mathcal{Y} = P_\Lambda \mathcal{X} \text{ and } \mathcal{Z} = Q_\Lambda \mathcal{X},$$

so that

$$\mathcal{X} = \mathcal{Y} \oplus \mathcal{Z}.$$

Now if the map G has an inertial manifold, the reduction of the map on this manifold gives a map on the finite-dimensional space \mathcal{Y} , defined by

$$p^{(n+1)} = P_\Lambda G(p^{(n)} + \Phi(p^{(n)})), \quad (5.2.4)$$

where $\Phi : \mathcal{Y} \rightarrow \mathcal{Z}$ is a Lipschitz mapping and the inertial manifold is representable as the graph of this function. The finite-dimensional map (5.2.4) is the inertial form of G and will have the same bounded invariant sets as G .

In order to prove the existence of an inertial manifold for G , using the method of Jones, Stuart and Titi, the following assumptions have to be made on G .

Assumptions \mathcal{G} The map G is dissipative with absorbing ball $\mathcal{B}_{\mathcal{X}^\alpha}(\rho)$, $\rho > 0$.

The linear operator $L \in \mathcal{L}(\mathcal{X}^\alpha)$ and the spaces \mathcal{Y} and \mathcal{Z} are invariant subspaces for L . Moreover there exists positive constants a, b depending on Λ, τ , positive constants K_1, K_2 depending on Λ, τ, ρ and $c \in (0, 1)$ depending on τ , such that

$$\|Lq\|_{\mathcal{X}^\alpha} \leq a\|q\|_{\mathcal{X}^\alpha}, \quad \forall q \in \mathcal{Z}, \quad (\mathcal{G}1)$$

$$b\|p\|_{\mathcal{X}^\alpha} \leq \|Lp\|_{\mathcal{X}^\alpha} \leq c\|p\|_{\mathcal{X}^\alpha}, \quad \forall p \in \mathcal{Y}. \quad (\mathcal{G}2)$$

We assume that there exists a $\sigma > \rho$, such that for all $u \in \mathcal{X}^\alpha$,

$$N(u) = 0 \quad \text{and} \quad DN(u) = 0, \quad \|u\|_{\mathcal{X}^\alpha} \geq \sigma, \quad (\mathcal{G}3)$$

and that $N \in C^1(\mathcal{X}^\alpha, \mathcal{X}^\alpha)$, such that

$$\|\mathcal{R}N(u)\|_{\mathcal{X}^\alpha} \leq K_1, \quad \forall u \in \mathcal{X}^\alpha, \quad (\mathcal{G}4)$$

$$\|\mathcal{R}DN(u)w\|_{\mathcal{X}^\alpha} \leq K_2\|w\|_{\mathcal{X}^\alpha}, \quad \forall u, w \in \mathcal{X}^\alpha, \quad (\mathcal{G}5)$$

where DN is the Fréchet derivative of N and $\mathcal{R} = I, P_\Lambda$ or Q_Λ .

Assumptions $(\mathcal{G}1)$ and $(\mathcal{G}2)$ are concerned with the spectrum of the operator A , $(\mathcal{G}3)$ implies the map G is in a prepared form and $(\mathcal{G}4)$ and $(\mathcal{G}5)$ are global bounds arising from the nonlinearity of G . The following conditions on the constants in Assumptions \mathcal{G} are also required.

Conditions \mathcal{C} Let $\delta, l \in (0, \infty)$ and $\mu \in (0, 1)$, be arbitrarily chosen but fixed and in addition we let $B_i = 2K_i$, $i = 1, 2$. We assume that there exists Λ and $\tau > 0$ depending on δ and l such the following inequalities hold

$$4B_2(1 + l) \leq b - a, \quad (\mathcal{C}1)$$

$$a\delta + B_1 \leq \delta, \quad (\mathcal{C}2)$$

$$al + B_2(1 + l) \leq l\phi, \quad (\mathcal{C}3)$$

where $\phi = b - B_2(1 + l) > 0$, and finally

$$a + B_2(1 + l) \leq \mu. \quad (\mathcal{C}4)$$

Conditions (C1) and (C3) correspond to the spectrum of A having sufficiently large gaps. We recall that this is a sufficient condition for proving the existence of inertial manifolds. Conditions (C2) and (C4) imply that the spectral gap occurs when the eigenvalues of A have sufficiently large real parts. The reason for enlarging the B_i 's from Assumptions \mathcal{G} will be apparent when the approximation theory is introduced later.

We now state the following result from Jones and Stuart [51].

Theorem 5.2.1 *Under Assumptions \mathcal{G} and Conditions \mathcal{C} the map G has an inertial manifold \mathcal{M} , representable as the graph of a function $\Phi : \mathcal{Y} \rightarrow \mathcal{Z}$. Moreover, $\Phi(p) = 0$ for $p \in \mathcal{Y}$ such that $\|p\|_{\mathcal{X}^\alpha} \geq c\sigma + B_1$ and*

$$\sup_{p \in \mathcal{Y}} \|\Phi(p)\|_{\mathcal{X}^\alpha} \leq \delta, \quad \|\Phi(p_1) - \Phi(p_2)\|_{\mathcal{X}^\alpha} \leq l\|p_1 - p_2\|_{\mathcal{X}^\alpha}, \quad \forall p_1, p_2 \in \mathcal{Y}.$$

Proof: See [51, Theorem 2.2]. The main idea in this proof is to find an invariant manifold which is the graph of a function in the space

$$\begin{aligned} \Gamma(\delta, l) = \{ & \Psi \in C(\mathcal{Y}, \mathcal{Z}) : \sup_{p \in \mathcal{Y}} \|\Psi(p)\|_{\mathcal{X}^\alpha} \leq \delta, \\ & \Psi(p) = 0, \forall p \in \mathcal{Y} : \|p\|_{\mathcal{X}^\alpha} \geq c\sigma + B_1, \\ & \|\Psi(p_1) - \Psi(p_2)\|_{\mathcal{X}^\alpha} \leq l\|p_1 - p_2\|_{\mathcal{X}^\alpha}, \forall p_1, p_2 \in \mathcal{Y} \}, \end{aligned}$$

Projecting (5.2.2) with the operators P_Λ and Q_Λ gives

$$p^{(m+1)} = Lp^{(m)} + P_\Lambda N(p^{(m)} + q^{(m)}), \quad (5.2.5)$$

$$q^{(m+1)} = Lq^{(m)} + Q_\Lambda N(p^{(m)} + q^{(m)}), \quad (5.2.6)$$

where $u^{(m)} = p^{(m)} + q^{(m)}$ is an arbitrary orbit with $p^{(m)} \in \mathcal{Y}$, $q^{(m)} \in \mathcal{Z}$ and $m \geq 0$. Therefore an invariant manifold will be the graph of the fixed point Φ of

the operator $T : \Gamma(\delta, l) \rightarrow \Gamma(\delta, l)$ defined by

$$p = L\xi + P_\Lambda N(\xi + \Psi(\xi)), \quad (5.2.7)$$

$$(T\Psi)(p) = L\Psi(\xi) + Q_\Lambda N(\xi + \Psi(\xi)). \quad (5.2.8)$$

The existence of the fixed point follows from the contraction mapping principle. \square

The main point to note from Theorem 5.2.1 is that \mathcal{M} is an inertial manifold for the discrete time τ map G . However this manifold can be shown to be the inertial manifold for equation (5.1.1) if τ is taken to be small, see [51, Theorem 4.2] for details.

The next step of the theory in [52] is to prove that the Φ , given in Theorem 5.2.1, is in the space $C^1(\mathcal{Y}, \mathcal{Z})$. This property is essential for applying the C^1 perturbation theory we mentioned earlier. However before stating this result we define the operator norm by

$$\|T\|_{op} := \sup_{u \in \mathcal{X}^\alpha} (\|Tu\|_{\mathcal{X}^\alpha} / \|u\|_{\mathcal{X}^\alpha}),$$

where T is an operator on \mathcal{X}^α and we define the space

$$\begin{aligned} \Gamma(l) = \{ \Upsilon \in C(\mathcal{Y}, L(\mathcal{Y}, \mathcal{Z})) : & \|\Upsilon\|_\Gamma := \sup_{p \in \mathcal{Y}} \|\Upsilon(p)\|_{op} \leq l, \\ & D\Upsilon(p) = 0, \forall p \in \mathcal{Y} : \|p\|_{\mathcal{X}^\alpha} \geq c\sigma + B_1 \}. \end{aligned}$$

Theorem 5.2.2 *Under Assumptions \mathcal{G} and Conditions \mathcal{C} the map G has an inertial manifold which is representable as the graph of the function $\Phi \in C^1(\mathcal{Y}, \mathcal{Z})$. Moreover $\Phi \in \Gamma(\delta, l)$ and $D\Phi \in \Gamma(l)$.*

Proof: See [52, Theorem 2.5]. The basic idea in this proof follows the work of Chow, Lu and Sell [6]. First of all it is assumed that the Φ given in Theorem 5.2.1 is Fréchet differentiable. A map is then formulated for which $D\Phi$ would be a fixed point and the contraction mapping principle is used to show that $D\Phi$ is indeed a fixed point which is the Fréchet derivative of Φ .

□

Having introduced the existence theory for C^1 inertial manifolds in [52], we now consider the approximation theory. This theory is an important development in the area of numerical analysis of PDE's, by the remarks we made earlier in this section.

We let $G_h^*(\tau, u)$ be the approximation to the map G considered above. This map could arise from a fully or semi-discrete approximation to equation (5.1.1). We assume that this map is defined on some finite-dimensional subspace \mathcal{X}_h of $D(A^\alpha)$ and we define the operator $P_h : \mathcal{X} \rightarrow \mathcal{X}_h$. It is convenient to express G_h^* as a map on the space $D(A^\alpha)$ and hence we define

$$G_h(v) := G_h^*(P_h v), \quad (5.2.9)$$

where we have dropped the explicit dependence τ . In order to prove that the bounded invariant sets of G persist under approximation by the mapping G_h , the following assumptions on G_h have to be made.

Assumptions \mathcal{G}_h

$$\|E(v)\|_{\mathcal{X}^\alpha} := \|G(v) - G_h(v)\|_{\mathcal{X}^\alpha} \leq K(\rho)h, \quad \forall v \in \mathcal{B}_{\mathcal{X}^\alpha}(2\rho), \quad (\mathcal{G}_h1)$$

$$\|DE(v)\|_{op} := \|DG(v) - DG_h(v)\|_{op} \leq K(\rho)h, \quad \forall v \in \mathcal{B}_{\mathcal{X}^\alpha}(2\rho), \quad (\mathcal{G}_h2)$$

where DE is the Fréchet derivative of E and ρ was previously given in Assumptions \mathcal{G} .

In these assumptions all we need to check is that the numerical discretization approximates the map G in the C^1 norm over the ball $\mathcal{B}_{\mathcal{X}^\alpha}(2\rho)$ which contains all the bounded invariant sets. This is an essential improvement over the work in [51] where it was necessary to obtain error estimates for the discretization of the prepared equation.

If we were to assume that the map G_h is dissipative then Assumptions \mathcal{G}_h would guarantee the existence of an inertial manifold for G_h , see [84] for details.

This assumption is not necessary to prove the persistence of the bounded invariant sets of G to its approximation. However, it is essential to prove the existence of an inertial form for a map related to G_h , in the ball $\mathcal{B}_{\mathcal{X}^\alpha}(\rho)$. Therefore we introduce a fixed cut-off function $\theta \in C^\infty([0, \infty); [0, 1])$, which satisfies

$$\theta(x) = \begin{cases} 1, & 0 \leq x \leq 2, \\ 0, & 4 \leq x, \end{cases}$$

with $|\theta'(x)| \leq 2$ for all $x \geq 0$. Given this function we define the $\theta_\rho(x) = \theta(x/\rho^2)$ and the map \tilde{G}_h by

$$\begin{aligned} \tilde{G}_h(v) &= Lv + N(v) - \theta_\rho(\|v\|_{\mathcal{X}^\alpha}^2)E(v), \\ &:= Lv + N_h(v), \end{aligned} \tag{5.2.10}$$

where L and N are defined in (5.2.1) and

$$N_h(v) := N(v) - \theta_\rho(\|v\|_{\mathcal{X}^\alpha}^2)E(v). \tag{5.2.11}$$

The map \tilde{G}_h agrees with the map G_h inside the ball $\mathcal{B}_{\mathcal{X}^\alpha}(\sqrt{2}\rho)$ and is dissipative. Also from (\mathcal{G}_h1) and (\mathcal{G}_h2) we have

$$\|G(v) - \tilde{G}_h(v)\|_{\mathcal{X}^\alpha} \leq K(\rho)h, \quad \forall v \in \mathcal{X}^\alpha, \tag{5.2.12}$$

$$\|DG(v) - D\tilde{G}_h(v)\|_{op} \leq K(\rho)h, \quad \forall v \in \mathcal{X}^\alpha. \tag{5.2.13}$$

The following theorem shows that \tilde{G}_h has an inertial manifold.

Theorem 5.2.3 *Under Assumptions \mathcal{G} , \mathcal{G}_h and Conditions \mathcal{C} , there exists a constant $h_1 > 0$ depending on $\tau, \Lambda, \epsilon, l$, such that the map \tilde{G}_h has an inertial manifold, \mathcal{M}_h , which is representable as the graph of a C^1 function $\Phi_h : \mathcal{Y} \rightarrow \mathcal{Z}$. Moreover $\Phi_h \in \Gamma(\epsilon, l)$ and $D\Phi_h \in \Gamma(l)$.*

Proof: See [52, Theorem 3.1]. This is a straight-forward application of Theorem 5.2.2. It is only necessary to show that $N_h(v)$ has similar properties to $N(v)$ in

Assumptions \mathcal{G} . From (5.2.11), we have that

$$\begin{aligned}\|\mathcal{R}N_h(v)\|_{\mathcal{X}^\alpha} &\leq \|\mathcal{R}N(v)\|_{\mathcal{X}^\alpha} + \|\theta_\rho(\|v\|_{\mathcal{X}^\alpha}^2)\mathcal{R}E(v)\|_{\mathcal{X}^\alpha}, \\ &\leq K_1 + K(\rho)h, \quad \forall v \in \mathcal{X}^\alpha.\end{aligned}$$

where \mathcal{R} is given in Assumptions \mathcal{G} . Similarly

$$\begin{aligned}\|\mathcal{R}DN_h(v)\|_{op} &= \|\mathcal{R}D[N(v) - \theta_\rho(\|v\|_{\mathcal{X}^\alpha}^2)E(v)]\|_{op}, \\ &\leq \|\mathcal{R}[DN(v) - \theta_\rho(\|v\|_{\mathcal{X}^\alpha}^2)DE(v)]\|_{op} + \|D\theta_\rho(\|v\|_{\mathcal{X}^\alpha}^2)\mathcal{R}E(v)\|_{op}, \\ &\leq K_2 + K(\rho)h + \frac{8}{\rho}K(\rho)h.\end{aligned}$$

Hence assuming that $\rho > 1$ we have that for some $h_1 > 0$,

$$\|N_h(v)\|_{\mathcal{X}^\alpha} \leq B_1, \quad \|DN_h(v)\|_{op} \leq B_2, \quad \forall v \in \mathcal{X}^\alpha,$$

for $h \leq h_1$, where B_1 and B_2 are the constants given in Conditions \mathcal{C} , which illustrates why it was necessary to increase the size of K_1 and K_2 earlier. \square

The map \tilde{G}_h restricted to its inertial manifold gives the following inertial form defined on \mathcal{Y} ,

$$p_{n+1} = P_\Lambda \tilde{G}_h(p_n + \Phi_h(p_n)),$$

where $p_n \in \mathcal{Y}$. This finite system will have the same dynamics as \tilde{G}_h and will agree with the map G_h in the ball $\mathcal{B}_{\mathcal{X}^\alpha}(\rho)$.

It is also possible to prove that the inertial manifolds of \tilde{G}_h converge to the inertial manifolds of G in the C^1 norm as $h \rightarrow 0^+$. This result is given in the following theorem.

Theorem 5.2.4 *Suppose that Assumptions \mathcal{G} , \mathcal{G}_h , Conditions \mathcal{C} and that $h \leq h_1$ so that the map \tilde{G}_h has an inertial manifold as in Theorem 5.2.3. Then for any*

$\epsilon > 0$, there exists an $h_0(\epsilon) > 0$ such that

$$\sup_{p \in \mathcal{Y}} \|\Phi(p) - \Phi_h(p)\|_{\mathcal{X}^\alpha} \leq K(\rho)h, \quad (5.2.14)$$

$$\sup_{p \in \mathcal{Y}} \|D\Phi(p) - D\Phi_h(p)\|_{\mathcal{X}^\alpha} \leq \epsilon, \quad (5.2.15)$$

for all $h \in (0, h_0)$.

Proof: See [52, Theorem 3.2].

□

Theorem 5.2.4 implies that Φ_h can be made close to the Φ , in the C^1 norm, if h is taken to be sufficiently small it is possible to make

$$P_\Lambda G(p + \Phi(p)) - P_\Lambda \tilde{G}_h(p + \Phi_h(p)),$$

arbitrarily small in the C^1 norm in $\mathcal{B}_{\mathcal{X}^\alpha}(\rho)$. Given these results one can apply the theory concerning the persistence of bounded invariant sets of finite-dimensional systems under C^1 perturbation. Also since G and \tilde{G}_h will have the same bounded invariant sets as their respective inertial forms, we can apply this theory to the PDE and its numerical approximation. Hence we can make deductions about the relationships between the true and approximate flows on the attractor.

5.3 Inertial manifolds for the Kuramoto-Sivashinsky equation

In this section we prove the existence of a C^1 inertial manifold for the K-S equation (2.4.3) using the existence theory outlined in the previous section. Therefore it is necessary to verify Assumptions \mathcal{G} and Conditions \mathcal{C} for this equation. We begin by truncating the nonlinear term in (2.4.3) and formulating a discrete time map.

We recall, from Lemma 4.2.2, that the K-S equation is dissipative in X^s , for all $s \geq 0$ with $4s \in \mathbb{N} \cup \{0\}$. We will therefore denote by $\mathcal{B}_{X^s}(\rho)$, $\rho > 0$, the

absorbing ball in this space. Given this ball, we consider the following prepared equation of (2.4.3),

$$\begin{aligned} \frac{du}{dt} + Au + F_\theta(u) &= 0, \\ u(0) &= u_0 \in X^s, \end{aligned} \tag{5.3.1}$$

where

$$F_\theta(u) = \theta_\rho(\|u\|_{X^s}^2)F(u). \tag{5.3.2}$$

Equation (5.3.1) will have the same long-time dynamics as (2.4.3) and if an inertial manifold exists for this equation, the intersection of this inertial manifold with the absorbing ball defines an inertial manifold for the K-S equation.

It is possible to write equation (5.3.1) in the form

$$G(u_0) = u(\tau) = L(\tau)u_0 + N(\tau, u_0), \tag{5.3.3}$$

for any fixed τ , where

$$L(\tau) = e^{-A\tau}, \quad N(\tau, u_0) = - \int_0^\tau e^{-A(\tau-s)} F_\theta(u(s)) ds.$$

Also, since the eigenfunctions of A in (5.3.1) form a complete orthonormal basis for the space X , we can set $P_\Lambda := P_m$, the projection onto the first m eigenfunctions $\{\omega_k\}_{k=1}^m$, and $Q_\Lambda := Q_m = I - P_m$, where P_Λ and Q_Λ were defined in the last section. This implies that the L , given in (5.3.3), trivially satisfies (G1) and (G2) with

$$a = e^{-\lambda_{m+1}\tau}, \quad b = e^{-\lambda_m\tau}, \quad c = e^{-\lambda_1\tau},$$

where the λ_i 's are the eigenvalues of A .

In order to verify the assumptions on the nonlinear terms N and DN we will need to use the results of Theorems 2.4.7 and 2.4.8, which imply that (2.4.3) has a unique solution, $u(t) \in C^1([0, \infty); X^s)$, for $s > 5/8$ with $4s \in \mathbb{N}$. These theorems

also hold for equation (5.3.1) by the properties of the mapping θ_ρ . Hence for N , we have that

$$\begin{aligned} \|N(\tau, u_0)\|_{X^s} &= \left\| \int_0^\tau A^{1/2} e^{-A(\tau-t)} A^{s-1/2} F_\theta(u(t)) dt \right\|_{L^2}, \\ &\leq \int_0^\tau \|A^{1/2} e^{-A(\tau-t)}\|_{L^2} \|F_\theta(u(t))\|_{X^{s-1/2}} dt, \\ &\leq \int_0^\tau \frac{C_1}{(\tau-t)^{1/2}} \|F_\theta(u(t))\|_{X^{s-1/2}} dt. \end{aligned} \quad (5.3.4)$$

Now from the proof of Lemma 2.4.6, for $0 \leq t \leq \tau$, it is possible to obtain the estimate

$$\|F_\theta(u(t))\|_{X^{s-1/2}} \leq M_1(\rho), \quad \forall u(t) \in X^s.$$

Hence (5.3.4) becomes

$$\begin{aligned} \|N(\tau, u_0)\|_{X^s} &\leq \int_0^\tau \frac{C_1 M_1}{(\tau-t)^{1/2}} dt, \\ &= K_1 \tau^{1/2}, \end{aligned} \quad (5.3.5)$$

where $K_1 = C_1 M_1$. Similarly for any $w_0 \in X^s$, we have that

$$\begin{aligned} \|DN(\tau, u_0)w_0\|_{X^s} &= \left\| \int_0^\tau A^{1/2} e^{-A(\tau-t)} A^{s-1/2} DF_\theta(u(t))w(t) dt \right\|_{L^2}, \\ &\leq \int_0^\tau \|A^{1/2} e^{-A(\tau-t)}\|_{L^2} \|DF_\theta(u(t))w(t)\|_{X^{s-1/2}} dt, \\ &\leq \int_0^\tau \frac{C_2}{(\tau-t)^{1/2}} \|DF_\theta(u(t))w(t)\|_{X^{s-1/2}} dt. \end{aligned} \quad (5.3.6)$$

Also from the proof of Theorem 2.4.8 it is possible to show that

$$\|DF_\theta(u(t))w(t)\|_{X^{s-1/2}} \leq M_2(\rho) \|w(t)\|_{X^s}, \quad \forall u(t) \in X^s,$$

Hence (5.3.6) becomes

$$\begin{aligned} \|DN(\tau, u_0)w_0\|_{X^s} &\leq \int_0^\tau \frac{C_2 M_2 \|w(t)\|_{X^s}}{(\tau - t)^{1/2}} dt, \\ &\leq \max_{t \in [0, \tau]} \|w(t)\|_{X^s} C_2 M_2 \tau^{1/2}. \end{aligned} \quad (5.3.7)$$

Now since $w(t)$ is the solution of the linearized equation of (5.3.1), we have that

$$\max_{t \in [0, \tau]} \|w(t)\|_{X^s} \leq K(\tau) \|w_0\|_{X^s},$$

so that (5.3.7) becomes

$$\|DN(\tau, u_0)w_0\|_{X^s} = K_2 \tau^{1/2} \|w_0\|_{X^s}, \quad (5.3.8)$$

where $K_2 = K(\tau)C_2 M_2$. Hence the estimates (5.3.5) and (5.3.8) show that (G4) and (G5) hold for the map (5.3.3). Also (G3) follows by definition of the operator F_θ . Having satisfied Assumptions \mathcal{G} we now show that Conditions \mathcal{C} follow for the map (5.3.3).

We recall, from the last section, that Conditions \mathcal{C} are related to properties of the spectrum of the linear operator. The following lemma is essential in establishing Conditions \mathcal{C} for the map (5.3.3) and represents a spectral gap condition.

Lemma 5.3.1 *For any positive real numbers K_3 and K_4 there exists $m \in \mathbb{N}$ such that*

$$\lambda_{m+1}^{1/2} \geq K_3, \quad \lambda_{m+1} - \lambda_m \geq K_4 \lambda_{m+1}^{1/2}, \quad (5.3.9)$$

where $\{\lambda_k\}_{k=1}^\infty$ are the eigenvalues of the operator A .

Proof: First we recall that the eigenvalues of A are given by $\lambda_k = 4k^4$. Let us choose $m \in \mathbb{N}$ such that

$$m \geq \max \left\{ \sqrt{\frac{K_3}{2}} - 1, \frac{2K_4 + 9}{16} \right\}. \quad (5.3.10)$$

Then

$$\lambda_{m+1}^{1/2} = 2(m+1)^2 \geq K_3,$$

by (5.3.10) and

$$\begin{aligned} \lambda_{m+1} - \lambda_m &= 4((m+1)^4 - m^4), \\ &= 4(4m^3 + 6m^2 + 4m + 1), \\ &\geq 2 \left(4(m+1) - \frac{25}{4} \right) 2(m+1)^2, \\ &\geq K_4 \lambda_{m+1}^{1/2}, \end{aligned}$$

by (5.3.10).

□

Given the existence of the spectral gap condition in the above lemma, we prove the following lemma.

Lemma 5.3.2 *Suppose that for any $K_3, K_4 > 0$ given in Lemma 5.3.1, there exists a natural number $m_0 > 0$ such that (5.3.9) holds for any $m \geq m_0$. Then Conditions C hold for the map (5.3.3).*

Proof: Let $\delta, l \in (0, \infty)$ and $\mu \in (e^{-1}, 1)$ be given and we define τ, K_3 and K_4 by

$$\tau = \frac{1}{\lambda_{m+1}}, \tag{5.3.11}$$

$$K_3 = \max \left\{ \frac{4K_1}{\delta}, \frac{2K_2(1+l)}{\mu - e^{-1}} \right\}, \tag{5.3.12}$$

$$K_4 = \max \left\{ 8K_2e(1+l), \frac{2K_2e(1+l)^2}{l} \right\}. \tag{5.3.13}$$

From (5.3.9) and (5.3.13) we obtain

$$(\lambda_{m+1} - \lambda_m)\tau \geq 8K_2\tau^{1/2}e(1+l),$$

which gives

$$e^{(\lambda_{m+1}-\lambda_m)\tau} - 1 \geq 8K_2\tau^{1/2}e(1+l),$$

since $e^x - 1 \geq x$, for $x \geq 0$. Hence we obtain

$$e^{-\lambda_m\tau} - e^{-\lambda_{m+1}\tau} \geq 8K_2\tau^{1/2}(1+l),$$

which can be written as $b - a \geq 4B_2(1+l)$, with $B_2 = 2K_2\tau^{1/2}$ and we have established (C1). Next, (5.3.9) and (5.3.12) imply that

$$\lambda_{m+1}^{1/2} \geq \frac{4K_1}{\delta},$$

which gives

$$\delta(\lambda_{m+1}\tau + 1) \geq 4K_1\tau^{1/2} + \delta.$$

Dividing by $1 + \lambda_{m+1}\tau$ and using the inequality $e^{-x} \leq 1/(1+x)$, for $x \geq 0$, gives

$$\delta \geq 2K_1\tau^{1/2} + \delta e^{-\lambda_{m+1}\tau},$$

which satisfies (C2) with $B_1 = K_1\tau^{1/2}$. From (5.3.9) and (5.3.13) we can also obtain

$$\lambda_{m+1} - \lambda_m \geq \lambda_{m+1}^{1/2} \frac{2K_2e(1+l)^2}{l},$$

so that

$$e^{(\lambda_{m+1}-\lambda_m)\tau} - 1 \geq \frac{2\tau^{1/2}K_2e(1+l)^2}{l}.$$

Since $(1+l)^2 = (1+l) + l(1+l)$, this last inequality becomes

$$l(e^{-\lambda_m\tau} - e^{-\lambda_{m+1}\tau}) \geq 2K_2\tau^{1/2}(1+l) + 2K_2\tau^{1/2}(1+l)l,$$

which can be written as

$$le^{-\lambda_{m+1}\tau} + 2K_2\tau^{1/2}(1+l) \leq l(e^{-\lambda_m\tau} - 2K_2\tau^{1/2}(1+l)).$$

Hence (C3) is established. Finally (5.3.9) and (5.3.12) imply that

$$\lambda_{m+1}^{1/2} \geq \frac{2K_2(1+l)}{\mu - e^{-1}},$$

which gives

$$\mu \geq 2\tau^{1/2}K_2(1+l) + e^{-1},$$

which satisfies (C4). □

We can now state the following existence theorem for an inertial manifold for the K-S equation.

Theorem 5.3.3 *Suppose that there exists a natural number $m_0 > 0$ such that (5.3.9) holds for all $m \geq m_0$. Then the K-S equation given by (2.4.3) has an inertial manifold, which is representable as the graph of a Lipschitz function $\Phi \in C^1(P_m X, Q_m X)$ within the ball $\mathcal{B}_{X^s}(\rho)$, for $s > 5/8$ with $4s \in \mathbb{N}$*

Proof: Having verified Assumptions \mathcal{G} and Conditions \mathcal{C} , we can apply Theorem 5.2.2 to the map (5.3.3). The inertial manifold for this map is an inertial manifold for (5.3.1) for sufficiently small τ , and this manifold defines an inertial manifold for the K-S equation (2.4.3) in the ball $\mathcal{B}_{X^s}(\rho)$. □

The K-S equation with periodic boundary conditions has also been shown to possess an inertial manifold in Foias *et al.* [8], [9], [22] and [24]. In the paper by Temam and Wang [90] it has been shown this inertial manifold in L^2 and in X^s , $4s \in \mathbb{N}$, has the following bound on its Euclidean dimension

$$\dim(\mathcal{M}) = \mathcal{O}(\alpha^{4/5}) \quad \text{and} \quad \dim(\mathcal{M}) = \mathcal{O}(\alpha^{0.5(3.28s+2.05)}),$$

respectively.

Many other dissipative PDE's modelling physical systems have been shown to possess an inertial manifold, these include the Cahn-Hilliard equation, see [8] and [69], the Ginzburg-Landau equation, see [14], several reaction-diffusion equations, see [8], [46], [65] and [63] and the Swift-Hohenberg equation, see [86]. It is still an open question as to whether the two-dimensional Navier-Stokes equation has an inertial manifold.

5.4 Convergence of the Fréchet derivative of the semi-discrete approximation

5.4.1 The Fréchet derivative

In order to apply the perturbation studies of Jones, Stuart and Titi [52] we need to verify Assumptions \mathcal{G}_h for our PS semi-discrete approximation (3.1.17). We can use the convergence results in Section 3.2 to satisfy (\mathcal{G}_h1) . However we must formulate a similar convergence result for the Fréchet derivatives of the solution, $u(t)$ and the approximation, $u_h(t)$. Hence we have to show that

$$\sup_{v_0 \in X^s} \frac{\| [Du(t) - Du_h(t)]v_0 \|_{X^s}}{\|v_0\|_{X^s}} \leq K(\rho)h, \quad t \in [0, T], \quad (5.4.1)$$

for all initial data in $\mathcal{B}_{X^s}(2\rho)$ and $T > 0$. We recall that $v(t) := Du(t)v_0$ is the derivative of $u(t)$ with respect to initial data applied to v_0 , which satisfies

$$\begin{aligned} \frac{\partial v}{\partial t} + 4 \frac{\partial^4 v}{\partial x^4} + \alpha \left(\frac{\partial^2 v}{\partial x^2} + u \frac{\partial v}{\partial x} + \frac{\partial u}{\partial x} v \right) &= 0, \\ v(0) &= v_0. \end{aligned} \quad (5.4.2)$$

by Theorem 2.4.8. In order to show that (5.4.1) holds we must find the linearized equation of the PS approximation and prove some regularity of the solutions of this equation.

Below we will state and prove an analogous result to Theorem 2.4.8 for the

PS approximation. We first consider the sectorial properties of the operator A_h .

Lemma 5.4.1 *The operator A_h is sectorial on X_h^s .*

Proof: The operator A_h is closed and densely defined on the space X_h^s , by its finite dimensionality. Also from Theorem 2.4.2 and Theorem 3.1.3 we have that

$$\|(\lambda - A_h)^{-1}\|_{L_h^2} \leq \frac{\sqrt{2}}{|\lambda - \lambda_1|}.$$

Therefore following the relevant part of the proof of Lemma 2.4.5 for the operator A , it is possible to show that

$$\|(\lambda - A_h)^{-1}\|_{X_h^s} \leq \frac{\sqrt{2}}{|\lambda - \lambda_1|},$$

and we have satisfied Definition 2.2.3. □

Lemma 5.4.2 *Let $u(x) \in X^s$, $s > 1/8$, then*

$$\|\mathbf{u}\|_{X_h^s} \leq (C + 1)\|u\|_{X^s},$$

where $\mathbf{u} = [u(x_1), u(x_2), \dots, u(x_{N-1})]^T$ and C is a positive constant independent of u .

Proof: From Lemma 3.2.3 we have that

$$\|I_h^o u - u\|_{X^s} \leq C\|u\|_{X^s},$$

and by definition of we also have

$$I_h^o u(x_j) = u(x_j), \quad 1 \leq j \leq N - 1,$$

so that

$$\|I_h^o u\|_{X^s} = \|\mathbf{u}\|_{X_h^s},$$

which implies that

$$\|\mathbf{u}\|_{X_h^s} \leq (C + 1)\|u\|_{X_h^s}.$$

□

We now state the following regularity result.

Theorem 5.4.3 *Let $\mathbf{U}(t)$ be the solution of the PS approximation (3.1.17) of the K-S equation. Then the semigroup for the approximation $S_h(t)$ is continuously differentiable from X_h^s into X_h^s , for $s > 5/8$ with $4s \in \mathbb{N}$, with respect to initial data \mathbf{U}_0 . This derivative applied to $\mathbf{V}_0 \in X_h^s$ gives $\mathbf{V}(t) = D\mathbf{U}(t)\mathbf{V}_0 \in X_h^s$ which satisfies the following equation*

$$\begin{aligned} \frac{d\mathbf{V}}{dt} + 4D_h^4\mathbf{V} + \alpha D_h^2\mathbf{V} + \frac{\alpha}{3}\mathbf{B}(\mathbf{U}, \mathbf{V}) &= \mathbf{0}, \\ \mathbf{V}(0) &= \mathbf{v}_0, \end{aligned} \quad (5.4.3)$$

where $\mathbf{B}(\mathbf{U}, \mathbf{V}) = [\mathbf{U} \otimes D_h^\circ\mathbf{V} + 2D_h^e(\mathbf{U} \otimes \mathbf{V}) + \mathbf{V} \otimes D_h^\circ\mathbf{U}]$.

Proof: We need to satisfy the assumptions of Theorem 2.2.14 for our PS approximation. We already have that A_h is sectorial on the space X_h^s , so it remains to show that $\mathbf{F} : X_h^s \rightarrow X_h^{s-1/2}$ defined by

$$\mathbf{F}(\mathbf{U}) := D_h^2\mathbf{U} + \frac{1}{3}[\mathbf{U} \otimes D_h^\circ\mathbf{U} + D_h^e(\mathbf{U} \otimes \mathbf{U})], \quad \mathbf{U} \in X_h^s,$$

is continuously differentiable on X_h^s . First of all if we let $\mathbf{u}, \mathbf{v} \in X_h^s$ then

$$\begin{aligned} \|\mathbf{F}(\mathbf{u}) - \mathbf{F}(\mathbf{v})\|_{X_h^{s-1/2}} &\leq \|D_h^2\mathbf{u} - D_h^2\mathbf{v}\|_{X_h^{s-1/2}} + \frac{1}{3}\|\mathbf{u} \otimes D_h^\circ\mathbf{u} - \mathbf{v} \otimes D_h^\circ\mathbf{v}\|_{X_h^{s-1/2}} \\ &\quad + \frac{1}{3}\|D_h^e(\mathbf{u} \otimes \mathbf{u}) - D_h^e(\mathbf{v} \otimes \mathbf{v})\|_{X_h^{s-1/2}}, \\ &\leq \|D_h^2(\mathbf{u} - \mathbf{v})\|_{X_h^{s-1/2}} + \frac{1}{3}\|(\mathbf{u} - \mathbf{v}) \otimes D_h^\circ\mathbf{u}\|_{X_h^{s-1/2}} \\ &\quad + \frac{1}{3}\|\mathbf{u} \otimes D_h^\circ(\mathbf{u} - \mathbf{v})\|_{X_h^{s-1/2}} \\ &\quad + \frac{1}{3}\|D_h^e(\mathbf{u} \otimes \mathbf{u} - \mathbf{v} \otimes \mathbf{v})\|_{X_h^{s-1/2}}, \end{aligned}$$

which gives

$$\begin{aligned} \|\mathbf{F}(\mathbf{U}) - \mathbf{F}(\mathbf{V})\|_{X_h^{s-1/2}} &\leq C_1 \left\| \frac{\partial^2}{\partial x^2} (u_h - v_h) \right\|_{X^{s-1/2}} + C_2 \left\| (u_h - v_h) \frac{\partial u_h}{\partial x} \right\|_{X^{s-1/2}} \\ &\quad + C_3 \left\| v_h \frac{\partial}{\partial x} (u_h - v_h) \right\|_{X^{s-1/2}} + C_4 \left\| \frac{\partial}{\partial x} (u_h^2 - v_h^2) \right\|_{X^{s-1/2}}, \end{aligned}$$

by Lemma 5.4.2 using the fact that $s > 5/8$, where u_h and v_h are the sine interpolants of the vectors \mathbf{U} and \mathbf{V} respectively. Applying Theorem 2.1.7 to the last equation gives

$$\begin{aligned} \|\mathbf{F}(\mathbf{U}) - \mathbf{F}(\mathbf{V})\|_{X_h^{s-1/2}} &\leq C'_1 \|u_h - v_h\|_{X^s} + C'_2 \|u_h - v_h\|_{X^{s-1/2}} \|u_h\|_{X^{s-1/4}} \\ &\quad + C'_3 \|v_h\|_{X^{s-1/2}} \|u_h - v_h\|_{X^{s-1/4}} \\ &\quad + C'_4 \|u_h - v_h\|_{X^{s-1/4}} \|u_h + v_h\|_{X^{s-1/4}}, \end{aligned}$$

which implies that

$$\|\mathbf{F}(\mathbf{U}) - \mathbf{F}(\mathbf{V})\|_{X_h^{s-1/2}} \leq C_5 (\|\mathbf{U}\|_{X^s}, \|\mathbf{V}\|_{X^s}) \|\mathbf{U} - \mathbf{V}\|_{X^s}.$$

The derivative of \mathbf{F} at a point $\mathbf{U} \in X_h^s$ is given by the linear operator $D\mathbf{F}(\mathbf{U}) : X_h^s \rightarrow X_h^s$, which is defined by

$$D\mathbf{F}(\mathbf{U})\mathbf{V} := D_h^2 \mathbf{V} + \frac{1}{3} [\mathbf{V} \otimes D_h^\circ \mathbf{U} + \mathbf{U} \otimes D_h^\circ \mathbf{V} + 2D_h^e(\mathbf{U} \otimes \mathbf{W})], \quad (5.4.4)$$

for $\mathbf{V} \in X_h^s$. We now show that the map $\mathbf{U} \rightarrow D\mathbf{F}(\mathbf{U})$ is also continuous. Hence for $\mathbf{U}, \mathbf{V}, \mathbf{W} \in X_h^s$ we have that

$$\begin{aligned} \| [D\mathbf{F}(\mathbf{U}) - D\mathbf{F}(\mathbf{V})] \mathbf{W} \|_{X_h^{s-1/2}} &\leq \frac{1}{3} \| \mathbf{W} \otimes D_h^\circ (\mathbf{U} - \mathbf{V}) \|_{X_h^{s-1/2}} \\ &\quad + \frac{1}{3} \| (\mathbf{U} - \mathbf{V}) \otimes D_h^\circ \mathbf{W} \|_{X_h^{s-1/2}} \\ &\quad + \frac{2}{3} \| D_h^e [(\mathbf{U} - \mathbf{V}) \otimes \mathbf{W}] \|_{X_h^{s-1/2}} \\ &\leq C_6 \|w_h\|_{X^{s-1/2}} \|u_h - v_h\|_{X^{s-1/4}} \\ &\quad + C_7 \|w_h\|_{X^{s-1/4}} \|u_h - v_h\|_{X^{s-1/2}} \\ &\quad + C_8 \|w_h\|_{X^{s-1/4}} \|u_h - v_h\|_{X^{s-1/4}}. \end{aligned}$$

by Lemma 5.4.2, where u_h, v_h, w_h are the sine interpolants of $\mathbf{u}, \mathbf{v}, \mathbf{w}$ respectively. Hence we obtain

$$\| [DF(\mathbf{u} - \mathbf{F}(\mathbf{v}))]\mathbf{w} \|_{X_h^{s-1/2}} \leq C_9 \|\mathbf{w}\|_{X^s} \|\mathbf{u} - \mathbf{v}\|_{X^s},$$

for $s > 5/8$. Therefore we have satisfied the assumptions of Theorem 2.2.14 as both \mathbf{F} and DF are continuous on X_h^s for $s > 5/8$. □

Next we need to prove a convergence result for the Fréchet derivatives of the solution and the approximation which is similar to the one we proved in Section 3.2.

5.4.2 Consistency

We substitute $\mathbf{u}(t)$ and $\mathbf{v}(t)$, the restrictions of the solution and its Fréchet derivative to the interior points of the grid (3.1.2), into the semi-discrete system (5.4.2), so that the vector of the truncation error at the grid points, $\tau_{\mathcal{F}}(t)$, is given by

$$\begin{aligned} \tau_{\mathcal{F}}(t) = & \frac{d\mathbf{v}}{dt} + 4D_h^4\mathbf{v} + \alpha D_h^2\mathbf{v} + \frac{\alpha}{3}[\mathbf{u} \otimes D_h^0\mathbf{v} \\ & + \mathbf{v} \otimes D_h^0\mathbf{u} + 2D_h^e(\mathbf{u} \otimes \mathbf{v})]. \end{aligned} \quad (5.4.5)$$

Theorem 5.4.4 *For $h > 0$ sufficiently small let $\tau_{\mathcal{F}}(t)$ be given in (5.4.5) and $u_0, v_0 \in X^s$ for $s > 9/8$ with $4s \in \mathbb{N}$, which are the initial data for (2.3.7) and (5.4.2) respectively. Then for any $T > 0$ there exists a constant C such that*

$$\|\tau_{\mathcal{F}}(t)\|_{L_h^2} \leq C(\alpha, T, \|u_0\|_{X^s}) \|v_0\|_{X^s} h^{4(s-1)}, \quad \forall t \in [0, T], \quad (5.4.6)$$

Proof: Subtracting (5.4.2), considered at the grid points, from (5.4.5) gives

$$\begin{aligned} \tau_{\mathcal{F}}(t) = & 4[D_h^4\mathbf{v} - \mathbf{v}_{xxxx}] + \alpha[D_h^2\mathbf{v} - \mathbf{v}_{xx}] \\ & + \frac{\alpha}{3}(\mathbf{u} \otimes [D_h^0\mathbf{v} - \mathbf{v}_x] + \mathbf{v} \otimes [D_h^0\mathbf{u} - \mathbf{u}_x] + 2[D_h^e(\mathbf{u} \otimes \mathbf{v}) - (\mathbf{u} \otimes \mathbf{v})_x]), \end{aligned}$$

where $\mathbf{v}_{xxxx}, \mathbf{v}_{xx}, \mathbf{v}_x, \mathbf{u}_x$ and $(\mathbf{u} \otimes \mathbf{v})_x$ are the grid restrictions of the functions $v_{xxxx}, v_{xx}, v_x, u_x$ and $(uv)_x$ respectively. Taking the L_h^2 norm of the last equation gives

$$\begin{aligned} \|\tau_{\mathcal{F}}(t)\|_{L_h^2} = & 4\|D_h^4 \mathbf{v} - \mathbf{v}_{xxxx}\|_{L_h^2} + \alpha\|D_h^2 \mathbf{v} - \mathbf{v}_{xx}\|_{L_h^2} + \frac{\alpha}{3} \left(\|\mathbf{u}\|_{L_h^\infty} \|D_h^2 \mathbf{v} - \mathbf{v}_{xx}\|_{L_h^2} \right. \\ & \left. + \|\mathbf{v}\|_{L_h^\infty} \|D_h^2 \mathbf{u} - \mathbf{u}_{xx}\|_{L_h^2} + 2\|D_h^e(\mathbf{u} \otimes \mathbf{v}) - (\mathbf{u} \otimes \mathbf{v})_x\|_{L_h^2} \right), \end{aligned}$$

which is equivalent to

$$\begin{aligned} \|\tau_{\mathcal{F}}(t)\|_{L_h^2} = & 4\|(I_h^o \mathbf{v})_{xxxx} - \mathbf{v}_{xxxx}\|_{L_h^2} + \alpha\|(I_h^o \mathbf{v})_{xx} - \mathbf{v}_{xx}\|_{L_h^2} \\ & + \frac{\alpha}{3} \left(\|\mathbf{u}\|_{L_h^\infty} \|(I_h^o \mathbf{v})_x - \mathbf{v}_x\|_{L_h^2} + \|\mathbf{v}\|_{L_h^\infty} \|(I_h^o \mathbf{u})_x - \mathbf{u}_x\|_{L_h^2} \right. \\ & \left. + \|I_h^o((\mathbf{u} \otimes \mathbf{v})_x) - (\mathbf{u} \otimes \mathbf{v})_x\|_{L_h^2} \right). \end{aligned}$$

Now since $s > 9/8$ we can apply Lemma 3.2.4 to this equation to give

$$\begin{aligned} \|\tau_{\mathcal{F}}(t)\|_{L_h^2} \leq & C_1 \|v_{xxxx}\|_{X^{s-1}} h^{4(s-1)} + C_2 \|v_{xx}\|_{X^{s-1/2}} h^{4(s-1/2)} \\ & + C_3 \|u\|_{L^\infty} \|v_x\|_{X^{s-1/4}} h^{4(s-1/4)} + C_4 \|v\|_{L^\infty} \|u_x\|_{X^{s-1/4}} h^{4(s-1/4)} \\ & + C_5 \|(uv)_x\|_{X^{s-1/4}} h^{4(s-1/4)}. \end{aligned} \quad (5.4.7)$$

Also Theorem 2.1.7 and Agmon's inequality imply that

$$\|uv\|_{X^s} \leq C_6 \|u\|_{X^s} \|v\|_{X^s} \quad \text{and} \quad \|u\|_{L^\infty} \leq \sqrt{2} \|u\|_{L^2} \|u\|_{X^{1/4}} \leq C_7 \|u\|_{X^s},$$

respectively. Therefore (5.4.7) becomes

$$\begin{aligned} \|\tau_{\mathcal{F}}(t)\|_{L_h^2} \leq & C_1 \|v\|_{X^s} h^{4(s-1)} + C_2 \|v\|_{X^s} h^{4(s-1/2)} \\ & + C_8 \|u\|_{X^s} \|v\|_{X^s} h^{4(s-1/4)}, \end{aligned}$$

which can be written as

$$\|\tau_{\mathcal{F}}(t)\|_{L_h^2} \leq C_9(\alpha, \|u(x, t)\|_{X^s}) \|v(x, t)\|_{X^s} h^{4(s-1)}, \quad t \in [0, T]. \quad (5.4.8)$$

Finally since $u_0, v_0 \in X^s$, Theorem 2.4.7 and Theorem 2.4.8 extended onto $[0, T]$ imply that the right hand side of (5.4.8) in terms of this initial data.

□

5.4.3 Convergence

Theorem 5.4.5 *Let $\mathbf{V}(t)$ and $\mathbf{v}(t)$ be the Fréchet derivative of K-S equation and its PS approximation respectively. If the initial data $u_0, v_0 \in X^s$, for $s > 9/8$ with $4s \in \mathbb{N}$, then for a given $T > 0$ and $h \leq h_1$ there exist a positive constant C such that*

$$\|\mathbf{V}(t) - \mathbf{v}(t)\|_{L_h^2} \leq C(\alpha, T, \|u_0\|_{X^s}) \|v_0\|_{X^s} h^{4(s-5/4)}, \quad \forall t \in [0, T], \quad (5.4.9)$$

Proof: Subtracting (5.4.3) from (5.4.5) gives

$$\begin{aligned} \frac{d\mathbf{E}_{\mathcal{F}}}{dt} + 4D_h^4\mathbf{E}_{\mathcal{F}} + \alpha D_h^2\mathbf{E}_{\mathcal{F}} + \frac{\alpha}{3}[(\mathbf{u} \otimes D_h^0\mathbf{v} - \mathbf{U} \otimes D_h^0\mathbf{V}) \\ + 2D_h^0(\mathbf{u} \otimes \mathbf{v} - \mathbf{U} \otimes \mathbf{V}) + (\mathbf{v} \otimes D_h^0\mathbf{u} - \mathbf{V} \otimes D_h^0\mathbf{U})] = \boldsymbol{\tau}_{\mathcal{F}}(t), \end{aligned}$$

where $\mathbf{E}_{\mathcal{F}} = \mathbf{v} - \mathbf{V}$. Premultiplying by $2h\mathbf{E}_{\mathcal{F}}^T$ gives

$$\begin{aligned} \frac{1}{2} \frac{d}{dt} \|\mathbf{E}_{\mathcal{F}}\|_{L_h^2}^2 = & -4\|D_h^2\mathbf{E}_{\mathcal{F}}\|_{L_h^2}^2 - \alpha \langle D_h^2\mathbf{E}_{\mathcal{F}}, \mathbf{E}_{\mathcal{F}} \rangle_{L_h^2} \\ & - \frac{\alpha}{3} \left[\langle \mathbf{u} \otimes D_h^0\mathbf{v} - \mathbf{U} \otimes D_h^0\mathbf{V}, \mathbf{E}_{\mathcal{F}} \rangle_{L_h^2} \right. \\ & + \langle \mathbf{v} \otimes D_h^0\mathbf{u} - \mathbf{V} \otimes D_h^0\mathbf{U}, \mathbf{E}_{\mathcal{F}} \rangle_{L_h^2} \\ & \left. - 2 \langle \mathbf{u} \otimes \mathbf{v} - \mathbf{U} \otimes \mathbf{V}, D_h^0\mathbf{E}_{\mathcal{F}} \rangle_{L_h^2} \right] + \langle \boldsymbol{\tau}_{\mathcal{F}}, \mathbf{E}_{\mathcal{F}} \rangle_{L_h^2}, \end{aligned}$$

which can be written as

$$\begin{aligned} \frac{1}{2} \frac{d}{dt} \|\mathbf{E}_{\mathcal{F}}\|_{L_h^2}^2 = & -4\|D_h^2\mathbf{E}_{\mathcal{F}}\|_{L_h^2}^2 - \alpha \langle D_h^2\mathbf{E}_{\mathcal{F}}, \mathbf{E}_{\mathcal{F}} \rangle_{L_h^2} \\ & - \frac{\alpha}{3} \left[\langle \mathbf{u} \otimes D_h^0(\mathbf{v} - \mathbf{V}) + (\mathbf{u} - \mathbf{U}) \otimes D_h^0\mathbf{V}, \mathbf{E}_{\mathcal{F}} \rangle_{L_h^2} \right. \\ & + \langle (\mathbf{v} - \mathbf{V}) \otimes D_h^0\mathbf{u} + \mathbf{V} \otimes D_h^0(\mathbf{u} - \mathbf{U}), \mathbf{E}_{\mathcal{F}} \rangle_{L_h^2} \\ & \left. - 2 \langle \mathbf{u} \otimes (\mathbf{v} - \mathbf{V}) + (\mathbf{u} - \mathbf{U}) \otimes \mathbf{V}, D_h^0\mathbf{E}_{\mathcal{F}} \rangle_{L_h^2} \right] \\ & + \langle \boldsymbol{\tau}_{\mathcal{F}}, \mathbf{E}_{\mathcal{F}} \rangle_{L_h^2}. \end{aligned}$$

Now if we set $\mathbf{E} = \mathbf{u} - \mathbf{U}$, this equation becomes

$$\begin{aligned}
\frac{1}{2} \frac{d}{dt} \|\mathbf{E}_{\mathcal{F}}\|_{L_h^2}^2 &= -4 \|D_h^2 \mathbf{E}_{\mathcal{F}}\|_{L_h^2}^2 - \alpha \langle D_h^2 \mathbf{E}_{\mathcal{F}}, \mathbf{E}_{\mathcal{F}} \rangle_{L_h^2} \\
&\quad - \frac{\alpha}{3} \left[\langle \mathbf{u} \otimes D_h^0 \mathbf{E}_{\mathcal{F}} - \mathbf{E} \otimes D_h^0 \mathbf{E}_{\mathcal{F}} + \mathbf{E} \otimes D_h^0 \mathbf{v}, \mathbf{E}_{\mathcal{F}} \rangle_{L_h^2} \right. \\
&\quad + \langle \mathbf{E}_{\mathcal{F}} \otimes D_h^0 \mathbf{u} - \mathbf{E}_{\mathcal{F}} \otimes D_h^0 \mathbf{E} + \mathbf{v} \otimes D_h^0 \mathbf{E}, \mathbf{E}_{\mathcal{F}} \rangle_{L_h^2} \\
&\quad \left. - 2 \langle \mathbf{u} \otimes \mathbf{E}_{\mathcal{F}} - \mathbf{E} \otimes \mathbf{E}_{\mathcal{F}} + \mathbf{E} \otimes \mathbf{v}, D_h^0 \mathbf{E}_{\mathcal{F}} \rangle_{L_h^2} \right] \\
&\quad + \langle \boldsymbol{\tau}_{\mathcal{F}}, \mathbf{E}_{\mathcal{F}} \rangle_{L_h^2}, \\
&\leq -4 \|D_h^2 \mathbf{E}_{\mathcal{F}}\|_{L_h^2}^2 - \alpha \langle D_h^2 \mathbf{E}_{\mathcal{F}}, \mathbf{E}_{\mathcal{F}} \rangle_{L_h^2} \\
&\quad - \frac{\alpha}{3} \left[\langle \mathbf{E} \otimes D_h^0 \mathbf{v}, \mathbf{E}_{\mathcal{F}} \rangle_{L_h^2} \right. \\
&\quad + \langle \mathbf{E}_{\mathcal{F}} \otimes D_h^0 \mathbf{u} - \mathbf{E}_{\mathcal{F}} \otimes D_h^0 \mathbf{E} + \mathbf{v} \otimes D_h^0 \mathbf{E}, \mathbf{E}_{\mathcal{F}} \rangle_{L_h^2} \\
&\quad \left. - \langle \mathbf{u} \otimes \mathbf{E}_{\mathcal{F}} - \mathbf{E} \otimes \mathbf{E}_{\mathcal{F}} + 2\mathbf{E} \otimes \mathbf{v}, D_h^0 \mathbf{E}_{\mathcal{F}} \rangle_{L_h^2} \right] \\
&\quad + \langle \boldsymbol{\tau}_{\mathcal{F}}, \mathbf{E}_{\mathcal{F}} \rangle_{L_h^2}.
\end{aligned}$$

which gives

$$\begin{aligned}
\frac{1}{2} \frac{d}{dt} \|\mathbf{E}_{\mathcal{F}}\|_{L_h^2}^2 &\leq -4 \|D_h^2 \mathbf{E}_{\mathcal{F}}\|_{L_h^2}^2 - \alpha \langle D_h^2 \mathbf{E}_{\mathcal{F}}, \mathbf{E}_{\mathcal{F}} \rangle_{L_h^2} \\
&\quad + \frac{\alpha}{3} \left[\|\mathbf{E} \otimes D_h^0 \mathbf{v}\|_{L_h^2} \|\mathbf{E}_{\mathcal{F}}\|_{L_h^2} + \|D_h^0 \mathbf{u}\|_{L_h^\infty} \|\mathbf{E}_{\mathcal{F}}\|_{L_h^2}^2 \right. \\
&\quad + \|D_h^0 \mathbf{E}\|_{L_h^\infty} \|\mathbf{E}_{\mathcal{F}}\|_{L_h^2}^2 + \|\mathbf{v} \otimes D_h^0 \mathbf{E}\|_{L_h^2} \|\mathbf{E}_{\mathcal{F}}\|_{L_h^2} \\
&\quad + \|\mathbf{u}\|_{L_h^\infty} \|\mathbf{E}_{\mathcal{F}}\|_{L_h^2} \|D_h^0 \mathbf{E}_{\mathcal{F}}\|_{L_h^2} + \|\mathbf{E}\|_{L_h^\infty} \|\mathbf{E}_{\mathcal{F}}\|_{L_h^2} \|D_h^0 \mathbf{E}_{\mathcal{F}}\|_{L_h^2} \\
&\quad \left. + 2 \|\mathbf{E} \otimes \mathbf{v}\|_{L_h^2} \|D_h^0 \mathbf{E}_{\mathcal{F}}\|_{L_h^2} \right] + \|\boldsymbol{\tau}_{\mathcal{F}}\|_{L_h^2} \|\mathbf{E}_{\mathcal{F}}\|_{L_h^2}.
\end{aligned}$$

Recalling the results of Lemmas 3.1.6 and 3.1.7, this last equation becomes

$$\begin{aligned}
\frac{1}{2} \frac{d}{dt} \|\mathbf{E}_{\mathcal{F}}\|_{L_h^2}^2 &\leq -4 \|D_h^2 \mathbf{E}_{\mathcal{F}}\|_{L_h^2}^2 + \alpha \|\widehat{D}_h^0 \mathbf{E}_{\mathcal{F}}\|_{L_h^2} \\
&\quad + \frac{\alpha}{3} \left[\|\mathbf{E} \otimes D_h^0 \mathbf{v}\|_{L_h^2} \|\mathbf{E}_{\mathcal{F}}\|_{L_h^2} + (\|D_h^0 \mathbf{u}\|_{L_h^\infty} + \|D_h^0 \mathbf{E}\|_{L_h^\infty}) \|\mathbf{E}_{\mathcal{F}}\|_{L_h^2}^2 \right. \\
&\quad + \|\mathbf{v} \otimes D_h^0 \mathbf{E}\|_{L_h^2} \|\mathbf{E}_{\mathcal{F}}\|_{L_h^2} + (\|\mathbf{u}\|_{L_h^\infty} + \|\mathbf{E}\|_{L_h^\infty}) \|\mathbf{E}_{\mathcal{F}}\|_{L_h^2} \|\widehat{D}_h^0 \mathbf{E}_{\mathcal{F}}\|_{L_h^2} \\
&\quad \left. + 2 \|\mathbf{E} \otimes \mathbf{v}\|_{L_h^2} \|\widehat{D}_h^0 \mathbf{E}_{\mathcal{F}}\|_{L_h^2} \right] + \|\boldsymbol{\tau}_{\mathcal{F}}\|_{L_h^2} \|\mathbf{E}_{\mathcal{F}}\|_{L_h^2}. \tag{5.4.10}
\end{aligned}$$

We note that in the above equation $\|\mathbf{u}\|_{L_h^\infty}$ and $\|D_h^\circ \mathbf{u}\|_{L_h^\infty}$ are bounded by the properties of the continuous K-S equation, see the proof of Theorem 3.2.7 and Lemma 3.2.5 for details. Also from our error analysis in Section 3.2 we have that

$$\|\mathbf{E}(t)\|_{L_h^2} \leq C_1(\alpha, T, \|u_0\|_{X^s}) h^{4(s-1)} \text{ and } \|D_h^\circ \mathbf{E}(t)\|_{L_h^2} \leq C_2(\alpha, T, \|u_0\|_{X^s}) h^{4(s-5/4)},$$

for all $t \in [0, T]$, which gives the following bounds

$$\begin{aligned} \|\mathbf{E}(t)\|_{L_h^\infty} &\leq \frac{N}{\pi} \|\mathbf{E}(t)\|_{L_h^2}, \\ &\leq C'_1(\alpha, T, \|u_0\|_{X^s}) h^{4(s-5/4)}, \end{aligned} \quad (5.4.11)$$

and

$$\begin{aligned} \|D_h^\circ \mathbf{E}(t)\|_{L_h^\infty} &\leq \frac{N}{\pi} \|D_h^\circ \mathbf{E}(t)\|_{L_h^2}, \\ &\leq C'_2(\alpha, T, \|u_0\|_{X^s}) h^{4(s-3/2)}. \end{aligned} \quad (5.4.12)$$

Therefore if we choose $s \geq 3/2$, (5.4.10) can be written as

$$\begin{aligned} \frac{1}{2} \frac{d}{dt} \|\mathbf{E}_{\mathcal{F}}\|_{L_h^2}^2 &\leq -4 \|D_h^2 \mathbf{E}_{\mathcal{F}}\|_{L_h^2}^2 + \alpha \|\widehat{D}_h^\circ \mathbf{E}_{\mathcal{F}}\|_{L_h^2}^2 \\ &\quad + \frac{\alpha}{3} \left[\|\mathbf{E} \otimes D_h^\circ \mathbf{v}\|_{L_h^2} \|\mathbf{E}_{\mathcal{F}}\|_{L_h^2} + C_3 \|\mathbf{E}_{\mathcal{F}}\|_{L_h^2}^2 \right. \\ &\quad + \|\mathbf{v} \otimes D_h^\circ \mathbf{E}\|_{L_h^2} \|\mathbf{E}_{\mathcal{F}}\|_{L_h^2} + C_4 \|\widehat{D}_h^\circ \mathbf{E}_{\mathcal{F}}\|_{L_h^2} \|\mathbf{E}_{\mathcal{F}}\|_{L_h^2} \\ &\quad \left. + 2 \|\mathbf{E} \otimes \mathbf{v}\|_{L_h^2} \|\widehat{D}_h^\circ \mathbf{E}_{\mathcal{F}}\|_{L_h^2} \right] + \|\tau_{\mathcal{F}}\|_{L_h^2} \|\mathbf{E}_{\mathcal{F}}\|_{L_h^2}, \end{aligned} \quad (5.4.13)$$

where we have bounded $\|D_h^\circ \mathbf{u}\|_{L_h^\infty} + \|D_h^\circ \mathbf{E}\|_{L_h^\infty}$ and $\|\mathbf{u}\|_{L_h^\infty} + \|\mathbf{E}\|_{L_h^\infty}$ by C_3 and C_4 respectively by using the bounds (5.4.11) and (5.4.12). These constants are bounded in terms of T , $\|u_0\|_{X^s}$ and some constant $h_1 \geq h$ for $s \geq 3/2$. Applying Young's inequality to (5.4.13) gives

$$\begin{aligned} \frac{d}{dt} \|\mathbf{E}_{\mathcal{F}}\|_{L_h^2}^2 &\leq -8 \|D_h^2 \mathbf{E}_{\mathcal{F}}\|_{L_h^2}^2 + K_1 \|\widehat{D}_h^\circ \mathbf{E}_{\mathcal{F}}\|_{L_h^2}^2 + K_2 \|\mathbf{E}_{\mathcal{F}}\|_{L_h^2}^2 \\ &\quad + \frac{\alpha}{3} \left[\|D_h^\circ \mathbf{v}\|_{L_h^\infty}^2 \|\mathbf{E}\|_{L_h^2}^2 + \|\mathbf{v}\|_{L_h^\infty}^2 \|D_h^\circ \mathbf{E}\|_{L_h^2}^2 \right. \\ &\quad \left. + 2 \|\mathbf{v}\|_{L_h^\infty}^2 \|\mathbf{E}\|_{L_h^2}^2 \right] + \|\tau_{\mathcal{F}}\|_{L_h^2}^2, \end{aligned} \quad (5.4.14)$$

where $K_1 = 2\alpha + (\alpha/3)[2 + C_4]$ and $K_2 = 1 + (\alpha/3)[2 + 2C_3 + C_4]$. Also since

$$-8\|D_h^2 \mathbf{E}_{\mathcal{F}}\|_{L_h^2}^2 + K_1 \|\widehat{D}_h^o \mathbf{E}_{\mathcal{F}}\|_{L_h^2}^2 \leq \frac{K_1^2}{32} \|\mathbf{E}_{\mathcal{F}}\|_{L_h^2}^2.$$

equation (5.4.14) becomes

$$\begin{aligned} \frac{d}{dt} \|\mathbf{E}_{\mathcal{F}}\|_{L_h^2}^2 - K_3 \|\mathbf{E}_{\mathcal{F}}\|_{L_h^2}^2 &\leq \frac{\alpha}{3} \left[\|D_h^o \mathbf{v}\|_{L_h^\infty}^2 \|\mathbf{E}\|_{L_h^2}^2 + \|\mathbf{v}\|_{L_h^\infty}^2 \|D_h^o \mathbf{E}\|_{L_h^2}^2 \right. \\ &\quad \left. + 2\|\mathbf{v}\|_{L_h^\infty}^2 \|\mathbf{E}\|_{L_h^2}^2 \right] + \|\boldsymbol{\tau}_{\mathcal{F}}\|_{L_h^2}^2, \end{aligned} \quad (5.4.15)$$

where $K_3 = K_1^2/32 + K_2$ and is dependent on T and $\|u_0\|_{X^s}$. Now substituting the bounds for \mathbf{E} and the truncation error into equation (5.4.15) gives

$$\frac{d}{dt} \|\mathbf{E}_{\mathcal{F}}\|_{L_h^2}^2 - K_3 \|\mathbf{E}_{\mathcal{F}}\|_{L_h^2}^2 \leq K_4(\alpha, T, \|u_0\|_{X^s}) \|v_0\|_{X^s}^2 h^{8(s-5/4)}.$$

where we have also used Theorem 2.4.8 to bound the terms involving $\mathbf{v}(t)$, $t \in [0, T]$, in terms of the initial data \mathbf{v}_0 . Integrating this equation with respect to time gives

$$\begin{aligned} \|\mathbf{E}_{\mathcal{F}}(t)\|_{L_h^2}^2 &\leq K_4 \|v_0\|_{X^s}^2 h^{8(s-5/4)} \int_0^t e^{K_3(t-r)} dr, \\ &\leq \frac{K_4}{K_3} e^{K_3 T} \|v_0\|_{X^s}^2 h^{8(s-5/4)}, \quad t \in [0, T], \end{aligned} \quad (5.4.16)$$

which gives

$$\|\mathbf{E}_{\mathcal{F}}(t)\|_{L_h^2} \leq C(\alpha, T, \|u_0\|_{X^s}) \|v_0\|_{X^s} h^{4(s-5/4)}, \quad \forall t \in [0, T].$$

□

Corollary 5.4.6 *Let $v_h(x, t)$ be interpolant, on the interval $[0, \pi]$, of the vector $\mathbf{V}(t)$ given in Theorem 5.4.5. Furthermore assume that $u_0, v_0 \in X^s$, for $s > 3/2$ with $4s \in \mathbb{N}$, then for a given $T > 0$ and $h \leq h_1$ there exists a positive constant*

C such that

$$\|v_h(x, t) - v(x, t)\|_{L^2} \leq C(\alpha, T, \|u_0\|_{X^s}) \|v_0\|_{X^s} h^{4(s-5/4)}, \quad \forall t \in [0, T]. \quad (5.4.17)$$

Proof: Similar to the proof of Corollary 3.2.8 in Section 3.2.

□

5.5 Persistence of bounded invariant sets for the semi-discrete approximation

We are now in a position to prove the persistence of bounded invariant sets under PS semi-discrete approximation. Let $u_h(x, t)$ be the PS interpolant of the approximation on the interval $[0, \pi]$. We can consider the map

$$G_h^*(\tau, u_0) := u_h(\tau), \quad (5.5.1)$$

where $\tau = \lambda_{m+1}^{-1}$, $m \in \mathbb{N}$, was defined in Section 5.3. Given this map we can define the perturbed map

$$G_h(u) = G_h^*(I_h^o u), \quad u \in X, \quad (5.5.2)$$

where we have dropped the explicit dependence on time. Hence it is possible to define the map

$$\tilde{G}_h(u) := G(u) - \theta_\rho(\|u\|_{X^s}) [G(u) - G_h(u)], \quad (5.5.3)$$

where G and θ_ρ are defined in Section 5.3. The map (5.5.3) therefore agrees with G_h in the ball $\mathcal{B}_{X^s}(\rho)$.

In order to state the main theorem in this section we will need the following two lemmas.

Lemma 5.5.1 *Let $s > 3/2$ and n be some natural number such that $n \geq \lfloor s \rfloor$, where $\lfloor s \rfloor$ denotes the largest integer less than s . Then for any fixed $\tau > 0$ we have that*

$$\|v(t)\|_{X^{n/2}} \leq C \|v_0\|_{X^s}, \quad \forall t \in (0, \tau],$$

where $v(t)$ is the solution of equation (5.4.2) and C is some constant dependent on τ .

Proof: Consider the sequence of numbers

$$0 < \alpha_{\lfloor s \rfloor} < \alpha_{\lfloor s \rfloor + 1} < \cdots < \alpha_{2\lceil ks \rceil} \leq \frac{1}{2},$$

where $\lceil s \rceil$ denotes the smallest integer greater than s and $k \in \mathbb{N}$. Let P_n be the statement

$$\|v(t)\|_{X^{n/2}} \leq C(n) \|v_0\|_{X^s}, \quad \forall t \in [\alpha_n \tau, \tau], \quad (5.5.4)$$

where $n \in [\lfloor s \rfloor, 2\lceil ks \rceil]$. For $n = \lfloor s \rfloor$, P_n is true by Theorem 2.4.8 since $s > 3/2$. Now assume that P_n is true for $n = m$ so that

$$\|v(t)\|_{X^{m/2}} \leq C(m) \|v_0\|_{X^s}, \quad \forall t \in [\alpha_m \tau, \tau].$$

From (2.4.10) we have that

$$v(t) = e^{-A(t-\alpha_m \tau)} v(\alpha_m \tau) - \int_{\alpha_m \tau}^t e^{-A(t-r)} DF(u(r)) v(r) dr,$$

for all $t \in [\alpha_m \tau, \tau]$. Multiplying by $A^{(m+1)/2}$ and taking the L^2 norm of this equation gives

$$\begin{aligned} \|v(t)\|_{X^{(m+1)/2}} &\leq C_1 (t - \alpha_m \tau)^{-1/2} \|v(\alpha_m \tau)\|_{X^{m/2}} \\ &\quad + C_2 \int_{\alpha_m \tau}^t (t - r)^{-1/2} \|u(r)\|_{X^{(m+1)/2}} \|v(r)\|_{X^{(m+1)/2}} dr, \end{aligned}$$

for all $t \in [\alpha_m \tau, \tau]$, where we have used the properties of the operator DF , see (2.4.9). By the assumption (5.5.4) and the fact that $u(t)$ is contained in a Gevrey class for all $t > 0$, this last equation becomes

$$\begin{aligned} \|v(t)\|_{X^{(m+1)/2}} &\leq C_1(t - \alpha_m \tau)^{-1/2} C(m) \|v(0)\|_{X^s} \\ &\quad + C_3 \int_{\alpha_m \tau}^t (t - r)^{-1/2} \|v(r)\|_{X^{(m+1)/2}} dr. \end{aligned}$$

Now applying Gronwall's Lemma gives

$$\|v(t)\|_{X^{(m+1)/2}} \leq C(m+1) \|v_0\|_{X^s},$$

so that P_{m+1} is true and hence P_n is true for all $n \geq \lfloor s \rfloor$.

□

Lemma 5.5.2 *Let $s > 3/2$ and n be some natural number such that $n \geq \lfloor s \rfloor$. Then for any fixed $\tau > 0$ we have that*

$$\|v_h(t)\|_{X^{n/2}} \leq C \|v_0\|_{X^s}, \quad \forall t \in (0, \tau],$$

where $v_h(t)$ is the PS interpolant of the solution of equation (5.4.3) and C is some constant dependent on τ .

Proof: This proof is identical to the proof of Lemma 5.5.1, and uses the properties of the operator DF given in Theorem 5.4.3 and the fact that the solutions of our PS approximation are contained in a Gevrey class for all $t > 0$.

□

Theorem 5.5.3 *For m sufficiently large the map G , (5.3.3), has an inertial manifold representable as the graph of a C^1 function Φ . The finite-dimensional system*

$$p_{n+1} = P_m G(p_n + \Phi(p_n)), \tag{5.5.5}$$

has the same dynamics as the map G . For h sufficiently small and $u_0, v_0 \in X^s$, $s > 3/2$, the map \tilde{G}_h , (5.5.3), has an inertial manifold representable as the graph of a C^1 function Φ^h . The finite-dimensional system

$$p_{n+1} = P_m \tilde{G}(p_n + \Phi^h(p_n)), \quad (5.5.6)$$

converges in the C^1 norm to (5.5.5) over the ball $\mathcal{B}_{X^s}(\rho)$ as h tends to zero with $\mathcal{O}(h^{4\epsilon(s-5/4)})$, $0 \leq \epsilon < 1$.

Proof: The first part of the proof follows from Theorem 5.3.3. In order for us to show that \tilde{G}_h has an inertial manifold we need to show that Assumptions \mathcal{G}_h hold for the map G_h . From Corollary 3.2.8 we have that

$$\|u_h(x, t) - u(x, t)\|_{L^2} \leq C(\alpha, T, \|u_0\|_{X^s}) h^{4(s-1)}, \quad 0 \leq t \leq T,$$

for some T , which implies that

$$\|G(u_0) - G_h(u_0)\|_{L^2} \leq C(\tau, \|u_0\|_{X^s}) h^{4(s-1)}, \quad (5.5.7)$$

where τ is given above and we have dropped the dependence on the parameter α . From the Gagliardo-Nirenberg Theorem 2.1.6 we have that

$$\|G(u_0) - G_h(u_0)\|_{X^s} \leq C_1 \|u(\tau) - u_h(\tau)\|_{X^{ks}}^{1-\epsilon} \|u(\tau) - u_h(\tau)\|_{L^2}^\epsilon,$$

where $\epsilon = 1 - 1/k$, $k \in \mathbb{N}$ such that $k \geq 2$. Hence substituting (5.5.7) into this equation gives

$$\|G(u_0) - G_h(u_0)\|_{X^s} \leq C_2(\tau, \|u_0\|_{X^s}) [\|u(\tau)\|_{X^{ks}} + \|u_h(\tau)\|_{X^{ks}}]^{1-\epsilon} h^{4\epsilon(s-1)}. \quad (5.5.8)$$

Now since $u_0 \in X^s$ for $s > 3/2$ we have that the solution and its PS approximation are both in a Gevrey class for $\tau > 0$, which implies that it is possible to bound

the norms in the square brackets in (5.5.8). Therefore this equation becomes

$$\|G(u_0) - G_h(u_0)\|_{X^s} \leq C_3(\tau, \|u_0\|_{X^s}) h^{4\epsilon(s-1)}. \quad (5.5.9)$$

Also from Corollary 5.4.6 we have that

$$\|v(t) - v_h(t)\|_{L^2} \leq C(T, \|u_0\|_{X^s}) \|v_0\|_{X^s} h^{4(s-5/4)}, \quad 0 \leq t \leq T,$$

for $s \geq 3/2$, which gives

$$\|[DG(u_0) - DG_h(u_0)]v_0\|_{L^2} \leq C(\tau, \|u_0\|_{X^s}) \|v_0\|_{X^s} h^{4(s-5/4)},$$

Once again using Theorem 2.1.6 we can obtain

$$\begin{aligned} \|[DG(u_0) - DG_h(u_0)]v_0\|_{X^s} &\leq C_4(\tau, \|u_0\|_{X^s}) [\|v(\tau)\|_{X^{ks}} + \|v_h(\tau)\|_{X^{ks}}]^{1-\epsilon} \\ &\quad \|v_0\|_{X^s}^\epsilon h^{4\epsilon(s-5/4)}, \end{aligned} \quad (5.5.10)$$

and the terms in the square brackets are bounded by Lemmas 5.5.1 and 5.5.2 respectively. Hence equation (5.5.10) becomes

$$\|[DG(u_0) - DG_h(u_0)]v_0\|_{X^s} \leq C_5(\tau, \|u_0\|_{X^s}) \|v_0\|_{X^s} h^{4\epsilon(s-5/4)},$$

which implies that

$$\|DG(u_0) - DG_h(u_0)\|_{op} \leq C_6(\tau, \|u_0\|_{X^s}) h^{4\epsilon(s-5/4)}, \quad (5.5.11)$$

We recall that Assumptions \mathcal{G}_h require only that the map G_h approximates the map G in the C^1 norm over the set $\mathcal{B}_{X^s}(0, 2\rho)$, which contains all the bounded invariant sets of the map G . Hence (5.5.9) and (5.5.11) can be written as

$$\|G(u_0) - G_h(u_0)\|_{X^s} \leq K(\rho) h^{4\epsilon(s-1)}, \quad (5.5.12)$$

$$\|DG(u_0) - DG_h(u_0)\|_{op} \leq K(\rho) h^{4\epsilon(s-5/4)} \quad (5.5.13)$$

for all $u_0 \in \mathcal{B}_{X^*}(2\rho)$. We can satisfy Assumptions \mathcal{G}_h for our approximation if

$$4\epsilon(s - 5/4) \geq 1,$$

which implies that

$$s \geq 5/4 + 1/(4\epsilon) > 3/2.$$

This allows us to apply Theorem 5.2.4, which implies that the map \tilde{G}_h can be reduced to an inertial form, defined by (5.5.6) which has the same asymptotic dynamics in the ball $\mathcal{B}_{X^*}(\rho)$. Equations (5.5.12) and (5.5.13) show that the inertial forms converge in the C^1 norm as h tends to zero with $\mathcal{O}(h^{4\epsilon(s-5/4)})$.

□

Let us now discuss the implications of Theorem 5.5.3. We first of all note that the map $P_m \tilde{G}_h$ agrees with the map $P_m G_h$ in the ball $\mathcal{B}_{X^*}(\rho)$. Hence these maps will have identical dynamical behaviour which is the same as the asymptotic behaviour of the PS approximation. We also have that the bounded invariant sets of the map $P_m G$ are the same as those of the K-S equation. We therefore conclude that the bounded invariant sets, known to persist under C^1 perturbation in the context of finite-dimensional systems, hold for the K-S equation and its PS approximation, for sufficiently small h .

The essential improvement of this result over previous studies, is the high order convergence estimate achieved in Theorem 5.5.3. In the papers [49], [51] and [52], spatial discretizations were analysed involving the finite difference method and the spectral Galerkin method which yield only low order estimates. In the case of the spectral method one may expect to be able to improve this as it is high order method. We have managed to show that this is the case for the PS approximation by using the smoothness of the solutions of the K-S equation and its Fréchet derivative.

Chapter 6

Numerical Analysis

6.1 Numerical study of the dynamics of the Kuramoto-Sivashinsky equation

In this section we carry out a detailed study of the dynamical behaviour of the K-S equation (2.3.7) for parameter values $0 \leq \alpha \leq 40$ using the PS discretization, considered in this thesis. Similar computations, using the PS method and other approximation methods, have been carried out for these particular values and higher ones in Hyman and Nicolaenko [43], Jolly, Kevrekidis and Titi [47], Kevrekidis, Nicolaenko and Scovel [55], Russell, Sloan and Trummer [78] and Papageorgiou and Smyrlis [73], [82]. We will outline the work in these papers where relevant.

6.1.1 Low dimensional attractor

In Chapter 5, we showed that the K-S equation has an inertial manifold. This means that it is possible to capture the asymptotic dynamics of the equation by a finite-dimensional system. Therefore it is important to find the number of grid points required by our PS discretization to obtain a good approximation to these dynamics. The best estimate for the dimension of the inertial manifold, in the

L^2 space, is

$$\dim(\mathcal{M}) \leq C\alpha^{4/5}, \quad (6.1.1)$$

where C is some constant. Although this gives us a bound on the power growth of α , the constant C is not known. Hence we carried out some computations of a steady state and a periodic solution, within our parameter range, to find the minimum size of N required for the PS discretization to capture the essential dynamical behaviour of the K-S equation. The numerical results that follow were obtained using the MATLAB time stepping routine ODE15S with our spatial discretization. This routine is a variable order and variable step size ODE solver for stiff systems of equations and was used for its robustness.

We initially considered how well our discretization approximated a steady state solution at $\alpha = 40$, given the initial condition $u_0(x) = \sin(x)$. For various sizes of N , we followed the solution of the approximation at $x = \pi/3$ and $x = 2\pi/3$ until it converged to ten decimal places. Table 6.1 shows the approximations to the steady state obtained for the different values of N . One can see that there is no difference in the solution values as we move from $N = 24$ to $N = 51$. Also for $N = 18$ the PS approximation is accurate to 7 decimal places. Figure 6-1 shows a picture of the steady state attractor of the K-S equation on the interval $[-\pi, \pi]$, for this particular parameter value and initial condition.

N	$x = \pi/3$	$x = 2\pi/3$
6	-2.07846097	2.07846097
9	-2.46191925	2.46191925
12	-2.45130368	2.45130368
15	-2.45139013	2.45139013
18	-2.45138226	2.45138225
21	-2.45138233	2.45138233
24	-2.45138232	2.45138232
51	-2.45138232	2.45138232

Table 6.1: PS approximation to a steady state solution of the K-S equation with $\alpha = 40$ at $x = \pi/3$ and $x = 2\pi/3$, for varying sizes of the discretization parameter N .

We next considered capturing the periodic behaviour of the K-S equation

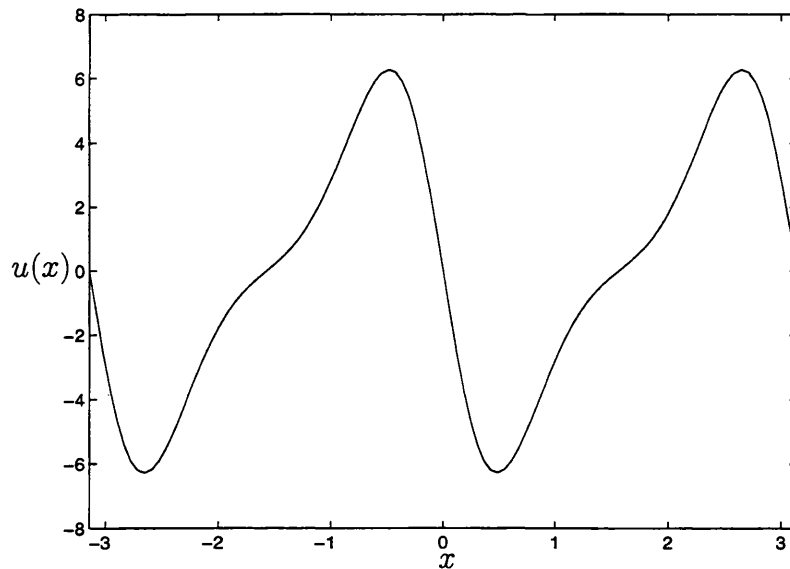


Figure 6-1: Bi-modal steady state attractor of the K-S equation with $\alpha = 40$ on the interval $[-\pi, \pi]$.

which is known to exist at $\alpha = 32.96$. We had to perturb the initial condition slightly so that $u_0(x) = 0.1 \sin(x)$, otherwise solutions would have been attracted to a steady state. Figure 6-2 shows the approximation to $u(\pi/3)$ plotted against the approximation to $u(2\pi/3)$ for varying sizes of N and Table 6.2 shows their respective periods. Clearly for this lower value of α , less grid points are required for convergence. Figure 6-3 shows a 3-dimensional colour plot of two periods of the solution when $\alpha = 32.96$.

N	Period
6	0.0884
9	0.0772
12	0.0773
51	0.0773

Table 6.2: The period of the PS approximations to a periodic solution of the K-S equation which exists at $\alpha = 32.96$.

The above two numerical experiments show that it is reasonable to take quite small values of N to capture the dynamics of the K-S equation for $0 \leq \alpha \leq 40$. In the rest of this section all the computations will involve our PS discretization with $N = 18$. We will assume that for this value the dynamics of the discretization give an accurate representation of the dynamics of the K-S equation.

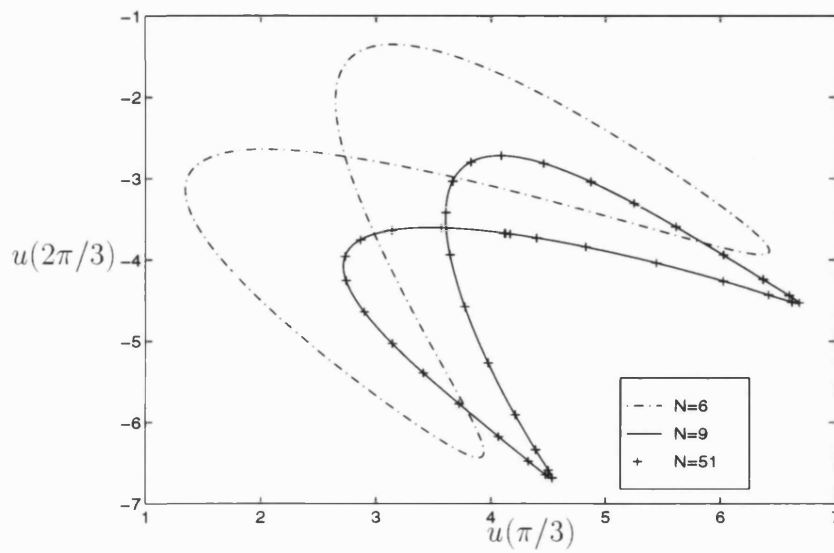


Figure 6-2: Periodic solutions of the PS approximation for increasing sizes of N .

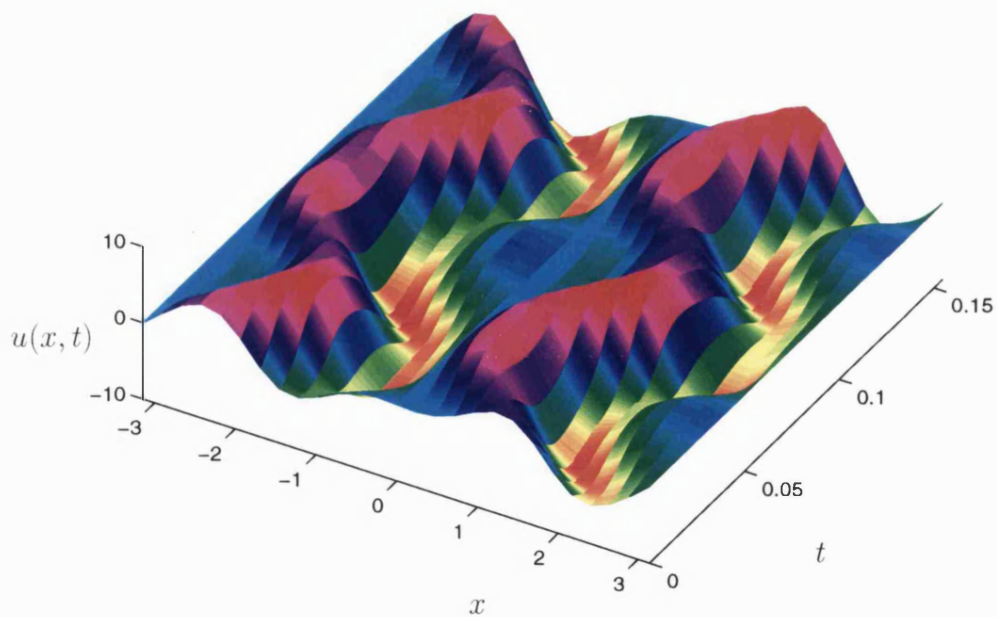


Figure 6-3: Solutions of the K-S equation with $\alpha = 32.96$ over two periods.

6.1.2 Steady states

To begin with we have computed the bifurcation diagram for the K-S equation using AUTO 97, which is a FORTRAN continuation and bifurcation software package for ODE's, developed by Doedel *et al.* [13]. Some of the bifurcation diagrams that follow show plots of the parameter α against the L^2 norm of the approximate solution. For a steady state solution, this norm is given by $\|\cdot\|_s$, which is defined by

$$\|\mathbf{U}\|_s = \left[\sum_{j=1}^{N-1} (U_j)^2 \right]^{1/2}, \quad \mathbf{U} \in \mathbb{R}^{N-1}, \quad (6.1.2)$$

and for a periodic solution, this norm is given by $\|\cdot\|_p$, which is defined by

$$\|\mathbf{U}(t)\|_p = \left[\frac{1}{T} \int_0^T \sum_{j=1}^{N-1} (U_j(t))^2 dt \right]^{1/2}, \quad \mathbf{U}(t) \in \mathbb{R}^{N-1}, \quad (6.1.3)$$

for $t \in [0, T]$, where T is the period. In the bifurcation diagrams solid curves correspond to stable solutions and broken curves correspond to unstable ones. The symbols \square denote bifurcation points, \blacksquare Hopf bifurcation points and \boxtimes period doubling bifurcations.

Figure 6-4 shows a bifurcation diagram of the L^2 norm of the steady state branches of the K-S equation against the parameter α . It is common for steady state solution branches of some equations to have the same L^2 norm, and this is in fact the case with the K-S equation. Therefore in order to get a detailed understanding of the the attracting steady states we have plotted the fourth solution component of the approximation against the parameter α in Figure 6-5. This figure gives us a much better idea of the overall bifurcation diagram. Similar diagrams can be obtained by plotting other solution components against α . These will contain exactly the same bifurcations and steady state branches and will only differ quantitatively.

For $0 \leq \alpha < 4$ the solutions are attracted to a stable trivial steady state. We note that if we take the inner product of the K-S equation (2.3.7) with $u \in \dot{H}_{per}^4$

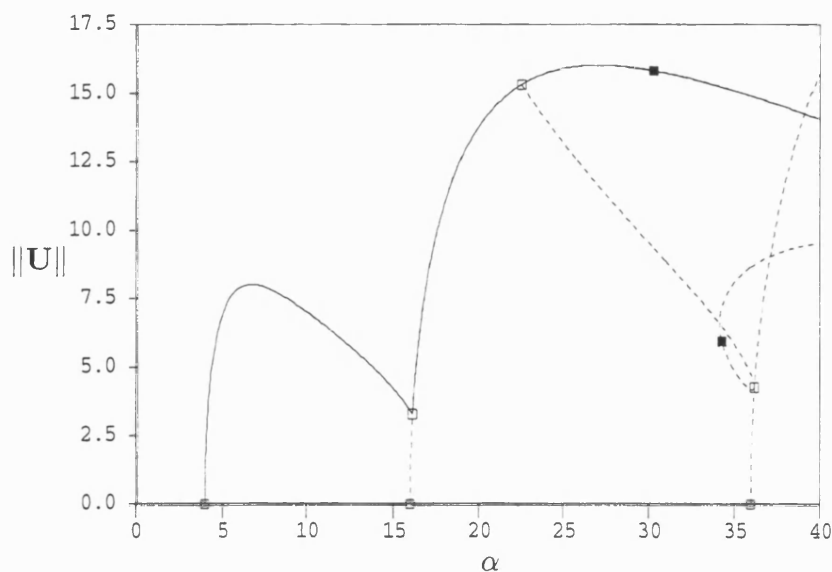


Figure 6-4: Bifurcation diagram of the K-S equation for $0 \leq \alpha \leq 40$, showing the L^2 norm plotted against α .

then we obtain

$$\frac{1}{2} \frac{d}{dt} \|u(\cdot, t)\|_{L^2}^2 = \alpha \|u_x(\cdot, t)\|_{L^2}^2 - 4 \|u_{xx}(\cdot, t)\|_{L^2}^2,$$

which gives

$$\frac{1}{2} \frac{d}{dt} \|u(\cdot, t)\|_{L^2}^2 \leq (\alpha - 4) \|u(\cdot, t)\|_{L^2}^2, \quad (6.1.4)$$

since

$$\|u\|_{L^2} \leq \|u_x\|_{L^2} \leq \|u_{xx}\|_{L^2},$$

by Theorem 2.1.5. Integrating (6.1.4) then gives

$$\|u(\cdot, t)\|_{L^2} \leq e^{(\alpha-4)t} \|u(\cdot, 0)\|_{L^2},$$

which implies that

$$\|u(\cdot, t)\|_{L^2} \rightarrow 0 \text{ as } t \rightarrow 0.$$

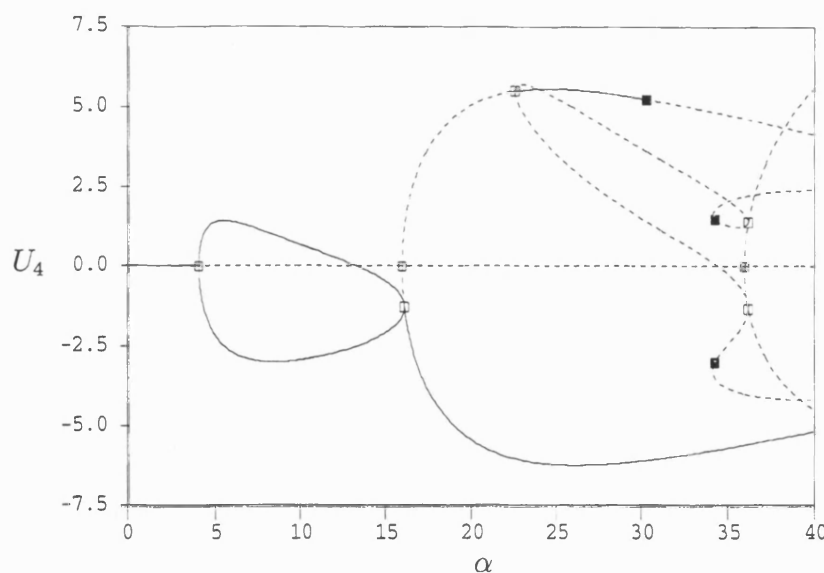


Figure 6-5: Bifurcation diagram of the K-S equation of the fourth solution component plotted against α .

We summarise all the details of the attracting states and their bifurcations, from Figure 6-5, in Table 6.3. The attracting states in this table correspond to the K-S equation with odd initial data. The attracting states of the K-S equations with general initial data are considered in [43]. In Table 6.3 we note the appearance of the supercritical Hopf bifurcation at $\alpha = 30.345$. Figure 6-6 shows the stable periodic solutions emanating from this Hopf bifurcation and these solutions will be examined in detail next.

6.1.3 Periodic states

From Figure 6-5, we can see that there are three Hopf bifurcation points in the parameter range which we are interested in. Therefore any periodic behaviour of the K-S equation will be produced at these points. Although we are mainly concerned with the behaviour at the Hopf bifurcation point at $\alpha = 30.345$, we will briefly discuss what happens at the other two points. The periodic solutions produced at $\alpha = 30.345$ have been studied previously in [47] and [78]. However the main motivation behind the studies in these papers was to test how well various approximation methods performed. In [47], it was observed that the

Parameter Values	Attracting States and Bifurcations
$0 \leq \alpha \leq 4$	trivial steady state branch
$\alpha = 4$	trivial branch undergoes a supercritical pitchfork bifurcation
$4 < \alpha \leq 16.140$	two nontrivial steady states branches
$\alpha = 16.140$	nontrivial branches intersect at a further supercritical pitchfork
$16.140 < \alpha \leq 40$	nontrivial steady state branch
$\alpha = 22.556$	subcritical pitchfork bifurcation
$22.556 < \alpha \leq 30.345$	second nontrivial steady state branch
$\alpha = 30.345$	second steady state branch undergoes a supercritical Hopf bifurcation
$30.345 \leq \alpha \leq 33.015$	periodic attracting state

Table 6.3: Attracting states of the K-S equation and their bifurcations.

periodic solutions eventually become chaotic, and it is for this reason that we have chosen to study these solutions in detail.

Figure 6-7 shows the branch of solutions if we continue the branch in Figure 6-6 for higher parameter values. We can see that the solutions lose stability at a bifurcation point at $\alpha = 32.853$. Although the two solution branches produced at this point have different norms and stability, the actual solutions have similar shape and period. We will consider what happens to the unstable solution branch later in this section. However we note that the stable branch undergoes a number of period doubling bifurcations. We managed to detect the first four using AUTO and a close-up of these can be seen in Figure 6-8.

In order to study the dynamics beyond the fourth period doubling bifurcation, a numerical code was written to implement the PS discretization in FORTRAN. We chose the external routine D02NBF to perform the time integration from the NAG (Numerical Algorithms Group) Library. This routine involves a variable order and variable step size BDF method.

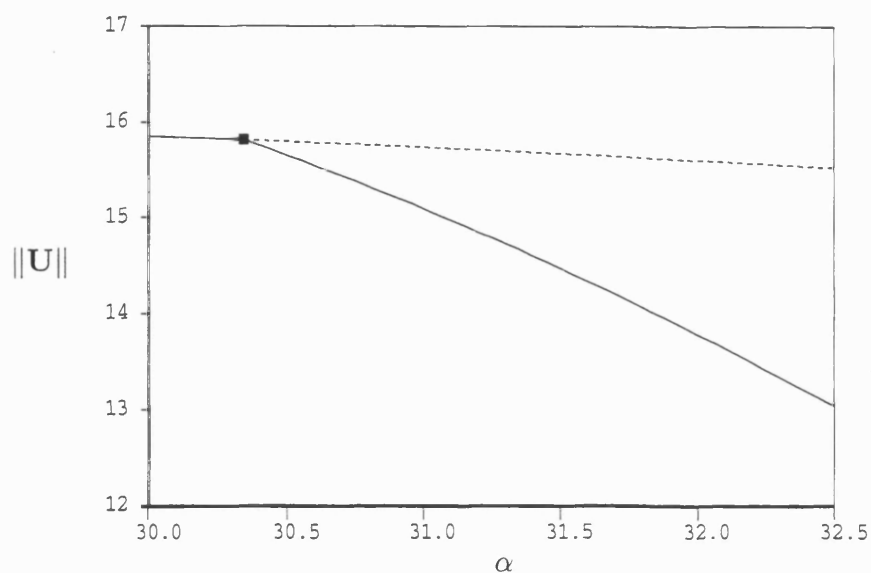


Figure 6-6: Close-up of stable periodic solutions emanating from the Hopf bifurcation at $\alpha = 30.345$.

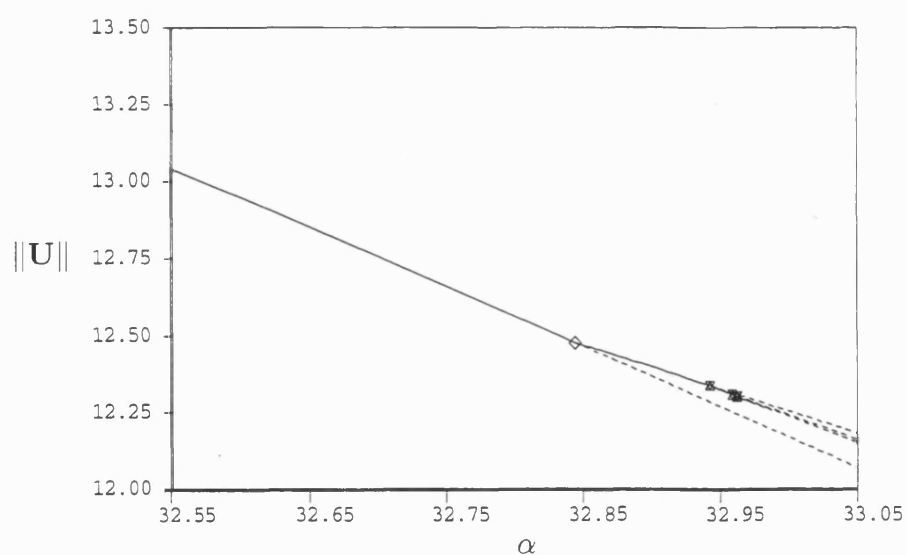


Figure 6-7: Periodic solutions losing stability at bifurcation and period doubling points.

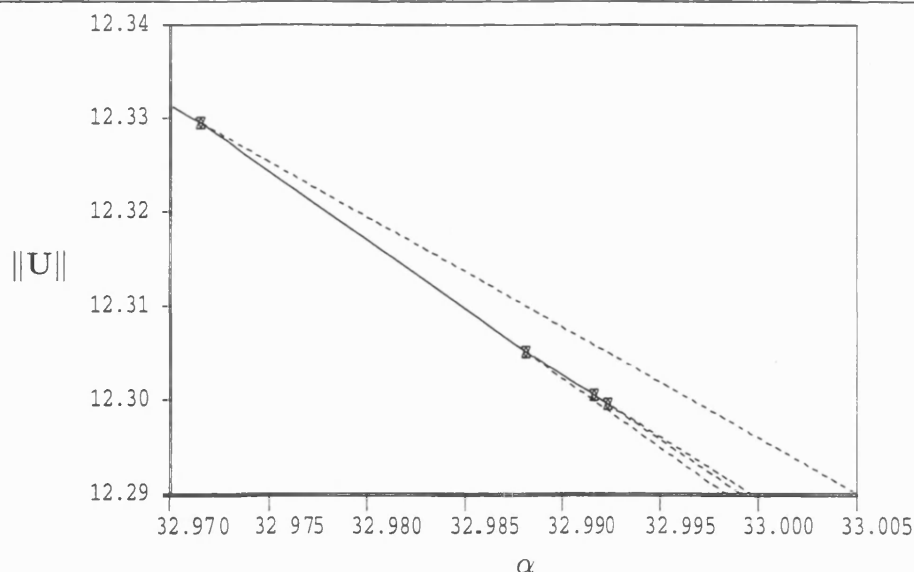


Figure 6-8: Close-up of the initial period doubling points.

We describe how our code computes the values of α where the period doublings take place, below

- We integrate an initial starting value over a sufficiently large time interval, say $[0, T_1]$, to eliminate transient behaviour.
- We then integrate the approximation at T_1 over a shorter interval, $[T_1, T_2]$, giving an approximation to $\mathbf{u}(t)$ at a set of discrete time points on $[T_1, T_2]$.
- We choose a solution component of the approximation, say $U_1(t)$, and interpolate it over the discrete time points using a piecewise cubic Bessel interpolation method, which gives approximations to $U_1'(t)$ and $U_1''(t)$.
- We use $U_1'(t)$ and $U_1''(t)$ to determine the critical points of $U_1(t)$. A change in the number of critical points corresponds to a change in the number of periodic orbits.

In our code we look for the minimum turning points of each orbit. As the period of the solution increases it is necessary to increase the size of the time intervals over which we must integrate.

We managed to detect 3 further period doubling points accurately using the above code, which appear to be the beginnings of a period doubling cascade. We

also used the code to compute the first four period doubling points, which we detected with AUTO, with a greater degree of accuracy. We expect to be able to find more points if we were to increase N . However this would greatly increase the CPU time of each computer run.

The period doubling route to chaos is well documented for certain low dimensional models which include the Lorenz equation and the forced Duffing's equation. Associated with this is the Feigenbaum universal constant

$$\delta = \lim_{n \rightarrow \infty} \frac{\alpha_n - \alpha_{n-1}}{\alpha_{n+1} - \alpha_n} = 4.669201609 \dots, \quad (6.1.5)$$

where the α_n 's are the parameter values at which period doubling bifurcations occur. This constant was originally found for discrete time maps and is believed to appear for other higher dimensional maps, which include ordinary and partial differential equations. Hence for completeness we have tested the successive ratios of period doublings which we observed for our approximation and the results can be seen in Table 6.4. The first column of the table gives our estimate for the subwindow boundaries (e.g. the first and second numbers in this column show the beginning and the end of the first periodic subwindow respectively). These points were calculated to eight decimal places. The second column shows the length of the subwindow, the third shows the successive ratios of the lengths and the fourth column shows the period of the solution at the respective parameter value.

Subwindow boundary	Length	Ratio	Period
32.97166311	-	-	0.16777555
32.99071753	1.90544×10^{-2}	-	0.34785657
32.99459246	3.94057×10^{-3}	4.835341080	0.70157517
32.99544233	8.4987×10^{-4}	4.636673844	1.45986242
32.99562538	1.8305×10^{-4}	4.642829828	2.99879927
32.99566467	3.9292×10^{-5}	4.658698423	6.00062756
32.99567289	8.215×10^{-6}	4.782836676	12.19519709

Table 6.4: First seven period doubling bifurcation points and the ratio of the successive subwindow lengths.

The ratios in the third column are quite close to the universal constant given in (6.1.5). This implies that Feigenbaum's theory for simple low dimensional maps is likely to apply to these periodic solutions. That is, there exists an accumulation point α_∞ , after which aperiodic solutions (or a *strange* attractor) can be observed. Table 6.4 also shows that the length of the subwindows shrinks rapidly, which makes the detection of further bifurcations difficult. Clearly there is insufficient accuracy in the calculation of the last bifurcation point.

Figure 6-9 shows a plot of the L^2 norm of the minimum turning point of the periodic solution against α , for $32.832 \leq \alpha \leq 33.014755$. The point where the branch splits into two represents the bifurcation point which we detected with AUTO in Figure 6-7. All the other points where the number of branches double represent period doubling bifurcations. After the first few period doublings, the attractor appears to become chaotic. It was impossible to find any attracting object beyond $\alpha = 33.014755$ using our code. However it may be possible to resolve this by increasing the size of N .

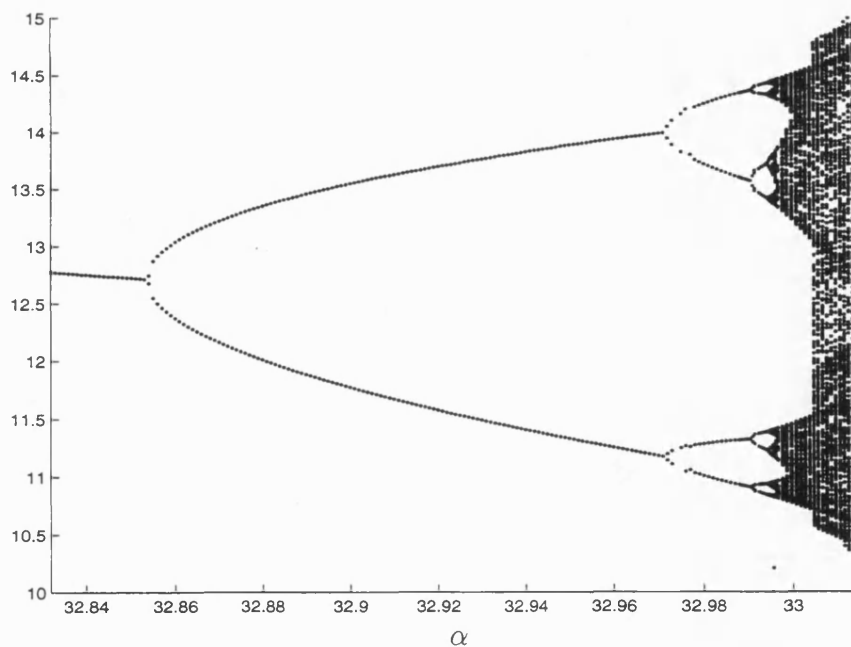


Figure 6-9: Minima of the L^2 norm of the periodic solutions plotted against α showing the period doubling cascade and beyond.

Figure 6-9 shows a sudden jump from a chaotic attractor in two narrow bands

to a chaotic attractor filling the entire interval at $\alpha \simeq 33.00465$. This jump discontinuity is usually referred to as an *interior crisis* point and is common in nonlinear dynamics. A close-up of the interior crisis bifurcation can be seen in Figure 6-10, the lines in this figure are separated by a distance of 1.0×10^{-4} . In the neighbourhood of this bifurcation the density of the points in the whole interval attractor concentrates in the bands and gradually spread out. An identical jump can be seen for the Hénon map in Parker and Chua [74, Ch.8, p.208].

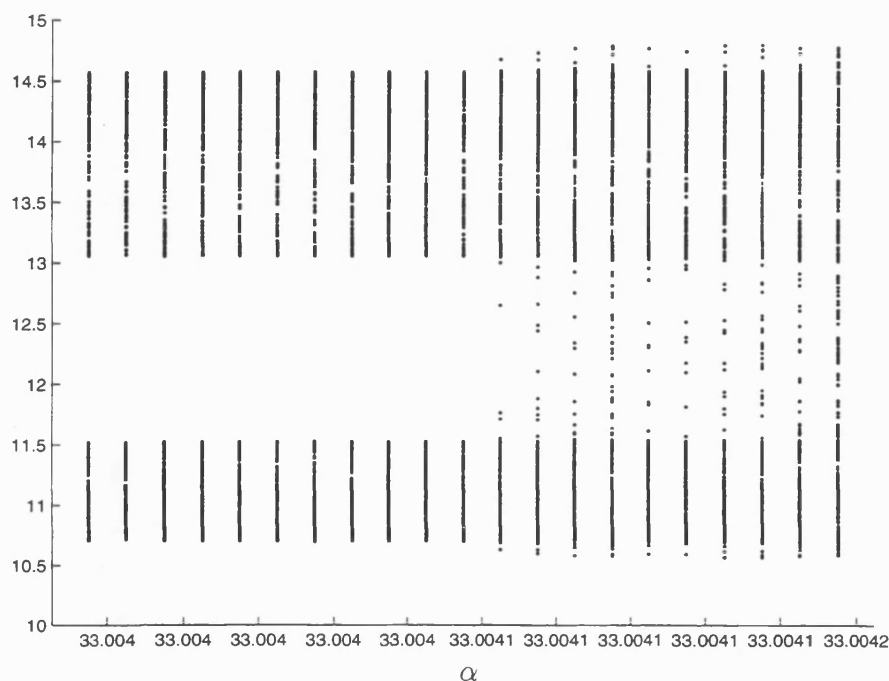


Figure 6-10: Interior crisis bifurcation at $\alpha \simeq 33.004$.

6.1.4 Homoclinic orbits

We now consider the implications of the Sil'nikov theory which we outlined in Section 4.1, for our PS discretization. In Figure 6-5 we showed that at $\alpha = 22.556$ there exists a pitchfork bifurcation which gives rise to two unstable steady state branches. These two branches consist entirely of saddle-focus points. That is, depending on the size of the discretization parameter, N , the eigenvalues of the linearization of our discretization will have the same form as the eigenvalues of the linearization of equation (4.5.10). Figure 6-11 shows the unstable branch of

solutions at $\alpha = 36$ followed by a sharp decrease. No further period doubling points were detected along the curve in Figure 6-12, however these are generally difficult to find, especially for complicated systems.

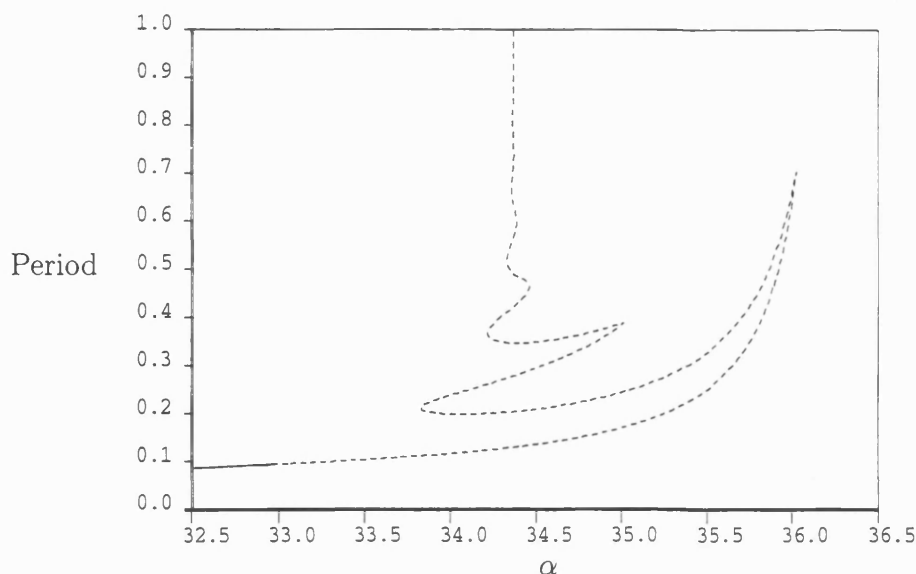


Figure 6-12: Behaviour of the periodic solutions produced at the supercritical Hopf bifurcation at $\alpha = 30.345$. Period plotted against α .

The homoclinic orbit, we have found, is in fact asymptotic to a saddle-focus point on the branch with the higher value for its fourth solution component in Figure 6-5. The eigenvalues of the linearized system at this point are shown in Figure 6-13a) and Figure 6-13b) shows a close up of the positive real eigenvalue, $\lambda_1 = 95.9239$, and the complex pair with negative real parts, $\lambda_{2,3} = -9.22122 \pm 42.0215i$.

The eigenvalues in Figure 6-13b) therefore satisfy the Sil'nikov inequality, given by (4.5.11) with $\delta = 0.09613$. This implies that our discretization has a route to chaos through the existence of a homoclinic orbit in its phase space and that the period doubling cascade we found earlier is a simple consequence of this orbit. Bifurcations to chaos through period doublings appears to be a common feature of systems which are approaching homoclinicity and can often be observed experimentally in dynamics experiments.

In Figure 6-14 we show some phase space projections of the branch of periodic solutions at various parameter values as they approach homoclinicity at

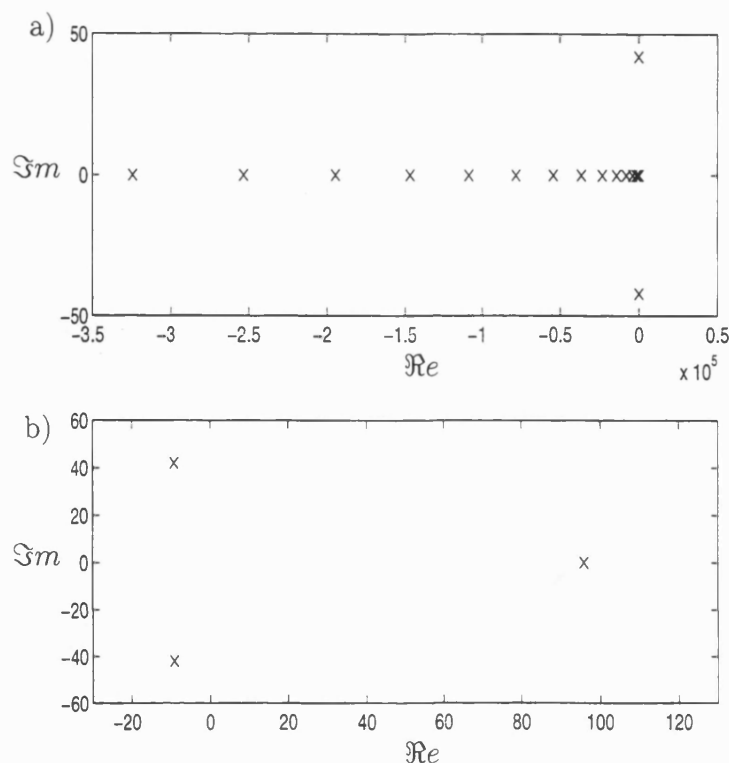


Figure 6-13: Eigenvalues of the linearization at the saddle-focus point at $\alpha = 34.366$. a) Complete spectrum; b) Close up of first three eigenvalues.

$\alpha = 34.366$. Figure 6-14a)-c) show the solutions undergoing a series of period doublings which eventually culminates in the existence of a strange attractor at $\alpha = 32.996$ given in Figure 6-14d). Then at $\alpha = 34.366$ the periodic solutions approach a homoclinic orbit of a saddle-focus point, see Figure 6-14e). At $\alpha = 34.3661$, see Figure 6-14f), this orbit collides with the stable manifold of a steady state (\times) and ultimately settles down to this steady state.

In order to obtain the picture of the homoclinic orbit in Figure 6-14e) we followed the unstable branch of periodic solutions produced at the first period doubling bifurcation at $\alpha = 32.971$ in Figure 6-8. If we follow the unstable branch from the second period doubling bifurcation in this figure, which contains double periodic solutions, then it is possible to find a double-pulse homoclinic orbit, see Figure 6-15, which exists at $\alpha = 34.3606$. If we could follow the unstable branch from an n^{th} period doubling bifurcation then we would obtain an orbit with 2^{n-1} loops before connecting back to the saddle point.

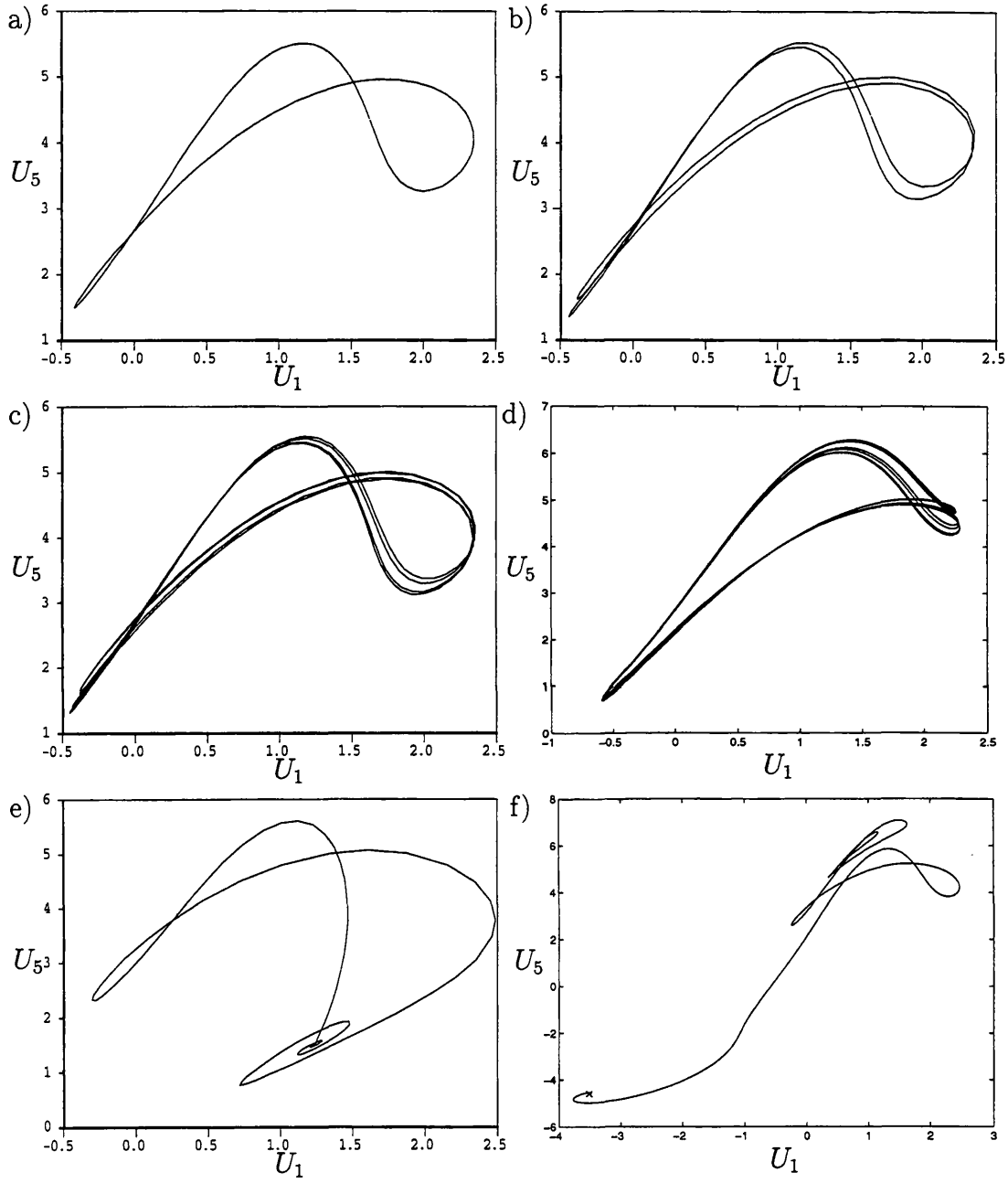


Figure 6-14: Phase plots of the periodic solutions. a) $\alpha = 32.971$; b) $\alpha = 32.990$; c) $\alpha = 32.994$; d) $\alpha = 32.996$; e) $\alpha = 34.336$; f) $\alpha = 34.3661$.

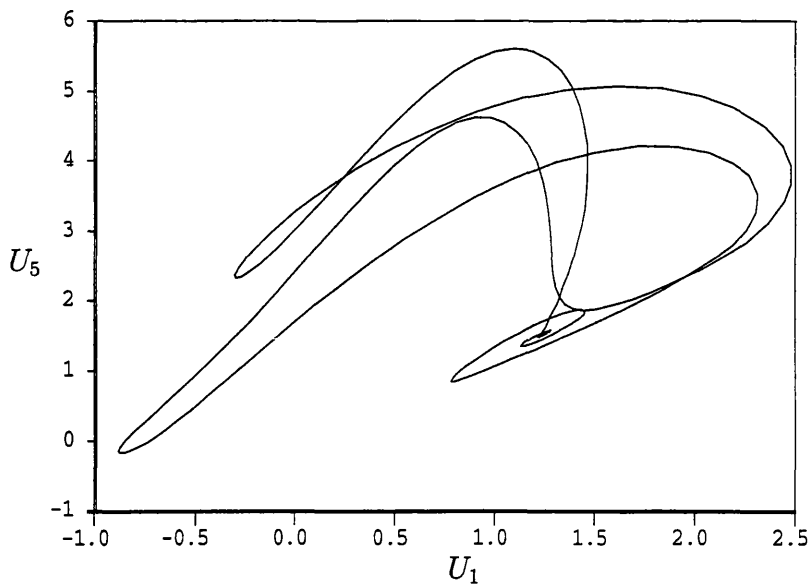


Figure 6-15: Double-pulse homoclinic orbit at $\alpha = 34.3606$.

6.1.5 A heteroclinic orbit

We now consider the unstable branch of periodic solutions which are produced at the bifurcation point at $\alpha = 32.853$. Figure 6-16 shows a close-up of the norm of these solutions. This branch has the same oscillatory behaviour which we observed when the solutions went homoclinic, however in this case the ‘wiggles’ appear to be more compressed and the branch joins the branch of saddle-focus points at $\alpha = 36.127$. In fact, at this point the solutions form a heteroclinic orbit connecting points on the two branches of saddle-focus points, this orbit is shown in Figure 6-17. The linearizations about the two saddle-focus points, which are connected by this orbit, both satisfy the Sil’nikov inequality. This is similar to the results in Glendinning and Sparrow [33] concerning a heteroclinic orbit for the Lorenz equations.

In Figure 6-18 we have plotted the evolution of the periodic solutions from the Hopf bifurcation at $\alpha = 30.345$, (+), up to the heteroclinic orbit. As far we are aware this is the first time this heteroclinic orbit has been observed.

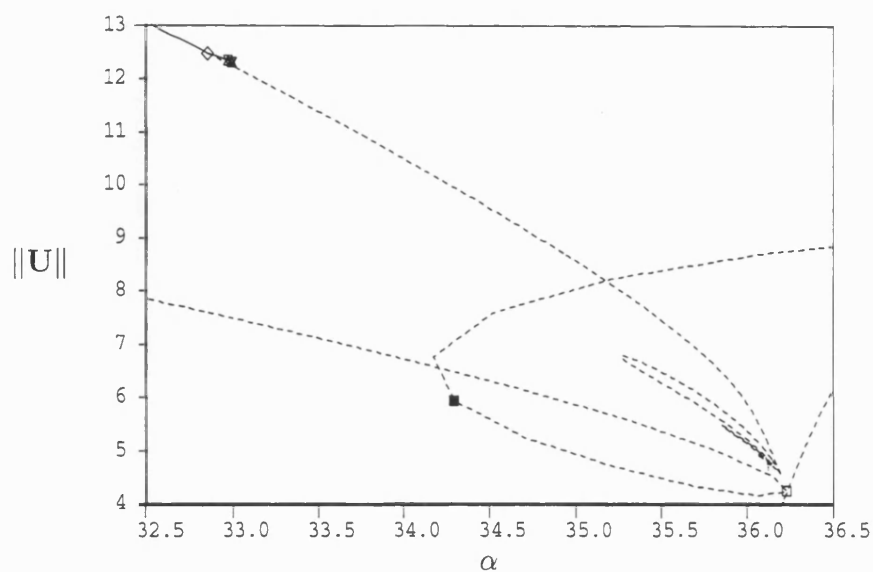


Figure 6-16: Unstable branch of periodic solutions emanating from the bifurcation point at $\alpha = 32.853$.

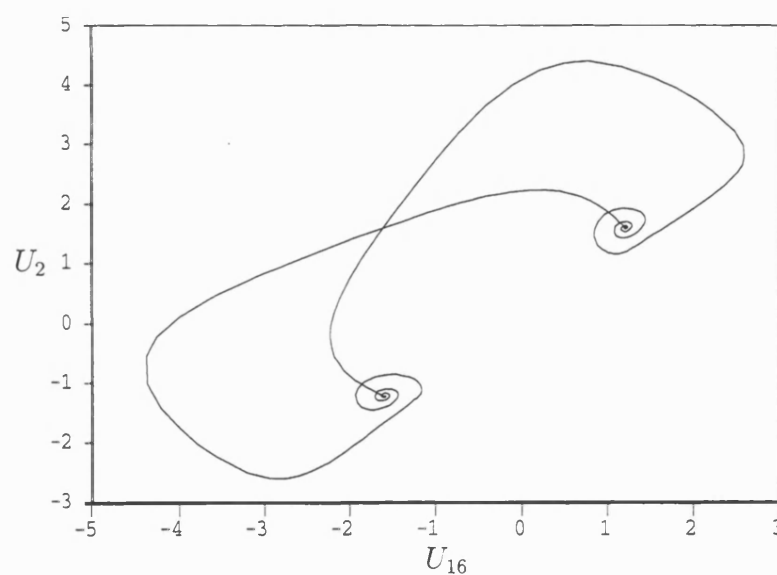


Figure 6-17: Heteroclinic orbit at $\alpha = 36.127$.

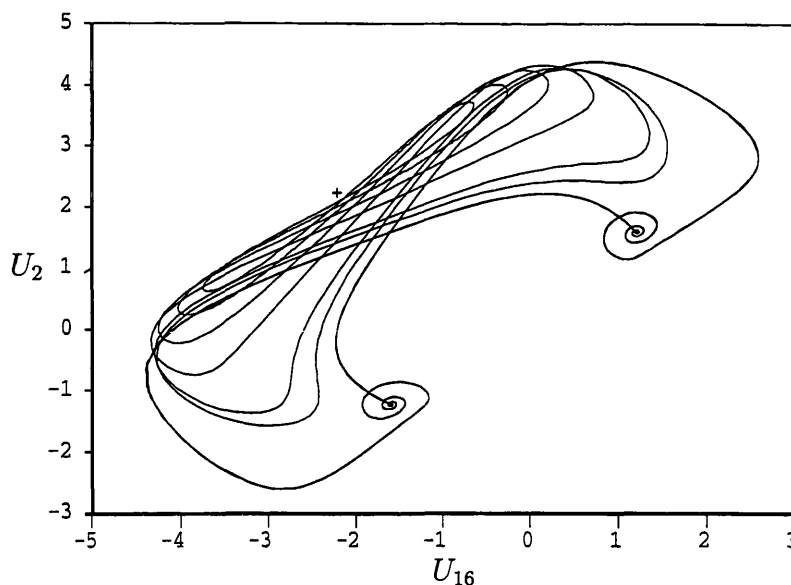


Figure 6-18: Periodic solutions as they approach the heteroclinic orbit.

6.1.6 Other periodic behaviour

Before concluding this section we briefly mention the periodic behaviour at the two Hopf bifurcation points at $\alpha = 34.345$, see Figure 6-5. The two bifurcations exhibit identical behaviour and we will only report on our findings for the one with the higher value in Figure 6-5. The periodic behaviour produced at this point can be seen in Figure 6-19. This looks similar to the behaviour we observed previously for the homoclinic orbits and the heteroclinic orbit, with the branches tending towards saddle-focus points.

In Figure 6-20 we have plotted the period of the solutions on the branch which tends to the saddle-focus branch with the higher norm value in Figure 6-19. It indicates that the period is winding itself around some accumulation point at $\alpha = 35.1745$. Also in Figure 6-21 we have plotted the homoclinic orbit which forms about the saddle-focus point for this value of α . Unlike the homoclinic orbits we observed earlier, the linearization about this point has a complex eigenvalue pair with positive real parts. The full spectrum at this saddle-focus point can be seen in Figure 6-22.

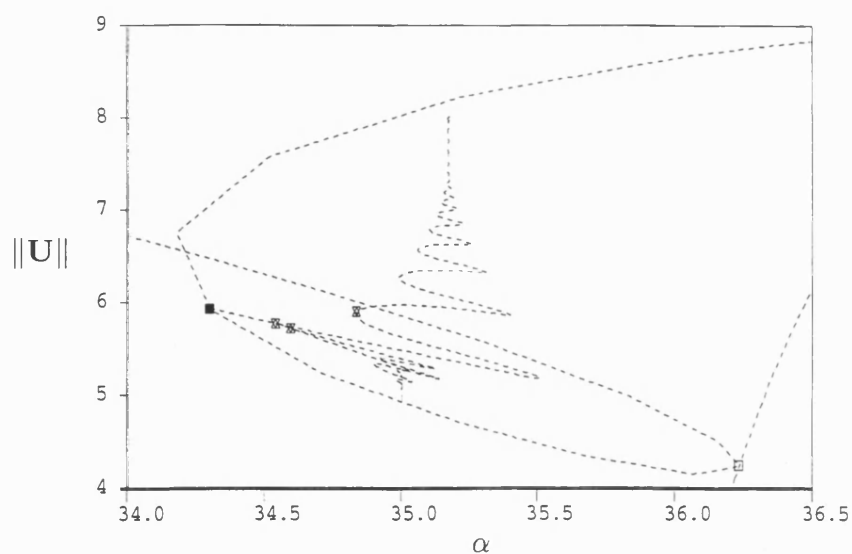


Figure 6-19: Periodic behaviour of the solutions at the Hopf bifurcation point at $\alpha = 34.345$.

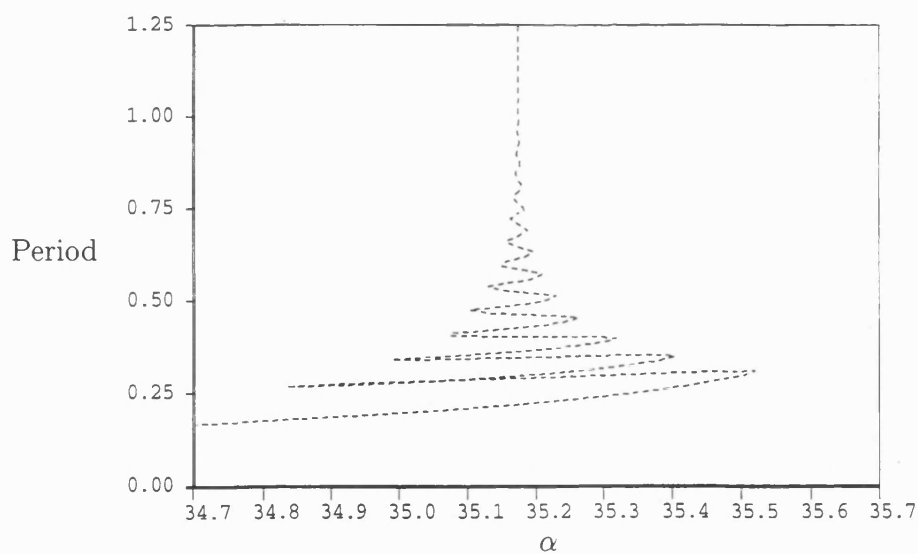


Figure 6-20: Behaviour of the upper branch of periodic solutions produced at Hopf bifurcation at $\alpha = 34.345$. Period plotted against α .

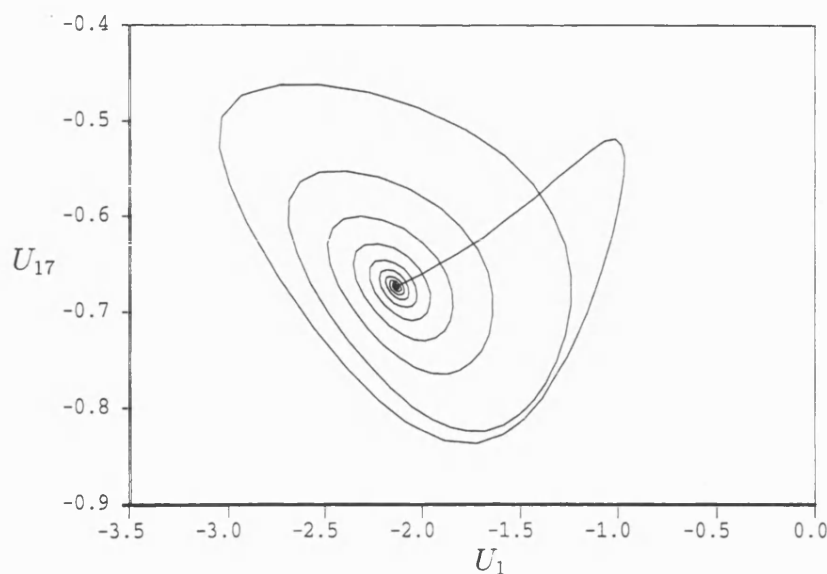


Figure 6-21: Behaviour of the upper branch of periodic solutions produced at Hopf bifurcation at $\alpha = 34.345$. Homoclinic orbit at $\alpha = 35.1745$.

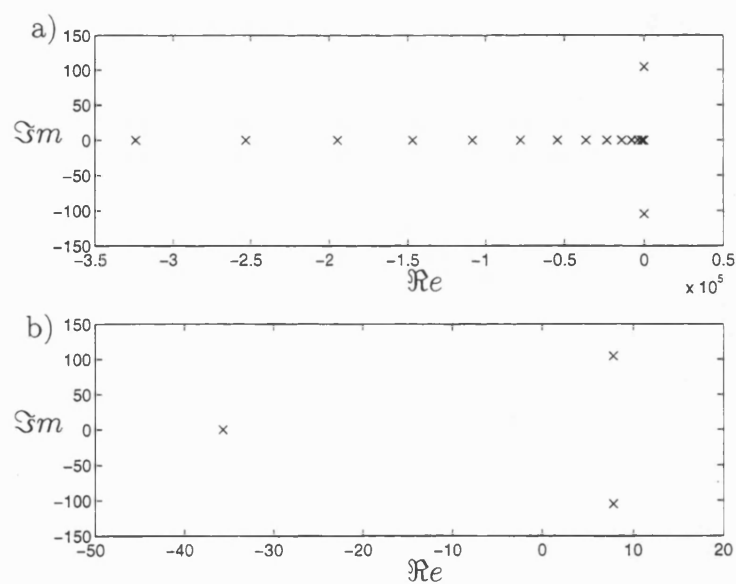


Figure 6-22: Eigenvalues of the linearization at the saddle-focus point at $\alpha = 35.1745$. a) Complete spectrum; b) Close-up of first three eigenvalues.

Therefore in this case the saddle-focus point has a two dimensional unstable manifold and hence the circumstances are different to those of the Sil'nikov case. If we follow the eigenvalues of the linearized system along the branches of saddle-focus points then at the Hopf bifurcation points at $\alpha = 34.345$, the complex pair of eigenvalues change from having a negative real part to having a positive real part at. Therefore the other branches in Figure 6-19 produced at the period doubling bifurcations do in fact approach homoclinicity and satisfy Sil'nikov's inequality.

In this section we have carried out a detailed study of the periodic solutions emanating from a supercritical Hopf bifurcation and illustrated numerically how these solutions become chaotic. It is worth noting that we have only considered small parameter values. However in Papageorgiou and Smyrlis [73], [82] much higher values were considered. In these papers at $\alpha = 115.5208$ a similar period doubling cascade was detected to the one which was studied here. It therefore may be the case that the K-S equation also has Sil'nikov chaotic behaviour for much higher parameter values.

6.2 Approximate inertial manifolds and nonlinear Galerkin methods

In Section 5.1 we showed that under certain conditions dissipative PDE's can be shown to possess inertial manifolds. These inertial manifolds can be represented in the form of graphs of Lipschitz functions, which relate the high and low Fourier modes of the solution. Unfortunately for some dissipative PDE's the existence of inertial manifolds is still an open question using the current existence methods. Also even when an equation is known to possess an inertial manifold there is no explicit representation for it.

It is because of these two reasons that the idea of *approximate inertial manifolds* (AIM's) has arisen. An AIM is a finite-dimensional Lipschitz manifold which attracts orbits of the equation into a small neighbourhood around it, exponen-

tially rapidly. AIM's were first introduced by Foias, Manley and Temam [21] in connection with the two-dimensional Navier-Stokes equations. These manifolds are another important development in the area of numerical analysis of dissipative equations because when an inertial manifold is known to exist, we can approximate it by an obtainable AIM. Also when an inertial manifold's existence is unknown we can use an AIM to provide a smooth approximation to the global attractor, in order to aid numerical computations.

6.2.1 Approximate inertial manifold theory

We now illustrate how AIM's are constructed in general. First of all we recall equation (5.1.1), given in Section 5.1,

$$\begin{aligned}\frac{du}{dt} + Au + R(u) &= 0, \\ u(0) &= u_0,\end{aligned}\tag{6.2.1}$$

on the separable Hilbert space \mathcal{X} . The space \mathcal{X} is spanned by the eigenfunctions of the linear operator A , which are given by $\{\psi_i\}_{i=1}^{\infty}$. We define P_n as the projection onto the first n eigenfunctions of A and Q_n as the orthogonal complement of P_n . Therefore projecting (6.2.1) with these operators gives the following equations

$$p_t + Ap + P_n R(p + q) = 0,\tag{6.2.2}$$

$$q_t + Aq + Q_n R(p + q) = 0,\tag{6.2.3}$$

where $p = P_n u$ and $q = Q_n u$. If (6.2.1) possesses an inertial manifold then for n sufficiently large there will exist a mapping Φ relating the spaces $P_n \mathcal{X}$ and $Q_n \mathcal{X}$. This implies that the asymptotic dynamics of the coupled system (6.2.2) and (6.2.3) will be identical to that of the inertial form of (6.2.1), which is given by

$$\begin{aligned}p_t + Ap + P_n R(p + \Phi(p)) &= 0, \\ p(0) &= P_n u_0.\end{aligned}\tag{6.2.4}$$

In AIM theory the mapping Φ is approximated by a map $\Phi_a : P_n\mathcal{X} \rightarrow Q_n\mathcal{X}$, which is known and explicitly computable. Hence the inertial form (6.2.4) is approximated by

$$\begin{aligned} p_t + Ap + P_n R(p + \Phi_a(p)) &= 0, \\ p(0) &= P_n u_0, \end{aligned} \tag{6.2.5}$$

which is called the *approximate inertial form*. This finite-dimensional system is used to obtain an approximation to the asymptotic dynamical behaviour of the original equation.

If $\Phi_a(p)$ is taken to be zero in (6.2.5), then this corresponds to solving (6.2.1) by an n -dimensional spectral Galerkin method and the AIM, in this case, will be given by the space $P_n\mathcal{X}$. If however $\Phi_a(p)$ is a non-trivial approximation to $\Phi(p)$, then the method of solution of (6.2.1) is referred as a nonlinear Galerkin (NLG) method. This is because the method involves the nonlinear mapping Φ_a . Hence NLG methods can basically be seen as extensions of the spectral Galerkin method, as they include some of the neglected terms, i.e. $q \in Q_n\mathcal{X}$.

The simplest way to construct an AIM for equation (6.2.1) is to use (6.2.3) to obtain a mapping which gives q in terms of p . For example, we note that the steady states of (6.2.1) will satisfy

$$Aq + Q_n R(p + q) = 0,$$

and are contained in the global attractor and hence an inertial manifold, should one exist. In this case, a possible AIM could be the graph of the function Φ_a , given by

$$\Phi_a(p) = -A^{-1}[Q_n R(p + \Phi_a(p))].$$

However, as this gives no explicit representation for Φ_a , we may consider the

following iterative scheme

$$\Phi_a^{(s+1)}(p) = -A^{-1}[Q_n R(p + \Phi_a^{(s)}(p))], \quad s \geq 0, \quad (6.2.6)$$

with initial approximation $\Phi^{(0)}(p) = 0$. The the first non-trivial manifold is therefore given by

$$\begin{cases} \Phi_a^{(1)}(p) = -A^{-1}[Q_n R(p)], \\ p \in P_n \mathcal{X}. \end{cases} \quad (6.2.7)$$

This AIM is called the *steady-AIM* and was introduced in Foias, Manley and Temam [21].

Debussche and Marion [10] and Temam [88] used the iterative scheme (6.2.6) to derive families of AIM's for the Navier-Stokes, reaction-diffusion and Cahn-Hilliard equations. The approximations to the q term are greatly improved with successive iterations. However it is sufficient to take only a few iterations of this scheme to obtain a good approximation and keep the computational cost at a minimum.

It is possible to use time-stepping methods to solve (6.2.3) to obtain an approximation for Φ_a . In Foias, Jolly, Kevrekidis, Sell and Titi [19] the so-called *Euler-AIM* was introduced. Here the backward Euler method with one iteration is used to solve (6.2.3), taking $q = 0$ as the initial approximation. If τ is the step size, then this AIM is given by

$$\begin{cases} \Phi_a(p) = -\tau(I + \tau A)^{-1} Q_n R(p), \\ p \in P_n H. \end{cases} \quad (6.2.8)$$

Smaller values of τ give better accuracy due to smaller truncation error.

It is also possible to use the Euler-AIM to construct families of approximations by using the following iterative scheme

$$\begin{cases} \Phi_a^{(s+1)}(p) = -\tau(I + \tau A)^{-1} Q_n R(p + \Phi_a^{(s)}(p)), & s \geq 0, \\ \Phi_a^{(1)}(p) = 0. \end{cases} \quad (6.2.9)$$

This particular scheme has been considered in Russell, Sloan and Trummer [78] for a reaction-diffusion equation and it is shown that particular values of τ are required for convergence.

Any of the AIM's given above could be substituted into (6.2.5) and the approximation method used to solve the resulting system would be an NLG method. Although NLG methods involve solving a much more complicated system, due to the AIM, it has been shown that in general their order of accuracy is $\mathcal{O}(\eta_{n+1}^{-(\beta+\sigma)})$, where η_{n+1} is the $(n+1)^{\text{th}}$ eigenvalue of A , σ is dependent on the regularity of the solutions of the equations under consideration and typically $\beta \in (1, 2]$. Here β is dependent on the particular AIM used in the approximation process and on the equation which is being approximated. This order of accuracy has been shown for a number of NLG methods, see [10], [21] and Jolly, Kevrekidis and Titi [47] and is an improvement over the spectral Galerkin method which is $\mathcal{O}(\eta_{n+1}^{-(1+\sigma)})$ accurate.

From a practical point of view in order to construct an NLG method it is necessary to ensure that the mapping Φ_a has a finite-dimensional range. This is achieved by redefining the projection operator Q_n as the projection onto the space

$$\text{span}\{\psi_{n+1}, \psi_{n+2}, \dots, \psi_{n+m}\},$$

where $m \in \mathbb{N}$. In practice m is usually taken to be n to keep the dimension of the whole system reasonably low, for computational efficiency. However in Jones, Margolin and Titi [50] it is argued that m should be taken to be $n^{\frac{\beta+\sigma}{1+\sigma}}$ where β is given above. This value will ensure that the additional accuracy of the NLG method is not lost through the truncation process. Obviously this choice of m has some practical implications for the methods, as the number of high modes required for an NLG method has a power growth. We will now consider some of the computational issues of the NLG methods.

6.2.2 Computational aspects of NLG methods

From a practical point of view it is not clear at present whether NLG methods offer an effective alternative to the spectral Galerkin method, due to their higher computational cost. To some extent this issue has been addressed in the papers García-Archilla and Frutos [31] and Jones, Margolin and Titi [50]. All the results in these papers correspond to particular example equations and we must empathise that there is little or no general theory in this area at present.

We now consider some of the results in [31] and [50] which correspond to Burgers' equation

$$\frac{\partial u}{\partial t} - \nu \frac{\partial^2 u}{\partial x^2} + u \frac{\partial u}{\partial x} = f(x), \quad (x, t) \in (0, \pi) \times (0, \infty), \quad (6.2.10)$$

and the reaction-diffusion equation

$$\frac{\partial u}{\partial t} - \nu \frac{\partial^2 u}{\partial x^2} + u^3 - u = f(x), \quad (x, t) \in (0, \pi) \times (0, \infty), \quad (6.2.11)$$

subject to the boundary conditions

$$u(0, t) = u(\pi, t) = 0, \quad t \in (0, \infty), \quad (6.2.12)$$

with initial condition $u(0, x) = u_0(x)$. Here f is some forcing term and ν is a positive parameter. These two equations can be formulated into abstract evolution equations, in a similar fashion as we did for the K-S equation, with $A = -\partial^2/\partial x^2$. The eigenvalues of A are then given by $\eta_j = j^2$ with corresponding eigenfunctions $\psi_j = \sqrt{2/\pi} \sin(jx)$, for $j \in \mathbb{N}$.

In (6.2.10) and (6.2.11) the function f is used to control the regularity of the solutions. If $f \in D(A^\sigma)$ and $u_0 \in L^2$, then it is possible to show that the spectral Galerkin method and NLG method based on the steady-AIM are $\mathcal{O}(\eta_{n+1}^{-(1+\sigma)})$ and $\mathcal{O}(\eta_{n+1}^{-(\beta+\sigma)})$ accurate respectively. Hence when σ is large the improvement due to the NLG method is less significant, since $\beta \in (1, 2]$. However for small σ the extra accuracy of the NLG method will be much more significant. This is illustrated

in [50] using equation (6.2.10) with $\nu = 1$, an appropriate initial condition and

$$f(x) = \sum_{j=1}^{\infty} \frac{1}{j^{2\gamma+1}} \sin(jx).$$

Hence $f \in D(A^\sigma)$, for $\sigma < \gamma + 1/4$. The solutions of equation (6.2.10) with this forcing term are attracted to a unique steady state. This steady state was computed using the spectral Galerkin method with 100 modes for various values of γ . Then for each of these values of γ the steady state was computed a number of times using the NLG method with $n = 10$ low modes and an increasing number of high modes, m . The L^2 error between these steady state approximations and the steady state obtained for the spectral Galerkin with $n = 100$ for the different values of γ can be seen in Figure 6-23.

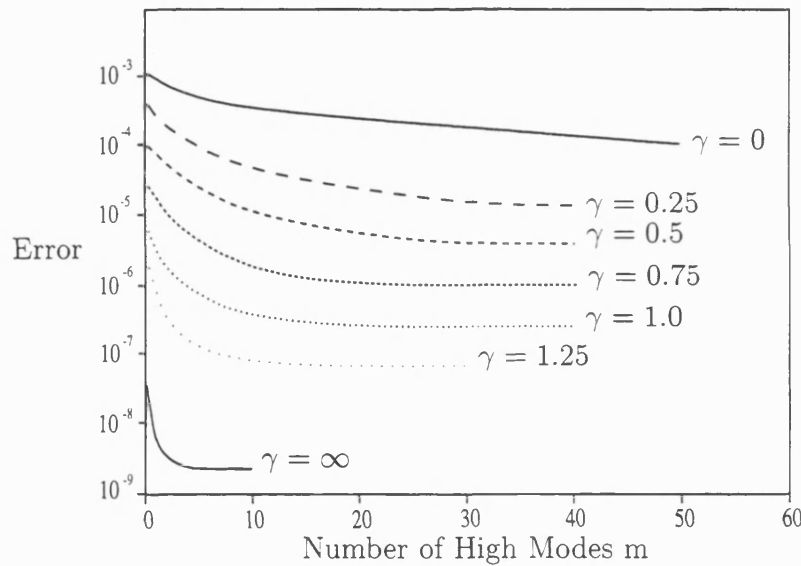


Figure 6-23: Approximation of the steady state attractor of Burgers' equation with $\nu = 1$. The L^2 error plotted against the number of high modes used by the NLG method.

Figure 6-23 confirms, for this particular example, that as the solution becomes more regular and satisfies more compatibility conditions, the less advantageous the NLG method becomes. The line with $\gamma = \infty$ corresponds to when the solutions of equation (6.2.10) are in a Gevrey class.

The question of whether NLG methods are superior over the spectral Galerkin

method, in terms of accuracy and computational efficiency, for equations with less smooth solutions is considered in [31]. In this paper the reaction-diffusion equation (6.2.11) with no forcing term was considered. This equation is known to possess two stable steady state solutions, whose gradients become large as ν becomes small. For increasingly small values of ν the two steady states were calculated using the spectral Galerkin method with a large number of modes to obtain reference solutions, which could be used to compare other approximations.

Next the spectral Galerkin method using a specified number of mode sizes, say n , and the NLG method using n low modes and $[2n/3]$ high modes were tested to see how well they approximated the reference solutions for the different values of ν . Efficiency diagrams for each value of ν considered can be seen in [31], which show the CPU time plotted against the L^2 error achieved for each method. The diagrams show that for a given accuracy requirement the NLG method never out-performed the spectral Galerkin method in terms of CPU time, even for very small values of ν . This will be illustrated more clearly when we show an efficiency diagram for this example with a different forcing term later in this section. These results therefore contradict the claims in [50] for the reaction-diffusion equation (6.2.11).

It has been shown that NLG methods are more accurate than the existing spectral Galerkin method. However it is unclear as to whether this additional accuracy is worth the extra computational cost of these methods, which comes from the evaluation of the AIM. It is because of these problems that the NLG methods have not been used by those engaged in numerical computation in the area of long-time dynamical behaviour.

6.2.3 The postprocessed Galerkin method

Before concluding this section it is worth looking at the recent paper by García-Archilla, Novo and Titi [32]. In this paper a method of postprocessing the spectral Galerkin method is introduced, which uses AIM techniques. This method enables one to exploit the increased accuracy of the NLG methods without the extra

computational cost.

In the postprocessed method one first of all obtains an approximation $p_n(t)$, by solving (6.2.1) by the spectral Galerkin method, i.e. solving

$$\begin{aligned} \frac{\partial p_n}{\partial t} + Ap_n + P_n R(p_n) &= 0, \\ p_n(0) &= P_n u_0. \end{aligned} \tag{6.2.13}$$

This approximation is then postprocessed using an AIM so that the final approximation, $u_{app}(t)$ is given by

$$u_{app}(t) = p_n(t) + \Phi_a(p_n(t)).$$

The Φ_a can be taken to be the steady-AIM or the Euler-AIM, which we described earlier.

In [32] it is shown that $u_{app}(t)$ is as accurate as an approximation obtained by a NLG method and the computational costs of the postprocessed methods are significantly less than the NLG method. This is illustrated by looking at the reaction-diffusion equation (6.2.11) with $\nu = 0.002$ and the following time dependent forcing term

$$f(x) = \begin{cases} 0, & 0 \leq x \leq \pi/4, \\ ((4/\pi)x - 1)(1 + \sin(2\pi t)/3), & \pi/4 \leq x \leq \pi/2, \\ (3 - (4/\pi)x)(1 + \sin(2\pi t)/3), & \pi/2 \leq x \leq 3\pi/4, \\ 0, & 3\pi/4 \leq x \leq \pi. \end{cases}$$

We note that $f \in D(A^\sigma)$ for $\sigma \in [0, 3/4)$, which implies that the order of convergence of the NLG method against that of the spectral Galerkin method should be more significant.

Given the initial condition $u_0(x) = \sin(x)$ the solutions of (6.2.11) become almost periodic in time. This behaviour was computed at $T = 15$ using a spectral Galerkin method with $n = 8000$ which was used as the reference solution. The same behaviour was then calculated using the spectral Galerkin method,

the postprocessed method and the NLG methods with various sizes of n . The postprocessed and NLG method used the steady-AIM. In accordance with the remarks previously made about truncating the term Φ_a , the number of high nodes used for the NLG method and the postprocessed method was taken so that

$$\eta_m^{-1-3/4} \leq \eta_n^{-\beta-3/4}.$$

In this case for equation (6.2.11) and the steady-AIM, $\beta = 3/2$, so that m was taken to be $n^{9/7}$. The L^2 errors of the approximations to the periodic behaviour obtained by the various methods can be seen in Figure 6-24. This figure shows

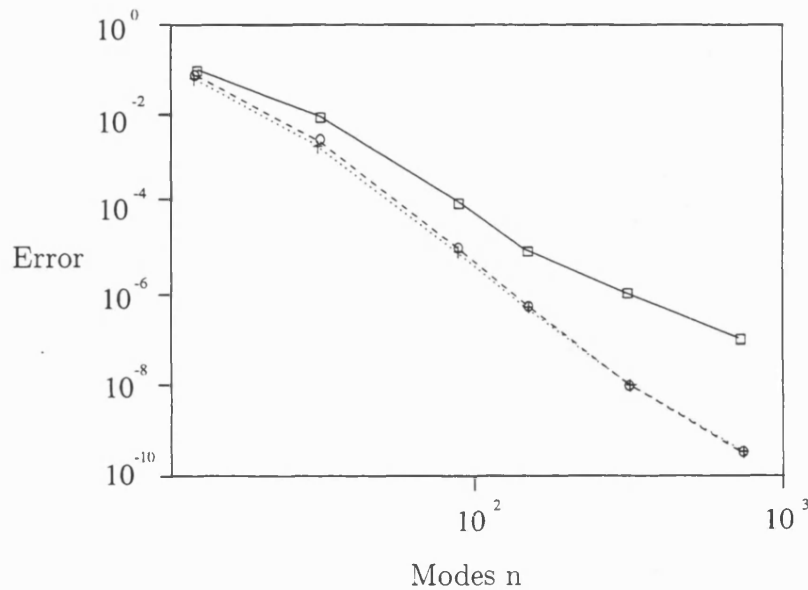


Figure 6-24: The L^2 error of the approximation to the periodic behaviour of the reaction-diffusion equation with $\nu = 0.002$ at $T = 15$ for different mode sizes n . — Spectral Galerkin Method, NLG method, --- Postprocessed Galerkin Method.

that for a given number of modes, the NLG and postprocessed method are between 10 and 100 times more accurate than the spectral Galerkin method. It also shows that the accuracy of the postprocessed method is almost identical to the NLG method. In Figure 6-25 some of the errors in Figure 6-24 were plotted against the CPU time that it took to achieve them. This shows that the least efficient method is the NLG method. Also the cost of the postprocessed method is slightly more than the spectral Galerkin method, however this is compensated

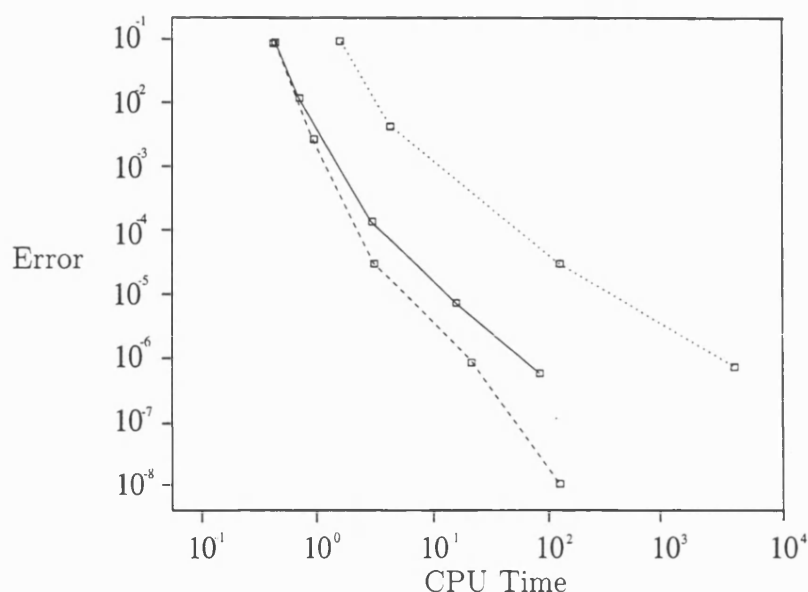


Figure 6-25: Efficiency diagram for the approximation of the periodic behaviour of the reaction-diffusion equation with $\nu = 0.002$ at $T = 15$. — Spectral Galerkin Method, NLG method, - - - Postprocessed Galerkin Method.

by the smaller error.

6.3 A nonlinear Galerkin method based on the pseudospectral method for the Kuramoto-Sivashinsky equation

In the previous section, we discussed AIM's which were constructed as graphs of functions relating the high and low eigenfunctions of linear operators of dissipative equations. The main drawback here is that these eigenfunctions are not always available, particularly when dealing with equations which have complicated boundary conditions. It is for this reason that in recent years attempts have been made to extend the theory of AIM's and their associated NLG methods to approximation schemes other than the spectral Galerkin method. Finite difference methods are considered in Margolin and Jones [64] and Temam [89], finite element methods are considered in Marion and Xu [66] and methods based on approximation by expansions of orthogonal polynomials are considered in Frutos,

García-Archilla and Novo [29], Gottlieb and Temam [35] and Wallace and Sloan [94]. Most of the NLG methods outlined in these papers use the steady-AIM described in the previous section. All the above papers basically mimic the slaving of high and low eigenfunctions through a Lipschitz function by relating nodal values of the solution on a coarse and fine grid. The NLG methods analysed in these papers all give rise to methods which have superior accuracy compared to existing methods. However in most cases no attempts have been made to analyse the practical implementation of these methods as was done in García-Archilla and Frutos [31].

In the next part of this section we look in detail at the work carried out by Wallace and Sloan [94] on their approach to AIM's.

6.3.1 Approximate inertial manifold approach of Wallace and Sloan

The motivation behind their work was to combine the pseudospectral method with the concept of AIM's in the hope of creating an efficient algorithm, in terms of computational efficiency and accuracy, to compute the asymptotic behaviour of dissipative PDE's. In their paper they illustrate their work using the renormalised one-dimensional K-S equation (2.3.7) with periodic boundary conditions and odd initial data. They formulate the same semi-discrete system that is considered in this thesis, which we recall is given by

$$\dot{\mathbf{U}} + 4D_h^4 \mathbf{U} + \alpha D_h^2 \mathbf{U} + \frac{\alpha}{3} [\mathbf{U} \otimes D_h^2 \mathbf{U} + D_h^2 (\mathbf{U} \otimes \mathbf{U})] = \mathbf{0}, \quad (6.3.1)$$

with initial condition $\mathbf{U}(0) = \mathbf{u}_0$, where the dot indicates time differentiation. This is a finite-dimensional, autonomous, nonlinear, discrete dynamical system of the form

$$\dot{\mathbf{U}} = \mathbf{G}(\mathbf{U}), \quad (6.3.2)$$

where \mathbf{G} is given by (3.4.2).

6.3.2 Algorithm with coarse and fine grid interactions

If we consider a spectral method with $N + 1$ high modes and N low modes then in a nodal sense this corresponds to the creation of a fine grid which matches a coarser grid at every second point. Therefore, in this context, we can replace the relation $q = \Phi(p)$ by a mapping which relates computed solutions on coarse and fine grids in physical space.

We now introduce some notation for the semi-discrete system (6.3.1) and we define a coarse grid

$$\{x_j\}_{j=1}^{N-1} : x_j = \frac{j\pi}{N} \equiv jh, \quad j = 1, \dots, N-1,$$

and a fine grid

$$\{y_j\}_{j=1}^{2N-1} : y_j = \frac{j\pi}{2N} \equiv jH, \quad j = 1, \dots, 2N-1.$$

The choice of $H = h/2$ ensures an overlap of the two uniform grids, see Figure 6-26. We also denote the approximations obtained by (6.3.1) at time t on the

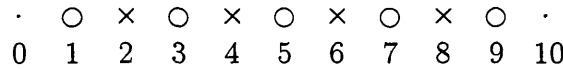


Figure 6-26: Coarse grid points (\times) and fine grid points (\times, \circ) on the interval $(0, \pi)$ for $N = 5$.

coarse grid by

$$\mathbf{U}^N = [U_1^N, U_2^N, \dots, U_{N-1}^N]^T, \quad (6.3.3)$$

and on the fine grid by

$$\mathbf{U}^{2N} = [U_1^{2N}, U_2^{2N}, \dots, U_{2N-1}^{2N}]^T. \quad (6.3.4)$$

The approximations on the fine grid can be split into their odd and even components

$$\begin{aligned}\mathbf{U}^o &= [U_1^{2N}, U_3^{2N}, \dots, U_{2N-1}^{2N}]^T, \\ \mathbf{U}^e &= [U_2^{2N}, U_4^{2N}, \dots, U_{2N-2}^{2N}]^T.\end{aligned}$$

Finally, we can use the discrete sine transform to obtain the discrete Fourier coefficients \mathbf{a}^N and \mathbf{a}^{2N} which are given by

$$\begin{aligned}\mathbf{a}^N &= S^N \mathbf{U}^N, \\ \mathbf{a}^{2N} &= S^{2N} \mathbf{U}^{2N},\end{aligned}$$

where S^i , $i = N, 2N$, are defined in (3.1.5) and are $(N-1) \times (N-1)$ and $(2N-1) \times (2N-1)$ square matrices respectively.

We now look at *Algorithm 2* introduced by Wallace and Sloan in [94]. In this algorithm, time integration is carried out using the Crank-Nicolson method which we analysed in Section 3.4. We recall that applying this method to (6.3.2) gives

$$\mathbf{U}^{(n)} - \frac{k}{2} \mathbf{G}(\mathbf{U}^{(n)}) = \mathbf{U}^{(n-1)} + \frac{k}{2} \mathbf{G}(\mathbf{U}^{(n-1)}), \quad (6.3.5)$$

where k is the time-step size and $\mathbf{U}^{(i)}$, $i = n, n-1$, is the approximation to $u(\cdot, t_i)$, where $t_i = ik$. If we take $\mathbf{U}^{(n-1)}$ as an initial guess we can solve (6.3.5) using a Newton iteration, i.e. we solve the system

$$\begin{cases} J^{(s)} \mathbf{U}^{(n,s+1)} = J^{(s)} \mathbf{U}^{(n,s)} - \mathbf{F}^{(s)}, & s \geq 0, \\ \mathbf{U}^{(n,0)} = \mathbf{U}^{(n-1)}, \end{cases} \quad (6.3.6)$$

for $\mathbf{U}^{(n,s+1)}$, where $\mathbf{F}^{(s)}$ is the function

$$\mathbf{F}^{(s)} = \mathbf{U}^{(n,s)} - \frac{k}{2} \mathbf{G}(\mathbf{U}^{(n,s)}) - \mathbf{U}^{(n-1)} - \frac{k}{2} \mathbf{G}(\mathbf{U}^{(n-1)}),$$

and $J^{(s)}$ is the Jacobian of $\mathbf{F}^{(s)}$ given by

$$J^{(s)} = I + \frac{k}{2}[4D_h^4 + \alpha D_h^2 + \frac{\alpha}{3}N^{(s)}],$$

where I is the identity matrix and N is the matrix given by

$$[N^{(s)}]_{i,j} = \begin{cases} U_i^{(n,s)} ([D_h^o]_{i,i} + 2[D_h^e]_{i,i}) + \sum_{k=1}^r [D_h^o]_{i,k} U_k^{(n,s)}, & i = j, \\ U_i^{(n,s)} [D_h^o]_{i,j} + 2[D_h^e]_{i,j} U_j^{(n,s)}, & i \neq j, \end{cases}$$

where $U_i^{(n,s)}$ are the components of $\mathbf{U}^{(n,s)}$. All the matrices given above are $r \times r$, where r is the number of internal grid points, so it will either take the value $N-1$ or $2N-1$ depending on which grid we are solving (6.3.5) on.

Algorithm 2 below gives an approximation to the solution on the coarse grid and improves this approximation by considering fine grid interactions.

Algorithm 2 (Wallace & Sloan [94])

1. Find \mathbf{U}^N by solving (6.3.5) by a Newton iteration with $r = N-1$ and set

$$\mathbf{U}^e := \mathbf{U}^N.$$

2. Approximate $\mathbf{G}(\mathbf{U}^{2N})$ on the coarse grid by $\mathbf{G}(\mathbf{U}^e)$ and use the discrete sine transform to obtain

$$\mathbf{a}^N = S^N \mathbf{G}(\mathbf{U}^e),$$

so that interpolation (which in this case is a sine series) can be used to obtain an approximation to $\mathbf{G}(\mathbf{U}^{2N})$ at the intermediate points of the fine grid, say $\mathcal{I}G(y_j)$, $j = 1, 3, \dots, 2N-1$, where \mathcal{I} stands for the interpolation operator, i.e.,

$$\mathcal{I}G(y_j) = \sum_{l=1}^N a_l \sin\left(\frac{l j \pi}{2N}\right), \quad j = 1, 3, \dots, 2N-1,$$

where a_l is the l^{th} component of \mathbf{a}^N .

3. Fix \mathbf{U}^e and use a Newton iteration to solve

$$\mathbf{G}(\mathbf{U}^{2N})|_{\text{odd}} = \mathcal{I}\mathbf{G}, \quad (6.3.7)$$

for \mathbf{U}^o . $\mathcal{I}\mathbf{G}$ is the vector of values $\mathcal{I}G(y_j)$ for $j = 1, 3, \dots, 2N - 1$ and $\mathbf{G}(\mathbf{U}^{2N})|_{\text{odd}}$ corresponds to $G_i(\mathbf{U}^{2N})$, for $i = 1, 3, \dots, 2N - 1$, which is considered to be a function of \mathbf{U}^o with fixed \mathbf{U}^e . Thus this solution process involves solving N nonlinear equations.

4. Fix \mathbf{U}^o and update \mathbf{U}^e by solving (6.3.5) for \mathbf{U}^e , this time using the PS derivatives on the complete fine grid. Here we are solving for $N - 1$ unknowns contained in the vector \mathbf{U}^e from the nonlinear equations which constitute the even rows of (6.3.5) for a fine grid discretization. This means that the Newton iteration, although related to solving (6.3.5) with $r = 2N - 1$, only involves the solution of $N - 1$ equations.
5. Compute the difference between the left hand side of (6.3.5), evaluated using the updated value of \mathbf{U}^e from step 4, and the right hand side of (6.3.5), evaluated using the \mathbf{U}^e value from the previous time step. If the difference is within a specified tolerance then go on to the next time step, otherwise return to step 2 with the updated \mathbf{U}^e value.

In step 3 since \mathbf{G} is considered to be a function of \mathbf{U}^o with \mathbf{U}^e fixed, the solution of the N equations in (6.3.7) for \mathbf{U}^o , could therefore be written as

$$\mathbf{U}^o = \Phi(\mathbf{U}^e). \quad (6.3.8)$$

This interaction between the fine and coarse grids can be seen to be an analogous representation of the interaction of high and low eigenfunctions in the NLG methods.

6.3.3 Numerical results

We now reproduce some of the numerical results from Wallace and Sloan [94]. We therefore examine how well the NLG algorithm outlined above computes the qualitative behaviour of the K-S equation using AUTO 97. Efficiency tests were carried for the algorithm in [94] and we will discuss the implications of these later.

Our previous studies of the dynamics of the K-S equation showed that for reasonably low parameter values the dimension of the attractor is also low. Therefore in order to demonstrate how well the dynamics are captured by the NLG algorithm we have computed bifurcation diagrams for parameter values $0 \leq \alpha \leq 80$. We begin by considering the steady states for these particular values. The main qualitative behaviour can be captured using the standard PS discretization with $N = 12$ (or 11 nodal points). There is little difference in the numerical results if N is increased above this value. However we shall see that using the NLG algorithm, the value of N can be decreased below 12 to obtain similar behaviour. Figure 6-27 shows the bifurcation diagram for the K-S equation using the PS discretization with $N = 12$. This diagram shows the solution component U_4 , which represents the approximation of the solution at $x = \pi/3$, plotted against the bifurcation parameter. We used U_4 so that comparisons could be made with the algorithm for different values of N .

Figure 6-28 shows the bifurcation diagram computed by the algorithm with $N = 6$ (5 coarse grid points). For parameter values $0 \leq \alpha \leq 50$ the diagrams are essentially the same. However beyond these values we notice a marked difference. Namely some of the steady state branches are missing and some bifurcation points and branches differ quantitatively. Although this demonstrates that for small values of N the algorithm has problems capturing the dynamics of the K-S equation, it performs well compared to the standard PS discretization with $N = 6$.

It was found that for $N = 9$ the algorithm produces an almost identical bifurcation diagram as the standard PS discretization with $N = 12$, see Figure

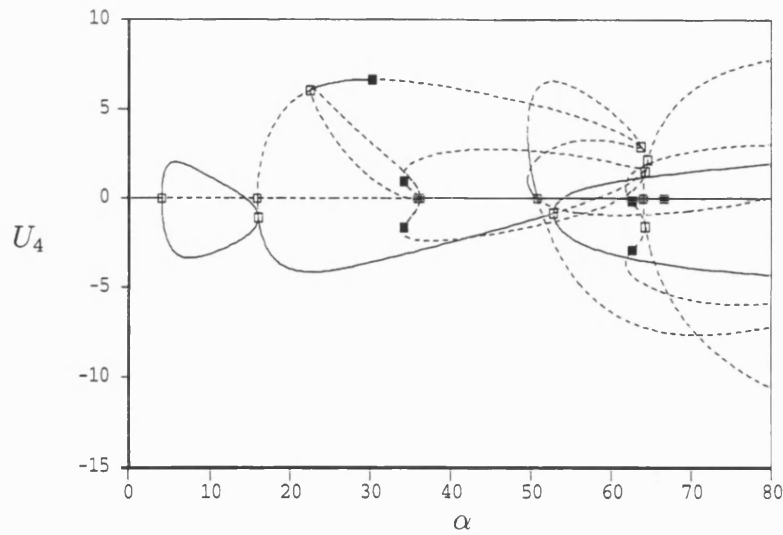


Figure 6-27: Bifurcation diagram for the K-S equation for $0 \leq \alpha \leq 80$ using the PS method with $N = 12$.

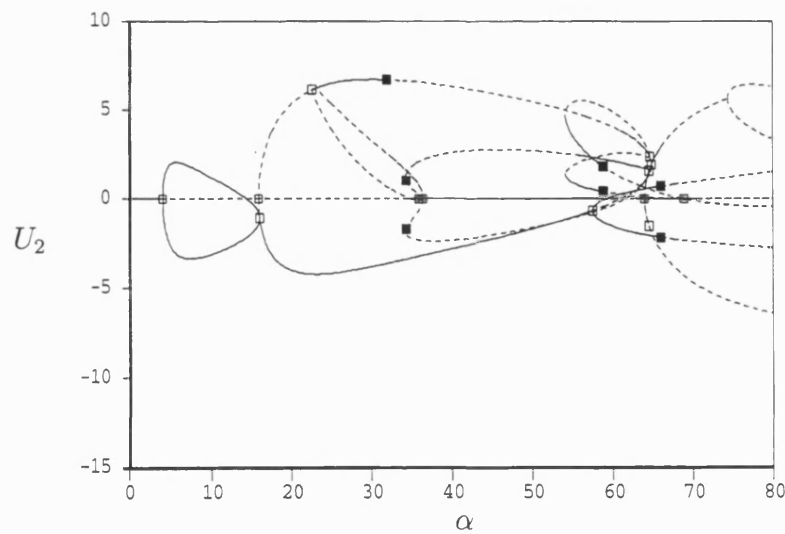


Figure 6-28: Bifurcation diagram for the K-S equation for $0 \leq \alpha \leq 80$ using Algorithm 2 with $N = 6$.

6-29. The only essential difference is there appears to be a missing bifurcation point at $\alpha = 64.275$, however it may be possible to resolve this by changing the parameter values of AUTO 97 (i.e. setting smaller tolerances or increasing the number of subintervals for the spline collocation).

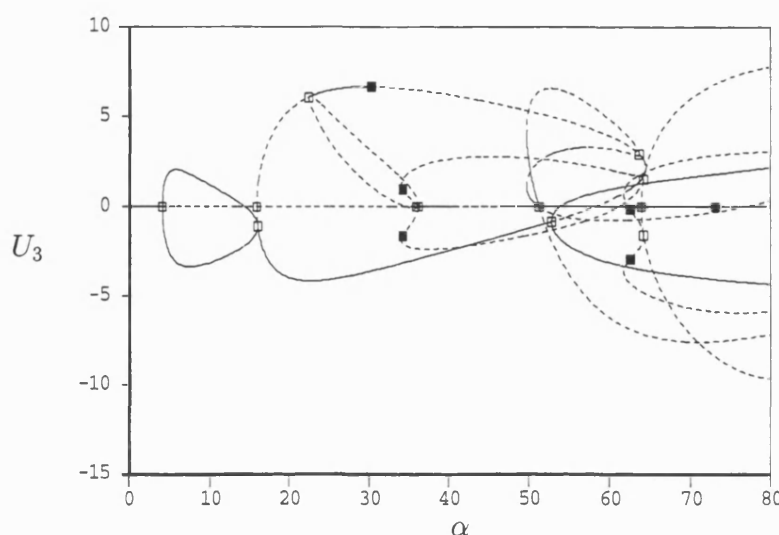


Figure 6-29: Bifurcation diagram for the K-S equation for $0 \leq \alpha \leq 80$ using Algorithm 2 with $N = 9$.

We next considered how well the algorithm captured the periodic behaviour of the K-S equation, which we observed in Section 6.1. Figure 6-30 shows that the algorithm with $N = 9$ captures the periodic solutions produced at the Hopf bifurcation at $\alpha = 30.345$ as well as the oscillatory behaviour as these solutions become heteroclinic at $\alpha = 36.127$. A picture of this heteroclinic orbit is given in Figure 6-31, where we have plotted the first solution component against the eighth component. The standard PS discretization with $N=9$ was unable to detect this orbit.

The numerical experiments carried out above and in the paper [94] show that Algorithm 2 is much more accurate than the standard PS method. It is also able to detect more of the dynamical behaviour of the K-S equation for lower discretization parameter values.

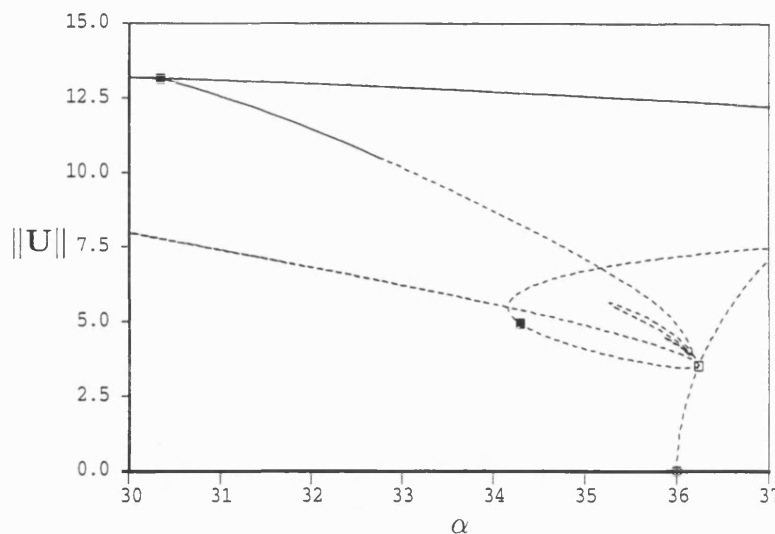


Figure 6-30: Periodic solutions produced by the Hopf bifurcation at $\alpha = 30.345$, computed using Algorithm 2 with $N = 9$.

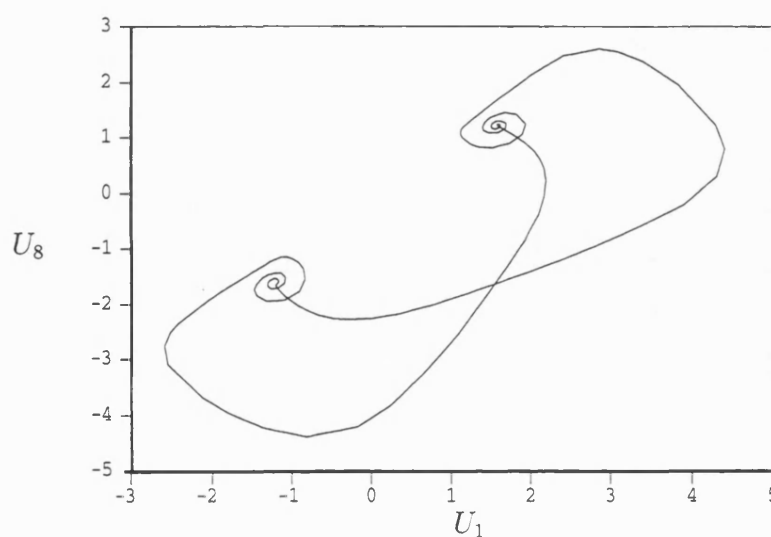


Figure 6-31: Heteroclinic orbit at $\alpha = 36.127$, computed using Algorithm 2 with $N = 9$.

The accuracy and efficiency tests carried out for the NLG algorithm in [94] showed that as the acceptable error diminishes the algorithm becomes increasingly more expensive than the standard PS discretization. This is in line with the results of García-Archilla and Frutos [31]. There is possibly a case for carrying out the time integration of (6.3.2) using a more efficient time integrator than the Crank-Nicolson method and possibly one which is stiffly stable, however this

is unlikely to produce an algorithm which is as efficient as the postprocessed methods which we described in the last section. A method of postprocessing using spectral methods based on orthogonal polynomials is introduced in Frutos, García-Archilla and Novo [29].

Chapter 7

Final Conclusions and Future Work

In this thesis we have carried out a detailed study of the numerical approximation of the asymptotic behaviour of the K-S equation using a semi-discrete pseudospectral approximation. We have improved upon an existing convergence result for this method applied to this particular equation and proved a convergence result for a fully-discrete approximation using the Trapezoidal rule for the time integration. We have also shown that the solutions of our semi-discrete approximation are in a Gevrey class. To our knowledge this is the first time that such a result has been proved for the pseudospectral method. Using this result we have applied the approach of Lord and Stuart [61] to prove an upper semi-continuity result for the attractors of our semi-discrete approximation. This approach avoids the use of rough initial data estimates by exploiting the regularity of the solutions of the continuous equation and its approximation. We have greatly reduced the assumptions of this approach to obtain our result and hence improved its applicability.

Also using the regularity of the solutions of the K-S equation and its pseudospectral approximation we have managed to apply the recent approximation theory of inertial manifolds in Jones, Stuart and Titi [52] to our semi-discrete approximation. This has enabled us to prove that the invariant sets of the K-S

equation persist under semi-discrete PS approximation. The essential improvement of our work here is that we have shown that these sets converge to each other with a high order of accuracy.

In this thesis we have managed to prove some mathematical results for a practical numerical method applied to the K-S equation with periodic boundary conditions. Possible future work may be to apply our results to fully-discrete approximations methods, such as our Crank-Nicolson method given in Section 3.4. It may also be interesting to try and prove similar results for time discretization methods which are generally used for the time integration of nonlinear problems. Another possible area of study may be to apply our results to the K-S equation with more applicable boundary conditions. In order to do this it will be essential to prove the existence of an inertial manifold under these conditions. A problem may arise also in proving that the solutions are contained in a Gevrey class, therefore an alternative method may be required to prove regularity of solutions and their approximations. One may also consider applying our results to other dissipative PDE's using the pseudospectral method or an alternative approximation method.

Bibliography

- [1] R.A. Adams. *Sobolev Spaces*. Academic Press, 1966.
 - [2] A.J. Babchin, A.L. Frenkel, B.G. Levich, and G.I. Sivashinsky. Nonlinear saturation of Rayleigh-Taylor instabilities in thin films. *Physics of Fluids*, **26**:3159–3161, 1983.
 - [3] D.J. Benney. Long waves in liquid film. *Journal of Mathematical Physics*, **45**:150–155, 1966.
 - [4] J.E. Billoti and J.P. LaSalle. Dissipative periodic processes. *Bulletin of the A.M.S.*, **77**:1082–1089, 1971.
 - [5] C. Canuto, M.Y. Hussaini, A. Quarteroni, and T.A. Zang. *Spectral Methods in Fluid Dynamics*. Computational Physics. Springer-Verlag, 1987.
 - [6] S.N. Chow, K. Lu, and G.R. Sell. Smoothness of inertial manifolds. *Journal of Mathematical Analysis and Applications*, **169**:283–321, 1992.
 - [7] P. Collet, J.P. Eckmann, H. Epstein, and J. Stuble. A global attracting set for the Kuramoto-Sivashinsky equation. *Communications in Mathematical Physics*, **152**:203–214, 1993.
 - [8] P. Constantin, C. Foias, B. Nicolaenko, and R. Temam. *Integral Manifolds and Inertial Manifolds for Dissipative Partial Differential Equations*, volume 70. Springer-Verlag, 1988.
-

-
- [9] P. Constantin, C. Foias, B. Nicolaenko, and R. Temam. Spectral barriers and inertial manifolds for dissipative partial differential equations. *Journal of Dynamics and Differential Equations*, 1(1):45–73, 1989.
 - [10] A. Debussche and M. Marion. On the construction of families of approximate inertial manifolds. *Journal of Differential Equations*, 100:173–201, 1992.
 - [11] L. Dettori, D. Gottlieb, and R. Temam. A nonlinear Galerkin method: The two-level Fourier-collocation case. ICOSAHOM 95.
 - [12] R. Devaney. *An Introduction to Chaotic Dynamical Systems*. Addison-Wesley, 2nd edition, 1989.
 - [13] E.J. Doedel, A.R. Champneys, T.F. Fairgrieve, Y.A. Kuznetsov, B. Sandstede, and X. Wang. **AUTO 97: Continuation and bifurcation software for ordinary differential equations (with homcont)**.
 - [14] C.R. Doering, J.D. Gibbon, D.D. Holm, and B. Nicolaenko. Low-dimensional behaviour in the complex Ginzburg-Landau equation. *Nonlinearity*, 1:279–309, 1988.
 - [15] P.G. Drazin. *Nonlinear Systems*. Cambridge Texts in Applied Mathematics, 1992.
 - [16] J. Duan, E.S. Titi, and P. Holmes. Regularity, approximation and asymptotic dynamics for a generalized Ginzburg-Landau equation. *Nonlinearity*, 6:915–933, 1993.
 - [17] D.E. Edmunds and W.D. Evans. *Spectral Theory and Differential Operators*. Clarendon Press, 1989.
 - [18] C.M. Elliott and S. Larsson. Error-estimates with smooth and nonsmooth data for a finite-element method for the Cahn-Hilliard equation. *Mathematics of Computations*, 58(198):603–630, 1992.
-

-
- [19] C. Foias, M.S. Jolly, I.G. Kevrekidis, G.R. Sell, and E.S. Titi. On the computation of inertial manifolds. *Physics Letters A*, **131**(7-8):433–436, 1988.
 - [20] C. Foias, M.S. Jolly, I.G. Kevrekidis, and E.S. Titi. Dissipativity of numerical schemes. *Nonlinearity*, **4**(3):591–613, 1991.
 - [21] C. Foias, O. Manley, and R. Temam. Modelling of the interaction of small and large eddies in two-dimensional turbulent flows. *Mathematical Modelling and Numerical Analysis*, **22**:93–114, 1988.
 - [22] C. Foias, B. Nicolaenko, G.R. Sell, and R. Temam. Inertial manifolds for the Kuramoto-Sivashinsky equation and an estimate of their lowest dimension. *Journal de Mathématiques Pures et Appliquées*, **67**:197–226, 1988.
 - [23] C. Foias, G.R. Sell, and R. Temam. Variétés inertielles des équations différentielles dissipatives. *Comptes Rendus de l'Académie des Sciences Série I-Mathématiques*, **301**:139–141, 1985.
 - [24] C. Foias, G.R. Sell, and R. Temam. Inertial manifolds for nonlinear evolutionary equations. *Journal of Differential Equations*, **73**:309–353, 1988.
 - [25] C. Foias and R. Temam. Structure of the set of stationary solutions of the Navier-Stokes equations. *Communications on Pure and Applied Mathematics*, **30**:149–164, 1979.
 - [26] C. Foias and R. Temam. Gevrey class regularity for the solutions of the Navier-Stokes equations. *Journal of Functional Analysis*, **87**:359–369, 1989.
 - [27] C. Foias and E.S. Titi. Determining nodes, finite difference schemes and inertial manifolds. *Nonlinearity*, **4**:135–153, 1991.
 - [28] B. Fornberg and D.M. Sloan. A review of pseudospectral methods for solving partial differential equations. In *Acta Numerica*, pages 203–267. Cambridge University Press, 1994.
-

-
- [29] J. De Frutos, B. García-Archilla, and J. Novo. A postprocessed Galerkin method with Chebyshev or Legendre polynomials. Applied mathematics and computation reports, University of Valladolid, July 1996.
- [30] B. García-Archilla. Some practical experience with the time integration of dissipative equations. *Journal of Computational Physics*, **122**:25–29, 1995.
- [31] B. García-Archilla and J. De Frutos. Time integration of the nonlinear Galerkin method. *IMA Journal of Numerical Analysis*, **15**:221–244, 1995.
- [32] B. García-Archilla, J. Novo, and E.S. Titi. Postprocessing the Galerkin method: A novel approach to approximate inertial manifolds. *SIAM Journal of Numerical Analysis*, **35**(3):941–972, 1998.
- [33] P. Glendinning and C. Sparrow. Local and global behaviour near homoclinic orbits. *Journal of Statistical Physics*, **38**:645–696, 1984.
- [34] D. Gottlieb and S.A. Orszag. *Numerical Analysis of Spectral Methods: Theory and Applications*. Regional Conference Series in Applied Mathematics. SIAM, 1977.
- [35] D. Gottlieb and R. Temam. Implementation of the nonlinear Galerkin method with pseudospectral (collocation) discretisations. *Applied Numerical Mathematics*, **12**:119–134, 1993.
- [36] J. Guckenheimer and P. Holmes. *Nonlinear Oscillations, Dynamical Systems and Bifurcation of Vector Fields*, volume 42 of *Applied Mathematical Sciences*. Springer-Verlag, 1983.
- [37] J.K. Hale. *Asymptotic Behaviour of Dissipative Systems*. A.M.S., 1988.
- [38] J.K. Hale, X.-B. Lin, and G. Raugel. Upper semicontinuity of attractors for approximations of semigroups and partial differential equations. *Mathematics of Computations*, **50**(181):89–123, 1988.
- [39] D. Henry. *Geometric Theory of Semilinear Parabolic Equations*, volume 840 of *Lecture Notes in Mathematics*. Springer-Verlag, 1981.
-

-
- [40] A.T. Hill and E. Süli. Upper semicontinuity of attractors for linear multi-step methods approximating sectorial evolution-equations. *Mathematics of Computation*, **64**(211):1097–1122, 1995.
 - [41] M.W. Hirsch and S. Smale. *Differential Equations, Dynamical Systems, and Linear Algebra*. Academic Press, 1974.
 - [42] N.W. Hirsch, C.C. Pugh, and M. Shub. *Invariant Manifolds*, volume 583. Springer-Verlag, 1977.
 - [43] J.M. Hyman and B. Nicolaenko. The Kuramoto-Sivashinsky equation: A bridge between PDE's and dynamical systems. *Physica D*, **18**(1-3):113–126, 1986.
 - [44] J.M. Hyman, B. Nicolaenko, and S. Zaleski. Order and complexity in the Kuramoto-Sivashinsky model of weakly turbulent interfaces. *Physica D*, **23**(1-3):265–292, 1986.
 - [45] F. John. *Partial Differential Equations*. Springer-Verlag, 4th edition, 1981.
 - [46] M.S. Jolly. Explicit construction of an inertial manifold for a reaction diffusion equation. *Journal of Dynamics and Differential Equations*, **78**:220–261, 1989.
 - [47] M.S. Jolly, I.G. Kevrekidis, and E.S. Titi. Approximate inertial manifolds for the Kuramoto-Sivashinsky equation: Analysis and computations. *Physica D*, **44**:38–60, 1990.
 - [48] M.S. Jolly, I.G. Kevrekidis, and E.S. Titi. Preserving dissipation in approximating inertial forms for the Kuramoto-Sivashinsky equation. *Journal of Dynamics and Differential Equations*, **3**(2):179–197, 1991.
 - [49] D.A. Jones. On the behaviour of attractors under finite-difference approximation. *Numerical Functional Analysis and Optimization*, **16**:1155–1180, 1995.
-

-
- [50] D.A. Jones, L.G. Margolin, and E.S. Titi. On the effectiveness of the approximate inertial manifold: A computational study. *Theoretical and Computational Fluid Dynamics*, **12**(4):243–260, 1995.
 - [51] D.A. Jones and A.M. Stuart. Attractive invariant manifolds under approximation. Inertial manifolds. *Journal of Differential Equations*, **123**:588–637, 1995.
 - [52] D.A. Jones, A.M. Stuart, and E.S. Titi. Persistence of invariant sets for dissipative evolution equations. *Journal of Mathematical Analysis and applications*, **219**:479–502, 1998.
 - [53] D.A. Jones and E.S. Titi. C^1 approximations of inertial manifolds for dissipative nonlinear equations. *Journal of Differential Equations*, **127**:54–86, 1996.
 - [54] K. Kassner, A.K. Hobbs, and P. Metzener. Dynamical patterns in directional solidification. *Physica D*, **93**(1-2):23–51, 1996.
 - [55] I.G. Kevrekidis, B. Nicolaenko, and J.C. Scovel. Back in the saddle again: A computer assisted study of the Kuramoto-Sivashinsky equation. *SIAM Journal of Applied Mathematics*, **50**(3):760–790, 1990.
 - [56] Y. Kuramoto. Diffusion induced chaos in reactions systems. *Progress of Theoretical Physics Supplement*, **3**:346–367, 1978.
 - [57] J.N. Kutz and W.L. Kath. Stability of pulses in nonlinear-optical fibres using phase-sensitive amplifiers. *SIAM Journal of Applied Mathematics*, **56**(2):611–626, 1996.
 - [58] X. Liu. Gevrey class regularity and approximate inertial manifolds for the Kuramoto-Sivashinsky equation. *Physica D*, **50**(1):135–151, 1991.
 - [59] X. Liu. A note on Gevrey class for the solution of the Navier-Stokes equations. *Journal of Mathematical Analysis and Applications*, **167**:588–595, 1992.
-

-
- [60] M.A. López-Marcos. Numerical-analysis of pseudospectral methods for the Kuramoto-Sivashinsky. *IMA Journal of Numerical Analysis*, **14**(2):233–242, 1994.
- [61] G.J. Lord and A.M. Stuart. Discrete Gevrey regularity, attractors and upper-semicontinuity for a finite difference approximation to the Ginzburg-Landau equation. *Numerical Functional Analysis and Optimization*, **16**(7-8):1003–1047, 1995.
- [62] J. Mallet-Paret. Negatively invariant sets of compact maps and extension of a theorem of Cartwright. *Journal of Differential Equations*, **22**:331–418, 1976.
- [63] J. Mallet-Paret and G.R. Sell. Inertial manifolds for reaction-diffusion equations in higher space dimensions. *Journal of the American Mathematical Society*, **1**(4):805–866, 1988.
- [64] L.G. Margolin and D.A. Jones. An approximate inertial manifold for computing Burgers' equation. *Physica D*, **60**:175–184, 1992.
- [65] M. Marion. Approximate inertial manifolds for reaction diffusion equations in high space dimension. *Journal of Dynamics and Differential Equations*, **1**:245–267, 1989.
- [66] M. Marion and J.C. Xu. Error-estimates on a new nonlinear Galerkin method based on 2-grid finite-elements. *SIAM Journal of Numerical Analysis*, **32**(4):1170–1184, 1995.
- [67] D. Michelson. Steady solutions of the Kuramoto-Sivashinsky equation. *Physica D*, **19**(1):89–111, 1986.
- [68] B. Nicolaenko, B. Scheurer, and R. Temam. Some global dynamical properties of the Kuramoto-Sivashinsky equation: Nonlinear stability and attractors. *Physica D*, **16**(2):155–183, 1985.
-

-
- [69] B. Nicolaenko, B. Scheurer, and R. Temam. Some global dynamical properties of a class of pattern formation equations. *Communications in Partial Differential Equations*, **14**:245–297, 1989.
- [70] L. Nirenberg. Remarks on strongly elliptic partial differential equations. *Communications on Pure and Applied Mathematics*, **8**:649–675, 1955.
- [71] A. Novick-Cohen and G.I. Sivashinsky. On the solidification fronts of a dilute binary alloy: Thermal diffusivity effects and breathing solutions. *Physica D*, **20**(2-3):237–258, 1986.
- [72] D.T. Papageorgiou, C. Maldarelli, and D.S. Rumschitzki. Nonlinear interfacial stability of core-annular film flow. *Physics of Fluids A-Fluid Dynamics*, **2**(3):340–352, 1990.
- [73] D.T. Papageorgiou and Y.S. Smyrlis. The route to chaos for the Kuramoto-Sivashinsky equation. *Theoretical and Computational Fluid Dynamics*, **3**:15–42, 1991.
- [74] T.S. Parker and L.O. Chua. *Practical Numerical Algorithms for Chaotic Systems*. Springer-Verlag, 1989.
- [75] A. Pazy. *Semigroups of Linear Operators and Applications to Partial Differential Equations*, volume 44 of *Applied Mathematical Sciences*. Springer-Verlag, 1983.
- [76] V.A. Pliss and G.R. Sell. Perturbations of attractors of differential equations. *Journal of Differential Equations*, **92**:687–728, 1991.
- [77] K. Promislow. Time analyticity and Gevrey regularity for solutions of a class of dissipative partial differential equations. *Nonlinear Analysis*, **16**(1):959–980, 1991.
- [78] R.D. Russell, D.M. Sloan, and M.R. Trummer. Some numerical aspects of computing inertial manifolds. *SIAM Journal of Scientific Computing*, **14**(1):19–43, 1993.
-

-
- [79] J.M. Sanz-Serna. Two topics in nonlinear stability. In W. Light, editor, *Advances in Numerical Analysis: Volume I: Nonlinear Partial Differential Equations and Dynamical Systems*, chapter 4, pages 147–174. Clarendon Press, 1991.
- [80] L.P. Sil'nikov. A case of the existence of a denumerable set of periodic motions. *Sov. Math. Dokl.*, 6:163–166, 1965.
- [81] G. Sivashinsky. Nonlinear analysis of hydrodynamics instability in laminar flames, Part I. Derivation of basic equations. *Acta Astronautica*, 4(11):1177–1206, 1977.
- [82] Y.S. Smyrlis and D.T. Papageorgiou. Predicting chaos for infinite dimensional dynamical systems: The Kuramoto-Sivashinsky equation, a case study. *Proceedings of the National Academy of Sciences of the U.S.A.*, 88:11129–11132, 1991.
- [83] H.J. Stetter. Stability of nonlinear discretization algorithms. In J.H. Bramble, editor, *Numerical Solution of Partial Differential Equations*, pages 111–123. Academic Press, 1966.
- [84] A.M. Stuart. Perturbation theory for infinite-dimensional systems. In W.A. Light M. Ainsworth, J. Levesley and M. Marletta, editors, *Theory and Numerics of Ordinary and Partial differential Equations*. Oxford Science Publications, 1995.
- [85] A.M. Stuart and A.R. Humphries. *Dynamical Systems and Numerical Analysis*. Cambridge University Press, 1996.
- [86] M. Taboada. Finite dimensional asymptotic behaviour for the Swift-Hohenberg model of convection. *Nonlinear Analysis-Theory Methods and Applications*, 14:43–54, 1990.
- [87] R. Temam. *Infinite-Dimensional Dynamical Systems in Mechanics and Physics*, volume 68 of *Applied Mathematical Sciences*. Springer-Verlag, 1988.
-

-
- [88] R. Temam. Induced trajectories and approximate inertial manifolds. *Mathematical Modelling and Numerical Analysis*, **23**:541–561, 1989.
 - [89] R. Temam. Inertial manifolds and multigrid methods. *SIAM Journal of Mathematical Analysis*, **21**:154–178, 1990.
 - [90] R. Temam and S.H. Wang. Estimates on the lowest dimension of inertial manifolds for the Kuramoto-Sivashinsky equation in the general case. *Differential and Integral Equations*, **7**:1095–1108, 1994.
 - [91] S. Toh. Statistical-model with localised structures describing the spatio-temporal chaos of Kuramoto-Sivashinsky equation. *Journal of the Physical Society of Japan*, **56**(3):949–962, 1987.
 - [92] R.G. Voigt, D. Gottlieb, and M.Y. Hussaini, editors. *Spectral Methods for Partial Differential Equations*, 1984.
 - [93] R. Wallace. *Numerical Solution of Nonlinear Dissipative Systems using Inertial Manifolds*. PhD thesis, University of Strathclyde, 1995.
 - [94] R. Wallace and D.M. Sloan. Numerical solution of a nonlinear dissipative system using a pseudospectral method and inertial manifolds. *SIAM Journal of Scientific Computing*, **5**(16):1049–1070, 1995.
 - [95] S. Wiggins. *Global Bifurcations and Chaos*. Number 73 in Text in Applied Mathematics. Springer-Verlag, 1988.
-